THE UNIVERSITY *of* EDINBURGH

Production of canine hepatocyte-like cells from stem cell sources

Adam George Gow

2014

Thesis submitted for the degree of Doctor of Philosophy

College of Medicine and Veterinary Medicine

University of Edinburgh

Contents

Declaration

The thesis presented is the work of the author except stated otherwise by reference and /or acknowledgement. Any work presented, which has been conducted by (or in collaboration with) others is explicitly acknowledged. No part of this work has been submitted for any other degree or professional qualification.

Adam George Gow …… Date: March 2014

Abstract

The cost of drug development is high with many drugs failing during toxicity testing. This is a particular problem in veterinary medicine where the pharmaceutical market size is so small that it may not be economically viable to develop drugs. The liver and specifically hepatocytes have a crucial role in drug metabolism via oxidation by cytochrome enzymes (CYP), conjugation and excretion into the biliary system. This drug metabolism is unpredictable between species as each has unique CYP profiles. Furthermore there is breed variation of CYP profiles within the canine species. The ability to produce an *in vitro* source of canine hepatocytes to model drug metabolism in this species and in different breeds would greatly reduce the expense of candidate drug testing. If an unlimited supply could be produced *in vitro* this would reduce the number of animals required in pre-clinical testing. The aim of this thesis was to produce an *in vitro* supply of canine hepatocyte-like cells from stem cell sources, namely hepatic progenitor cells (HPC), mesenchymal stem cells (MSC) or induced pluripotent stem cells (iPSC). Cultures of canine primary hepatocytes were produced to use as a gold standard, but also to develop and refine tests of hepatocyte characterisation and function. A panel of primers was developed for use in real time polymerase chain reaction (PCR) as well as optimising tests for low density lipoprotein (LDL) and indocyanine green uptake, albumin production, periodic acid-Schiff staining for glycogen and CYP activity using a luciferase-based system. As primary hepatocytes rapidly lost their defining characteristics and function *in vitro*, methods of maintaining function using CYP inducers and culture substrates were assessed.

Isodensity centrifugation and magnetic-activated cell sorting was employed to isolate HPCs. Selection of cells from the non-parenchymal cell fraction with stem cell marker Prominin 1 demonstrated that these were keratin 7 positive, a HPC marker. Cells morphologically consistent with HPC appeared and expanded in culture after 2 weeks. On passaging, these cells failed to continue expanding, despite plating onto collagen, laminin, SNL feeder cells or using Kubota's medium (known to allow rapid expansion of rodent and human HPCs).

Canine adipose (Ad-MSC) and bone marrow-derived mesenchymal stromal cells (BM-MSC) were isolated *post mortem*. These were characterised as CD45, 105 and STRO-1 positive, CD11b, 19 and 45 negative cells which could be differentiated into adipocytes, chondrocytes and osteocytes based on staining characteristics and relative gene expression. Protocols published for other species were used to differentiate both Ad-MSC and BM-MSC towards a hepatocyte phenotype. Although a dramatic change in morphology and a reduction in vimentin gene expression were noted, suggesting a loss of mesenchymal phenotype, these protocols did not induce a hepatocyte phenotype. Pre-treatment with 5-Aza-2′-deoxycytidine to cause DNA demethylation and valproic acid to inhibit histone deacetylation also failed to allow transdifferentiation.

A polycistronic vector containing *Oct-4*, *c-Myc*, *Sox2* and *Klf4* was successfully transfected into canine epidermal keratinocyte progenitor cells which became alkaline phosphatase positive and assumed a morphology consistent with iPSC. After colony selection and expansion, PCR evidence of plasmid presence was lost, colony morphology changed, and alkaline phosphatase activity reduced, consistent with vector expression factor and pluripotency loss.

Canine iPSCs produced by lentiviral method were then differentiated towards hepatocyte phenotype using a published protocol for mouse and human iPSC. These cells were then assessed for hepatocyte characteristics using the developed reagents and primers. These cells demonstrated increased gene expression and morphology consistent with differentiation towards a hepatocyte-like phenotype.

This thesis demonstrates successful culture of canine primary hepatocytes and validation of tests of hepatocyte phenotype. This provides a basis for optimising primary hepatocyte function *in vitro* and assessment of the success of differentiation protocols on stem cell sources. Canine mesenchymal stromal cells do not appear to transdifferentiate towards a hepatocyte-like phenotype using published protocols for other species. Canine iPSC are a promising candidate for an *in-vitro* source of hepatocyte-like cells.

Acknowledgements

First, I would like to thank my supervisors Prof David Argyle and Dr David Hay for all their support and guidance throughout my PhD. Thanks also go to all members of the Argyle Group, past and present, for their help and support. I'd particularly like to thank Rhona Muirhead whose unfailing ability to multitask, find reagents and equipment at short notice and generally be willing to efficiently deal with any bizarre request is nothing short of miraculous. Thanks also go to Dr Lisa Pang for guidance on laboratory techniques as well as Indy Cat, and latterly Wofful, cat chat.

Personally, I am eternally grateful to the wonderful and amazing Debbie Gow for her love, support and being the first two adjectives. Joseph Gow needs special thanks for allowing me to be "Batdog" (or occasionally "Batpuppy"), to his Batman which helped break the thesis writing up nicely. Many thanks also to my parents for their love and support in our lives.

Contributions of work

Chapter 1: Keratin 7 staining of canine hepatic tissue blue was performed by Neil MacIntyre and the R(D)SVS pathology laboratory

Chapter 5: Assistance in isolation of BM-MSCs, Rhona Muirhead. Blocking, sectioning of cartilage pellets and staining with Toluidine blue was performed by Neil MacIntyre and the R(D)SVS pathology laboratory

Abstracts

Oral presentations

Gow, A.G., Pang,L., Hay, D., Argyle, D.J Magnetic assisted cell sorting of hepatic non-parenchymal cells for CD133 enriches for hepatic progenitor cells. European Veterinary Internal Medicine Congress, September 2012

Canine hepatocytes from stem cell sources. Presented at The Roslin Institute student research seminar series, June 2013

Gow, A.G., Hay, D., Argyle, D.J . Low density lipoprotein (LDL) and acetylated-LDL (Ac-LDL) uptake of primary canine hepatocytes and canine mesenchymal stem cells (MSC). European Veterinary Internal Medicine Congress, September 2013

Gow, A.G., Hay, D., Argyle, D.J. Characterisation of canine adipose and bone marrow-derived mesenchymal stem cells and hepatocyte differentiation capacity. European Veterinary Internal Medicine Congress, September 2013

Poster Presentations

Gow, A.G., Hay, D., Argyle, D.J. A study of canine hepatic stem cells. Poster abstract presented at The Roslin Institute & R(D)SVS student research day May 2011

Gow, A.G., Hay, D., Argyle, D.J. Canine mesenchymal stem cells to hepatocytes induction. Poster abstract presented at The Roslin Institute & R(D)SVS student research day May 2013

Figures

Tables

Chapter 1: Introduction

1.1 The liver

The liver is the largest internal organ in the body and contains an extensive network of afferent and efferent vessels transporting blood, bile and lymph that interdigitate. The vasculature, and its surrounding connective tissue, which make up approximately 22% of the organ's weight, provides structural support in the liver. Resting blood flow is approximately 25% of cardiac output, reflecting its high metabolic activity. Only 25% of this blood flow is fully oxygenated and supplied by the hepatic artery. The remainder is partially oxygen depleted, supplied by the portal vein draining the splanchnic viscera including the gastrointestinal tract (Arias et al., 2011).

1.1.1 Structure of the liver

The liver is composed of lobules which can be seen histologically as hexagonally shaped and consist of cords of hepatocytes radiating from a central vein. Located at each corner of the hexagon are three vessels, artery, vein and bile duct, known as the portal triad. Functionally, the liver acinus, defined by hepatocytes supplied by one triad, is the most useful method of demarcation. The hepatocytes in the acinus are subjected to an oxygen and biochemical gradient with a drop in oxygen concentration from the peri-portal to peri-venous zone.

The liver contains an array of cell types; hepatocytes, cholangiocytes, endothelial cells, macrophages (known as Kupffer cells in location), lymphocytes and stellate cells are all intimately involved in contributing to the liver's function.

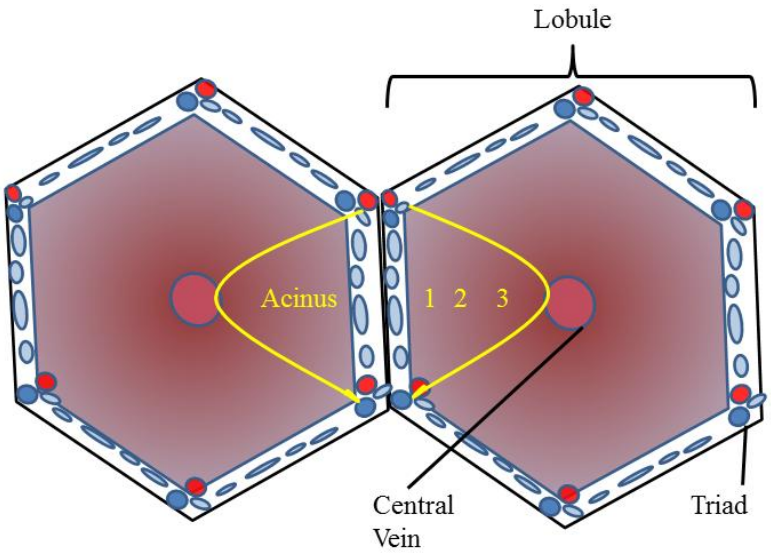

Figure 1.1 Organisation of the liver lobule and acinus
Although histologically the triad is easily defined, the acinus, demarcated by the yellow line, is the most applicable. The acinus can be sub-divided into three zones; 1- periportal, 2- transitional, and 3 – perivenous.

The liver has a diverse array of functions and as a result has a heterogeneous mix of cells. As the liver receives all venous blood from the gastrointestinal system, many of the functions involve processing products in this blood supply.

1.1.2 Main cells of the liver and function

1.1.2.1 Endothelial cells

These differ from endothelial cells elsewhere in the body as they lack a basement membrane, are fenestrated and intimately attached to stellate cells. They separate hepatocytes from sinusoidal blood and act as a selective filter for substances. As well as simple filtration they also have the ability to endocytose, and phagocytose substances (Kmiec, 2001).

1.1.2.2 Kupffer cells

These are resident macrophages in the liver and as stated above are intimately linked with the endothelial cells with the cell membrane reaching through the fenestrations of the endothelial cells into the space of Disse to contact stellate cells and hepatocytes. They are located in the greatest density peri-centrally and as a result are exposed to and clear lipopolysaccharides, bacterial toxins and translocated bacteria from the gastrointestinal tract (Kmiec, 2001). They make up 80-90% of the total tissue macrophage population in the body, highlighting their importance as an initial defence against gastrointestinal bacteria and toxins (Bilzer et al., 2006).

1.1.2.3 Stellate cells

These are situated between hepatocytes and endothelial cells, interdigitating with both, and contribute up to 15% of cell number in the normal liver (Hellerbrand, 2013). These cells store vitamin A and also regulate the extracellular matrix by production of matrix and also secretion of matrix metalloproteinases (MMP) as well as inhibitors of MMPs (TIMPS).

1.1.2.4 Cholangiocytes

These are epithelial cells that line the biliary tree. Their function is to modify bile which is produced by hepatocytes. These differ in morphology and derivation in different parts of the biliary tree. The intra-hepatic component of the biliary tree contains cells derived from hepatic progenitor cells whilst the extra-hepatic component has the same origin as the pancreas and duodenum. Cholangiocytes secrete chloride, bicarbonate and water and reabsorb bile acids, amino acids and glucose (Tabibian et al., 2013).

1.1.2.5 The Hepatocyte

Hepatocytes make up approximately 80% of the liver by weight and are also known as hepatic parenchymal cells (Si-Tayeb et al., 2010). They are large, polygonal, functionally complex cells with endocrine and exocrine functions (Arias et al., 2011). *In vivo* hepatocytes have several functionally distinct surfaces. Approximately 50% is adjacent to surrounding hepatocytes with areas containing microvilli which form bile caniliculi making up 13%. A further 35% face towards sinusoids with microvilli extending into the space of Disse (Arias et al., 2011) (Figure 1.2).

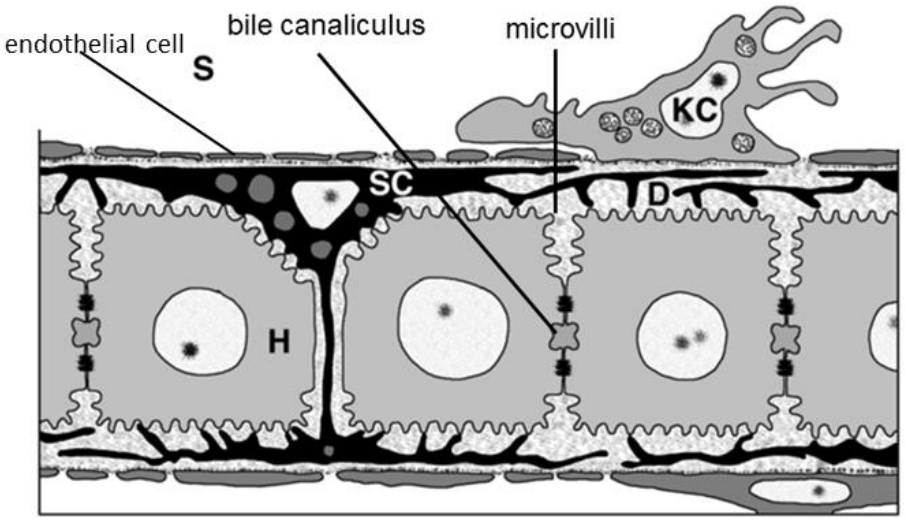

Figure 1.2 Hepatocyte structure and surrounding architecture
Between the layers of hepatocytes are fenestrated endothelial cells separated by the space of Disse. Macrophages (Kupffer cells) are present within the sinusoids. H – Hepatocyte, SC – Stellate cell, KC – Kupffer cell, D – Space of Disse, S – Sinusoid. Figure adapted from Frevert et al., 2005.

Hepatocytes are responsible for production of many proteins including albumin and the majority of clotting factors. Hepatocytes are the major centre for gluconeogenesis as well as providing a store of glucose in the form of glycogen. The hepatocyte is also a key player in lipid metabolism, producing bile acids, which emulsify ingested fat allowing efficient absorption, as well as synthesising apoproteins which facilitate lipid distribution throughout the body via lymphatics and blood vessels (Fraczek et al., 2013).

Another crucial hepatocyte function is the transformation and detoxification of endogenous substances. Endogenous compounds include hormones, for example steroid hormones, but also ammonia which is produced in the gastro-intestinal tract from protein metabolism and delivered via the portal vein directly to hepatocytes Ammonia is then efficiently converted to the much less toxic compound urea, before the blood enters the systemic circulation (Kaneko et al., 2008). Compounds may also be removed from the systemic circulation by hepatocytes secreting the substance through their bile canalicular membrane, ultimately causing the substance to be excreted in faeces (Tomlin, 2010). There appears to be remarkable zonation of hepatocyte function which is related to haemodynamics and which hepatocytes are exposed to the highest concentrations of substances. For example, peri-portal hepatocytes are exposed to the highest ammonia concentrations and have the greatest activity of carbamoyl phosphate synthetase I which is the first enzyme used in the urea cycle for ammonia detoxification (Arias et al., 2011).

1.1.3 Liver development

The liver forms from endoderm and mesoderm. Hepatocytes and cholangiocytes are formed from endoderm whilst other non-parenchymal cells have a mesodermal origin. The primitive gut tube endoderm forms fore, mid and hindgut regions, with the liver arising from the foregut (Figure 1.3). The endodermal portion then joins with the septum transversum mesenchyme to form a liver bud.

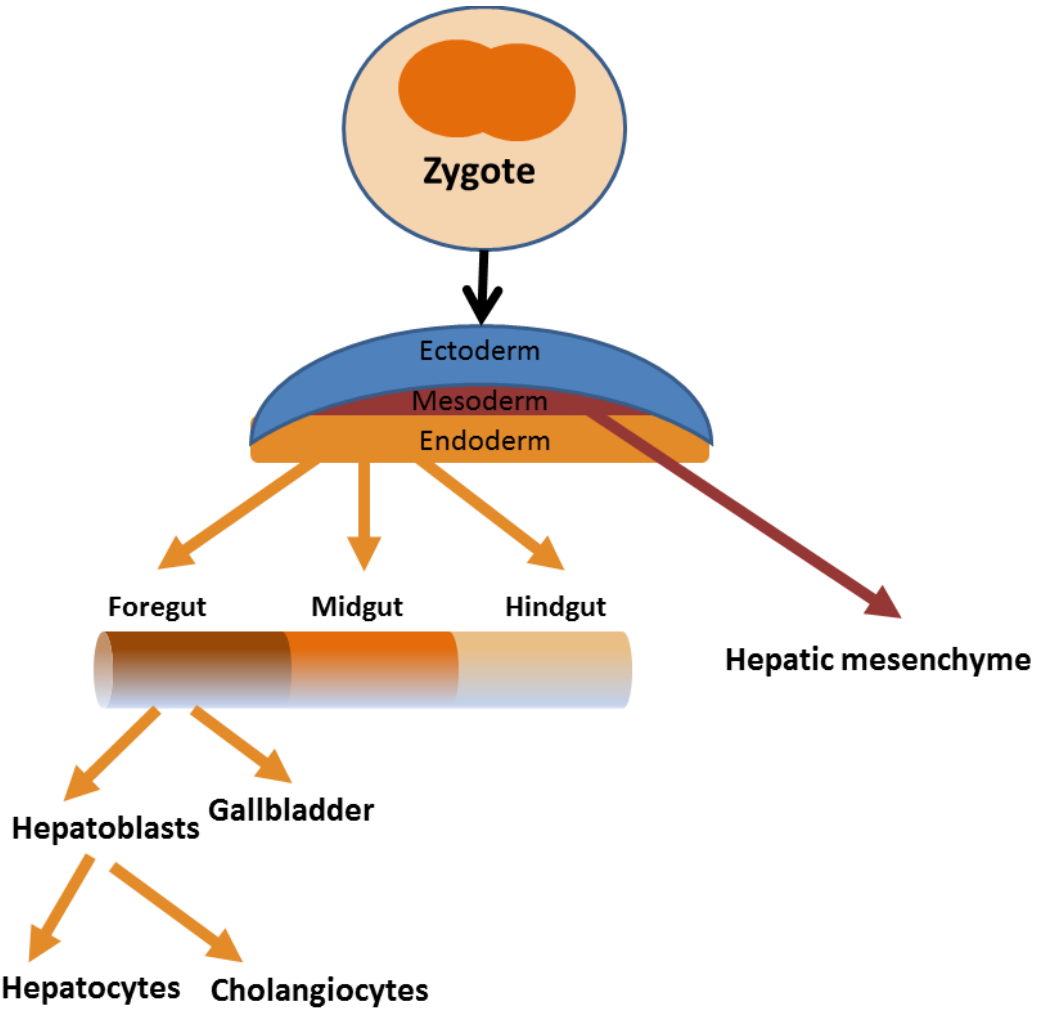

Figure 1.3 Origin of liver lineage
Both hepatocytes and cholangiocytes arise from foregut endoderm whilst the non-parenchymal cell compartment is mesenchymal in origin.

1.1.3.1 Signalling in liver development

Formation of both endoderm and mesoderm is controlled by Nodal with high concentrations forming endoderm and lower concentrations mesoderm (Zorn, 2008). Thereafter, fibroblast growth factor (FGF), Wnt, bone morphogenic protein (BMP) and retinoic acid combinations produced by the mesoderm stimulate specific endodermal zonation. For liver development, FGF from cardiac tissue along with BMP from the septum transversum cause hepatic development from the foregut endoderm (Figure 1.4). Wnt is also produced from the adjacent mesoderm; the function of this in hepatic development has not been elucidated (Zorn, 2008).

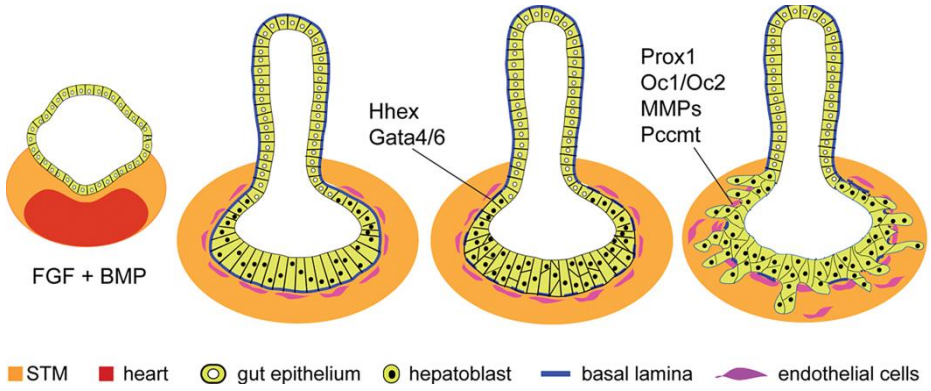

Figure 1.4 Liver bud development
Transverse section schematic demonstrating hepatic endoderm invaginating and subsequent migration into septum transversum mesenchyme. STM – septum transversum mesenchyme From Zorn (2008).

1.2 *In vivo* liver regeneration

The liver, as an organ, has very low cell turnover in health with approximately 1 year taken for complete cell turnover (Dolle et al., 2010). Despite this, mature hepatocytes have tremendous hyperplastic capacity. The original experiments by Higgins and Anderson in 1931 demonstrated that rats undergoing 2/3 hepatectomy regained their original liver weight within 7 days of the procedure (Higgins and Anderson, 1931). Although often termed "liver regeneration" in the literature, technically regeneration is defined by replacement of like with like e.g. limb replacement in many amphibians. The resultant replaced liver tissue is due to hypertrophy of the remaining lobes therefore the term "compensatory hypertrophy" is more accurate (Miyaoka and Miyajima, 2013). This response is thought to be due to cytokine queues of TNFα and IL-6. Further growth factors including hepatocyte growth factor (HGF), epidermal growth factor (EGF) and transforming growth factor (TGFα) then cause progression through the cell cycle. It has classically been thought that almost all quiescent mature hepatocytes enter the S phase of the cell division cycle and that the number of cell divisions per hepatocyte is low, between 1 and 2 (Fausto et al.,

2006). This was based on studies examining incorporation of radioactive nucleotides into hepatocytes (Bucher and Oakman, 1969).

Recently, this view has been questioned. Mature hepatocytes are often binucleate and it has been recognised for almost 70 years that the number of binucleate cells decreases after compensatory hypertrophy (St Aubin and Bucher, 1952). Genetic tracing of labelled hepatocytes indicates that after 70% partial hepatectomy, 40% of hepatocytes do not undergo division and that after 30% hepatectomy, only a small fraction entered the S phase and no hepatocytes divided, despite rapid restoration of liver mass. It appears that cellular hypertrophy i.e. increase in hepatocyte cell size accounts for a significant part of liver weight restoration and that this occurs as an early response. Hepatocytes will then only enter the cell cycle if cellular hypertrophy is insufficient to restore mass (Miyaoka et al., 2012). Furthermore the mature binucleate cells undergo cell division where one binucleate cell produces two mononuclear daughter cells which are more polyploid than the mother (Miyaoka and Miyajima, 2013). The factors that govern liver mass are still being investigated but blood flow, blood bile acid and glucose concentration have been shown to be important (Meng et al., 2011; Schoen et al., 2001; Simek et al., 1965). Additionally, hepatocyte paracrine signalling with TGFβ has been suggested as a mechanism to terminate proliferation (Carr et al., 1986).

1.3 Hepatic progenitor cells

If mature hepatocytes are unable to multiply, for example due to chronic hepatitis causing hepatocyte loss and fibrosis, then there are adult stem cells within the liver termed hepatic progenitor cells (HPC) or oval cells in rodents (Dolle et al., 2010). HPC are thought to be present in the Canals of Hering (Figure 1.2), anatomically located between hepatocytes and the biliary tree by the portal triads of zone 1 (Figure 1.5) (Roskams, 2006). These are present in very low numbers in healthy adult livers, approximately 0.5-2% of the parenchyma (Turner et al., 2011). It is thought that these HPC sequentially mature as they pass from periportal to pericentral in zone 3. HPCs have been sub-divided into hepatic stem cells (HpSCs) and hepatoblasts (HBs)

although this subdivision is not used universally (Schmelzer et al., 2007). HpSCs are bi-potential, in that they can differentiate into cholangiocytes or hepatocytes depending on need. As they differentiate towards hepatocytes, 8 distinct stages are recognised with cells increasing in size as they progress towards mature hepatocytes. Hepatoblasts are the second stage when differentiation towards cholangiocytes is still possible before the cells become committed progenitors. There is debate as to the phenotypic markers present on HPC as there has been no specific marker identified at present (Darwiche and Petersen, 2010). This presents a difficulty in research into HPC as different groups use different selection panels and markers may not apply across different species. Among the markers identified in human and rodent HPCs are CD133, epithelial cell adhesion molecule (EpCAM), neural cell adhesion molecule (NCAM), SOX9, keratins 7,8,18,19 (Figure 1.6) (Darwiche and Petersen, 2010; Roskams, 2006). Some authors state that αfoetal protein (AFP) is present on HPC, whilst others state this is not expressed until the hepatoblast has been reached (Darwiche and Petersen, 2010; Roskams, 2006). As with all tissue stem cells, they are protected within a "niche" of surrounding cell types and extracellular matrix that is required for their maintenance and self-renewal (Kordes and Haussinger, 2013). Among the cell types thought to be important in HPC maintenance are periportal fibroblasts, stellate cells, endothelial cells, hepatocytes, cholangiocytes, and immune cells (Darwiche and Petersen, 2010). It is thought angioblasts, associated mesenchymal cells, mature in concert with NPC and as a result provides sequential soluble factors and matrices to direct differentiation (Turner et al., 2011; Wang et al., 2010). In chronic liver disease a "ductular reaction" occurs where intermediate hepatocytes arise, surrounding fine biliary ducts (Schotanus et al., 2009; Yoshioka et al., 2004). Activation of these HPCs appears to be stimulated by release of Hedgehog ligand from damaged hepatocytes (Jung et al., 2010).

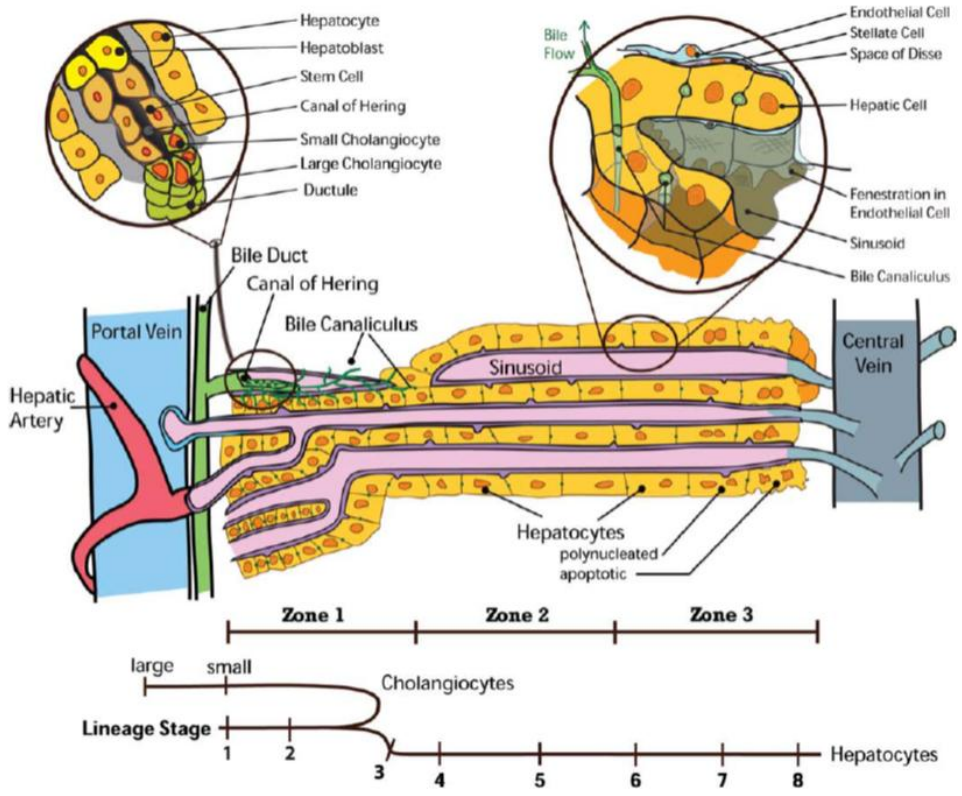

Figure 1.5 Schematic diagram demonstrating location of hepatic stem cells in the liver and sequential lineage between canal of Hering and central vein.
Image from Turner et al,. 2011.

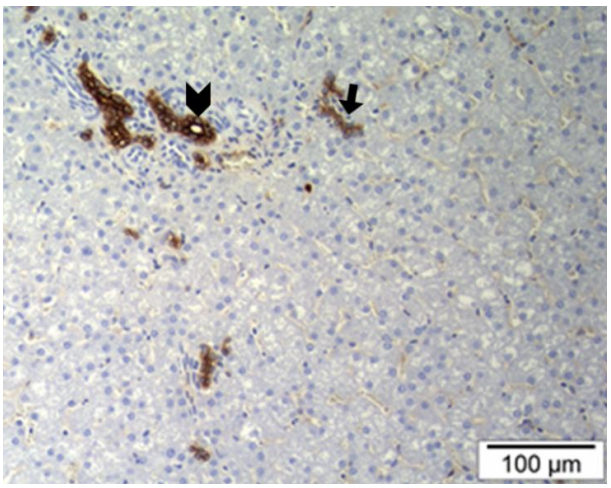

Figure 1.6 Keratin 7 staining of canine hepatic parenchyma.
Staining with monoclonal mouse antibody (OV-TL 12/30, Dako) 1:500 with Hypoxanthine-guanine phosphoribosyltransferase (HPRT). Black arrowhead indicated staining of cholangiocytes in bile duct. Black arrow indicates hepatic progenitor cells. Staining performed by Neil MacKintyre, R(D)SVS Pathology Laboratory.

1.4 Hepatic metabolism of xenobiotics

The liver also has the remarkable ability to metabolise a wide variety of synthetic drugs. This is performed by hepatocytes. To allow this, hepatocytes contain a large group of oxidative enzymes which are membrane bound haemoproteins, known as the cytochrome (CYP) P450 superfamily (Sevior et al., 2012). At present 1056 distinct forms have been identified in mammals with 116 in humans and 35 in the dog (Nelson, 2009). These individual enzymes are identified by the abbreviation CYP followed by a number for the gene family, a letter for the subfamily and finally a number for the individual gene e.g. CYP2D15. There is marked species variation in the cytochrome P450 profile with many species having unique enzymes and also response to induction by drugs (Graham and Lake, 2008; Martignoni et al., 2006). Comparable enzymes or orthologues to these unique enzymes can be identified in other species; however there can be marked differences in substrate specificity between orthologues, making extrapolation of drug pharmacokinetics between species unpredictable (Martignoni et al., 2006).

In the dog, the CYP family has not been fully characterised, however unique canine orthologues have been identified (Trepanier, 2006). Table 1.1 demonstrates known canine CYP orthologues, comparable human enzymes and known metabolic differences. In addition, there are polymorphisms within species which can cause increased or reduced drug metabolism depending on whether the variation increases or reduces function (Martignoni et al., 2006). Human directed breeding of dogs into specific morphologies (designated pedigree breeds), and subsequent genetic restriction within some breeds due to high levels of inbreeding has meant that some breeds have low genetic diversity with the consequence that different dog breeds may have specific CYP profiles (Fleischer et al., 2008; Rimbault and Ostrander, 2012). This has not been thoroughly investigated at present, although breed differences in CYP profiles and drug metabolising ability have been recognised (Table 1.2) (Fleischer et al., 2008). The implications of this are that pharmacokinetics, pharmacodynamics and effects of drugs may vary widely between different breeds and that drug testing using the laboratory Beagle, for example, may not ensure the drug is safe to use in the Greyhound or Labrador Retriever. To add to

the difficulty of assessing drug metabolism and hepatotoxicity within the canine population, there have been five CYP enzymes identified at present in the dog that are polymorphic (CYP1A2, CYP2C41, CYP2D15, CYP2E1 and CYP3A12), therefore testing drugs with a range of breeds may not be enough to predict toxicity (Table 1.2) (Blaisdell et al., 1998; Kamimura, 2006; Lankford et al., 2000; Mise et al., 2004).

Cytochrome P450 human	Human substrates	Cytochrome P450 canine	Known canine substrates
CYP1A	Dioxin, other environmental chemicals	CYP1A	Induced by environmental toxins (e.g., polychlorinated biphenyls)
CYP1A2	Caffeine, theophylline	Canine ortholog of CYP1A2	Fluoroquinolones (?), theophylline (?), Induced by omeprazole
CYP2B6	Propofol	CYP2B11 Possible second gene?	Propofol, diazepam, progesterone, androstenedione, testosterone (16-α-hydroxylation), diclofenac, cyclophosphamide Induced by phenobarbital
CYP2E1	Ethanol, chlorzoxazone, Bioactivation of acetaminophen	CYP2E ortholog	Chlorzoxazone
CYP2C9	Phenytoin, fluconazole, warfarin, glipizide, flurbiprofen, piroxicam, ibuprofen, celecoxib, naproxen, meloxicam	CYP2C21	Testosterone (16-α-hydroxylation), diclofenac Modest induction by phenobarbital
CYP2D6	Codeine, tramadol, propranolol and other beta-blockers, phenothiazines, quinidine, dextromethorphan, chlorpheniramine, imipramine, fluoxetine, amitriptyline, chlorpromazine, metoclopramide	CYP2D15	Celecoxib, dextromethorphan, imipramine, metoprolol, propranolol
CYP3A4	Ketoconazole, itraconazole, ciclosporin, tacrolimus, lincosamides, cisapride, diazepam, midazolam, diltiazem, digoxin, quinidine, verapamil, aflatoxin, budesonide Induced by rifampicin	CYP3A12 CYP3A26	Erythromycin, tacrolimus, ciclosporin, midazolam, diazepam, nordiazepam progesterone, testosterone (6-β-hydroxylation) Induced by phenobarbital, rifampicin

Table 1.1 Canine and human cytochrome P450 enzyme orthologues and known substrates
Modified from Trepanier, 2006 and Martinez et al., 2013

Breed	Enzyme Linked to Finding	Metabolic Effects
Beagle	CYP1A	Polymorphism/genotypic variation in CYP1A2 activity (due to differences in enzyme expression). Poor metabolizers and extensive metabolizers result in significant polymorphic hydroxylation of a novel benzodiazepine
Greyhound	CYP2B11	Deficient in CYP2B11. Canine CYP2B11 is responsible for propofol hydroxylation in dogs
Mixed Breeds	CYP2B11	14-fold variance in CYP2B11 activity in mixed breed dogs. Mixed breed dogs tended to span range of Vmax seen in Beagles (high) and Greyhounds (low)
Beagle	CYP2D15	Significant pharmacogenetic variation in gene encoding CYP2D15 (counterpart to human CYP2D6). Other undefined CYPs may also be involved. Significant pharmacogenetic variation in celecoxib metabolism in purebred Beagles. Celecoxib is primarily a CYP2D15 substrate in dogs. Extensive metabolizers (about 50% of those tested) have an elimination half-life of 1.5–2 h. Poor metabolizers have an elimination half-life of approximately 5 h.

Table 1.2 Known CYP variations in canine breeds
Adapted from Fleischer 2008

1.5 Liver disease in the dog

The most common type of liver disease in dog and man is inflammatory .i.e. hepatitis. Whereas in man, the cause of hepatitis is often recognised e.g. viral, alcohol-induced or due to fat accumulation, in the dog despite searching, no specific underlying cause has been identified in the vast majority of cases (Boomkens et al., 2004; Boomkens et al., 2005; Van den Ingh et al., 2006). A recently discovered hepacivirus in dogs, which is the closest genetic relative of hepatitis C virus, was not found to be associated with chronic liver disease in the dog (Bexfield et al., 2014). This is not to say that all cases of hepatitis in the dog are idiopathic. Copper associated hepatitis is well recognised in the dog and is similar to Wilson's disease in humans (Favier et al., 2012).

Chronic hepatitis (CH) is thought to be the most common liver disease in the dog although prevalence rates vary. Poldervaart et al. (2009) reported a prevalence of 0.5% in a referral population, whilst Watson et al. (2010) found evidence of CH in 12% of post-mortem examination of 200 unselected dogs. As the cause is unknown, treatment is symptomatic and the prognosis for dogs with chronic hepatitis is poor. A median survival time of 18.3 months is reported (Poldervaart et al., 2009; Watson, 2004).

Chronic hepatitis is characterised by hepatocyte apoptosis and necrosis with an inflammatory infiltrate which is mononuclear or mixed (Watson, 2004). Fibrosis occurs and is progressive in the majority of cases to the point of cirrhosis. Regenerative nodules are often present within the liver (Van den Ingh et al., 2006). Fibrosis results from increased extracellular matrix (ECM) deposition, particularly type I and III collagen (Mallat and Lotersztajn, 2013). This increase in ECM is due to activation of hepatic stellate cells to a myofibroblast morphology which upregulate ECM production and TIMPS, which inhibit degradation of ECM (Hellerbrand, 2013). This transformation is induced by TGFβ. It is thought that myofibroblasts further contribute to inflammation by cytokine production which attracts further leucocytes. Portal fibroblasts have also been shown to transform to myofibroblasts and there is evidence that bone marrow fibrocytes may localise within the liver

(Forbes et al., 2004; Mallat and Lotersztajn, 2013). *In vitro* studies have demonstrated that TGFβ can induce epithelial to mesenchymal transition of hepatocytes and cholangiocytes; however, evidence of this has not been found *in vivo* (Mallat and Lotersztajn, 2013). As suggested by their name, myofibroblasts are contractile cells. This contractility along with deposition of ECM disrupts the normal hepatic architecture causing portal hypertension by altering sinusoidal tone and blood flow as well as intrahepatic cholestasis. Continued portal hypertension causes the recruitment of collateral porto-systemic shunting vessels allowing portal blood direct access to the systemic circulation (Szatmari and Rothuizen, 2009; Watson, 2004). Intrahepatic cholestasis causes the development of jaundice, portal hypertension may result in ascites, particularly if combined with hypoalbuminaemia as a result of reduced hepatocyte number. Porto-systemic shunting results in the development of hepatic encephalopathy (HE) which is a clinical syndrome of neurological dysfunction. A key player in HE is high systemic ammonia concentrations ,which are neurotoxic (Shawcross et al., 2005). This thought not to be the only factor in HE development and there is evidence for a role of inflammation and manganese (Mn) (Ahboucha, 2011; Shawcross and Jalan, 2005). Increased systemic delivery of these factors results from the failure of portal blood to pass through the liver. Ammonia is converted to the less toxic compound urea by hepatocytes. Similarly manganese is efficiently extracted by hepatocytes and secreted in bile such that only approximately 2% of portal Mn normally reaches the systemic circulation (Davis et al., 1993). As stated above, the liver has a large population of tissue macrophages which act to remove potential inflammatory mediators from portal blood before it reaches the systemic circulation.

As the liver has a huge reserve capacity of hepatocytes, a large proportion must be lost before there is a noticeable reduction in hepatocyte function. Once this occurs, reduced serum albumin can further contribute to the development of ascites. Inability to maintain adequate concentrations of clotting factors may cause coagulopathy; however, this is further compounded by pre-disposition to disseminated intravascular coagulation and potentially vitamin K deficiency (Szatmari and Rothuizen, 2009).

1.6 Human *in vitro* hepatocyte production

In human medicine, the increase in prevalence of chronic liver disease, coupled with a shortage of healthy livers for transplantation, has stimulated much research to produce and expand hepatocytes *in vitro* (Palakkan et al., 2013). In human medicine it is anticipated that these would be used in a variety of ways, for transplantation; in bio-artificial liver devices to support patients as a bridge until a transplant was available, or allow sufficient regeneration in cases of acute hepatic failure; as an *in vitro* model of liver disease; or as an *in vitro* system for modelling hepatic metabolism of candidate drugs (Dalgetty et al., 2009). The source of these hepatocytes may be derived from primary hepatic tissue, cell lines or stem cell sources (Donato et al., 2013; Fraczek et al., 2013; Greenhough et al., 2010).

1.7 Rational for *in vitro* canine hepatocyte production

In dogs, chronic hepatitis is common. A small percentage of chronic hepatitis cases are caused by infectious agents (e.g. leptospirosis), toxins (e.g. aflatoxicosis) or associated with abnormal hepatic copper accumulation, however to date, in contrast to human medicine, the initiating cause is unknown in the vast majority of canine cases (Boomkens et al., 2004; Boomkens et al., 2005; Van den Ingh et al., 2006; Watson, 2004). As a result, therefore, potentially these patients would benefit from liver transplant in a similar manner to human patients with liver disease. Although liver transplant is frequently performed experimentally in the dog as a model for the human procedure, the ethics, logistics and financial cost makes clinical liver transplantation for dogs with liver disease unlikely (Liu et al., 2013; Pan et al., 2013). Hepatocyte transplantation/transfusion is used clinically in humans as a "bridge" to transplantation (Pareja et al., 2013). There is concern that the pre-existing disruption in architecture with fibrosis and conditions causing hepatocyte death would be too harsh for transfused cells; the "rocky ground" (Forbes, 2008). Therefore this may also be the case in dogs with chronic hepatitis. There may however still be utility in veterinary medicine; dogs with acute hepatic failure may

benefit where a transient improvement in hepatic function via hepatocyte transfusion or stem cell derived hepatocytes may act as a "bridge" until sufficient endogenous hepatic regeneration has occurred.

The ability to provide liver support via an extracorporeal device populated with hepatocytes (Bioartifical liver device, BAL) is also another potential use for in-vitro canine hepatocytes (Leckie et al., 2012). The number of cells required for these devices is a potential stumbling-block (Chan et al., 2004). Again this is envisaged to be used as a bridge to transplantation in human medicine. In veterinary medicine, this could be used as a bridge in acute hepatic failure until sufficient hepatic regeneration has taken place, although again the expense and logistics of this producing the required cell numbers may be prohibitive.

There has also been much interest in the ability to correct hepatic metabolism disorders in man by transfusion of autologous stem cell derived hepatocytes which have undergone genetic correction e.g. α1-antitrypsin deficiency (Yusa et al., 2011). Many dog breeds have hepatic metabolic defects e.g. the Dalmatian and Cavalier King Charles Spaniel's defects in hepatic purine metabolism and the Bedlington Terrier's hepatic defect in copper transport (Forman et al., 2005; Gow et al., 2011; Safra et al., 2006). Hepatocyte transfusions have been used the Dalmatian as a human model for treatment of hepatic metabolic defects. Technically, this procedure is straightforward with the cells delivered intra-splenically although immunosuppression was required as these were allotransplants (Benedetti et al., 1997; Dunn et al., 2000). If autologous stem cells were utilised, immunosuppression would not be required. The expense and effort involved in correction of these genetic defects in individual dogs would be ethically difficult to defend as veterinary medicine has the luxury of genetic manipulation via breeding selection to which effort and money would be better put, for example testing of Bedlington Terriers for a mutation in the *COMMD1* gene which causes copper accumulation within hepatocytes and subsequent genetic selection of the future generation (Mellersh, 2012).

The most immediate reason for producing an *in vitro* source of canine hepatocytes is the ability to model hepatocyte functions *in vitro*, particularly with regard to drug metabolism. Drug development is expensive and many candidate drugs fail during toxicity testing (Kola, 2008). Preclinical studies on candidate drugs are usually performed on laboratory animals to assess pharmacodynamics, pharmacokinetics as well as possible toxicities. The hepatocyte plays a crucial role in metabolism of many drugs via three main phases: Phase I - oxidation via the cytochrome P450 monooxygenases, Phase II – conjugation of phase I products, Phase III – transport ofthe product out of the hepatocyte (Sevior et al., 2012). Pre-clinical testing may initially be in non-target species e.g. rodents to reduce cost. As different species have different CYP profiles, these studies may not always predict potential toxicities in the target species (Graham and Lake, 2008). The ability to utilise species specific *in vitro* hepatocytes to monitor candidate drug metabolic products and assess hepatotoxicity would have the potential to greatly reduce the expense of drug development and also the number of animals used in pre-clinical drug testing. Furthermore, if these cells were derived from an unlimited stem cell source then this would further reduce the number of animals required for testing. The most commonly used laboratory dog breed is the Beagle (Home Office, 2012). As stated earlier, many breeds have different CYP profiles therefore proof of safety in a limited number of breeds will not predict safety in all pedigrees. Some drugs fail at phase III clinical trials when they are used in a large group of individuals and drug induced liver injury is the most common reason that drugs are withdrawn from market (after phase III trials) (Kaplowitz 2007, Suzuki 2010). As an example of this, in the human medical field, between 1995-2005 13 drugs were withdrawn due to hepatotoxic effects which were not evident in phase I,II or III trials (Need et al., 2005). This has not only economic consequences of the costs of development to that point but also ethical consequences in that individuals receiving that drug may have been harmed (Dieppe et al., 2004; Kola, 2008). In veterinary medicine, canine pre-clinical data such as pharmacokinetics, pharmacodynamics and toxicology on new drugs which have been developed for human medicine but are being considered for

the canine veterinary market can be available as dogs are occasionally used as a human model in pre-clinical testing (Peters, 2005). Ironically, if better *in-vitro* human models are developed then this resource would reduce.

The ability to produce *in vitro* canine hepatocytes with species specific CYP profiles would allow rapid screening of candidate drugs for potential hepatotoxicity not only of the parent drug but also the hepatic metabolic products. This would greatly reduce the cost of drug development for the veterinary market but also contribute to reducing the number of animals required in pre-clinical testing in line with the aims of the National Centre for the Replacement, Refinement and Reduction of Animals in Research (http://www.nc3rs.org.uk/). Furthermore, the ability to screen different breed phenotypes *in vitro* would hopefully avoid idiosyncratic breed reactions once the drug has been licensed, reducing the number of drugs withdrawn from the market and also reducing canine patients harmed.

To be a useful model of drug metabolism *in vitro*, the cells should be able to perform fully as hepatocytes with functional and inducible drug metabolising pathways including CYP activity (Hengstler et al., 2005). Practically, one metabolic function and one synthetic function are commonly accepted as demonstrating a hepatocyte-like cell *in vitro* (Meier et al., 2013).

1.8 Sources of in-vitro hepatocytes

1.8.1 Primary liver tissue as a source of *in vitro* hepatocytes

As primary hepatocytes have tremendous capacity for replication *in vivo*, this would seem the obvious choice (Higgins and Anderson, 1931). Primary hepatocyte cultures can be readily derived from hepatic tissue via collagenase digestion (Berry and

Friend, 1969). In human medicine there is the same problem as for liver transplantation i.e. shortage of supply of healthy hepatic tissue. Disappointingly, despite primary hepatocyte isolation being described for over 40 years in many species, culture conditions that allow mature hepatocyte division *in vitro* have not been achieved and hepatocytes in culture do not multiply to any appreciable extent. Furthermore, the majority of functions that would be desired of a hepatocyte e.g. protein production, CYP activity are lost rapidly *in vitro* (Elaut et al., 2006). A final problem with primary hepatocyte cultures is batch variability depending on donor source and time between death and processing (Donato et al., 2013). Although production of *in vitro* canine primary hepatocytes would be less limited than in human medicine in the sense that dogs may be specifically bred for this purpose, the continual sacrifice of these animals would not be the ideal solution especially at a time when much effort is being directed towards the mantra of the 3 R's (replace, reduce, refine) in animal research.

1.8.2 Stem Cells as a source of hepatocytes

Stem cells may be broadly divided into two main types– adult determined stem cells and pluripotent stem cells. Adult determined stem cells may be further sub-divided into organ specific stem cells and mesenchymal stem cells.

1.8.3 Hepatic progenitor cells

Many organs of the body have multipotent rather than pluripotent stem cells i.e. can differentiate into all the cells of the organ from which they have been derived, for example, as stated above, HPC in the liver are bipotent, producing both hepatocytes and cholangiocytes. At present, no unique HPC marker has been identified, which hampers isolation and enrichment. HPC have been isolated from many species including humans, rodents and dogs (Arends et al., 2009b; Gerbal-Chaloin et al., 2010; Yovchev et al., 2008). It has been demonstrated that human and rodent HPC can be expanded *in vitro* with specialized media and differentiated into hepatocytes

(Li et al., 2013b; McClelland et al., 2008; Wauthier et al., 2008). Hepatic progenitor cells have been identified in normal and diseased canine liver and also cultured *in vitro* (Arends et al., 2009a; Schotanus et al., 2009). If these cells could be expanded sufficiently and differentiation directed to hepatocyte lineage, as has been done for rodents, these could be a useful source of canine hepatocytes *in vitro* (Chen et al., 2010).

1.8.4 Pluripotent stem cells

The first pluripotent stem cells identified were embryonic stem cells (ESC) and derived from the inner cell mass of mouse embryos (Evans and Kaufman, 1981). These cells are naturally pluripotent i.e. have the ability to differentiate into many cells types. ESC have now been described in the human, cat and dog (Gomez et al., 2010; Hatoya et al., 2006; Thomson et al., 1998). Since the first description of canine ESC by Hatoya et al.(2006), there have been three other reports (Hayes et al., 2008; Schneider et al., 2007; Vaags et al., 2009). There has at present been little further work detailing directed differentiation of these cells, suggesting that culture conditions allowing self-renewal may require optimization.

In 2006, differentiated cells which were induced to become pluripotent (induced pluripotent stem cells, iPSC) by the addition of four transcription factors (Oct3/4, Sox2, cMyc & Klf4) were described (Yamanaka 2006). These behaved in a similar manner to ESC in that that they appear to have limitless expansion potential. iPSC have now been described in a range of species, including human, pig, rat, dog and cat (Esteban et al., 2009; Shimada et al., 2010; Takahashi et al., 2007; Verma et al., 2012).

Both stem cell types are an attractive potential source of hepatocytes as their pluripotency and expansion ability offer the potential for a limitless supply of hepatocytes (Palakkan et al., 2013). There are concerns with using both ESC and iPSCs *in vivo* as teratoma formation is common with ESC implantation, and the

majority of iPSC have been produced using retroviral vectors and oncogenic transgenes which are integrated into the host cell's genome (Palakkan et al., 2013). This raises issues of mutations and tumour formation with this cell type also. Much progress has been made in production of iPSC's without genomic abnormalities or oncogenes and will be further discussed in Chapter 6. iPSC's have the advantage in that if they are derived from the patient requiring treatment, autologous therapy would not require immunosuppression although some studies have demonstrated an immune rejection response (Guha et al., 2013; Zhao et al., 2011). If these stem cell types are used as an *in vitro* source then this avoids the problem for tumour formation, although mutations may cause the resultant hepatocytes to behave differently to primary cells.

1.8.5 Mesenchymal stem cells

Cells termed mesenchymal stem cells (MSC) were first isolated more than 50 years ago from bone marrow (Friedenstein et al., 1966). These cells arise from the neural crest and mesoderm and have been shown to have the capacity to differentiate into any mesodermal lineage (e.g. bone, cartilage, fat and tendon) (Pittenger et al., 1999). Since then, it has been realized that these cells can be isolated from any vascularized tissue and that they are derived from pericytes (Crisan et al., 2011; Crisan et al., 2008), however the differentiation capacity does appear to vary dependent on source (Innes et al., 2013; Kern et al., 2006; Ock et al., 2012). There has been huge interest in MSC in regenerative medicine, due to their ease of isolation, simple cryopreservation and also the ability to differentiate into bone, cartilage and tendon. As a result, they have been used clinically to effect enhanced repair to these tissue (Steinert et al., 2012). Furthermore, MSC appear to have beneficial effects on tissues not of mesodermal origin including liver, kidney and lung (Tanimoto et al., 2013; Wang et al., 2013b; Xu et al., 2013). In-vitro, it has been shown that MSC can trans-differentiate into ectodermal and endodermal cell fates, albeit at low efficiencies e.g. hepatocytes and are a potential *in vitro* source of these cells (Dezawa et al., 2004;

Lee et al., 2004). There has been much debate as to the action and fate of MSC once transfused into non-mesenchymal organs. It appears that many of their apparent *in vivo* therapeutic effects are not due to their differentiation capacity but due to a paracrine effect and as a result their name has been modified to mesenchymal stromal cell and then medicinal signalling cells (Caplan, 2009; Horwitz et al., 2005; Parekkadan and Milwid, 2010; Parekkadan et al., 2007). The two most common tissues from which MSC's are isolated are the bone marrow and adipose tissue, although as stated above any tissue may potentially yield MSC's (Caplan and Bruder, 2001).

MSC do not appear to have the same expansion abilities as ESC and iPSC with many reporting senescence and reduced differentiation capacity at varying passage numbers which also appears species, site and donor dependent (Bernardo et al., 2007; Izadpanah et al., 2006; Kern et al., 2006). The advantage that MSC have is the ability to rapidly expand an individual's MSC from adipose or bone marrow for use therapeutically either as MSC's or after terminal differentiation, thus avoiding the need for immunosuppression.

1.9 Use of undifferentiated stem cells in liver disease

1.9.1 Bone marrow cells

There has been interest in the potential of bone marrow cells (BMCs) to promote hepatic regeneration since bone marrow cells were identified in human livers after both bone marrow transplantation and after partial hepatectomy or full transplantation (De Silvestro et al., 2004). In experimental rodent models of fibrosis, autologous BMCs injected into the tail vein improved fibrosis and stimulated regeneration (Sakaida et al., 2004). BMCs are an unselected population which contains both haematopoietic stem cells (HSC) and MSC. A further study showed that mice with fumarylacetoacetate hydrolase deficiency, a model of tyrosinemia type I a hepatocyte metabolic defect in humans, had restored hepatic

metabolic function after transfusion of haematopoietic stem cells (Lagasse et al., 2000). Subsequent work showed that this was due to fusion of monocytes with hepatocytes and that the high selection pressure of the experimental model meant that this was unlikely to be clinically useful (Willenbring et al., 2004). Clinical trials in human have been performed with autologous mononuclear bone marrow cells. Improved serum albumin concentrations, and clinical scoring was noted; however the number of subjects was small and no control groups were used (Terai et al., 2006). A further study involving 15 treated and 15 control patients demonstrated an improvement in liver function in the treated group that was maintained for 90 days (Lyra et al., 2010). HSC have been shown to differentiate into hepatocyte like cells *in vitro* and that as small percentage of these were found integrated into liver *in vivo* after transfusion (Khurana and Mukhopadhyay, 2008)

1.9.2 Mesenchymal stem cells

There is debate as to whether BM-MSC's promote liver repair by differentiation to hepatocytes, producing growth factors or via an immune-modulatory route to reduce immune-mediated damage (Zhang et al., 2012). Recent work has shown that BM-MSC's appear to possess potent anti-inflammatory properties, exhibiting an inhibitory effect on T and B cell, dendritic and natural killer cell proliferation (Asari et al., 2009; Sato et al., 2007; Spaggiari et al., 2009; Spaggiari et al., 2006). Experimentally, BM-MSC have been shown to reduce hepatic fibrosis in NOD-SCID mice, however other studies have shown that MSC can potentiate fibrosis by becoming myofibroblasts (Baertschiger et al., 2009; Forbes et al., 2004; Tanimoto et al., 2013). In human clinical studies, MSC have been shown to improve patients with steroid resistant graft versus host and also decreased rejection rate, risk of postoperative infection and increased renal function of transplanted kidneys (Le Blanc et al., 2008; Le Blanc et al., 2004; Tan et al., 2012). Experimental studies have demonstrated that both BM and adipose-derived mesenchymal stem cells (AD-MSC) rescued immunodeficient mice with acute liver failure (Banas et al., 2008; Kuo et al., 2008). As of November 2014, 362 human clinical trials using MSC's are registered

with the National Institute of Health's www.clinicaltrials.gov website, treating diverse diseases including multiple sclerosis, dilated cardiomyopathy, ulcerative colitis and chronic renal failure. Twenty-nine studies are listed for liver disease, 23 for cirrhosis. Seven of these trials have completed and been published (Meier et al., 2013). Six of these used autologous BM-MSC and one allogeneic umbilical cord derived MSC's. In two studies hepatocyte differentiation *in vitro* was performed. The majority of the studies involved small numbers of patients (5 studies involved <20 patients). Although the studies differed in patient selection and route of delivery, the majority of patients exhibited no negative effects and only minor side-effects were noted. The results of these studies have been summarised as suggesting "that autologous MSC infusion allows mild biological improvements in patients with liver diseases, but clear and significant clinical benefit was not yet reported" (Meier et al., 2013). Interestingly the one study which used both undifferentiated and hepatocyte differentiated MSC noted no difference in efficacy between the two (El-Ansary et al., 2012). Criticisms include: no investigation of histological improvements, poor characterisation of the MSC, poor experiment power and lack of control groups (Meier et al., 2013). One small study (of 11 humans) has since been published which assessed histology after MSC transfusion and noted improvement, however this study lacked a control group (Jang et al., 2013). Potential risks of MSC treatment that have been raised are genetic mutations during *in vitro* expansion and spontaneous malignant transformation (Miura et al., 2006; Zhou et al., 2006). Finally, there is evidence that MSC can stimulate tumour growth of occult tumours or pre-cancerous lesions (Bian et al., 2010; Karnoub et al., 2007; Kucerova et al., 2010). This is of concern in human medicine where chronic hepatitis predisposes to hepatocellular carcinoma (HCC) development therefore the very patients that would be receiving MSC treatment would have high risk of pre-cancerous or cancerous lesions (Moradpour and Blum, 2005). Despite chronic hepatitis being common in the dog, HCC occurrence is infrequent therefore this risk may be of lesser consequence in the dog (Charles et al., 2006).

As stated earlier in the chapter, chronic hepatitis is common idiopathic inflammatory in the dog resulting in fibrosis and cirrhosis, the mainstay of treatment consists of immunosuppression with prednisolone. Despite treatment, prognosis is poor. With the increasing evidence of an immune-modulatory effect of MSC there is the potential to study the effect of MSC transfusion on the course of disease in the dog. It has been stated that there is a lack of large animal models of fibrosis for translational research to human medicine. The dog with naturally occurring hepatic fibrosis may make a useful model to inform human medicine (Meier et al., 2013).

1.10 Aims of Thesis

The aim of this project was to produce an *in vitro* source of canine hepatocytes from stem cell sources. To facilitate this, primary canine hepatocytes were cultured and used as a gold-standard to allow development and optimisation of methods to assess hepatocyte characteristics and function. As many of the function of canine primary hepatocytes were lost rapidly *in vitro*, methods of maintaining function by utilising CYP inducers and culture substrates were also assessed.

The project isolated adult hepatic stem cells, also known as hepatic progenitor cells as well as canine AD-MSC and BM-MSC. The MSC's were characterised using criteria developed by the International Society for Cellular Therapy (Dominici et al., 2006). A number of methods shown to be effective in other species were used to differentiate canine MSC's towards hepatocyte-like cells.

Finally, primary hepatocytes and canine keratinocytes were transfected with a plasmid containing the Yamanaka factors (Oct3/4, Sox2, cMyc & Klf4) to induce pluripotency. Canine iPSC's were differentiated according to published protocols in other species and hepatocyte phenotype assessed using the previously optimised tests.

Chapter 2: Materials and Methods

2.1 Tissue culture plastic coating

Tissue culture plates were coated with agents to improve cell attachment when required.

2.1.1 Collagen type I

Tissue culture plates were coated with 0.05mg/ml collagen type I. This solution was made by addition of 1 part 5mg/ml bovine collagen type I (Gibco) to 99 parts phosphate buffered saline (PBS). Sufficient was added to completely cover the base of the vessel and the plates incubated at 37^{o}C overnight. The solution was then aspirated and plates rinsed with PBS before drying and storing at 4^{o}C for up to 1 week.

2.1.2 Laminin

Laminin (Sigma-Aldrich) was thawed on ice slowly and diluted to 50µg/ml with Hank's balanced salt solution (HBSS, Invitrogen). A volume of 2.4mls was added to each well of a 6 well plate and incubated at 37^{o}C for 2 hours. The remaining solution was aspirated and the plate washed with HBSS.

2.1.3 Gelatin

A 0.1%w/v gelatine solution was prepared by dissolving 0.5g of Gelatine type A (Sigma-Aldrich) in 500mls of distilled water. This was then autoclaved and cooled. Sufficient solution was added to plates to cover the base. Plates were then incubated at room temperature for 10 minutes before the solution aspirated and plates washed with PBS.

2.2 Cell counting

Cells were suspended in a known volume of medium and 20µl of suspension added to an equal volume of Trypan blue (Sigma-Aldrich). The solution was loaded onto a haemocytometer (Menzel-Glaser, Germany) and cells counted. The result was

multiplied by two to give a starting cell concentration. Positively stained Trypan blue cells were non-viable.

2.3 RNA extraction and quantification

The RNeasy mini kit (Qiagen, UK) was used according to the manufacturer's instructions. Cell pellets were disrupted in 350µl of lysis buffer using a Qiashredder (Qiagen, UK). DNA digestion was performed using DNase I (Qiagen, UK) at the recommended point in the RNA extraction protocol. Total RNA was quantified and purity checked using absorbance spectrophotometry at 260 and 289nm (Nanodrop 1000, Thermo, UK).

2.4 Reverse transcription

RNA was converted to cDNA using the Omniscript reverse transcription kit (Qiagen, UK) according to the manufacturer's instructions using random nanomers (Sigma-Aldrich, UK) and RNase inhibitor (Promega, UK). One µg of RNA was added per reaction.

2.5 Primer design and preparation

Where available, previously published primers were checked using NCBI Primer-blast. For primer design, the NCBI nucleotide database was used. Primers spanning an intron were designed if possible. All primers were ordered from MWG Eurofins, diluted to 100 pmol/µL with nuclease-free water and stored at -20 °C.

2.6 Real-time polymerase chain reaction (qPCR)

The Platinum Sybr Green Qpcr Kit (Invitrogen, UK) was used in all qPCR reactions. The master mix is outlined in Table 2.1. Reactions were performed on the Stratagene MX3000P (Agilent, UK). For primer optimisation, cDNA from freshly isolated canine hepatocytes was diluted in ten-fold steps to 100,000 and 9.5µl of this added to each well. Primer efficiency, and dissociation curve calculated using MXPro software (Agilent, UK), specificity was assessed by agarose gel electrophoresis. Relative gene expression was performed using cDNA, diluted 1:20 and 9.5µl of this added to each well. Each reaction was performed in triplicate and three no template controls were also included for each primer using 9.5 µl of nuclease-free water.

Reference genes are specified in the specific chapters. Data were analysed using Microsoft Office Excel 2003 program using the method described by Pfaffl (2001) to calculate relative gene expression.

Component	Volume (µl per reaction)
SYBR Green mix	12.5
Forward primers	1.25
Reverse primers	1.25
Rox	0.5
TOTAL	15.5

Table 2.1 qPCR master mix

Reaction conditions are were 2 minutes at 50^{o}C, 2 minutes at 95^{o}C, then 40 cycles of 95^{o}C x 15secs and 60^{o}C x 30secs. The final cycle was 95^{o}C for 1 minute then cooling to 60^{o}C before monitoring for dissociation to 95^{o}C. The dissociation curve produced and lack of amplification of the no template controls were checked using MXPro Software (Agilent, UK).

2.7 Agarose gel and product analysis

PCR products were run on a 2% agarose gel. This was prepared by melting 2g of agarose (Sigma, UK) in100 mL of 1 x Tris Acetate EDTA (TAE, Gibco, UK). A volume of 10 µL Gel Red 10,000X (Biotium) was added to the 100 mL melted agarose and the agarose was poured into a setting tray with inserted comb and allowed to set at room temperature. A volume of 12 µL of PCR product was added to 4 µL of 6 X Blue/Orange Loading Dye (Promega, UK). This was loaded into the cell. A 100 base pair ladder (Promega, UK) was used to assess product size. A Bio-Rad transformer was used to create 80V differential. Gels were run for approximately 2 hours and then visualized using a BioRad Molecular Imager GelDoc.

2.8 1,1'-dioctadecyl-3,3,3'3'-tetramethylindocarbocyanine perchlorate-LDL (DiI-LDL) and 1,1'-dioctadecyl-3,3,3'3'-tetramethylindocarbocyanine perchlorate - acetylated-LDL uptake

DiI-LDL and acetylated DiI-LDL (both Invitrogen, UK) were diluted to 20µg/ml in appropriate culture medium and added to cell culture wells for 3 hours. Wells were then washed with phosphate-buffered saline (PBS) three times and fixed with 4% paraformaldehyde for 30 minutes. The cells were washed with PBS three times and 4',6-diamidino-2-phenylindole (DAPI) at a concentration of 200ng/ml for 30 minutes added. The slides were then washed with phosphate buffered saline with 0.1% Tween (Sigma) (PBST) and examined using fluorescent microscopy. No LDL controls were also performed.

2.9 Immunofluorescence assay for LDL receptor

Mesenchymal cells were cultured in four chambered slides (BD Biosciences) until they were approximately 50% confluent. Canine primary hepatocytes were cultured on collagen type I coated plastic at a seeding density of $1x10^5/cm^2$. Medium was removed, the cells washed with PBS and then fixed with 4% paraformaldehyde for 30 minutes. The cells were washed with PBS three times, permeabilised with 100% ethanol for 5 minutes before repeating the wash step. Blocking buffer (PBS containing 10% goat serum (Invitrogen) and 0.1% Tween 20 (Sigma) was added for 1 hour at room temperature. This was then aspirated and rabbit anti-human LDL receptor antibody with known cross-reactivity with the dog (ABIN672111, antibodies-online) was diluted to 1:500 with PBS containing 1% goat serum, 0.1% Tween added. This was then incubated at 4^oC overnight and then washed three times in PBST. Fluorescently tagged goat anti-rabbit secondary antibody (Alexa Fluor 594 goat anti-rabbit IgG, Life Technologies), diluted 1:1000 in PBS containing 1% goat serum and 0.1% Tween was added and incubated at room temperature in the dark for 1 hour. Slides were then rinsed three times with PBST and the 4', 6-diamidino-2-phenylindole (DAPI) added at a concentration of 200ng/ml for 30 minutes. The slides were then washed with PBST and examined using fluorescent microscopy

(Zeiss, Aviovert 40) and Zeiss Aviovision 4.7 software. Secondary only and no antibody controls were also indluded for each cell type and antibody.

2.10 Cytochrome P45 activity and Cyp induction

The Promega PFBE-Luciferase assay was used to assess Cyp activity. Cells cultured in a 96 well plate were used. Experiments were performed in triplicate and no cell control wells were measured and this value subtracted from the sample wells. For Cyp induction, phenobarbital and rifampicin (both Sigma-Aldrich, UK) were used. Phenobarbital was diluted in medium to a stock 200mM solution and rifampicin to 20mM. Drugs were added to a final concentration of 250µM and 25µM respectively for 72 hours as well as a basal no drug control before the wells were rinsed with PBS and 60µl of PFBE-Luciferase added to the wells in appropriate medium at a 1:40 dilution. Cells were then incubated at 37^{o}C and 5% CO_2 for 3 hours. A volume of 25µL of supernatant was added to a white 96 well plate in duplicate from each well. This was then mixed with 25µl of the detection buffer for 20 minutes before luminescence was read using a plate reader (Victor3, Perkin Elmer, USA).

2.11 3-(4,5-dimethylthiazol-2-yl)-2,5-diphenyltetrazolium bromide (MTT) assay

5mg/ml) of MTT (Sigma Aldrich M5655) stock solution diluted in appropriate cell culture medium well to achieve a final concentration of 1mg/ml and 50µl incubated at 37^{o}C for 3 hours. The MTT solution was removed and tetrazolium salt solubilised with 100µl of solubilisation agent (0.1M HCL, 10% Triton x -100 and isopropanol) added. The plates were then placed on an orbital shaker at 100rpm for 10 minutes before being read at 570nm in a plate reader (Victor3, Perkin Elmer, USA). No cell control wells were used to measure background and this value was removed from the sample values.

A chapter-specific materials and methods section is included in each chapter.

Chapter 3: Establishment and characterisation of primary canine hepatocyte cultures

3.1 Abstract

In preparation of experiments to differentiate canine stem cells to hepatocyte-like cells it was necessary to optimise and validate qualitative and quantitative tests that would be anticipated to be useful and also provide a positive control to which hepatocyte-like cells could be compared.

In this chapter the tests that are often performed on stem cell-derived hepatocyte-like cells are discussed followed by the description of the isolation and culture of canine primary hepatocytes from ischaemic tissue as a positive control. Quantitative and qualitative tests were validated using these cells. A panel of primers for genes expressed by hepatocytes was validated along with a canine-specific ELISA for albumin, DiI-LDL and DiI-Ac-LDL uptake, Luciferase-based cytochrome activity test and periodic acid-Schiff staining for glycogen. Indocyanine green uptake was found not to occur in viable canine primary hepatocyte cultures and appeared to stain only dead hepatocytes.

The ability of rifampicin and phenobarbital to induce cytochrome activity was assessed along with changes in gene expression and albumin secretion in primary hepatocyte cultures over time. The effect of Matrigel on *in vitro* function over time was examined. Although a Matrigel overlay improved cell attachment, no consistent improvement in gene expression or albumin production was demonstrated.

3.2 Introduction

Primary hepatocyte cultures are still considered to be the gold standard for *in vitro* toxicological testing (Fraczek et al., 2013; Kia et al., 2013). Isolation of primary hepatocytes was first described by Berry and Friend (1969) and subsequently modified by Selgen (1976). These protocols involve a two-step collagenase digestion of the surrounding matrix to dissociate the hepatocytes, producing a cell suspension. Hepatocytes are fragile cells and this process causes oxidation as well as loss of surrounding cells and extracellular matrix (Wang et al., 1998). The resultant isolated hepatocytes are plated onto a rigid substrate, commonly type I collagen (Pichard et al., 2006). This results in a "2D" or monolayer culture system in which the cells undergo dramatic changes in morphology and polarity, becoming polygonal and similar to epithelial cells in culture (Dunn et al., 1989). These factors all contribute to a reduction in gene expression and hepatocyte-specific functions which is termed de-differentiation. This is reported to remain the greatest barrier to *in vitro* drug toxicity testing (Soldatow et al., 2013). As stated in Chapter 1, hepatocytes can be defined by a range of functions and genes expressed. One of the crucial functions for drug toxicity testing is maintenance of cytochrome P450 expression and activity, in primary hepatocytes these are lost rapidly *in vitro*, stated to be within the first 24-48 hour of culture (Knobeloch et al., 2012; Soldatow et al., 2013). There appear to be species differences in the rapidity of this de-differentiation process with Nelson et al. (2013) reporting that porcine hepatocytes retained function for longer than human hepatocytes. In comparison of rat, human and canine hepatocytes in 2D culture, total cytochrome content declined most rapidly in the rat; 50% with the first 24-48 to 23% after 48 hours. Canine P450 content was stable for 24 hours then reduced to 50% at 48 hours whereas human were stable for 48 hours and reduced to 20% at 72 hours (Ubeaud et al., 2001). Ditewig et al. (2013) reported canine primary hepatocytes exhibited a 1000-fold decrease in *CYP* expression after 120 hours in culture. Maintenance of CYP function appears also highly culture condition dependent (Nelson et al., 2013). Utilising a sandwich method of culturing hepatocytes with a Matrigel overlay has been shown to improve constitutive and induced *CYP* gene expression in human and rodent primary hepatocytes (Gross-Steinmeyer et al., 2005; Sellaro et al., 2010; Sidhu et al., 1993). However, this has also been shown to be

species specific leading Olsavsky Goyak et al. (2010) to conclude that "considering species specific responses to *in vitro* conditions, a thorough evaluation of any primary hepatocyte culture system is warranted to secure confidence in its use."

3.2.1 Methods of assessing hepatocyte phenotype and function

As hepatocytes are functionally highly complex cells, there are arrays of tests of phenotype and function that can be used to demonstrate differentiation to a hepatocyte-like cell. Figure 3.1 gives a summary of commonly used characteristics that have been used to demonstrate hepatocyte-like properties during directed stem cell differentiation.

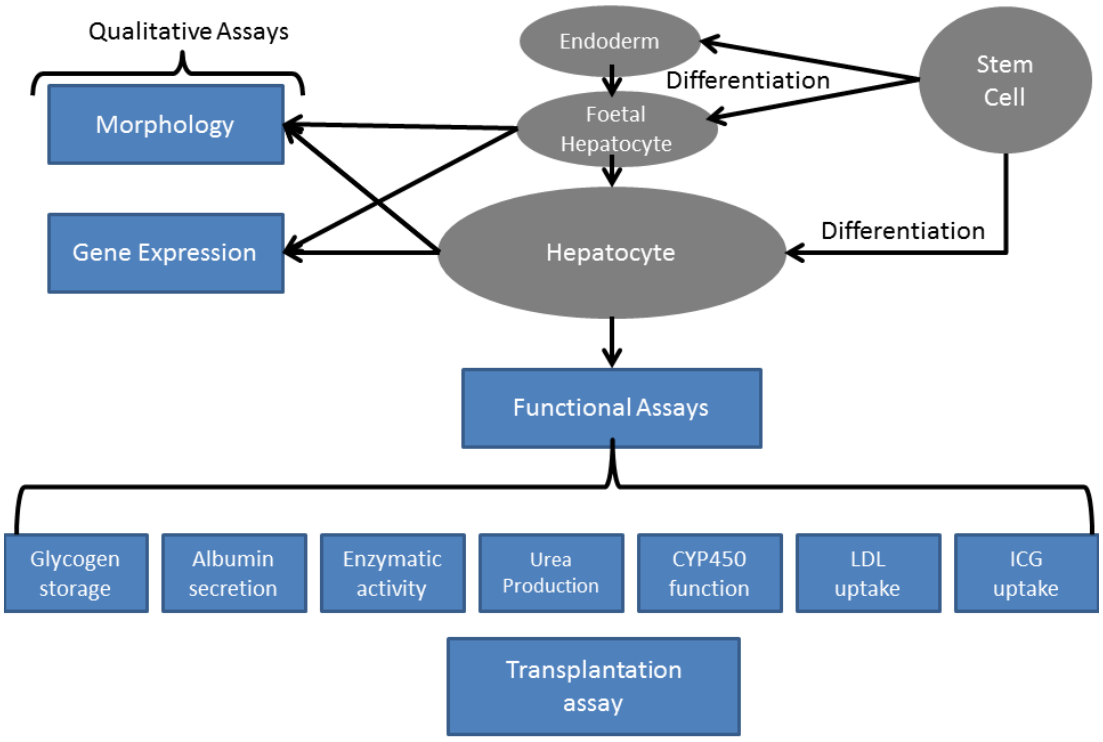

Figure 3.1 Summary of commonly used qualitative and functional characteristics that are used to define hepatocyte-like cells.
LDL – Low-density lipoprotein, ICG – Indocyanine green. Modified from Zhang et al. (2013c).

3.2.2 Morphology

Mature hepatocytes in 2D culture systems assume a polygonal shape, are often binucleate, with a large cytoplasm to nucleus ratio and intracytoplasmic granules which may be lipid or glycogen. Refractive borders between cells in the form of bile caniliculi may be present (Figure 3.2) (Nelson et al., 2013; Sancho-Bru et al., 2009).

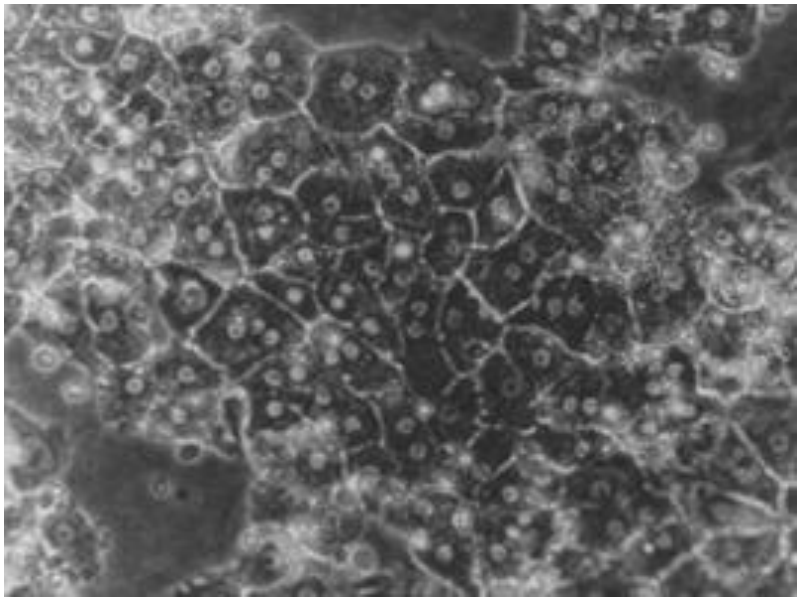

Figure 3.2 Porcine primary hepatocyte morphology on collagen type I.
Primary hepatocytes in 2D culture exhibiting high cytoplasm to nuclear ratio, sharp demarcation between borders and many binucleate cells. From Wang et al. (2004).

3.2.3 Gene expression

There are panels of genes that are generally accepted as representing stages of differentiation, although few genes are specific. Table 3.1 lists genes expressed at different stages of hepatocyte differentiation.

Cell Type	Markers
Definitive endoderm	Hex, Mixl1, Cxcr4, Tm4sf2, Gsc, Sox17, E-cadherin; not Sox7
Hepatic stem cell	OV6, Albumin, Keratin 8,18,7,19, c-kit, CD34
Hepatoblast	α1-antitrypsin, α-foetal protein, Albumin, Keratin 8,18 , Transthyretin
Mature hepatocyte	α1-antitrypsin, Albumin, ApoAII, ApoF, CEBP, Keratin 8,18, Cytochrome P450 enzymes, Hepatocyte nuclear factor 3b, 4a,6 Glucose 6-phosphate, liver-specific organic anion transporter-1, phosphoenolpyruvate carboxykinase, Tyrosine aminotransferase, tryptophan-2,3-dioxygenase, Transferrin, Transthyretin

Table 3.1 Gene expression markers used to assess hepatocyte-like cells.
Modified from Zhang et al. 2012 and Sancho-Bru et al. 2009.

3.2.4 Indocyanine green uptake

Indocyanine green (ICG) is a cyanine fluorescent dye which has been used intravenously as a test of liver function as it is extracted by hepatocytes and excreted in bile (Cherrick et al., 1960). It is commonly used as a test of hepatocyte-like cells *in vitro* whereby a positive result is defined as uptake after incubation with ICG and subsequent secretion of the compound when cells are placed in fresh medium. The first report of ICG use *in vitro* is by Watanabe et al. (1976) who stated that human oval cells vitally stained with ICG. For hepatocyte-like cell differentiation of stem cells, Yamada et al. (2002) described ICG positive cells in embroid bodies which expressed liver specific genes such as albumin and transthyretin. The first description of ICG uptake and subsequent secretion was demonstrating hepatocyte-like differentiation of human umbilical cord cells (Wang et al., 2005). These two papers incubated cells at 1mg/ml for 15 minutes. Other authors have used the same concentrations for 60-90 minutes (Agarwal et al., 2008; Hay et al., 2007). Neutrophils and reticulocytes have been shown to take up ICG; it is therefore not hepatocyte-specific (Wei et al., 2003).

3.2.5 Albumin secretion

Albumin is the main plasma protein in circulation and responsible for controlling blood volume by providing oncotic pressure as well as acting as a carrier for many hydrophobic compounds, such as steroid hormones. Hepatocytes are the chief source of albumin and therefore gene expression and secretion is often used to demonstrate a hepatocyte-like state (Fanali et al., 2012; Hengstler et al., 2005). Albumin gene expression has however also been documented in adipose tissue, bone, kidney, mammary gland as well as T cells and pancreatic and hepatic stellate cells, suggesting that albumin gene expression is not specific for a hepatocyte-like state (Kim et al., 2009; Mor and Cohen, 2013; Nahon et al., 1988; Shamay et al., 2005; Sirico et al., 2012; Yamaguchi et al., 2003; Yoo et al., 2010). It is unknown whether these extra-hepatic sources of gene expression can synthesise albumin.

3.2.6 Low density lipoprotein (LDL) uptake

LDL is a transport molecule for lipids, including cholesterol and triglycerides, in extracellular fluid. Specific LDL receptors on the cells membrane bind LDL and allow endocytosis. *In vivo*, most LDL receptors are present on hepatocytes to supply cholesterol for bile secretion, conversion to bile acids and production of *de novo* lipoproteins (Goldstein and Brown, 1987). Harada-Shiba et al. (2004) demonstrated that cultures of wild-type murine primary hepatocytes avidly took up fluorescently labelled LDL; however, hepatocytes from LDL receptor knock-out mice failed to do so. As a result, demonstration of LDL uptake is commonly used as a test of hepatocyte like cells. Commercially, two types of fluorescently tagged LDL are available, native LDL and acetylated LDL (AcLDL), a synthetic analogue of naturally occurring oxidised LDL. Acetylated LDL (and oxidised LDL) is not recognised by the LDL receptor but is taken up by scavenging receptors, present chiefly on macrophages and endothelial cells (Horiuchi et al., 2003). Oxidised LDL is responsible for endothelial dysfunction leading to atherosclerosis (Li and Mehta, 2005). Nahhmias et al. (2006) showed that human and rat primary hepatocytes took up LDL but not AcLDL and as stated above, Harada-Shiba et al. (2004)

demonstrated that LDL uptake is receptor-dependent on hepatocytes. Despite this apparent clear-cut division, in the field of stem cell differentiation to hepatocyte-like cells there appears to be confusion. There is variation in whether LDL or AcLDL is used, with many papers describing LDL use in the abstract yet stating use of AcLDL in the materials. Table 3.2 documents recent papers using a form of LDL as a test of hepatocyte-like cells and which compound is listed in the abstract and in materials and methods.

Study	Abstract	Materials & Methods
Prasajak and Leeanansaksiri, 2013	LDL	AcLDL
Vosough et al., 2013	Ac-LDL	Ac-LDL
Asgari et al., 2013	LDL	Ac-LDL
Cao et al., 2012	Not Stated	LDL
Takayama et al., 2012	LDL	LDL
Pournasr et al., 2011	LDL	Ac-LDL
Huang et al., 2011	Not stated	Ac-LDL
Ouyang et al., 2010	LDL	Ac-LDL
Si-Tayeb et al., 2010	LDL	LDL

Table 3.2 Papers detailing stem cell to hepatocyte differentiation and type of LDL used.
Detailing type of LDL documented in abstract and materials and methods in paper. LDL- low-density lipoprotein, Ac-LDL – acetylated low-density lipoprotein.

3.2.7 Urea production

Hepatocytes are responsible for the detoxification of ammonia. In peri-portal hepatocytes this occurs via the urea cycle whereby the net effect is that one molecule of urea and water is produced from two of ammonia and one carbon dioxide. In peri-venous hepatocytes, ammonia is utilised in the reaction of glutamate to glutamine (Kuntz and Kuntz, 2009). The synthesis and increase in supernatant urea concentration *in vitro* is commonly used to demonstrate hepatocyte-like activity (Zhang et al., 2013c).

3.2.8 Cytochrome P450 activity

One of the main advantages of developing canine *in vitro* hepatocytes would be the ability to model drug metabolism. The CypP450 enzyme system is the most important component of hepatocyte drug metabolism and, as a result, demonstration of CYP is an important characteristic. As genes may be expressed but non-functional, gene expression of *CYP* is insufficient (Sancho-Bru et al., 2009). Demonstration of CYP activity may be either by the use of commercially available kits which a results in colour change, fluorescence or luminescence (such as pentoxyresorufin dealkylation to resorufin by CYP2 subfamily), or by measurement of the products of drug metabolism such as hydroxylation of testosterone via testosterone 6β-hydroxylase activity of CYP3A12 (Abass et al., 2012; Graham et al., 2006; Lubet et al., 1985). One testing method commonly used during stem cell differentiation to hepatocyte-like cells adds luciferin-pentafluorobenzylether (Luciferin-PFBE) from which luciferin (a fluorescent compound) is dissociated by CYP3A4 and subsequently measured using luminometry (Cao et al., 2012; Shiraki et al., 2011; Sullivan et al., 2010). CYP activity can be induced *in vivo* and *in vitro* by certain drugs. Common compounds used are dexamethasone, rifampicin and phenobarbital. Dexamethasone is reported to be ineffective in causing CYP induction in the dog, causing a decrease in CYP3A enzymes (Zhang et al., 2006). Both rifampicin and phenobarbital are known to induce CYP3A12 and CYP3A26 in the Beagle, with phenobarbital also inducing CYP2C21 and CYP2B11. See Table 1.1 for known induction activity on human and canine CYP enzymes (Trepanier, 2006).

3.2.9 Transplantation assay

These are a crucial test for hepatocyte-like cells whose final purpose is to be used *in vivo*. Tests that have been recommended include, rescue of liver/metabolic failure models, such as the FAH mouse, a model of fumarylacetoacetase deficiency, leading to tyrosinaemia, progressive liver/renal dysfunction and neurological abnormalities (Sancho-Bru et al., 2009).

3.3 Aims

The aims were to assess if canine primary hepatocytes could be isolated from ischaemic liver. This *in vitro* source of hepatocytes would then be used to validate methods which would be used in testing stem cell derived hepatocyte-cells as well as providing a gold-standard against which these hepatocyte-like cells can be compared. Finally, the effect of different culture substrates on primary hepatocytes will be examined as this may impact on functionality of stem-cell derived hepatocytes.

3.4 Materials and Methods

3.4.1 Primary hepatocyte isolation

Dogs euthanased for a reason unrelated to the study were used. Liver tissue was acquired within 20 minutes of euthanasia. A wedge of hepatic tissue with one cut surface and intact Glisson's capsule was sectioned (between 20-100g). This was placed in William's Medium E (Invitrogen, UK) and transported to the laboratory on ice. The tissue was rinsed with Hank's balanced salt solution (HBSS, Invitrogen, UK), placed in a Petri dish and 20-22g plastic catheters (Vygon, UK) inserted into the vessels on the cut surface. Chelating buffer (Appendix 1) at 37^{o}C was perfused at approximately 6mls/minute using a 20ml syringe (BD, UK) for 15 minutes. HBSS was then perfused at the same rate for 10 minutes. Finally collagenase buffer (Appendix 1) was perfused for between 30-45 minutes until the tissue appeared spongy and digested. The tissue was moved to a fresh Petri dish and 25mls of William's medium E with 10% FCS and 100 U/mL penicillin G and 100 µg/mL streptomycin (all Invitrogen, UK) at 37^{o}C added. The liver capsule was then torn and the tissue gently agitated to release dissociated hepatocytes. The cell suspension was filtered through a 70µ cell strainer (BD, UK). The remaining liver tissue was rinsed with a further 25mls of medium and this suspension also filtered. The resultant 50ml suspension was centrifuged at 50g for 3 minutes to pellet mature hepatocytes. The supernatant was removed, the pellet re-suspended and centrifugation repeated.

3.4.2 Plating density of hepatocytes

Hepatocytes were plated at a density of 1 x10^5/cm^2 in William's media E with 10% FCS and 100 U/mL penicillin G and 100 µg/mL streptomycin (all Invitrogen, UK) on collagen-coated wells. After 3 hours to allow attachment, the wells were gently rinsed with PBS at 37^{o}C before Hepatocyte culture medium (Lonza, UK) was added.

3.4.3 Matrigel overlay

Matrigel (BD, UK) was thawed overnight on ice at 4^{o}C. A 0.25mg/ml dilution using cold HCM was prepared and then warmed to room temperature. After hepatocytes had attached and had been rinsed with PBS, this solution was added to the wells; 2ml per 6 well, 1ml in 12 well and 0.1ml in 96 well. These were then incubated overnight and solution gently aspirated and HCM used.

3.4.4 Albumin ELISA optimisation

The ELISA kit (Dog albumin ELISA kit, Immunology Consultants Laboratory, Inc., Texas) was labelled as specific for canine albumin for use with serum, plasma and urine. Recommended dilutions for serum were 1:20,000 and urine 1:1000. Therefore to assess dilution required for culture media supernatant and also any cross reaction with bovine albumin in the media, optimisation was required. A volume of 100µl of HCM was added to each well of a 96 well plate. Media from canine primary hepatocytes in the first 24 hours of culture was used as this would be expected to yield the highest concentrations of albumin. Media which had not been exposed to cells was included as a negative control. These were serially diluted 1:10 to give concentrations: neat, 1:10, 1:100, 1:1000, 1:10,000 and 1:100,000. The kit was used according to the manufacturer's instructions and the plate read using a Victor3 plate reader (Perkin Elmer, USA).

3.4.5 Albumin measurement

100µl of culture media was added to each well of a 96 well plate containing the cells of interest. After 24 hours this was removed and albumin concentration measured as above. Experiments were performed in triplicate and concentration in supernatant measured in duplicate. Culture media was added to blank wells to give background readings. This result was subtracted from the results.

3.4.6 Indocyanine green uptake

Indocyanine green (MP Biomedicals, UK) was diluted to 5mg/ml in DMSO (Sigma-Aldrich, UK). This stock was diluted in the appropriate culture medium to a final working concentration of 1mg/ml and cells incubated in this solution for 30 minutes at 37^{o}C and 5%CO_2. Wells were then washed three times in PBS, culture media replaced and cells imaged.

3.5 Results

3.5.1 Canine primary hepatocytes can be isolated from ischaemic liver

A total of 23 primary canine hepatocyte isolations and cultures were undertaken. Cell viability ranged from 10-92% (Appendix 2). Initial viability was poor but generally improved to >75% after the first 9 isolations, which is described as being acceptable for hepatocyte culture experiments (Knobeloch et al., 2012). Total cell yield varied markedly, again tending to increase with number of perfusions performed, ranging from 1.3 x10^3-2.4 x 10^8. It is likely that this was due to a combination of amount of liver perfused, age of dog, amount of fibrous tissue present in the liver, time and uniformity of perfusion.

3.5.2 Canine primary hepatocytes can be cultured *in vitro*

After 24 hours, large polygonal cells, which were often binucleate with a high cytoplasm to nucleus ratio, were attached to the collagen-coated wells (Figure 3.3). Refractive borders were present between cells consistent with bile caniliculi. These cells maintained their morphology for approximately 7-10 days before changing

morphology, gradually detaching and/or being replaced by colonies of smaller cells of a similar morphology or outgrowths of fibroblastic cells.

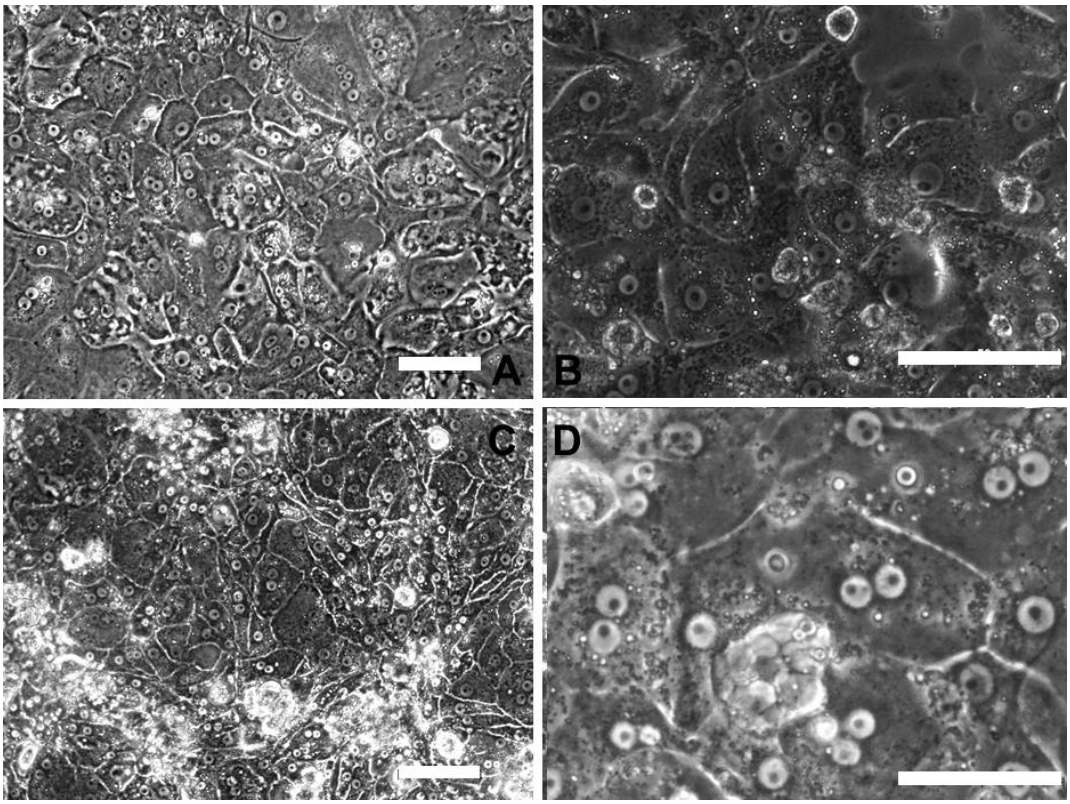

Figure 3.3 Morphology of canine primary hepatocyte cultures
Canine primary hepatocytes were seeded at a density of 1 x 10^5/cm^2 on type I collagen in William's media E containing 10% foetal calf serum. After 4 hours to allow attachment, media was replaced with serum-free hepatocyte culture media. Cells were imaged after 24 hours culture. A & B show hepatocytes from a 3 year old, entire male Rottweiler and C & D from 2 year entire male Mastiff. White bar represents 100µm.

3.5.3 Viable canine hepatocytes do not accumulate indocyanine green

Primary hepatocytes were assessed for ICG uptake after between 1-3 days in culture. Uptake appeared patchy with the majority of hepatocytes showing no uptake and dead cells/cell debris on the top of the mono-layer staining (Figure 3.4A). Cells around the periphery, which were less confluent took up the stain most readily with small contiguous areas also staining heavily (Figure 3.4B, C). Addition of ICG to hepatocytes which had been briefly exposed to 70% ethanol for 5 seconds before

washing with PBS and replacing culture media produced uniform uptake (Figure 3.4D). Scratch assay damaged hepatocytes also demonstrated strong uptake compared to undamaged cells (Figure 3.4E). Finally, culture of hepatocytes in media containing MTT after exposure to ICG demonstrated no purple granule formation in cells stained with ICG (Figure 3.4F). This lack of overlap between tetrazolium production and ICG staining of the hepatocytes indicated that cells which were stained with ICG had poor viability.

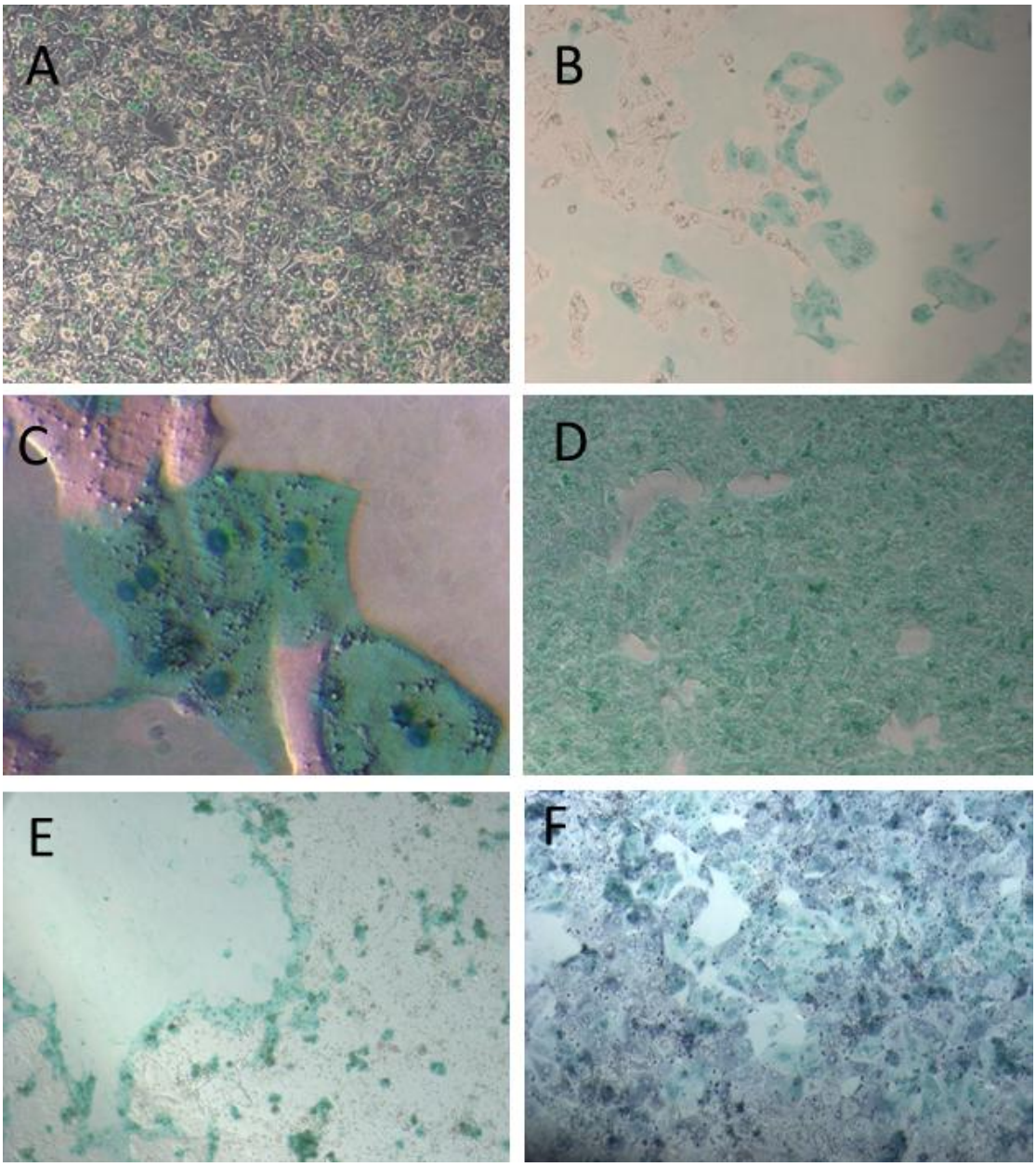

Figure 3.4 Indocyanine green (ICG) uptake by canine primary hepatocytes
A,B,C - Canine primary hepatocytes were cultured in media containing 1mg/ml indocyanine for 30 minutes, media aspirated, cells washed three times with PBS, fresh media replaced and cells photographed. D – Hepatocytes were washed for 5 seconds with 70% ethanol before rinsing in PBS prior to ICG incubation. E- Scratch assay, cell monolayer was disrupted by drawing a 20µl pipette tip through it prior to ICG incubation. F – After ICG incubation and washing, cells were then incubated in 1mg/ml MTT for 2 hours before washing three times in PBS. All images x100 apart from C x400. These images were representative from 3 primary hepatocyte cultures.

3.5.4 Canine hepatocytes stain with Periodic acid Schiff

Canine primary hepatocytes demonstrated strong PAS staining between days 1-3; this became less pronounced in prolonged culture. Figure 3.5A shows PAS staining of canine primary hepatocytes after 24 hours' culture, demonstrating intense pink staining consistent with the presence of intra-cytoplasmic glycogen. Figure 3.5B shows PAS staining of hepatocytes after 6 days in culture. Patchy, weak staining of cells is seen, consistent with loss of glycogen during culture.

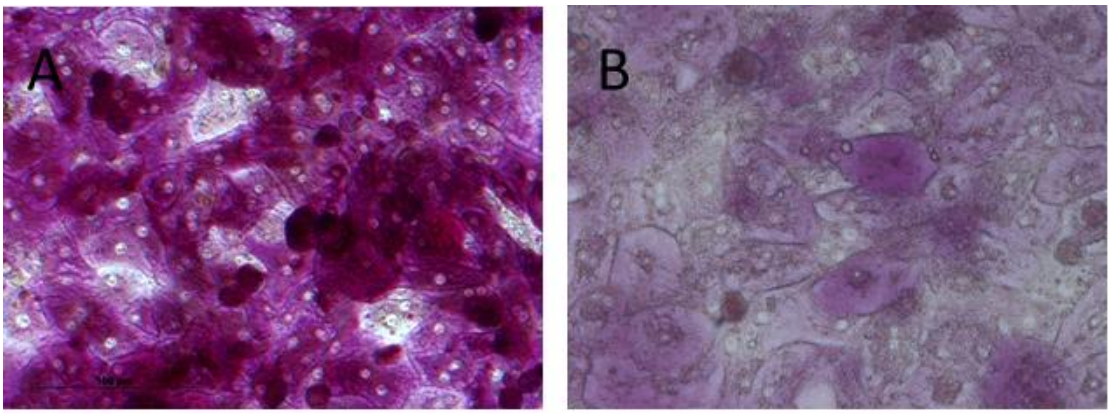

Figure 3.5 Periodic acid-Schiff staining of canine primary hepatocytes.
Canine primary hepatocytes were cultured on type I collagen in HCM, washed with PBS and fixed in 4% paraformaldehyde for 30 minutes. Cells were then stained with periodic acid-Schiff and photographed. A – D17913 hepatocytes after 1 day culture. B –Canine hepatocytes after 6 days culture (From dog ID- D17913). Images x 200. These images were representative of 3 primary hepatocyte cultures.

3.5.5 Primer optimisation of hepatocyte gene expression

Primers were optimised and efficiency calculated using cDNA from D10513 day 0 canine primary hepatocytes. Primers which had acceptable efficiency, dissociation curve and band size on gel electrophoresis were: β2 microglobulin, hypoxanthine guanine phosphoribosyl transferase, ribosomal protein L8, αfoetal protein, albumin, keratin 7, keratin 18, transthyretin, low-density lipoprotein receptor, glycogen synthase, α1-antitrypsin, *CYP1A2*, *CYP2B11*, *CYP2C18*,*CYP2D15*,*CYP3A12* and *CYP3A26*. Table 3.3 shows primers, sequence, calculated efficiencies, quality of dissociation curve and gel size of product.

Gene	Sequence	Product size (bp)	Efficiency %	TM ^{o}C (forward/reverse)	Dissociation curve	Gel size
HPRT	F– TTATGGACAGGACTGAGCGG R - TTGAGCACAGAGGGCTAC	82	98.3	59.18/56.23	√	√
B2MG	F– TCCTCATCC TCCTCGCT R - TTCTCTGCTGGGTGTCG	85	96.7	55.97/56.03	√	√
RPL8	F – CCATGAATCCTGTGGAGC R - GTAGAGGGTTTGCCGAT	64	96.6	55.07/53.2	√	√
Albumin	F – GTTCCTGGGCACGTTTTTGTA R- GCTTCATATTCCTTGGCGAGTCT	92	97.4	60.94/62.78	√	√
Keratin 18	F – TTGCTACCTACCGTCGCCTGT TGG R - ATCTTGCGGGTGGTGGTCTTC TGG	109	98	58.33/58.33	√	√
Keratin 19	F– GCCCAGCTGAGCGATGTG C R -TGCTCCAGCCGTGACTTGATGT	86	321	64.29/64.47	X	√
Trans-thyretin	F – CGCTGGACTGGTACTTGTGT R -TCGGACAGCGTCTAGGACTT	91	93.9	59.4/60.32	√	√
α1-antitrypsin	F– AAGAGATACGCCAGGTCTGC R- TGCTCAGGACGCTTTTCAGA	82	96.1	59.54/59.61	√	√
Glycogen synthase	F – AGGCTCTCCGATCTTCTGGA R - CTTCGGTCGTTGGTGGTGAT	127	96.6	59.74/60.32	√	√
HNF4	F – GAG ATG TTG CTG GGA GGG TCC R- CAC TCA CAC ATC TGT CCA TTGC	146	77.3	62.46/59.84	X	√
LDL-Receptor	F– ATTGTGGTGGATCCCGTGC R - GAAAGATCCAGGGTGATGCCATT	149	105	60.38/60.94	√	√
αfoetal protein	F- GCTGCTCCGCCATCCATCC R- GGGGTGCCTTCTTGCTATCTCA	123	61	63.48/62.07	X	
αfoetal protein	F – ACCCCACCTGAGCTGATGGC R- TAAGATCAGCCGCTCCCTCGC	112	72.5	64.39/64.31	X	

αfoetal protein	F- CTG AAA ACC CTC TTG AAT GCC A R - TTT CTG GAA GAG GCC ACA GCT	104	98.2	59.11/61.67	√	√
αfoetal protein	F – TAG AAA ACC AGC TCC CTG CC R - CTG CAG CAA TCT GCA AGT CC	85	73.7	59.67/59.83	√	√
CYP1A2	F – ACCATCCCCCACAGCACAACAAA R - GCTCTGGCCGGAATGCAAATGGAT	140	101	65.87/66.12	√	√
CYP2B11	F – CTGCCCATCTTGGGGAACTT R- CCGTATGGCGTCTATCCCAC	147	61.6	59.96/60.04	√	
CYP2B11	F - TGCGGAAAACTGAGGGAGTC R- CGCAGGAACTCAGGGTCTTT	121	96.8	59.97/59.96	√	√
CYP2B11	F – AAAGGCTTATGGCCACCTCC R- TCTTGGAGCCTGAGGAAGGA	108	74.3	60.03/59.88		
CYP2C18	F– TGGACCATACAGGGATTAGGAAT R- TCCGCAAAACTGTCAGGGAA	85	91.9	58.42/59.82	√	√
CYP2D15	F – TGGTGTCCACCTCAATCACG R- GGGTCTGGTCTCCCATCTCT	135	98.3	59.97/60.03	√	√
CYP3A12	F – GGCTATTTGGAAAGAAAGTTACTG R- AGTCCACTCGGTGCTTTTGT	97	91.3	57.79/59.82	√	√
CYP3A26	F – AGAAACACAGATCTCCCTGAGAA R- CCTTAGGAAAGTCAGGCTCCA	117	90	58.84/59.09	√	√
Keratin 7	F– GCG TGG GAGCCGTGAACATC R- CCG CCGCCGCTGGAGAA	112	99.4	64.04/65.36	√	√
TAT	F – TGCTCTGTCTATTGGCGACC R- CGAGTCCAGGGCATCTTTCA	88	127	59.82/59.72		

Table 3.3 Primers tested for efficiency and specificity using cDNA from canine primary hepatocytes
Primers assessed for specificity by dissociation curve and gel electrophoresis. Efficiency of between 90-105% was deemed acceptable. Primers in grey were not utilised as efficiency was unacceptable. HPRT - Hypoxanthine-guanine phosphoribosyltransferase, B2MG - β2 microglobulin, RPL8 – ribosomal protein L8, TAT - tyrosine aminotransferase, HNF4 – hepatocyte nuclear factor 4.

3.5.6 The albumin ELISA kit is specific for canine albumin in hepatocyte supernatant

Media unexposed to canine hepatocytes gave near identical readings to the 0 standard, demonstrating no detection of bovine albumin or cross-reaction with other substances in the medium. Of the 10-fold dilutions of supernatant which had been exposed to canine primary hepatocytes for 24 hours, the 1:100 and 1:1000 dilutions produced an optical density that lay within the standard curve (Table 3.4). The 1:1000 sample produced an OD which was within the values obtained by the standards but towards the lower range. Dilutions of 1:100 were selected for use in subsequent experiments as it was expected that albumin concentrations would decrease over time and that stem cell derived hepatocyte-like cells would have less albumin production than primary hepatocytes. This dilution would allow lower values to remain on the standard curve. Therefore the canine specific ELISA would be a useful test of albumin production in hepatocyte-like cells and the antibody did not cross-react with bovine albumin which is in the culture medium.

Albumin standard (ng/ml)	Optical density (450nm)	Dilution of supernatant	Optical density (450nm)
0	0.064	0	3.316
12.5	0.233	1:10	3.018
25	0.424	1:100	1.667
50	0.766	1:1000	0.301
100	1.352	1:10,000	0.091
200	2.112	1:100,000	0.078
400	2.763	Control media	0.069

Table 3.4 Optimisation of cell culture supernatant in canine albumin ELISA
Canine albumin standards were prepared according to manufacturer's directions. Cell media which had been incubated with freshly isolated canine primary hepatocytes for 24 hours was used as test media along with media which had not been exposed to cells as a negative control. Test media was diluted in ten-fold steps. Optical density of the plate was read at 450nm. Shading on the right hand side table indicates dilutions which fell within the optical density of the standards.

3.5.7 Canine hepatocytes take up LDL but not Ac-LDL

Canine primary hepatocytes from dogs D21113, D17513 and D19713 were used. In each experiment, the negative control demonstrated very mild auto-fluorescence: the majority of cells strongly took up native DiI-LDL and only a few cells strongly took up DiI-Ac-LDL (Figure 3.6). Canine primary hepatocytes appear to endocytose LDL strongly but not Ac-LDL. This would suggest that this occurs by specific LDL-receptor transport rather than scavenging receptors. The cells which strongly

endocytose Ac-LDL in the hepatocyte culture are most likely either macrophages (Kupffer cells if resident in the liver), or endothelial cells, as contaminants. From these results, when assessing differentiation of stem cells to hepatocyte-like cells, at least in the canine species, LDL and not Ac-LDL should be used. This is consistent with the literature describing the LDL receptor which is present on hepatocytes as specific for native LDL and not oxidised or acetylated LDL.

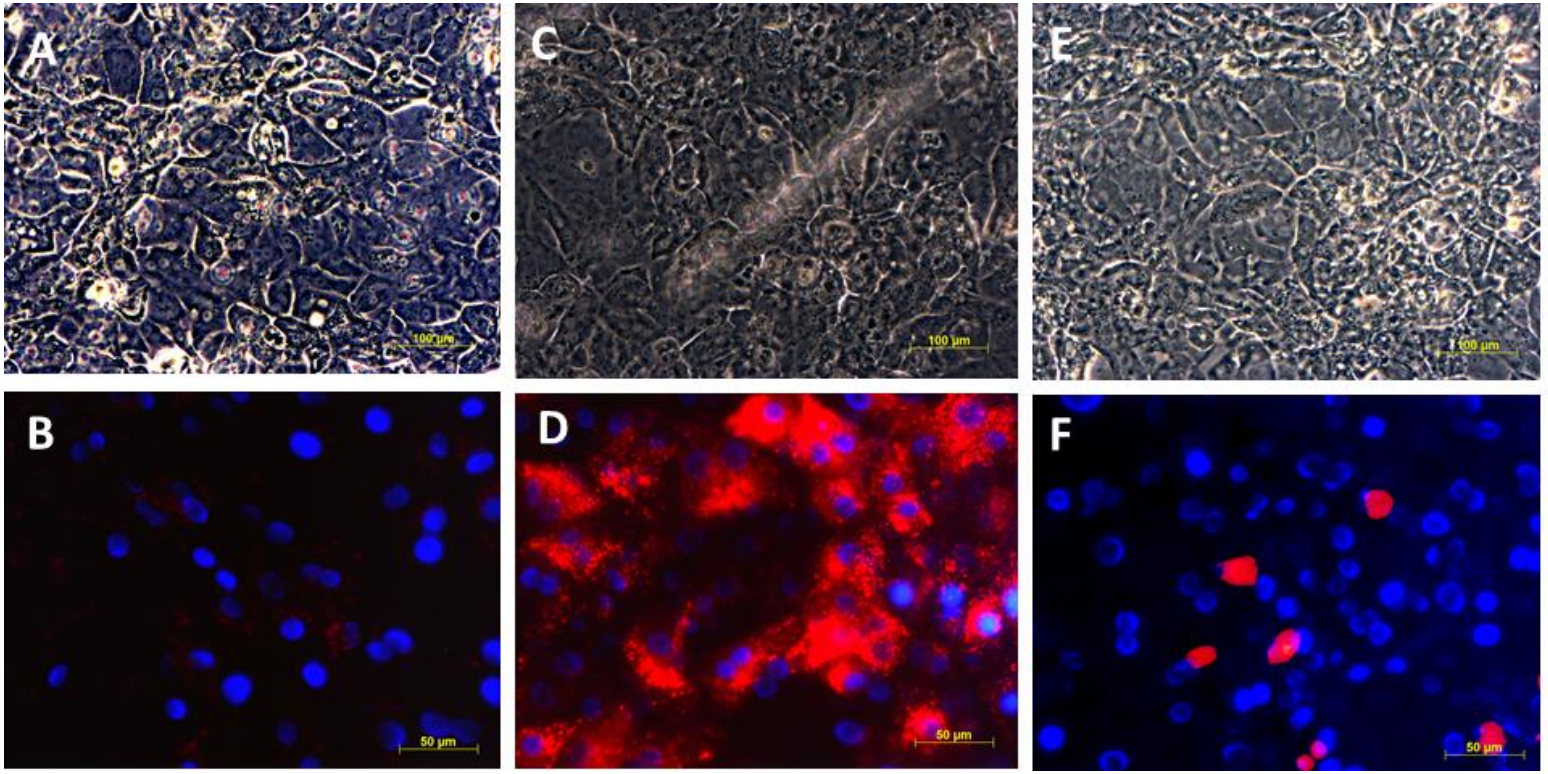

Figure 3.6 LDL and AcLDL uptake of primary hepatocyte cultures
A, C, E – Phase contrast images of primary hepatocytes x 10
B, D, F – x 20, DAPI as nuclear stain. B - negative control demonstrating low auto-fluorescence of hepatocytes, D – Hepatocytes incubated with 20µg/ml DiI-LDL for 3 hours demonstrating almost uniform LDL uptake. F – Hepatocytes incubated with 20µg/ml DiI-AcLDL for 3 hours. A minority of cells fluoresce with Ac-LDL strongly with the majority of the hepatocytes remaining negative. These images are representative of three primary hepatocyte cultures.

3.5.8 *In vitro* canine primary hepatocytes lose phenotype over time

To assess how rapidly hepatocyte-specific gene expression decreased *in vitro*, cell pellets were collected daily from day 0-6 for gene expression. Primary hepatocytes from dogs 17513, 19713 and 41013 were used in these experiments.

For all *CYP* genes examined there was a dramatic decrease over 48 hours, with greatest expression in freshly isolated hepatocytes (Figure 3.7).

Albumin gene expression also reduced dramatically during the 6 days in culture (Figure 3.8). Although transthyretin and glycogen synthase decreased from hepatocyte isolation to the first 24 hours in culture, they remained stably expressed for the remaining culture period (Figure 3.8). α1-Antitrypsin increased in the first 24 hours culture in 17513 and 41013 but not 19713 and then reduced to remain stable and a similar order of magnitude as fresh hepatocytes (Figure 3.8). LDL receptor expression increased slightly in D41013, remained stable in D19713 for the 6 day period and stable for the first 3 days in D17513 before decreasing slightly (Figure 3.8). Keratin 7 and 18 increased after 24 hours culture and remained increased compared to primary hepatocytes during the 6 days in culture (Figure 3.9).

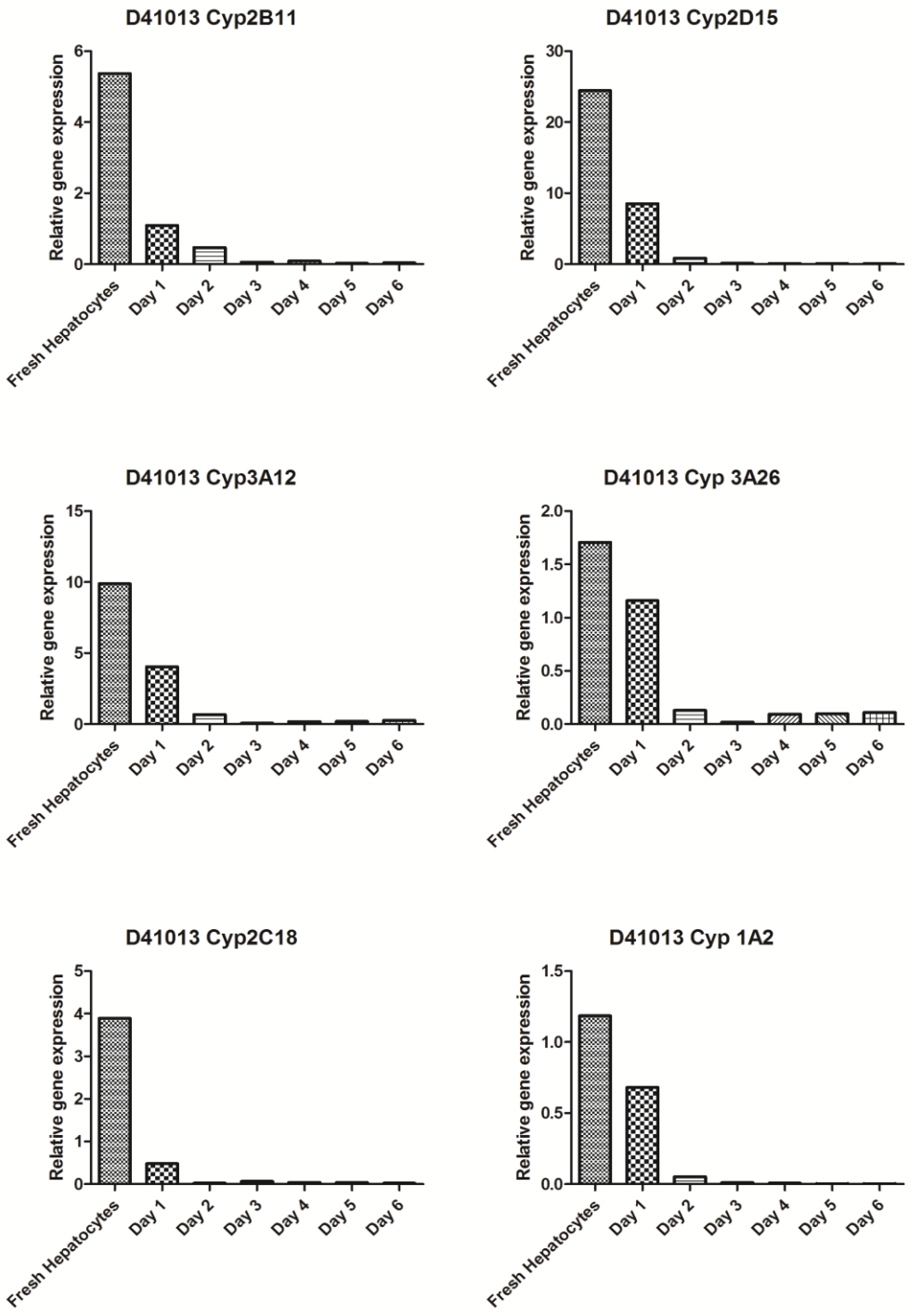

Figure 3.7 Relative gene expression of canine specific CYP in D41013 canine primary hepatocytes over time.
Reactions were performed in triplicate and genes of interest were normalised to three reference genes. Experiment was performed in triplicate with hepatocytes D17513, D19713 also used.

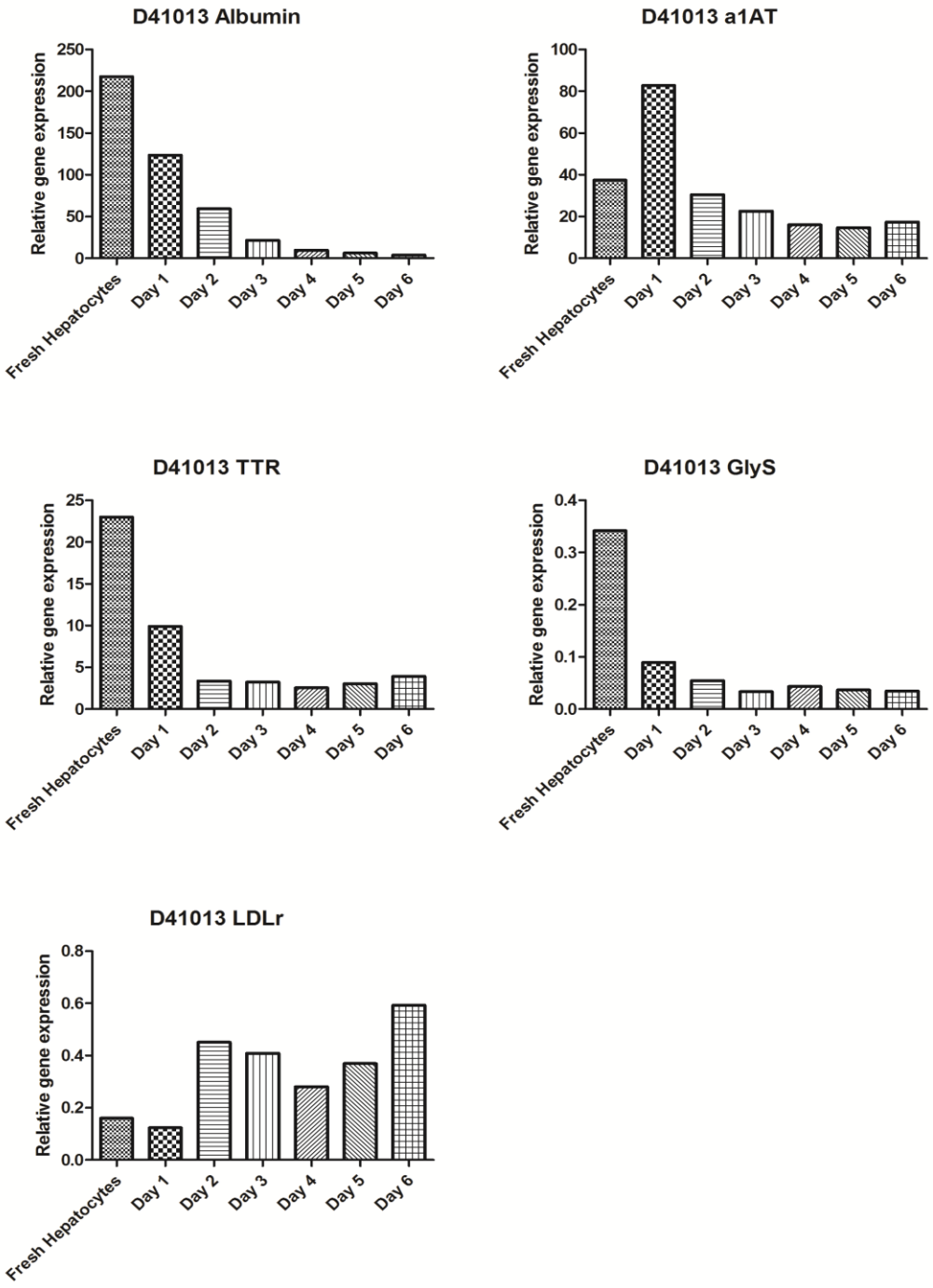

Figure 3.8 Relative gene expression of albumin (ALB), α1-antitrypsin (a1AT), transthyretin (TTR), glycogen synthase (GlyS) and low-density lipoprotein receptor (LDLr) in canine primary hepatocytes over time.
Reactions were performed in triplicate and genes of interest were normalised to three reference genes. Experiment was performed in triplicate with hepatocytes D17513, D19713 also used.

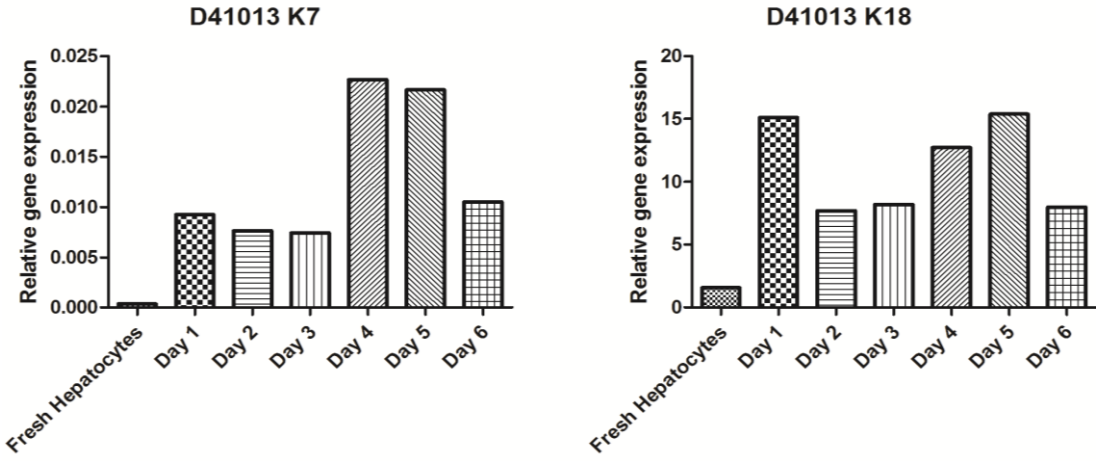

Figure 3.9 Relative gene expression of keratin 7 (K7) and keratin 18 (K18) in canine primary hepatocytes over time.
Reactions were performed in triplicate and genes of interest were normalised to three reference genes. Experiment was performed in triplicate with hepatocytes D17513, D19713 also used.

3.5.9 Rifampicin and phenobarbital induces *CYP* gene expression in canine hepatocytes

Induction of cytochrome P450 enzymes by drugs is one important factor in drug-drug interactions and alterations in pharmacokinetics. In production of canine hepatocyte-like cells for *in vitro* drug metabolism studies, this ability would be a prerequisite (Tsuchiya et al., 2012). Therefore this experiment was performed to assess the ability to induce *CYP* gene expression in the gold standard of primary canine hepatocytes and then provide a positive control during testing of possible hepatocyte-like cells derived from stem cell sources. Drugs which are commonly used *in vitro* to induce CYP activity are rifampicin (an antibiotic), dexamethasone and phenobarbital. Additionally, these drugs are used to boost the metabolic activity of cultured hepatocytes (Fraczek et al., 2013). As dexamethasone is not reported to cause CYP induction in the dog, rifampicin and phenobarbital were used (Zhang et al., 2006). D19713 primary hepatocytes were cultured with rifampicin and phenobarbital for 72 hour before qPCR gene expression of *CYP*, and fold increase compared to unexposed controls was calculated (Figure 3.10 & Figure 3.11).

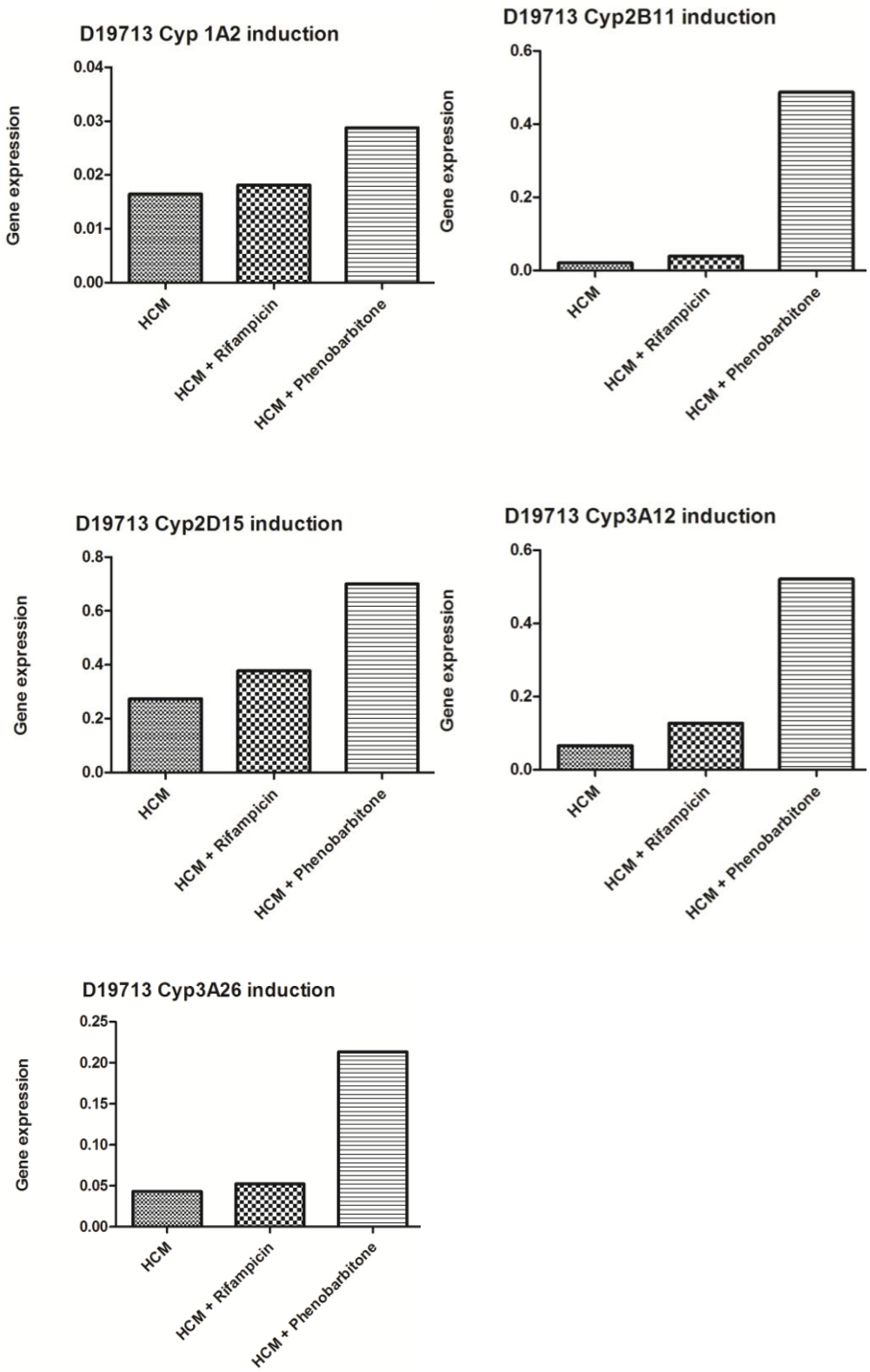

Figure 3.10 CYP gene expression of canine primary hepatocytes after 72 hours exposure to control medium(HCM), 25µM rifampicin and 250 µM phenobarbitone.Relative expression of selected *CYP* genes. Gene expression was normalised to three reference genes.

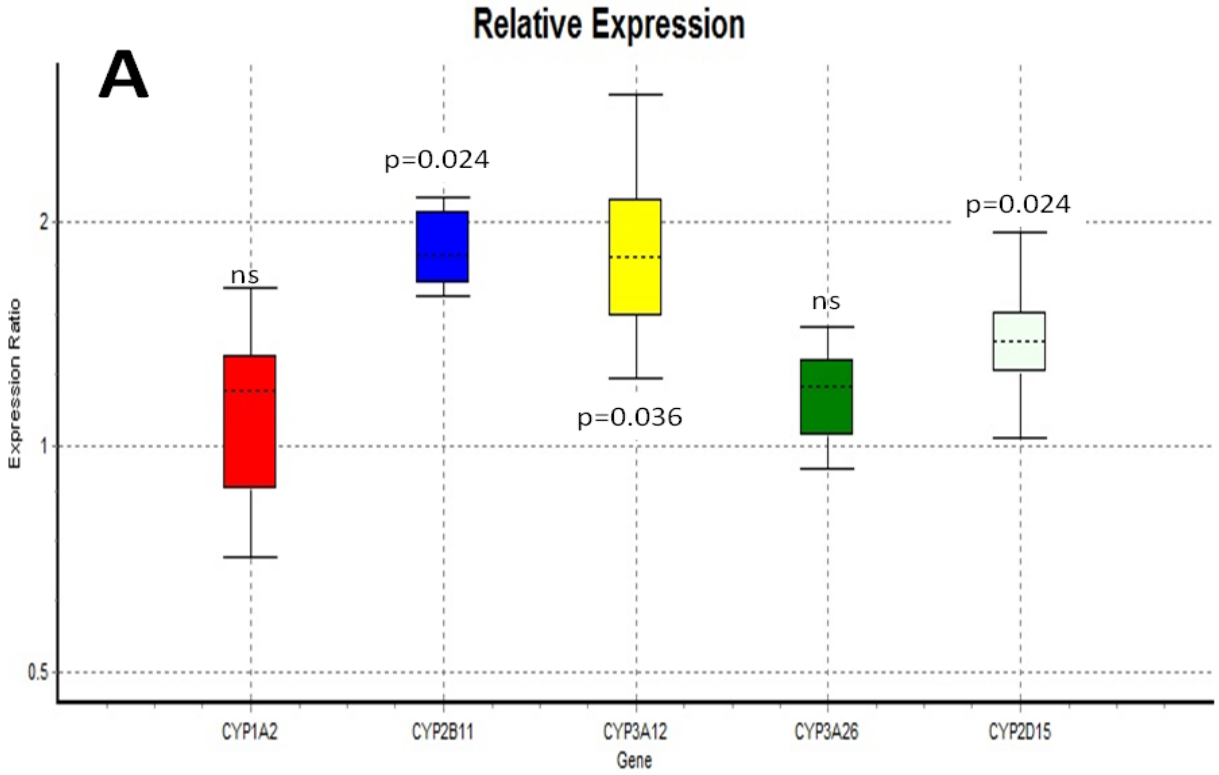
Relative Expression
A
p=0.024
p=0.024
ns
ns
p=0.036
2
1
0.5
Expression Ratio
CYP1A2
CYP2B11
CYP3A12
CYP3A26
CYP2D15
Gene

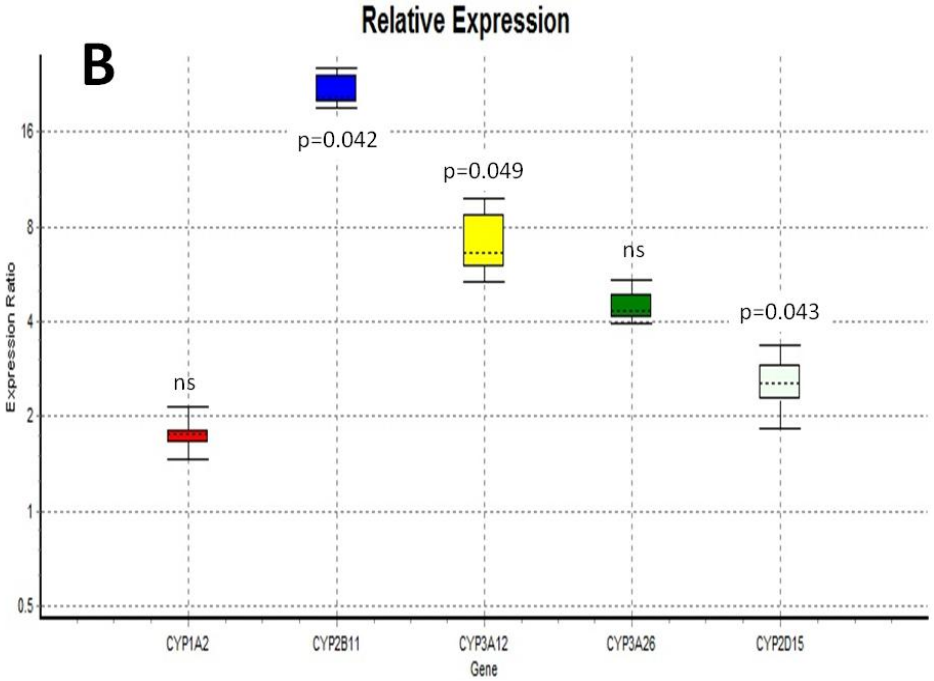

Figure 3.11 Fold increase of CYP gene expression after 72 hours of induction with A- 25µM rifampicin and B- 250µM phenobarbital.

Primary hepatocytes 19713 were used. Fold increase was calculated using the Pfaffl method after normalising to three reference genes (Pfaffl, 2001). Boxes represent the interquartile range, or the middle 50% of observations. The dotted line represents the median gene expression. Whiskers represent the minimum and maximum observations. Expression ratios were tested for significance by a pair wise fixed reallocation randomisation test. A – With rifampicin *CYP3A12*, *CYP2B11* and *CYP2D15* were significantly up-regulated (p=0.036, 0.024 and 0.024 respectively). With phenobarbital, *CYP3A12*, *CYP2B11* and *CYP2D15* were significantly up-regulated (p= 0.049, 0.042 and 0.043 respectively).

3.5.10 Rifampicin and phenobarbital do not significantly increase *CYP* activity as measured by cleaving PFBE-Luciferin

Various methods of assessing CYP activity *in vitro* have been used for primary hepatocyte cultures and also hepatocyte-like cells derived from stem cell sources (Asgari et al., 2013). A luciferase assay system suitable for use with intact cell monolayers was used in this case (Promega P450-Glo Assay Luciferin-PFBE). To allow for variation in cell number, the results were normalised against the optical density of the MTT cell viability assay. The results from 24 hours and 72 hours culture of canine primary hepatocytes with control media, rifampicin and phenobarbital are shown in Figure 3.12. No significant difference was detected after 24 hours' culture. Although values were higher than basal after 72 hours' culture with rifampicin and phenobarbital, this was not statistically significant. Activity was significantly lower in the 72 hour sample compared to the 24 hour sample in both basal and rifampicin treated cells. This reduction is consistent with the reduction in *CYP* gene expression noted between 24 and 72 hours.

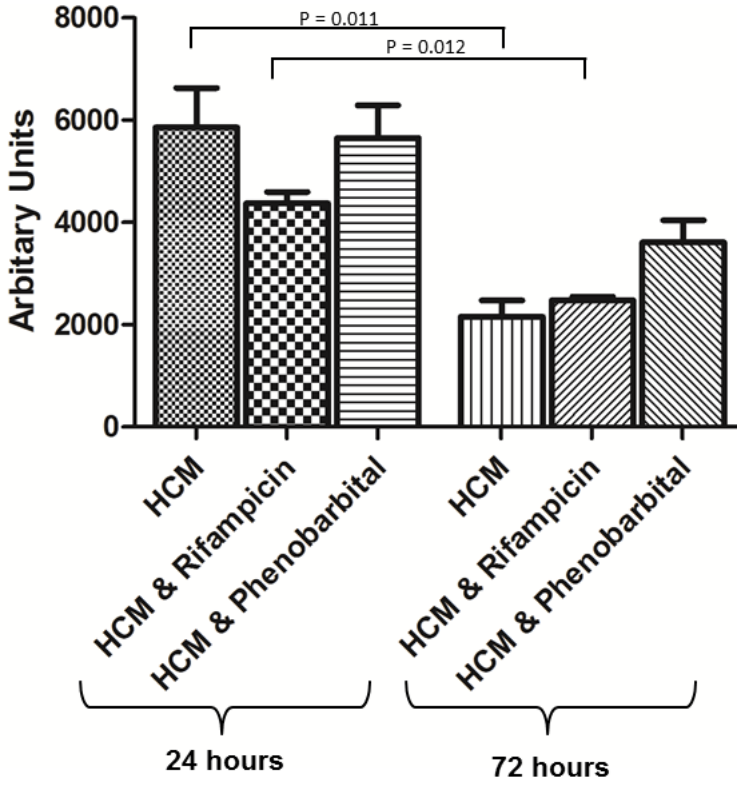

Figure 3.12 CYP activity of canine primary hepatocytes at 24 hours and 72 hours culture.
CYP activity was measured using Promega Pro-Glo Luciferase-PFBE which was added to culture media for 3 hours. The medium removed, detection buffer added and luminescence measured using a luminometer. MTT was used to assess cell viability. Luminescence was then divided by optical density to normalise for variation in cell number. There was a significant decrease in activity between the HCM 24 and 72 hours and also the rifampicin 24 and 72 hours. HCM - hepatocyte culture medium, basal activity. Rifampicin added at 25µM, phenobarbital at 250µM.

3.5.11 Albumin production of primary hepatocytes reduces over time

Albumin concentration of the supernatant was performed using D17513 and D41013. Consistent with the dramatic reduction in albumin gene expression previously noted, concentration reduced dramatically with a statistically significant difference over the first 24 hours (p=0.0128) and by approximately 50% between day 1 and 3 (Figure 3.13).

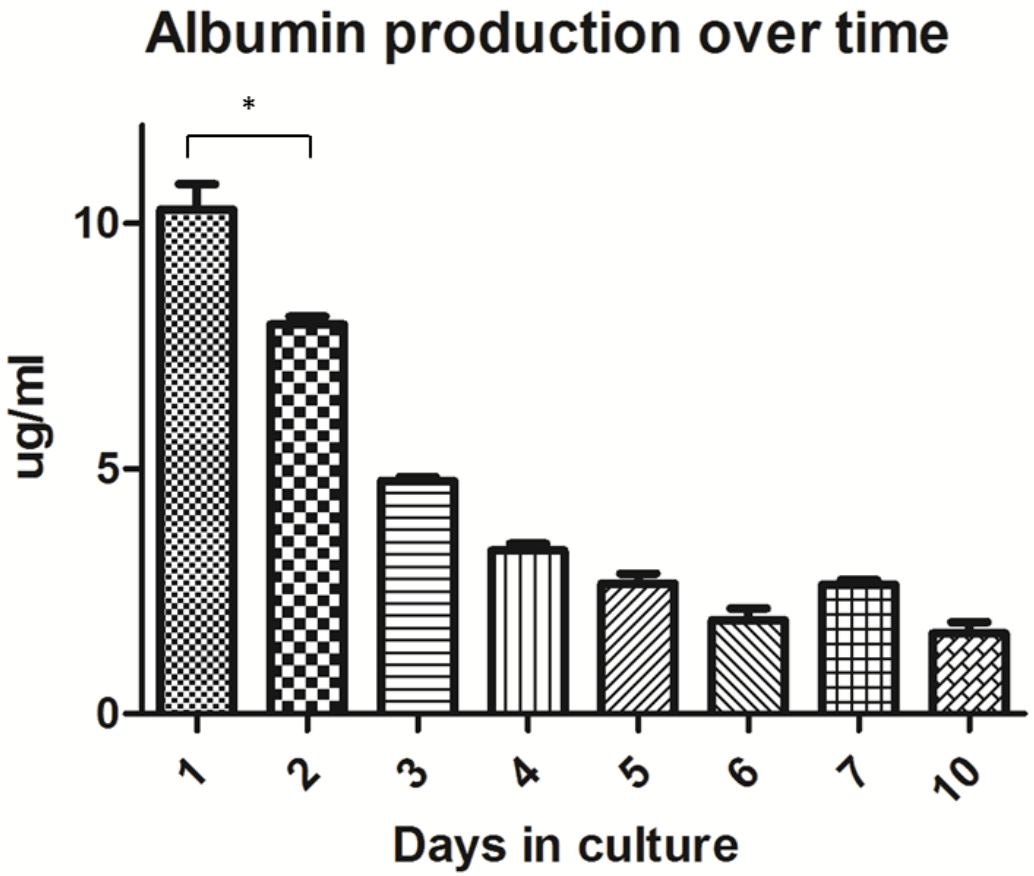

Figure 3.13 Albumin production per 24 hours in µg/ml from D17513 primary hepatocytes.
Canine albumin specific ELISA kit was used (Immunology Consultants Ltd). Media was collected every 24 hours and diluted 1:100. There was a significant reduction in albumin concentration between day 1 and 2 (* p=0.0128).

3.5.12 Matrigel overlay improves hepatocyte viability

As primary hepatocyte function decreased so dramatically, an experiment was designed to assess the effect of sandwich culture using Matrigel as an overlay. If an improvement in qualitative or quantitative tests were demonstrated then these culture conditions may also improve function in hepatocyte-like cells derived from stem cell sources. Matrigel at 0.25mg/ml in HCM was overlain primary hepatocytes cultured on collagen type I. These were compared with hepatocytes cultured on collagen type I. Cell morphology was examined and pellets for RNA extraction and real-time PCR

were collected on day 1 and 3 as well as freshly isolated hepatocytes. Subjectively, hepatocytes with Matrigel appeared more confluent, with sharper demarcations between cells, consistent with bile caniliculi formation (Figure 3.14).

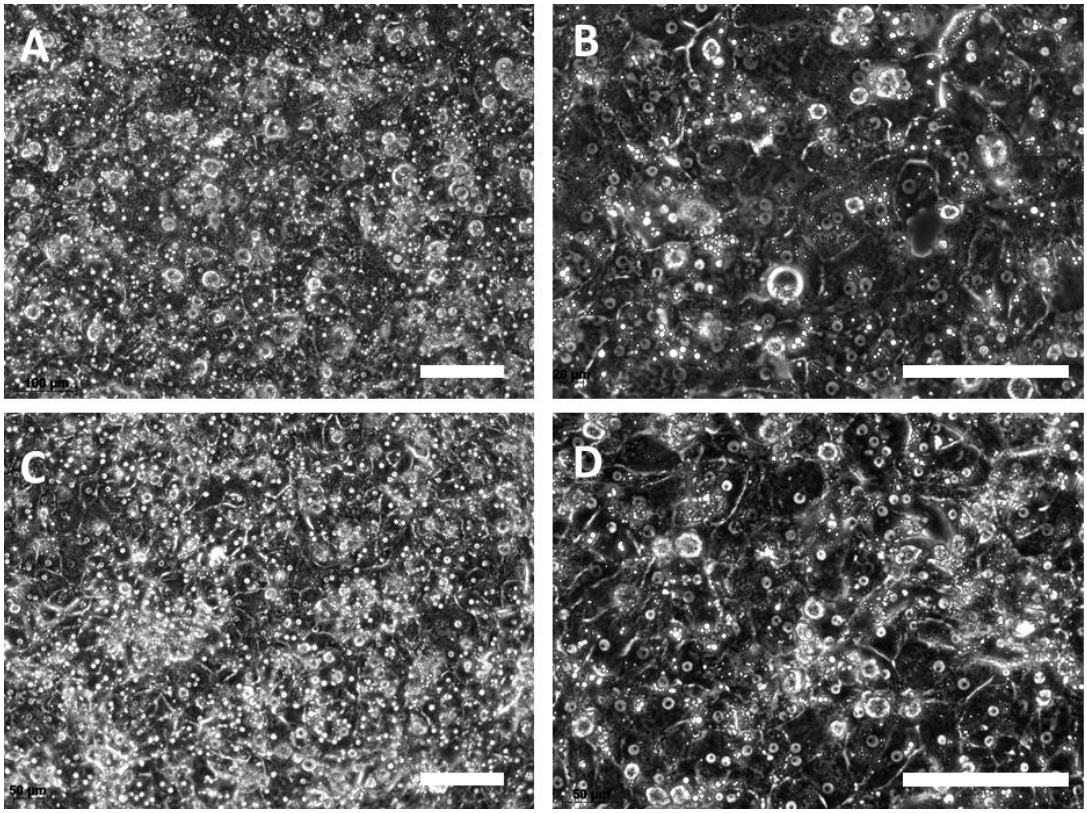

Figure 3.14 Morphology of canine primary hepatocytes on type I collagen and type I collagen with Matrigel overlay.
Canine primary hepatocytes from D41013 were plated at 1 x10^5/cm^2. After 4 hours to attach media was changed to either standard culture media or standard culture media supplemented with 0.25mg/ml Matrigel. Hepatocytes were photographed after 24 hours culture *in vitro*. Images A and B are hepatocytes on standard collagen type I, images C and D are hepatocytes on collagen type I that were then overlain with 0.25mg/mml of Matrigel. White bar represents 100µm.

To assess the effect of the Matrigel overlay on hepatocyte viability, a cell viability assay was performed after 1, 3 and 6 days culture. This was performed using canine primary hepatocytes D17513 and D41013. Wells cultured with an overlay of Matrigel had statistically significant higher cell viability at all time points with all hepatocyte cultures (Figure 3.15).

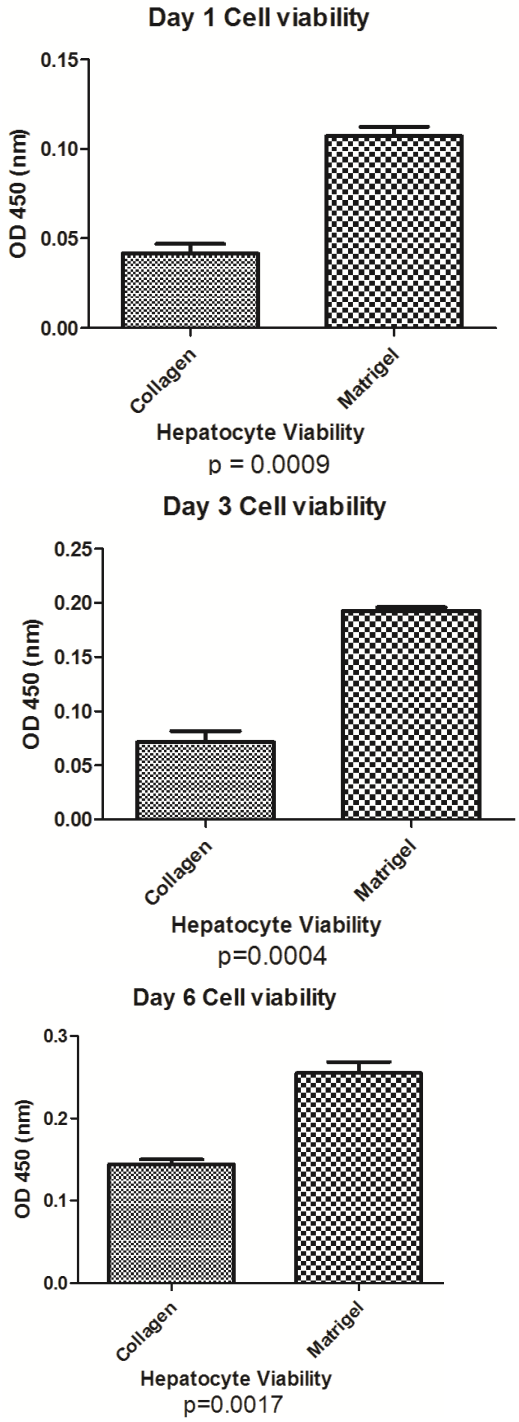

Figure 3.15 Cell viability of canine primary hepatocytes D19713 on collagen type I and Matrigel overlay on days' 1,3 and 6.

Canine primary hepatocytes from D41013 were plated as described in Figure 3.14. Following addition of 1mg/ml MTT solution, incubation for 3 hours and subsequent solubilisation, the optical density was read at 570nm using a plate reader. Results are the average of triplicate determinations ± SEM and the experiment repeated three times.

3.5.12.1 Hepatocyte gene expression is not consistently higher with Matrigel overlay

Canine primary hepatocytes from D41013 were used and analysed at time points 1,3 and 6 days. Matrigel overlay was changed daily. Fold increase in the Matrigel overlain hepatocytes in comparison to standard culture was calculated (Figure 3.16). No genes analysed were consistently significantly up-regulated at all time points. Glycogen synthase was mildly but significantly up-regulated at days 1 and 6 ($p=0.01$ and 0.02 respectively). Albumin was significantly up-regulated at day 6 ($p=0.02$).

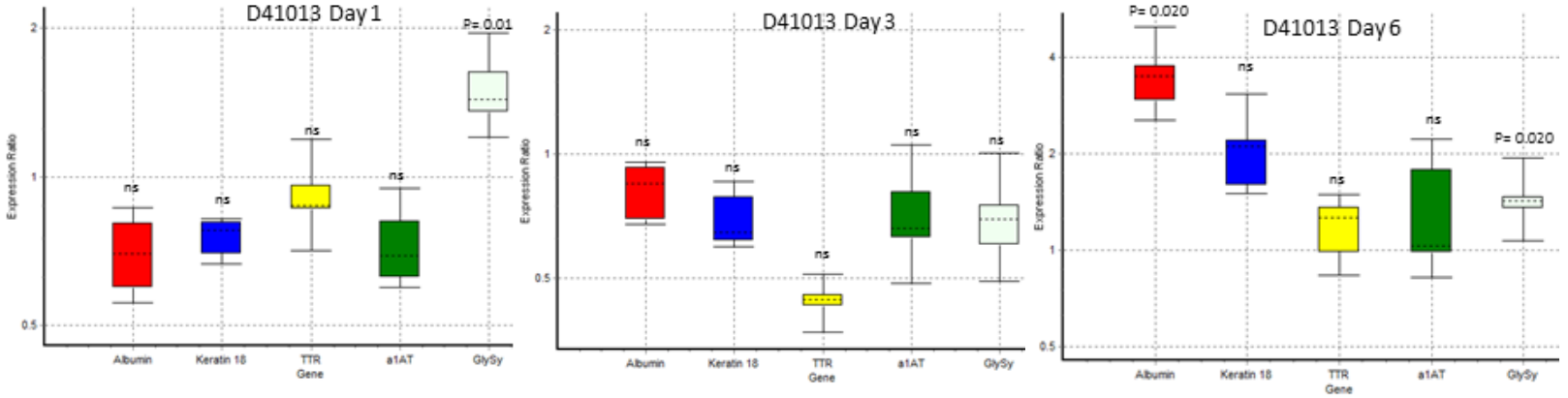

Figure 3.16 Fold increase in gene expression of albumin, keratin18, transthyretin (TTR), α1-antitrypsin (a1AT) and glycogen synthase(GlySy) in Matrigel overlain hepatocytes compared to standard culture.
Fold increase was calculated using the Pfaffl method (Pfaffl, 2001). Boxes represent the interquartile range, or the middle 50% of observations. The dotted line represents the median gene expression. Whiskers represent the minimum and maximum observations. Experiment was performed in triplicate. ns = not significant.

3.5.12.2 Matrigel overlay does not improve albumin production.

Supernatant from D17913 canine primary hepatocytes was collected from standard culture and Matrigel overlain hepatocytes after 24 and 72 hours and analysed for albumin concentration using the canine albumin specific ELISA. Cells were quantified using an MTT assay and albumin concentration was divided by this optical density to normalise for variation in cell number (Figure 3.17). Although normalised values were higher on day 1 and 3 in the Matrigel overlain hepatocytes this was not statistically significant.

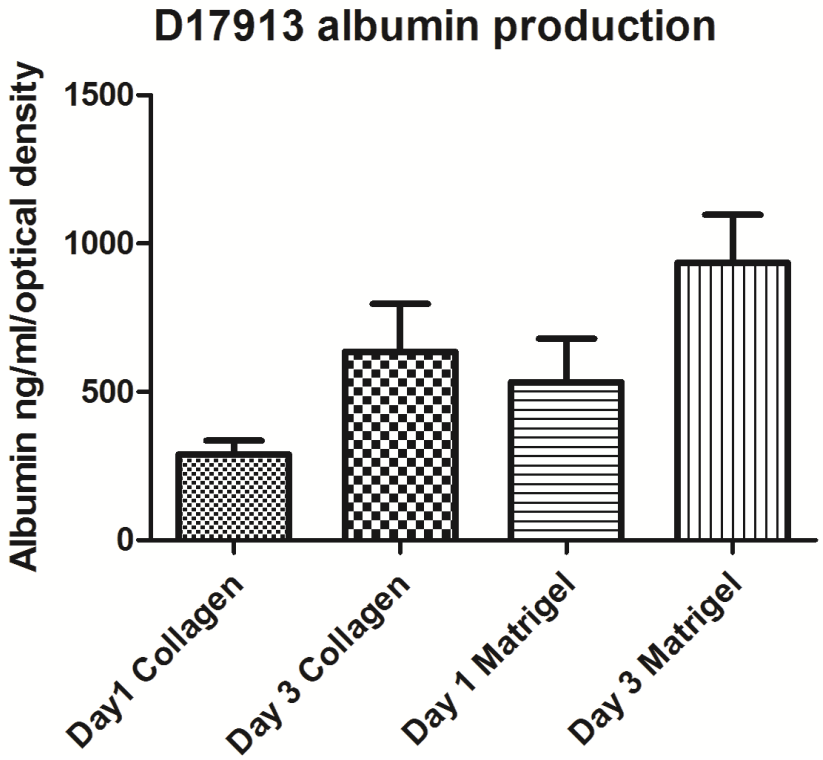

Figure 3.17 Comparison of albumin concentration of canine primary hepatocytes in standard culture and overlain with Matrigel.
Hepatocytes were plated as described in Figure 3.14. Experiment was performed in triplicate. Media was collected at day 1 and day 3. An MTT assay was then used to define cell number variation. Albumin concentration was measured in duplicate using ELISA and result was divided by MTT optical density to normalise for variation in cell number. Error bars represent standard error of mean.

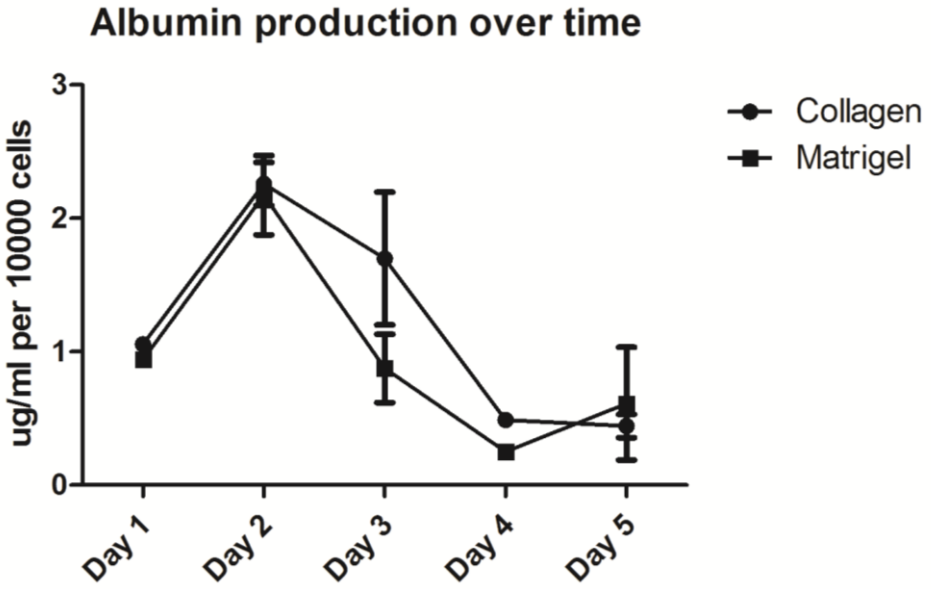

Figure 3.18 Albumin production of D41013 hepatocytes on collagen and Matrigel overlay
Hepatocytes were plated as described in Figure 3.14. Experiment was performed in triplicate. Medium was collected daily on days 1-5. Cells were trypsinised and counted. Albumin concentration was measured in duplicate using ELISA and the result was normalised to 1 x10^4 cells. Values were analysed using a repeated measures ANOVA.

Media from D41013 standard culture and Matrigel overlain hepatocytes was also analysed for albumin concentration. In this experiment, as there was concern that the MTT assay results may not be directly comparable between days, the cells were trypsinised and counted. Supernatant was collected every 24 hours for 5days. The experiment was performed in triplicate and samples were analysed in duplicate. Albumin concentration was normalised to 1 x10^4 cells (Figure 3.18). There was no significant difference between albumin production in standard culture and Matrigel overlain hepatocytes at any time point. There appeared to be an increase in albumin production in both standard culture and Matrigel overlain hepatocytes between days 1 and 2.

3.5.12.3 Matrigel overlay did not consistently increase hepatocyte CYP expression.

Real time PCR was performed at time points 1, 3 and 6 days to compare *CYP* gene expression in canine primary hepatocytes on standard collagen type I to hepatocytes on collagen type I with a Matrigel overlay. This was performed using D19713 and D41013 canine primary hepatocytes. Relative gene expression of Matrigel overlain hepatocytes was compared to control hepatocytes (Figure 3.19,Figure 3.20 & Figure 3.21). Any fold increase in *CYP* expression was mild (maximum of 4, generally <2) and not consistent apart from possibly *CYP1A2* which was significantly increased in D17913 at time points 1 and 3 and in D41013 at time points 3 and 6 days.

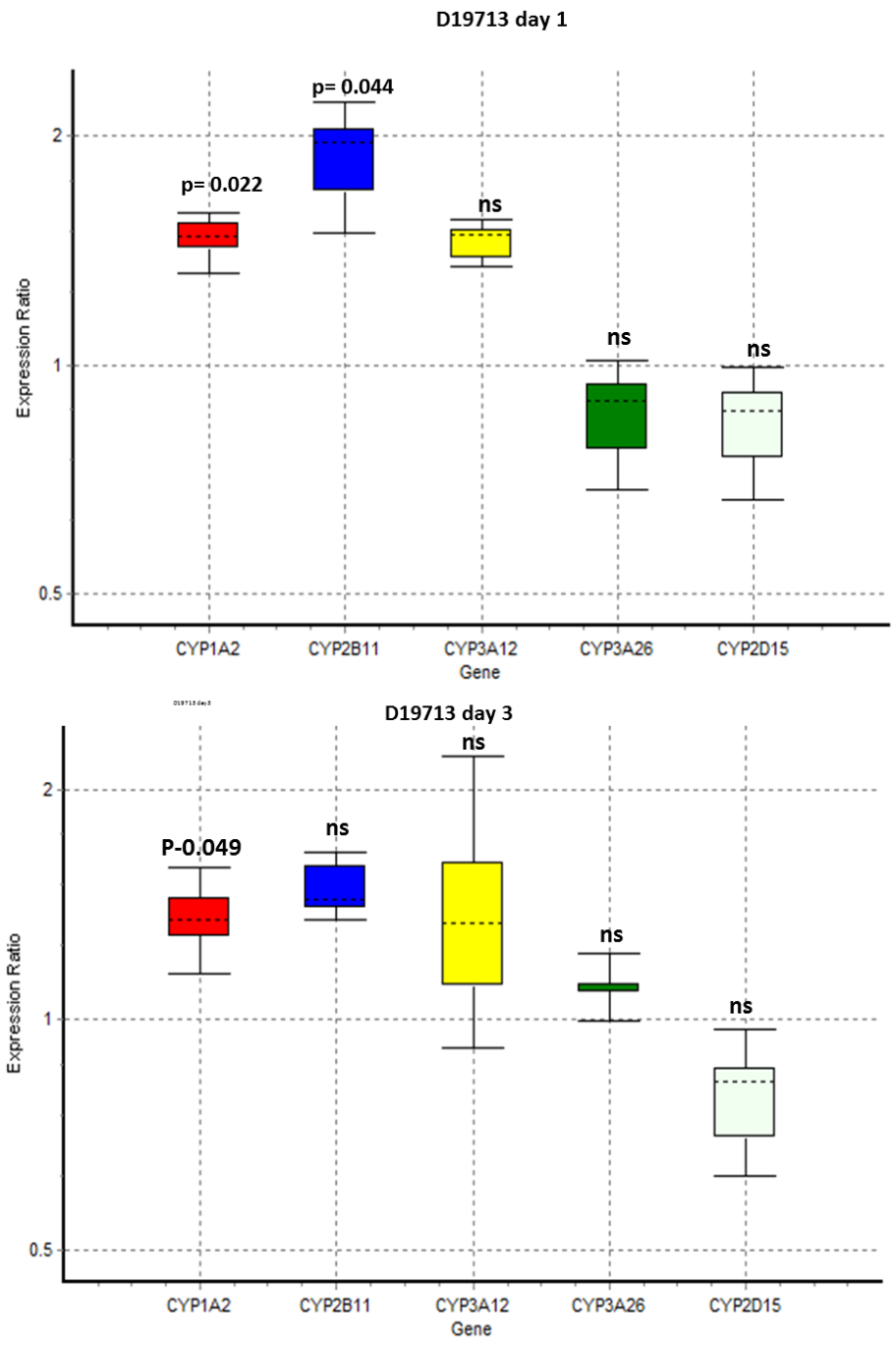

Figure 3.19 **Fold increase of CYP expression in D19713 canine primary hepatocytes with Matrigel overlay days 1 and 3.**
Hepatocytes with Matrigel overlay were compared to hepatocyte with standard collagen type I basal substrate. *CYP* genes were normalised to three reference genes. Fold increase was calculated using the Pfaffl method (Pfaffl, 2001). Boxes represent the interquartile range, or the middle 50% of observations. The dotted line represents the median gene expression. Whiskers represent the minimum and maximum observations. ns = not significant.

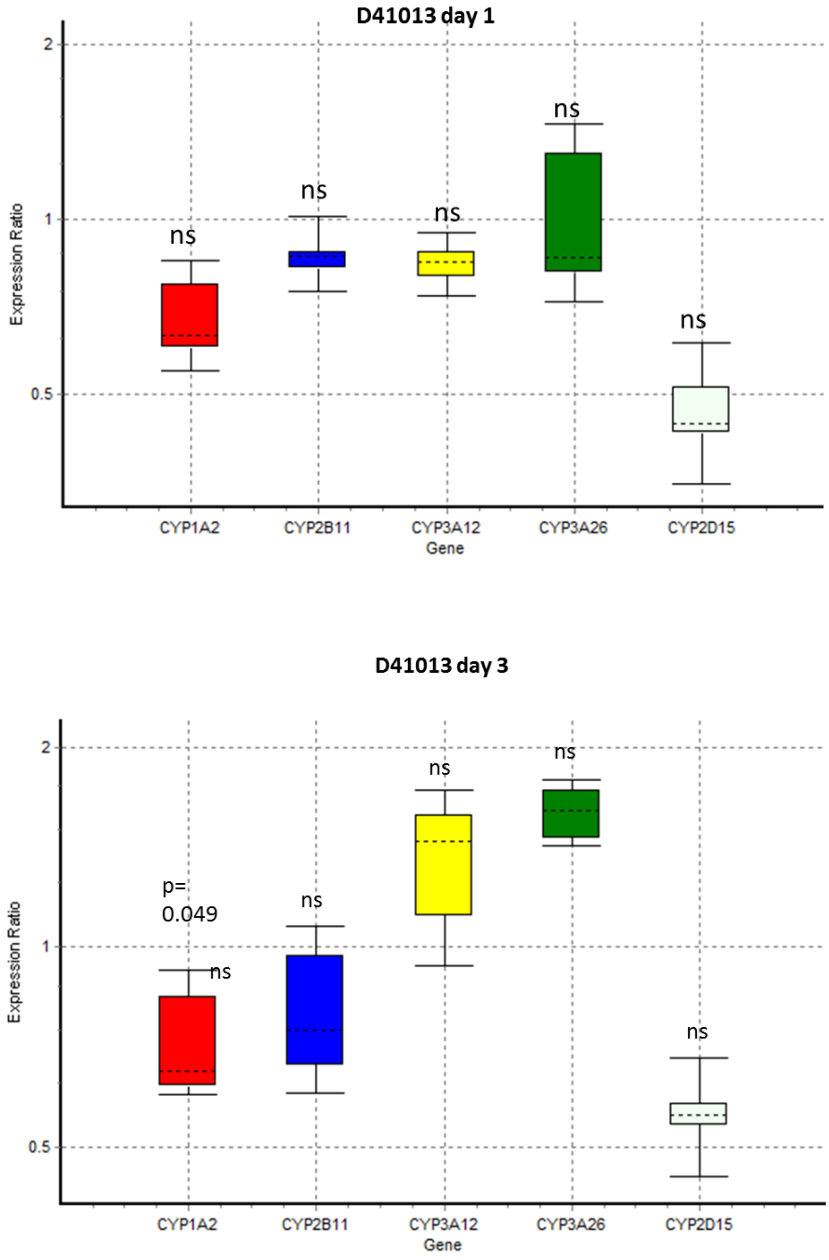

Figure 3.20 **Fold increase of CYP expression in D41913 canine primary hepatocytes with Matrigel overlay days 1 and 3.**
Hepatocytes with Matrigel overlay were compared to hepatocyte with standard collagen type I basal substrate. *CYP* genes were normalised to three reference genes. Fold increase was calculated using the Pfaffl method (Pfaffl, 2001). Boxes represent the interquartile range, or the middle 50% of observations. The dotted line represents the median gene expression. Whiskers represent the minimum and maximum observations. ns = not significant.

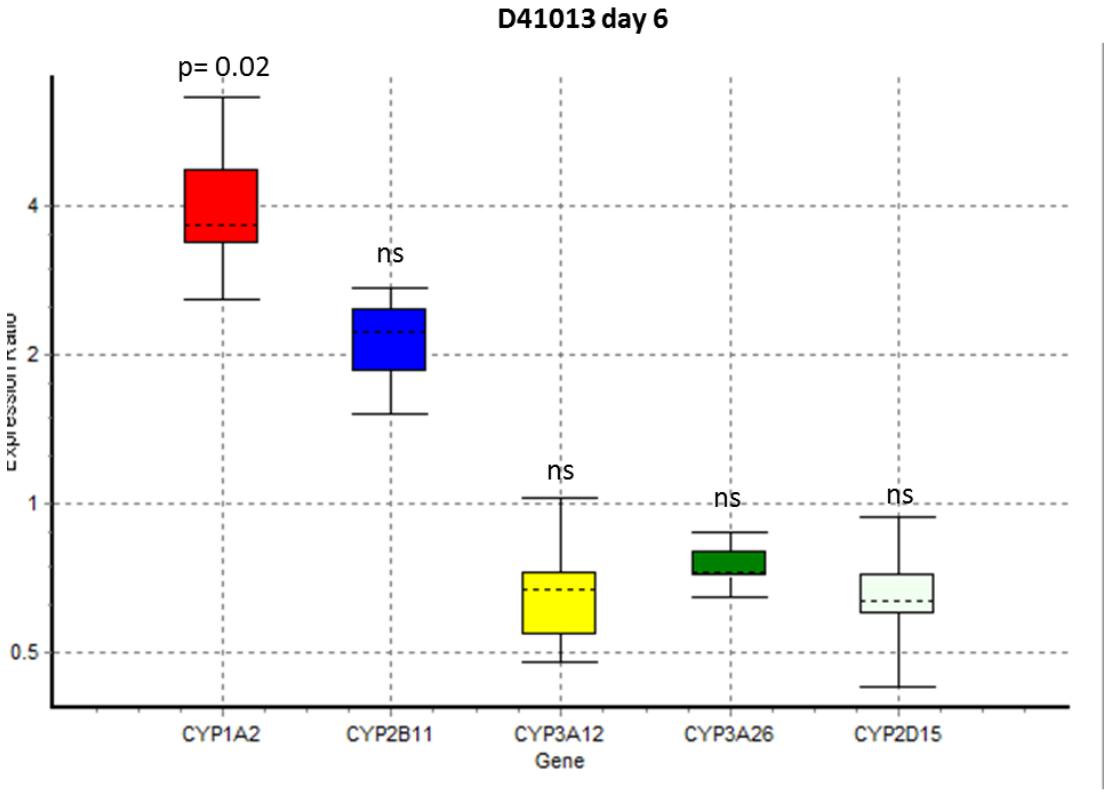

Figure 3.21 **Fold increase of CYP expression in D41913 canine primary hepatocytes with Matrigel overlay day 6.**

Hepatocytes with Matrigel overlay were compared to hepatocyte with standard collagen type I basal substrate. *CYP* genes were normalised to three reference genes. Fold increase was calculated using the Pfaffl method (Pfaffl, 2001). Boxes represent the interquartile range, or the middle 50% of observations. The dotted line represents the median gene expression. Whiskers represent the minimum and maximum observations. ns = not significant.

3.5.12.4 Induced CYP activity is not increased by Matrigel overlay.

D41013 hepatocytes were cultured with 50µM rifampicin, 500µM phenobarbital or control media. CYP activity was measured using the luciferase assay with normalisation against cell viability at time points 1 and 3 days (Figure 3.22). Basal CYP activity was significantly lower on day 1and 3 in the Matrigel cells compared to control cells (p=0.0178 and 0.0157 respectively). Although on Matrigel day 1, rifampicin and phenobarbital treated cells had higher values, these were not significantly different to basal Matrigel CYP activity (p=0.0822). By day 3, Matrigel phenobarbital but not rifampicin treated cells had significantly higher activity than the basal cells (p=0.0098). There was no significant difference in CYP activity after phenobarbital treatment between collagen and Matrigel hepatocytes on day 1 or 3 (p= 0.098 and 0.894).

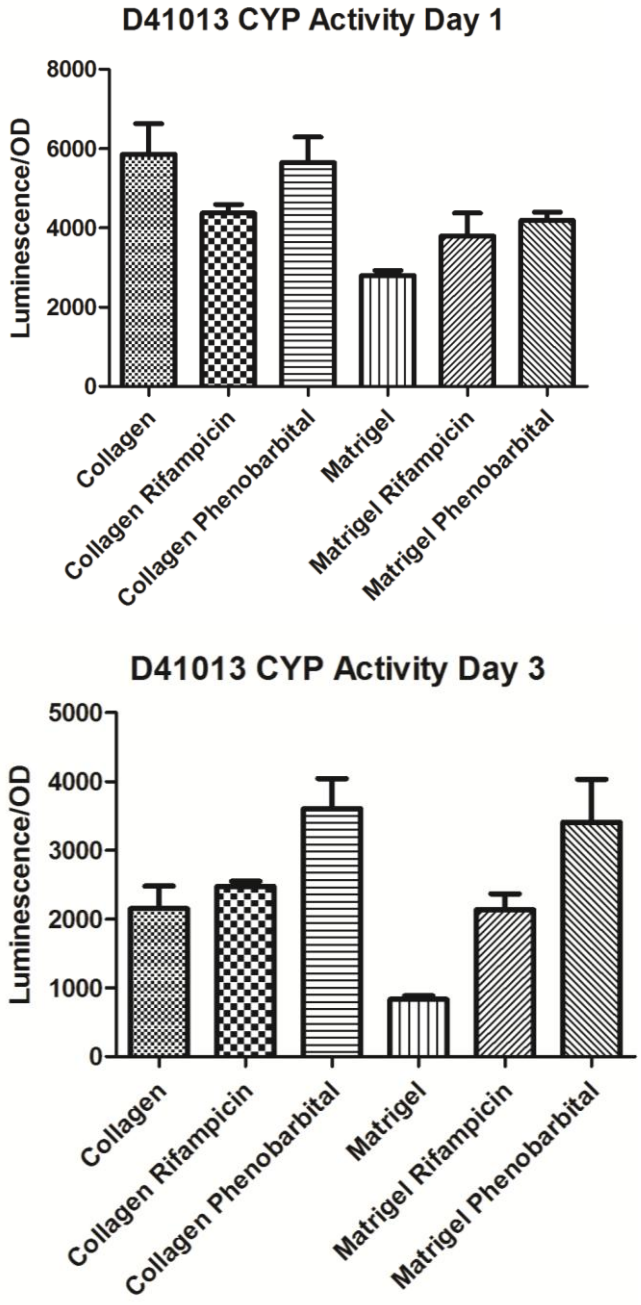

Figure 3.22 CYP activity of collagen and Matrigel overlain canine primary hepatocytes.

Hepatocytes were cultured in triplicate either on collagen or collagen/Matrigel overlay with HCM + vehicle, HCM + rifampicin or HCM+phenobarbital for 24 and 72 hours. Luciferin-PFBE was added and cell cultured from 3 hours. Media was then aspirated, added to detection reagent and read in duplicate in a luminometer at 1 second detection per well. Experiment was performed in triplicate and empty wells containing no cells were used as controls for background fluorescence. Background fluorescence was subtracted from results. Cells were then cultured in 1mg/ml MTT for 2 hours, and optical density measured. Luminescence was then divided by optical density.

3.6 Discussion

After a period of familiarisation with techniques, confluent cell cultures could be reliably derived from ischaemic canine hepatic tissue. Variation in cell number and viability was likely to be due to multiple factors including, age and health of the dog, time between euthanasia and processing of tissue, temperature of storage, size of liver wedge perfused, amount of connective tissue and length of time of the perfusion performed for. However after initial perfusions, many more hepatocytes than were required for each experiment were isolated. Hepatocytes are fragile, cryopreservation tends to cause poor viability and loss of function (Terry et al., 2006). As a result, this option was not explored for these hepatocytes especially as the main use was to provide a gold-standard with which to compare stem cell derived hepatocyte-like cells. As there is a shortage of human hepatocytes for clinical use, much effort has been put to improving cryopreservation techniques of human hepatocytes. At present, the most effective method involves purifying only high viability cells, pre-culturing with media supplements and using a programmable freezer which varies the rate of temperature decline and includes a "shock freezing" step to counteract the latent heat of fusion when ice crystals form (Hewitt, 2010). The cell density at which they are frozen at also appears critical, which is species specific (Hewitt, 2010). As after some successful perfusions, the majority of hepatocytes were discarded as surplus to requirements, investigation of the optimal cryopreservation methods for canine hepatocytes would be a useful avenue of further investigation, allowing these cells to be available on demand rather than being limited to fresh liver tissue availability.

The resultant cells were as described for *in vitro* hepatocyte preparations in multiple species, namely large polygonal cells, often bi-nucleate with a large cytoplasm to nucleus ratio. The change in morphology over 7-10 days has also been described in multiple species (Knobeloch et al., 2012).

Surprisingly, the majority of canine primary hepatocytes did not take up ICG and only damaged cells stained well. The first two papers that used ICG to demonstrate hepatocyte-like characteristics of differentiated stem cells both stated that "no effect

on viability was noted at 1mg/ml for 15 minutes", suggesting that higher concentrations and/or longer incubation times may have affected viability (Wang et al., 2005; Yamada et al., 2002). Zamule et al. (2011) stated that 1mg/ml for 15 minutes caused toxicity in human embryonic stem cells and used 100µg/ml. ICG has been used as a method of assessing human hepatocyte viability, however concentrations greater than 1mg/ml were toxic to the hepatocytes (Ho et al., 2012). ICG is used in ophthalmic surgery however there is increasing concern over its use, as toxicity to retinal glial, ganglion and pigmented epithelial cells *in vitro* is reported at 0.25mg/ml for 15 minutes (Balaiya et al., 2011; Kawahara et al., 2007). Therefore there is evidence that ICG has the potential to be cytotoxic *in vitro*. As a cell viability assay, MTT is reduced to formazan by NAD(P)H-dependent oxidoreductase enzymes in the cell cytoplasm. This occurs in metabolically active cells with a solubilisation step of the insoluble purple formazan granules to allow absorbance measurement (Berridge and Tan, 1993). This was used without the final solubilisation step in order that viable cells would be highlighted with the presence of intracytoplasmic purple granules. This demonstrated that cells which took up ICG were subsequently not metabolically active and by inference were non-viable. From this test it is unclear if viable cells may have been killed by subsequent toxicity from ICG uptake or the cells were non-viable prior to ICG addition. As chemically and physically damaged cells also took up ICG with the same degree of avidity, it is likely that dead/damaged canine hepatocytes stain with ICG. The second step in ICG testing is subsequent release of intracellular ICG after washing cells and replacing with fresh media, which would be consistent with active transport into bile caniliculi. One potential confounder is that as the dye solution is replaced with fresh media, diffusion would cause a loss of intracellular dye, potentially mimicking active excretion. This was seen in the stained canine primary hepatocytes (data not shown).

Aside from one study using ICG on suspensions of primary human hepatocytes, there is very little in the literature on using ICG *in vitro* in primary hepatocytes (Ho et al., 2012). Zemel et al. (2009) noted that clusters of undifferentiated adipose-derived mesenchymal stem cells took up ICG, again raising concern about the purported specificity of the test.

Therefore ICG uptake does not appear to be a useful test of function in canine primary hepatocytes and would not then be used for assessing the success of stem cell differentiation into hepatocytes.

Periodic acid-Schiff staining stained fresh canine primary hepatocytes intensely and after a period in culture, staining became patchy and less distinct. This did appear to be a good test of the presence of intra-cytoplasmic glycogen and would be used for testing the ability of hepatocyte-like cells to store glycogen.

From culturing canine hepatocytes in LDL and Ac-LDL it was clear that canine hepatocytes avidly took up native LDL which was consistent with gene expression for the LDL receptor. Unlike many other hepatocyte tests, LDL uptake did not seem to decrease during culture (data not shown) which was also consistent with gene expression as LDL receptor gene expression was one of the few hepatocyte function genes that increased during culture (Figure 3.8). In contrast, only a few cells in culture endocytosed Ac-LDL. Although the hepatic parenchyma consists mainly of hepatocytes it contains a wide variety of cells including macrophages and endothelial cells which are known to take up Ac-LDL (Arias et al., 2011; Horiuchi et al., 2003). It is probable that these cells would also be isolated and survive during culture and therefore it is suspected that these sparse Ac-LDL positive cells are macrophages, or endothelial cells, or both. This is consistent with the report by Babaev et al. (1989) who found that human primary hepatocyte cultures almost uniformly took up LDL with only 5% of cells in culture taking up modified LDL. These were identified as macrophages or endothelial cells based on their ability to take up tagged formaldehyde-treated albumin and carboxylate microspheres.

It is intriguing that Ac-LDL is used frequently as a test of hepatocyte-like cells from stem cell sources and testing LDL/Ac-LDL uptake of hepatocytes from a variety of species would help define if there are species differences in uptake. To verify canine hepatocyte-like function, it is clear that LDL uptake and not Ac-LDL uptake should be used and this appeared to be a useful test of hepatocyte-like function.

In addition, a panel of genes optimised for real-time PCR were developed to test hepatocyte like cells. These included 3 reference genes (RLP8, B2MG, HPRT), three for proteins secreted by hepatocytes – albumin, α1-antitrypsin and transthyretin, one protein produced by hepatoblasts (αfoetal protein), two structural proteins – K7 found in hepatic progenitors and K18 found in mature hepatocytes, glycogen synthase an enzyme causing hepatic glycogen deposition, and LDL-receptor, encoding for the LDL-specific receptor. Primers for 6 genes encoding for *CYP* enzymes, 1A2, 2B11, 2C18, 2D15, 3A12 and 3A26 were also validated. Of these, 1A2, 2B11, 2D15, 3A12 and 3A26 are known canine specific enzymes. In particular *CYP3A12* and *CYP3A26* are orthologues of the human enzyme *CYP3A4* which is responsible for biotransformation of over 50% of pharmaceuticals (Fraczek et al., 2013).

Consistent with the literature in many species, canine primary hepatocytes rapidly de-differentiated in culture with a rapid reduction in expression of many genes over time (Beigel et al., 2008; Fraczek et al., 2013; Rodriguez-Antona et al., 2002; Ubeaud et al., 2001). Of most concern is the rapid reduction in *CYP* expression as continued expression and activity is crucial for toxicological studies.

Culturing canine primary hepatocytes for 72 hours with rifampicin and phenobarbital caused significant up-regulation of *CYP3A12*, *CYP2B11* and *CYP2D15* genes with both drugs. In the literature, Makino et al. (2009) noted that phenobarbital increased *CYP2B11* and *CYP3A12* gene expression significantly, *CYP3A26* was non-significantly increased whilst *CYP1A2* was significantly down-regulated. Examining protein expression, CYP1A2 was down regulated, and CYP2B11 and CYP3A12 increased, consistent with gene expression (CYP3A26 was not examined). In a study by Graham et al. (2006), both drugs were noted to up-regulate *CYP3A12* and *CYP3A26* with only phenobarbital up-regulating *CYP2B11*. It was stated that this lack of *CYP2B11* induction by rifampicin was a previously overlooked species difference. Phenobarbital but not rifampicin was noted to increase CYP2B11 activity and both compounds increased CYP3A12 activity (Graham et al., 2002). The notable differences in the present study are that *CYP1A2* was not decreased with phenobarbital and that *CYP2B11* was significantly up-regulated with rifampicin in

contrast to the findings of Makino et al. (2009) and Graham et al.(2002). Additionally, *CYP3A26* was not significantly increased with phenobarbital, consistent with Makino et al., (2009) but contrary to Graham et al.(2002). The previous studies used Beagle dogs whereas the present study utilised hepatocytes from a Staffordshire Bull-Terrier; therefore it is possible that there may be breed differences to induction of *CYP* gene expression which could be further investigated.

Keratin 7 and 18 gene expression increased after plating and remained elevated during the whole period. These are cytoskeletal proteins and an increase in structural genes has been noted in other studies (Beigel et al., 2008; Fraczek et al., 2013). Suggested explanations are de-differentiation, an increase in proliferating fibroblasts in culture or, most plausibly, hepatocytes reacting to cellular stress and sudden loss of surrounding architecture synthesising more cytoskeletal filaments.

Of the three proteins examined, both albumin and transthyretin gene expression reduced dramatically over time whilst α1 acid-glycoprotein increased in the first 24 hours then reduced to similar expression levels as primary hepatocytes. This was consistent in all three experiments. This has been noted in other species and one hypothesis, other than straightforward de-differentiation reducing gene expression, is that hepatocytes are demonstrating an acute-phase response as a result of the dissociation process, with negative acute phase proteins such as albumin and transthyretin decreasing, whist positive acute phase proteins such as α2-macroglobulin and α1 acid-glycoprotein increase (Beigel et al., 2008).

The Promega Pro-Glo CYP34A Luciferase-PFBE kit provided luminescent readings which reduced over time (Figure 3.12), consistent with the reduction in CYP gene expression. No significant effect of culture with rifampicin or phenobarbital was noted. The substrate is selectively metabolised by CYP3A enzymes, in the rat specifically by CYP3A1 and CYP3A2 and in human CYP3A4 with some CYP3A5 and CYP3A7 activity (Garcia et al., 2008; Promega Technical Manual P450-Glo

Assays, 2013). In the dog, the orthologues to CYP3A4 would be CYP3A12 and CYP3A26. From the *CYP* gene induction experiment, *CYP3A12* but not *CYP3A26* is significantly induced by both rifampicin and phenobarbital (Figure 3.10). Therefore if the substrate is metabolised specifically by CYP3A26 in the dog this may account for the lack of significant difference in this assay between basal and CYP induced hepatocytes. One of the fundamental reasons for this project's production of *in vitro* canine hepatocytes is the problem of species differences in xenobiotic metabolism and this may be a case in point. It is possible that Luciferin-PFBE may be metabolised by another member of the CYP family in the dog. Therefore the assay appears useful in measuring basal CYP activity but not the ability to induce CYP activity with phenobarbital or rifampicin.

The albumin ELISA test was optimised and was specific for canine albumin. A 1:100 dilution of media which, coming from primary hepatocytes in the first 24 hours of culture, would be reasonably be expected to contain the highest concentrations of albumin was selected as the dilution to be used for subsequent experiments as it was mid-way between the standard range and would allow a sufficiently dynamic range to be measured. There was no cross-reactivity with bovine serum albumin in the culture media and consistent results were achieved. Albumin production in primary hepatocytes over time appeared consistent with the reduction in gene expression i.e. it fell dramatically, although from Figure 3.18 it appears that albumin production increased after 24 hours in both the standard culture and Matrigel overlain cells. Although this is possible, it is more likely that these are artefacts especially as in Figure 3.13 albumin production of D17513 decreased dramatically from day 1 onwards and from Figure 3.17, albumin production in the first 24 hours appears to provide the bulk of the total 72 hour production. In respect of the D41013 experiment where cell numbers were directly counted, a far higher cell number was counted for the day 1 wells (average 3.1 $x10^5$ on collagen and 3.6 $x10^5$ on Matrigel compared to 1.4 $x10^5$and 1.94 $x10^5$ respectively thereafter), which likely included non-viable and non-hepatocyte cells and therefore would have reduced the final value. As the media was changed daily, these cells would have been removed by day 2 and indeed cell numbers were approximately half day 1 counts for

the remaining days. Therefore comparing albumin production between days with these methods is problematic and using total albumin concentration is likely to be more accurate providing plating density remains similar. However comparing different culture substrates effect on albumin production on the same day would be less likely to suffer from these problems and more likely to have differences in cell density therefore normalising to cell number by one of these methods would be more accurate.

From the Matrigel overlay experiments, the hepatocytes morphologically appeared less flattened with more distinct borders compared to controls, also from the MTT assay, cell number was higher. Despite this, no consistent significant differences were seen in gene expression, CYP induction or albumin production. In fact, basal CYP activity as measured by the luciferase assay was statistically significantly lower in the Matrigel overlain cells compared to the standard collagen cells. This is in contrast to what has been reported in human and rat primary hepatocytes where Matrigel overlay allowed higher gene expression, enzyme basal activity and inducibility (Gross-Steinmeyer et al., 2005; Kocarek et al., 1993). Repeating these culture conditions with other canine hepatocytes of various breeds would ensure this was a consistent finding. At present, there appears to be no significant advantage to Matrigel overlay in primary hepatocyte or for hepatocyte-like cell culture. LeCluyse et al. (2000) found that type of overlay did not appear to be significant, however restoration of cell shape and cell to cell contact may be most important, therefore altering culture conditions to allow a 3D culture system may reduce dedifferentiation.

In summary this work has achieved:

- Reliable methods of producing viable canine primary hepatocytes to use as a gold standard when assessing stem cell-derived hepatocyte-like cells.
- A panel of primers optimised for real-time PCR. These included 6 *CYP* genes, a crucial component in cells for toxicological testing.
- Induction of *CYP* gene expression using phenobarbital and rifampicin
- Luciferin-PFBE produced reliable results on canine hepatocytes to assess CYP activity however induction was not demonstrated
- Optimisation of a canine-specific albumin ELISA for culture media
- Clarification that native LDL and not Ac-LDL should be used for canine primary hepatocytes
- Indocyanine green is not a useful test for canine primary hepatocytes, staining non-viable cells.
- Matrigel overlay appears to offer no significant advantage to standard collagen culture for canine primary hepatocytes

Chapter 4: Isolation and culture of hepatic progenitor cells

4.1 Abstract

The liver contains hepatic progenitor cells (HPC) that have the potential to differentiate into functional hepatocytes. If these can be isolated and expanded *in vitro*, they could provide a limitless supply of functional hepatocytes.

In this chapter, the location and phenotype of hepatic progenitor cells (HPC) is discussed followed by methods of isolation that have been described in various species, including the dog. Density centrifugation using Percoll and Ficoll to isolate the HPC compartment from normal canine liver was performed as well as immuno-selection selection for CD133 positive cells using magnetic assisted cell sorting (MACS). The Percoll method isolated very few cells, which were of a morphology consistent with HPC; however these failed to expand in culture. Ficoll isolation yielded a much larger cell population of mixed morphology, appearing to be composed mainly of fibroblasts and macrophages.

CD133 selection yielded a population apparently lower purity which was improved subsequently using dissociative enzymes. Colonies of cells morphologically consistent with hepatic stem cells and hepatoblasts expanded in culture. Mechanical passaging appeared superior to using dissociative enzymes and laminin-coated tissue-culture plastic supported colony attachment.

Further expansion of these cell types could not be achieved however CD133 selection appears a viable method of HPC selection in the dog and would allow further characterisation and optimisation of culture techniques.

4.2 Introduction

As hepatic progenitor cells have the ability to differentiate into hepatocytes when the ability of mature hepatocytes to contribute has been overwhelmed, there has been interest in isolating and expanding these cells *in vitro*. This source could then be used as a source of hepatocytes. As discussed in the introduction, these cells are located in the Canals of Hering, the junction between hepatocytes and cholangiocytes. It is stated that there are two main types of hepatic progenitor cell; the true hepatic stem cell (HpSC) and the hepatoblast (HB), although this point is still debated as to whether these are in fact the same cell type (Zhang et al., 2008). This contention may be due to the fact that HpSC differentiate to HBs and therefore the two cell populations are not distinct entities. HpSC also have the ability to produce biliary progenitor cells whereas HBs are committed to the hepatocyte lineage. Oval cells in rodents proliferate in response to hepatic injury and are bipotential progenitor cells, it is thought that these may be derived from HpSC and are variably described as being either in very low numbers or absent in normal livers (Conigliaro et al., 2010; Dolle et al., 2010).

4.2.1 Phenotype of HPCs

There is debate as to the phenotype of these cells which is made more complex by apparent species differences and the fact that as these cells differentiate, morphology and phenotype, including marker profiles, change (Darwiche and Petersen, 2010). Furthermore, the act of processing tissue with dissociative enzymes to access and isolate the cellular compartment of interest, in this case hepatic progenitor cells, has been shown to potentially cause loss of cell membrane cluster of differentiation (CD) expression (Panchision et al., 2007). Differences between HpSC and HB have been defined upon marker expression e.g. HpSC do not express αfoetal protein whereas HB do. Figure 4.1 highlights markers of hepatic progenitor cells in the human, rat and mouse. Marker profile varies between species and known markers are often expressed on many other cells. The fact that the liver is a heterogeneous organ

composed of many cell types makes this especially problematic when using markers for cell isolation. Specific markers tend to be intracellular and therefore prevent their use for isolation of viable cells for culture (Conigliaro et al., 2010).

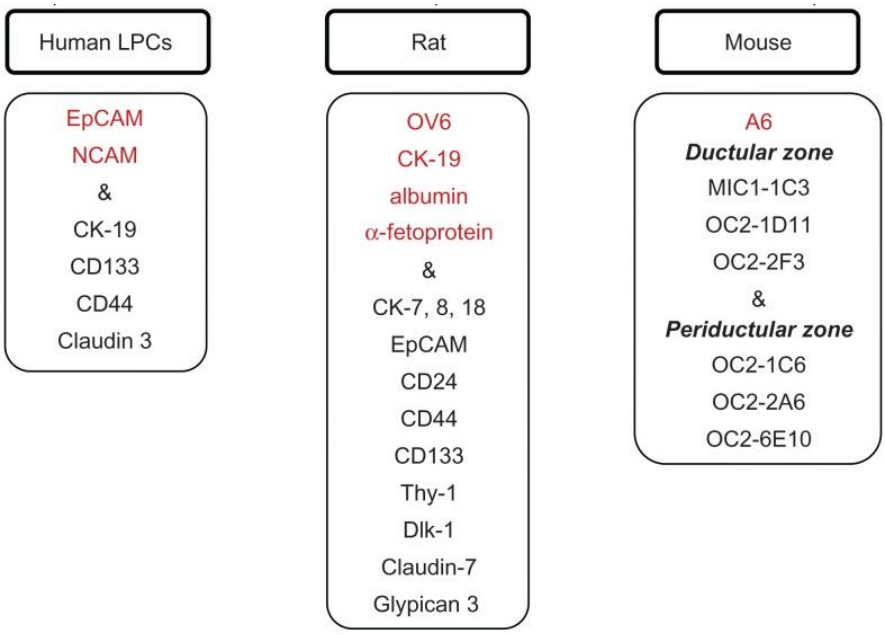

Figure 4.1 Markers of liver progenitor cells (LPC) or oval cells in human, mouse and rat.
Figure from Conigliaro et al. (2010).

4.2.2 Methods of hepatic progenitor cell isolation

There are three main methods which have been utilised, to isolate the hepatic progenitor cell compartment described in turn in the next three sections. All three begin with the standard collagenase perfusion digestion of either the whole liver *in situ* in rodents or a wedge perfusion in larger animals. Once single cell dissociation has been performed, hepatocytes are removed by low speed centrifugation to leave the non-parenchymal cell compartment which also contains the hepatic progenitor cells (Dolle et al., 2010). It is likely that many HPCs are aggregated along with mature hepatocytes at this stage due to cell-cell adhesion, which reduces the available cells. At this point, there are three main methods which have been utilized;

4.2.2.1 Isopycnic or density gradient centrifugation

This consists of layering the non-parenchymal cell suspension over Percoll, Optiprep, Nycodenz or Ficoll, followed by centrifugation and removal of the fraction

of interest containing the HPCs. This selects for cells based on density. The cells are then washed before being cultured.

4.2.2.2 Immunoselection

Magnetic assisted cell sorting (MACS) and fluorescence-activated cell sorting (FACS) have both been used to enrich populations based on positive and negative cell surface markers. Markers which have been employed include: c-Kit, CD45, TER119, c-Met, EpCAM, Sca-1, CD133 (Prominin-1) (Dolle et al., 2010). As stated earlier, markers are not specific and, as the liver is a heterogeneous organ with many cell types, pure populations are not achieved. Wauthier et al. (2008) stated that human hepatic progenitor cells are highly susceptible to shear-stress during FACS and also buffer composition such that few human progenitor cells are viable for culture after the FACS process. As a result, this group has used MACS exclusively since to isolate HPCs. Although MACS has the potential for much higher viability of the resultant cells, the purity is much lower (Wauthier et al., 2008).

4.2.2.3 Antigen selection for MACS sorting

Epithelial cell adhesion molecule (EpCAM), which is a transmembrane glycoprotein responsible for cell to cell adhesion in epithelial cells has been used to for MACS selection for both human and rodent HpSC and HB (Schmelzer and Reid, 2008; Schmelzer et al., 2007). These HPC co-expressed CD133 and keratin 19. Keratin 19 is an intracellular cytoskeletal protein and thus not available for viable cell selection. CD133 is another transmembrane protein, the function of which is unclear but has been shown to be expressed on haematopoietic and endothelial progenitor cells, as well as a marker for a putative cancer stem cell population (Irollo and Pirozzi, 2013). CD133 has been used to select for hepatic progenitor cells in rodents (Rountree et al., 2011; Suzuki et al., 2008). Canine hepatic progenitor cells have been shown to have increased gene expression of CD133 compared to primary hepatocytes whereas the status of EpCAM expression on canine HPCs is unknown. (Arends et al., 2009a).

4.2.2.4 Side population isolation

The ability of cells to efflux the dye Hoechst33343 due to expression of the ABCG2 transporter, coded by the multidrug resistance gene (MDR1), has been used to isolate a fraction of cells known as the "side population" (SP). In the murine and human liver, the SP has been shown to have HPC characteristics. Some studies have selected against CD45 which is found on many cells of haematopoietic origin however, both CD45 positive and negative fractions can demonstrate hepatocyte differentiation *in vitro* (Hussain et al., 2005; Shimano et al., 2003; Terrace et al., 2009). Many other cells in the liver other than HPC also express this transporter protein including haematopoietic stem cells (Forbes and Alison, 2006)

It is of note that the vast majority of studies isolating the HPC compartment in rodents do so after experimental induction of a ductular reaction e.g. using carbon tetrachloride or galactosamine (Shupe et al., 2009). This greatly increased the HPC percentage in the liver and as a result the number of cells isolated. In human tissue, a period of ischaemia (up to 168 hours) has been shown to select for HPC by their apparent resistance to cold ischemia compared to the other resident cell types (Aupet et al., 2013; Stachelscheid et al., 2009). The number or percentage of HPC isolated depends therefore not only on the starting tissue but also the method of selection. As an approximate percentage, human hepatic stem cells are stated to make up approximately 0.5-2.5% of the parenchyma (Schmelzer et al., 2007).

4.2.3 Culture of hepatic progenitor cells

Many different substrates and culture media have been described for expansion of HPC. For culture substrates, collagen type I is most commonly documented, although hyaluronic acid has been used (Fiegel et al., 2006; Gerbal-Chaloin et al., 2010; Sasaki et al., 2008). One group which has advanced the understanding of hepatic progenitor cells and the subdivision between HpSC and HB have published a

detailed methods paper describing the options for culture, expansion and differentiation of human HpSC and HBs (Wauthier et al., 2008). There is evidence that *in vivo*, HpSC are coordinated with angioblasts and hepatic stellate cell precursors and these cells interact, stimulating co-differentiation. This is termed an epithelial-mesenchymal relationship. Culturing HpSCs with mesenchymal co-cultures, mimicking co-culture with conditioned media or, if paracrine signals are known, in defined media is likely to be most successful. Media has also been described by the methods paper, with Kubota's media allowing expansion of human and rodent HpSC (Kubota and Reid, 2000).

4.2.4 Morphology of HPC *in vitro*

In vitro HpSC are reported be 7-10μm and form colonies which are densely packed whilst HB cells are approximately 10-20μm and form cord-like morphology with clear channels between cells (Schmelzer et al., 2007).

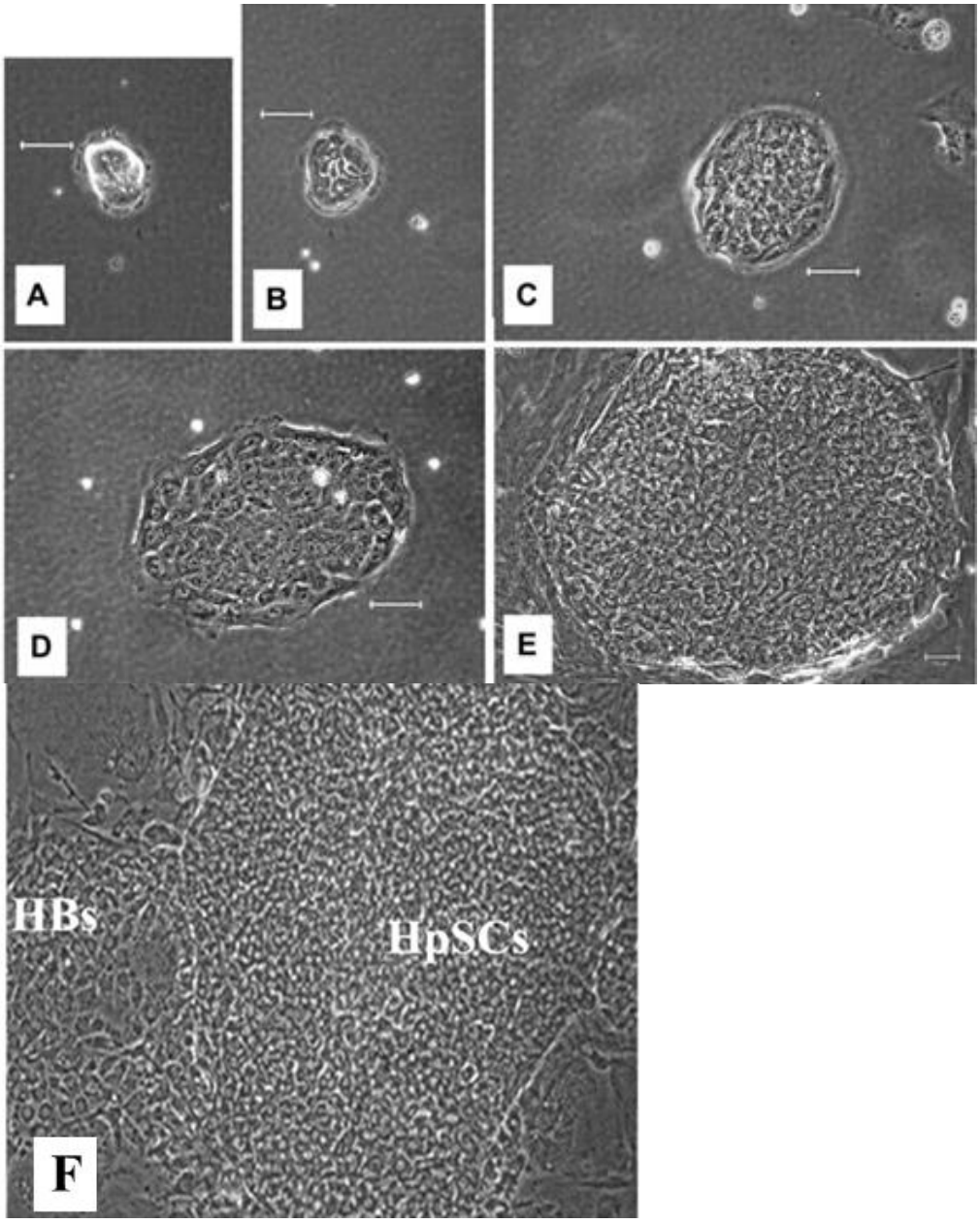

Figure 4.2 Human hepatic stem cells (HpSC) and hepatoblasts (HBs) in vitro. A-E demonstrate HpSC colony at days 2, 4,8,10 and 14. F demonstrates the morphological difference between hepatic stem cells and hepatoblasts. White bar represents 20µm. Images from Schmelzer et al. (2007).

4.2.5 Canine hepatic progenitor cells

There have been two reports investigating isolation of the hepatic progenitor cell compartment of canine liver. Arends et al. (2009b) utilized Hoechst 33343 after density centrifugation to isolate the side population from four normal canine livers. The SP comprised 2.8% $\pm$ 1.2% of the total non-parenchymal fraction. Thirty percent

of these were CD45 negative by FACS. The cells were reported to be small (8-10μm) and keratin7 positive on immune-staining. There was significantly higher ABCG2 gene expression between the CD45-ve SP and main population (MP) but it is not stated if the SP had significantly higher ABCG2 compared to the MP. Transporter inhibitors verapamil and reserpine also did not completely remove the SP and therefore lack of Hoechst 33343 fluorescence may not be specific for the presence of the ABCG2 transporter. Extremely low cell numbers were isolated (approximately 1 $x10^4$ cells in the SP) which prevented culture.

Culture of canine hepatic progenitor cells has also been described (Arends et al., 2009a). Prior to euthanasia the dogs received 10,000IU of heparin. After cell dissociation, the cell suspension was centrifuged in 55% Percoll to remove large hepatocytes (50g for 10 minutes) and the resultant cellular supernatant was pelleted and re-suspended in a proprietary hepatocyte culture media HCM (Hepatozyme, Invitrogen) or William's media E and supplements (WME). Cells cultured in WME were stated to be fibroblastic and died after 14 days. Cells in HCM exhibited mature hepatocyte morphology with binucleate cells. After 2 weeks smaller cell colonies appeared which expanded and then appeared to differentiate towards hepatocyte-like cells (Figure 4.3). These were stated to occur at a frequency of one colony per 4.5 – 80 x 10^4 cells.

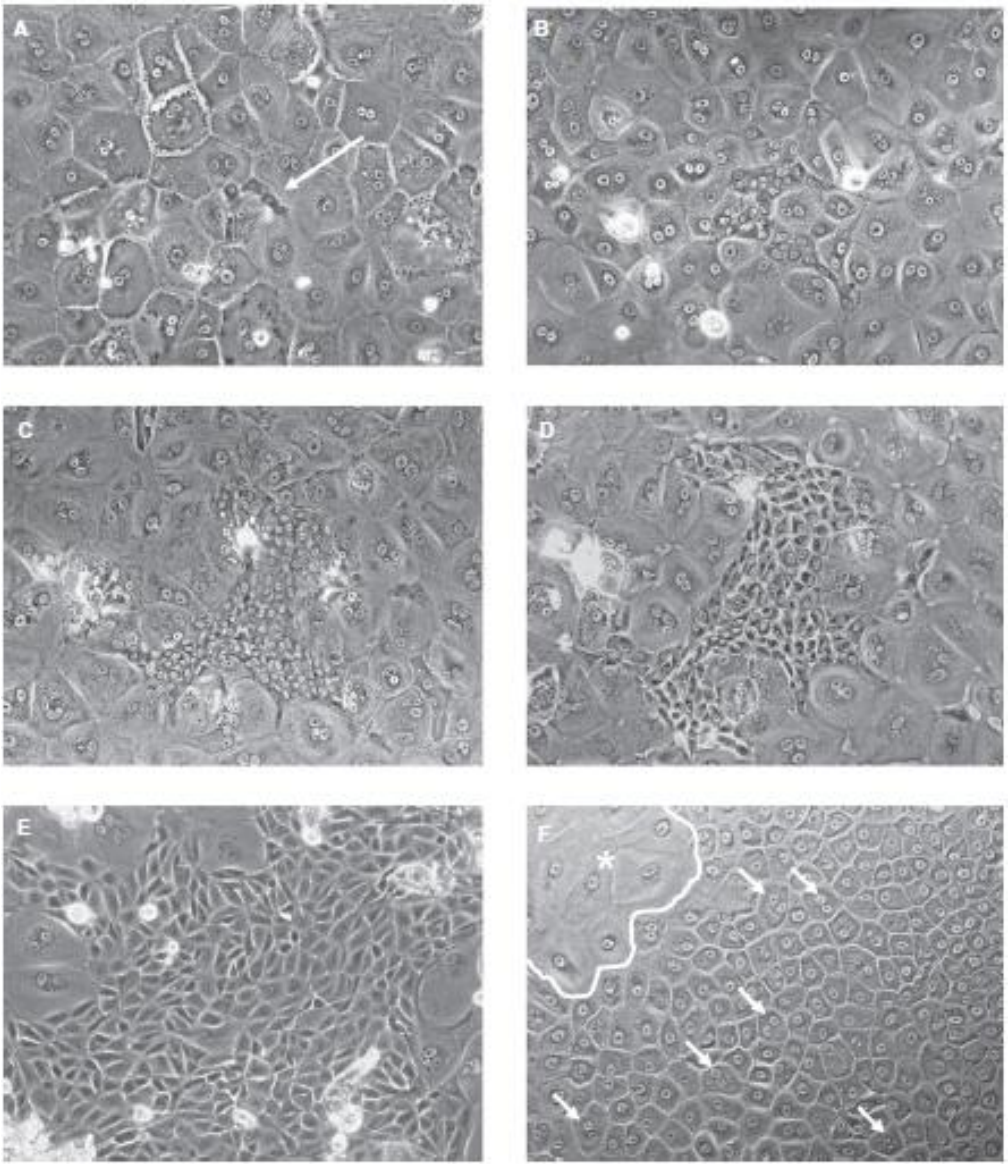

Figure 4.3 Figure from Arends et al. (2009a) demonstrating morphology of cultured cells.
Initial mature hepatocyte morphology with few smaller cells after 2 weeks arrowed (A), gradual expansion of small cells (B-D) and eventual increase in cytoplasm to nuclear ratio with some binucleate cells arrowed (F). Images x200.

Cells were stated not to passage and expand readily and appeared to require surrounding hepatocytes or Matrigel. The smaller colonies were positive for keratin 7 by immunostaining. At the 2 week point, gene expression demonstrated that the colonies expressed significantly more *Cyp1A2*, albumin, keratin 7, 18, 19, αfoetal protein and CD133 than surrounding hepatocytes.

4.3 Aims

The aims of this chapter were to assess if hepatic progenitor cells could be isolated and expanded from euthanased dogs without prior treatment with heparin. Additionally, methods to improve the selection of the hepatic progenitor compartment compared to the previous canine study were examined, specifically, density centrifugation with Percoll and Ficoll as described in human and rodent HPC isolations as well as MACS for $CD133^{+}$ cells.

The effect of Kubota's culture media, which has been described as supporting the expansion of rodent and human HpSC was examined on the ability to expand and passage canine HPC. Passaging using standard 0.25% trypsin, Accutase and mechanical dissociation was assessed. Finally, laminin and collagen Type I coated tissue culture plastic was compared for passaged colonies.

4.4 Methods

4.4.1 Isolation of non-parenchymal cell fraction

Canine hepatic tissue was processed as described in Chapter 3 to isolate a suspension of dissociated cells. The suspension was centrifuged for 5 minutes at 30g to pellet mature hepatocytes. The supernatant was transferred to a fresh Falcon tube and centrifugation repeated to pellet any remaining mature hepatocytes. The supernatant containing the non-parenchymal cell (NPC) fraction was then centrifuged at 400g for 30 minutes to pellet these cells. The cell pellet was re-suspended in HCM with 10% FCS (Lonza).

4.4.2 Density centrifugation

4.4.2.1 Percoll

Nine parts Percoll (GE Healthcare) was diluted with 1part 1.5M NaCl to give a stock solution. This was then further diluted to 20% and 50% with 0.15M NaCl. A volume of 10mls of 20% was layered over 20mls of 50% in a 50ml Falcon tube. The NPC suspension was layered over this and the tubes centrifuged for 15 minutes at 500*g*. The cell layer between the two Percoll concentrations was removed, resuspended and washed in HCM twice before being re-suspended in HCM and transferred to collagen-coated 6 well plates.

4.4.2.2 Ficoll-Paque

The NPC fraction was layered onto Ficoll-Paque (GE Healthcare) and centrifuged for 15 minutes at 500g. The cell layer to the top of the interface was removed, washed and plated as described in the Percoll section.

4.4.3 Magnetic assisted cell sorting for CD133

The system supplied by Miltenyi Biotech was used for MACS sorting. NPC were re-suspended in PBS containing 0.5% bovine serum albumin. Positive selection CD133/1 columns (Miltenyi Biotech) were used according to the manufacturer's instructions. Briefly, the column was placed in the magnetic holder and the cell

suspension passed through the column. Negative cells passed through the column and were collected. Positive cells were bound by the column until it was removed from the magnetic field, the column flushed with buffer and the resultant cells collected.

4.4.4 PCR analysis of fold increase in gene expression

Relative gene expression of CD133 and keratin 7 was calculated using B2MG and RLP8 as reference genes using MXPro QPCR software.

4.4.5 Passaging of HPC colonies

4.4.5.1 Enzymatic

Cloning cylinders (ScienceLab, USA) were placed around selected colonies and 0.25% trypsin EDTA (Invitrogen) or Accutase (Life Technologies) was added. Plates were then incubated at 37^{o}C until dissociation was evident using microscopy.

4.4.5.2 Mechanical passaging

A 200µl pipette tip was used to gently loosen the edges of a colony which was then aspirated into a 1000 µl pipette for passaging.

4.4.5.3 Kubota's medium preparation

Kubota's medium was prepared as described by Kubota and Reid (2000) and the formulation detailed in Appendix 3.

4.5 Results

4.5.1 Percoll isolated cells are few in number and fail to expand

Six HPC isolations were performed using Percoll (Appendix 4 lists HPC isolations performed). The initial four appeared to have very few viable cells and a large amount of cellular debris after washing. This made cell counting impossible. After removing debris at 48 hours and culture for a further 4 days, few cells adhered to the collagen coated-plate and these appeared to be mixed morphology (Figure 4.4 A and B). In subsequent experiments, likely due to improved perfusion/digestion and cell handling techniques, there was less debris present and small clusters of adherent cells were visible (Figure 4.4C and D). These were of morphology consistent with HpSC i.e. compact rounded cells; however, these cells did not expand and over the subsequent seven days, gradually became detached or died during culture. Insufficient cells were present to allow further analysis

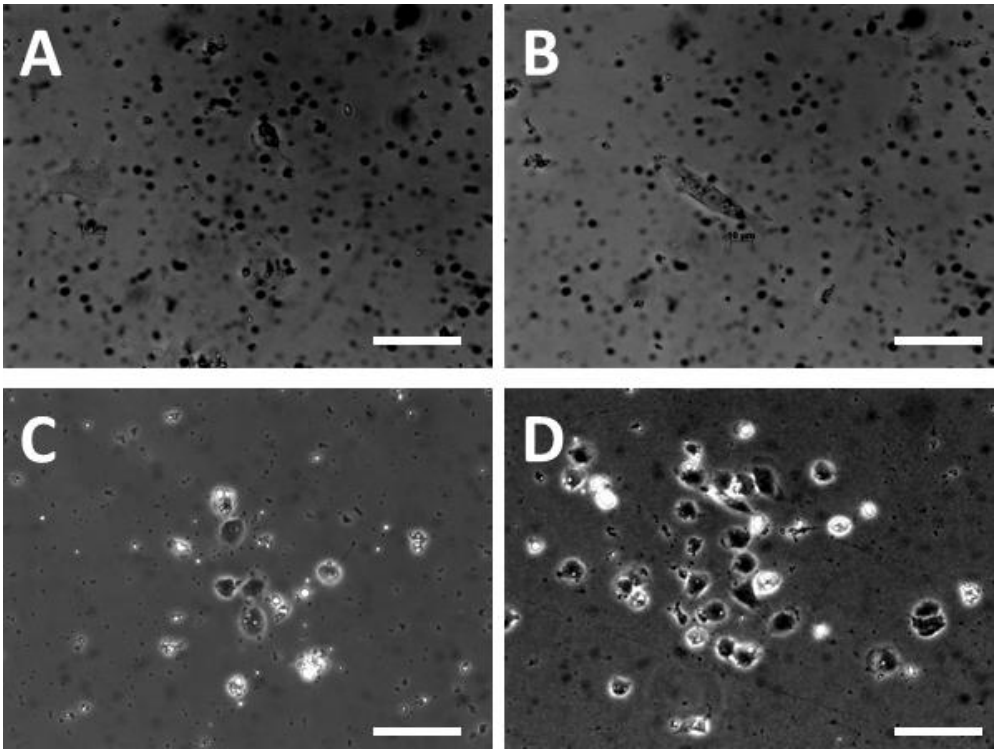

Figure 4.4 Morphology of cells after initial Percoll isolation
Representative images from first four experiments (D19811a), a large amount of debris present with very sparse cells of mixed morphology (A, B). Representative images from experiments 5-6, much less debris present and few colonies of compact round cells present (C, D). White scale bar represents 50µm.

4.5.2 Ficoll centrifugation isolates a mixed cell population

Three experiments were performed using Ficoll to isolate the HPC compartment using the NPC fraction from animals D18112a, D18112b and D8212. In the first two, no viable cells were present after 48 hours' culture. In the last experiment, an extremely heterogeneous cell population was cultured with cells resembling macrophages and fibroblasts present in the largest quantities after 6 days' culture (Figure 4.5). Few cells consistent with HpSC or HB morphology were evident and the culture was discarded after 14 days' due to fibroblast overgrowth.

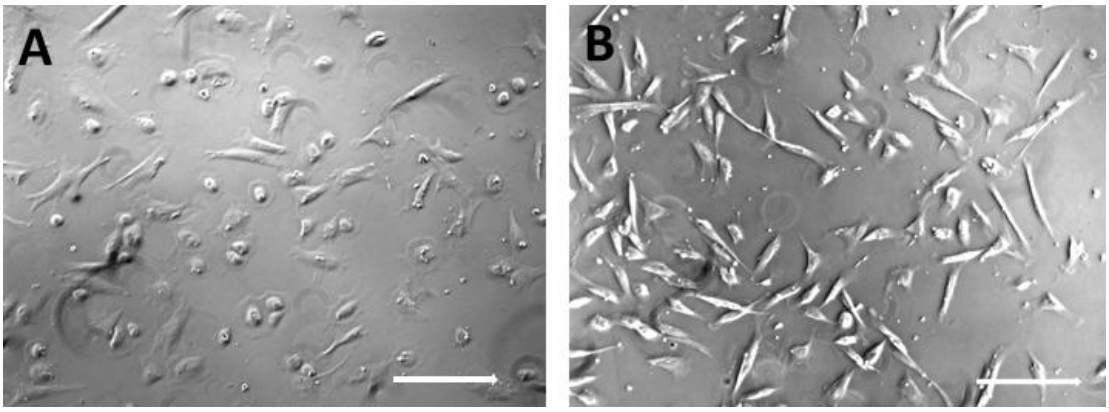

Figure 4.5 Cell morphology after Ficoll isolation and 6 days' culture.
Two representative fields shown (A and B). White bar represents 50µm.

4.5.3 CD133 selection enriches for hepatic progenitor cells

As expression of EpCAM on canine HPC was unknown, $EpCAM^+$ HPC in other species co-express CD133, and Arends et al. (2009a) demonstrated CD133 expression by canine HPC, CD133 was used for canine HPC isolation.

4.5.3.1 Cell numbers

The NPC fraction from D22212 was used for this experiment: 1.5 $x10^8$ cells were sorted and a total of 1.3 $x10^8$ cells were retrieved; 8.5 $x10^7$ were in the negative fraction with 5.2 $x10^7$ in the positive fraction. This gave a positive percentage of 38%.

4.5.3.2 Morphology

Twenty-four hours' after attachment, the morphology of the two cells types appeared similar, with the majority of cells having the morphology of small hepatocytes with a large cytoplasm to nuclear ratio and, polygonal structure with clear demarcation between cells (Figure 4.6).

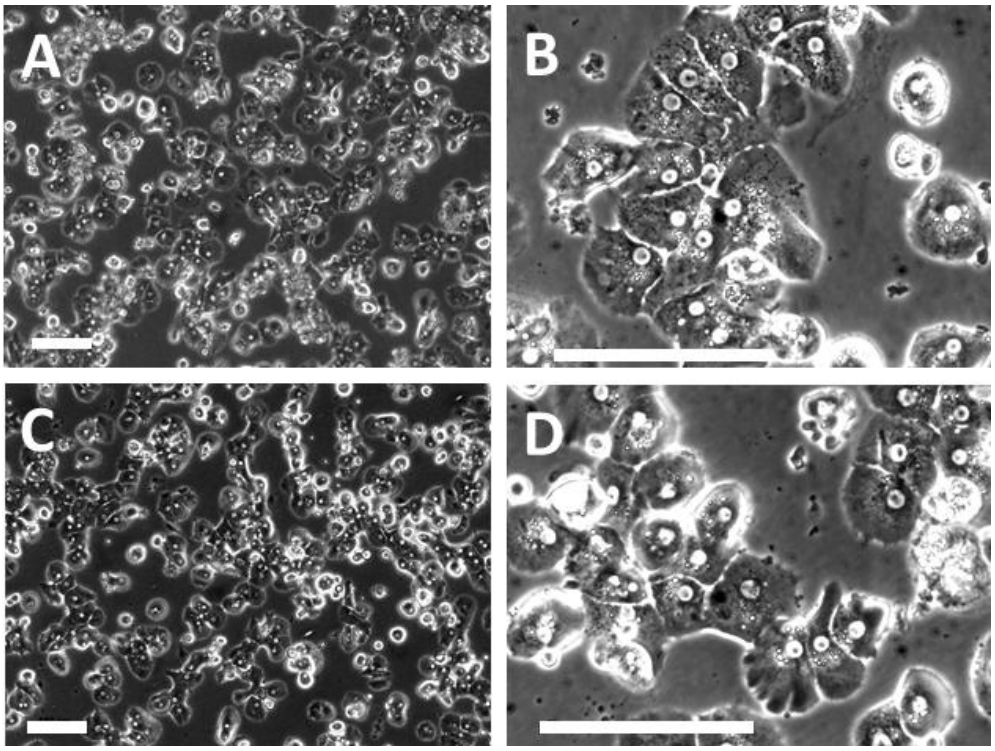

Figure 4.6 Morphology of CD133 positive and negative cells 24 hours after sorting
$CD133^+$ fraction (A, B) and negative fraction (C, D). Both contain small hepatocyte-like cells with no obvious difference between the two cultures. White scale bar represents 100µm.

These cultures were continued with a media change every 2-3 days. By day 7, mainly, but not exclusively in the CD133 positive cultures, small colonies of HB type cells appeared which expanded slowly, appearing to force out the resident cells. In the CD133 negative cultures, many more fibroblastic appearing cells were present which expanded and overgrew the plate. By 14 these differences were dramatic (Figure 4.7). Clusters of small round loosely adherent cells which appeared to attach to the underlying monolayer were also present in the CD133 positive population.

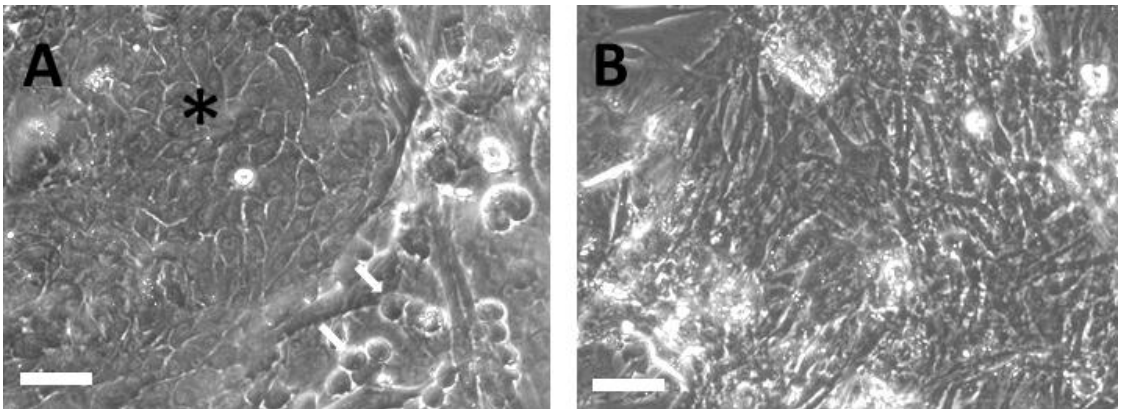

Figure 4.7 Morphology of CD133 positive and negative cultures after 14 days. $CD133^+$ cells (A) demonstrating expansion of hepatoblast like cells (*). Loosely adherent round cells marked by white arrows. $CD133^-$ cells containing a majority of fibroblast-like cells. White scale bar represents 50µm.

4.5.3.3 Keratin 7 gene expression is higher in CD 133 positive fraction.

RNA was extracted at the time of the initial sort and after culture for 14 days. After the initial sort, both CD133 and keratin 7 gene expression was higher in the $CD133^+$ fraction (Figure 4.8). After 14 days' culture, a differential between positive and negatively sorted cells remained but was less marked (Figure 4.9). When the $CD133^+$ cells at initial sort and adherent cells were compared, culture had caused a dramatic reduction in both CD133 and K7 expression (Figure 4.10).

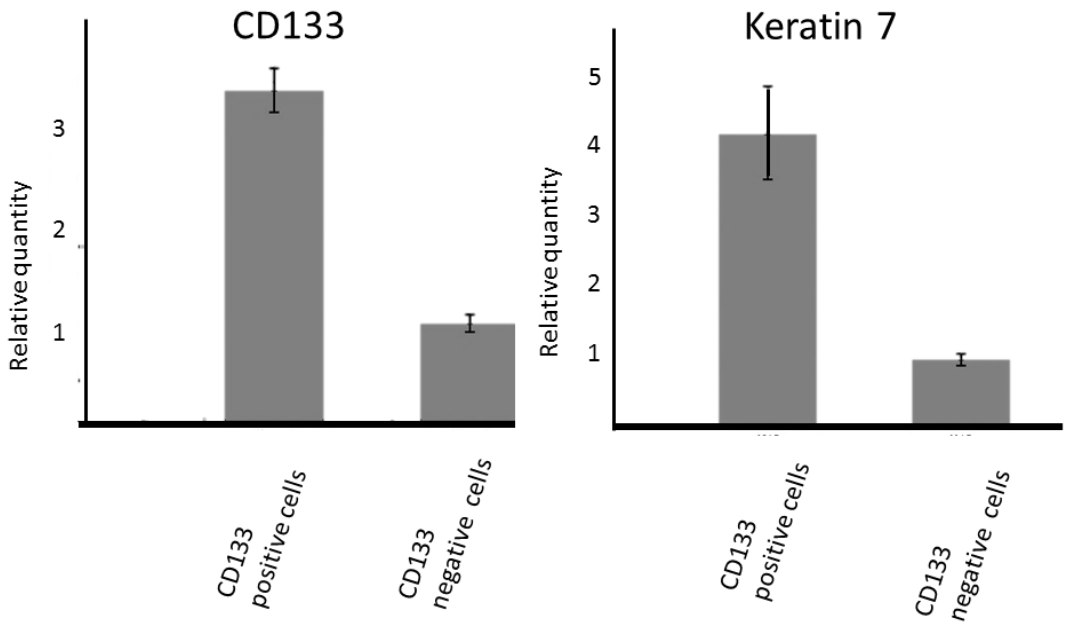

Figure 4.8 Fold increase of CD133 positive cells compared to CD133 negative cells of CD133 and Keratin 7.
CD133 negative cells are used as the calibrator. Error bars represent standard error of the mean.

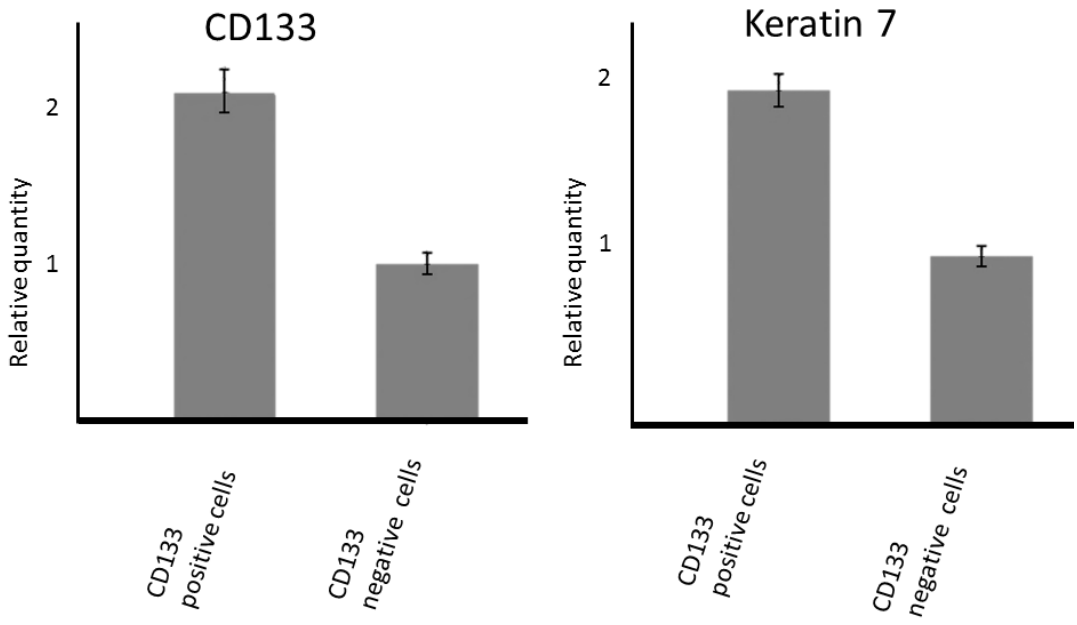

Figure 4.9 Fold increase of CD133 positive cells compared to CD133 negative cells of CD133 and Keratin 7 after 14 days in culture.
CD133 negative cells are used as the calibrator. Error bars represent standard error of the mean.

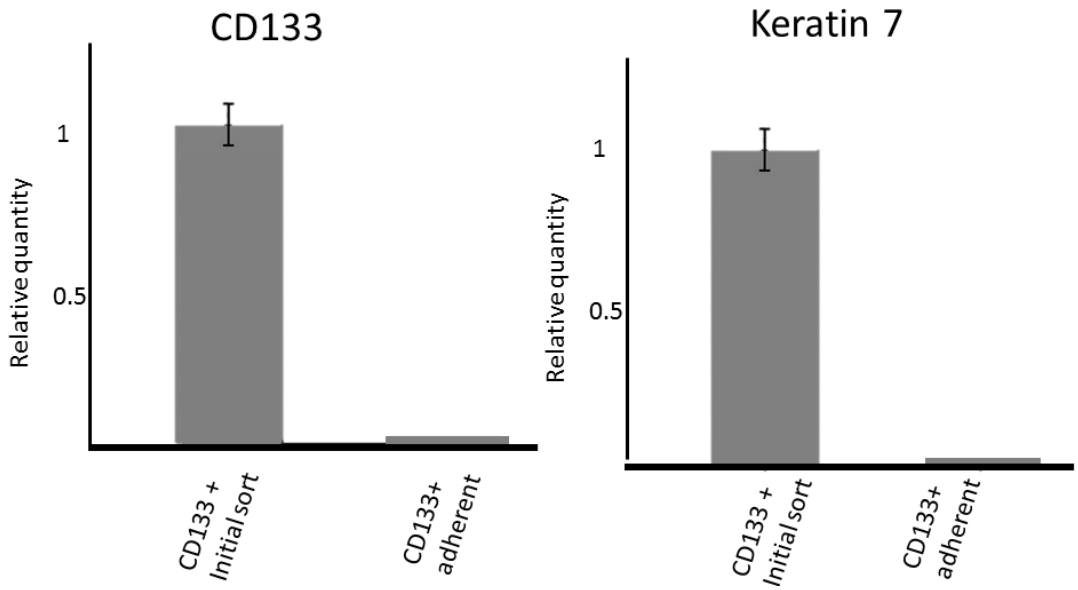

Figure 4.10 Comparison of CD133 and keratin 7 expression of CD133 positive cells before and after culture.
Initial sort cells are used as the calibrator. Error bars represent standard error of the mean.

4.5.4 Mechanical passaging is more effective than enzymatic

Colonies from the CD133 positive cells were passaged using 0.25% trypsin, Accutase® and mechanical dissociation onto fresh 0.01% collagen-coated and 100µg/ml laminin-coated wells. Between 3-6 colonies were passaged by each method to each matrix type. All enzymatic methods failed to yield viable cells after transfer onto collagen and laminin plates. Mechanical passaging achieved viable colonies on both collagen and laminin. These cells formed colonies with the smaller round loosely adherent cells in the centre and larger HB-like cells at the periphery (Figure 4.11). This appeared to be most organized in the laminin wells where the HB-like cells formed corded structures. The structure of the colonies and morphology of both cell types appeared very similar to that described by Schmelzer et al. (2007) for human HpSC and HBs (Figure 4.12). The canine colonies failed to continue expanding in both substrates and detached from the collagen-coated wells. The largest colony on laminin-coated wells was 900µm.

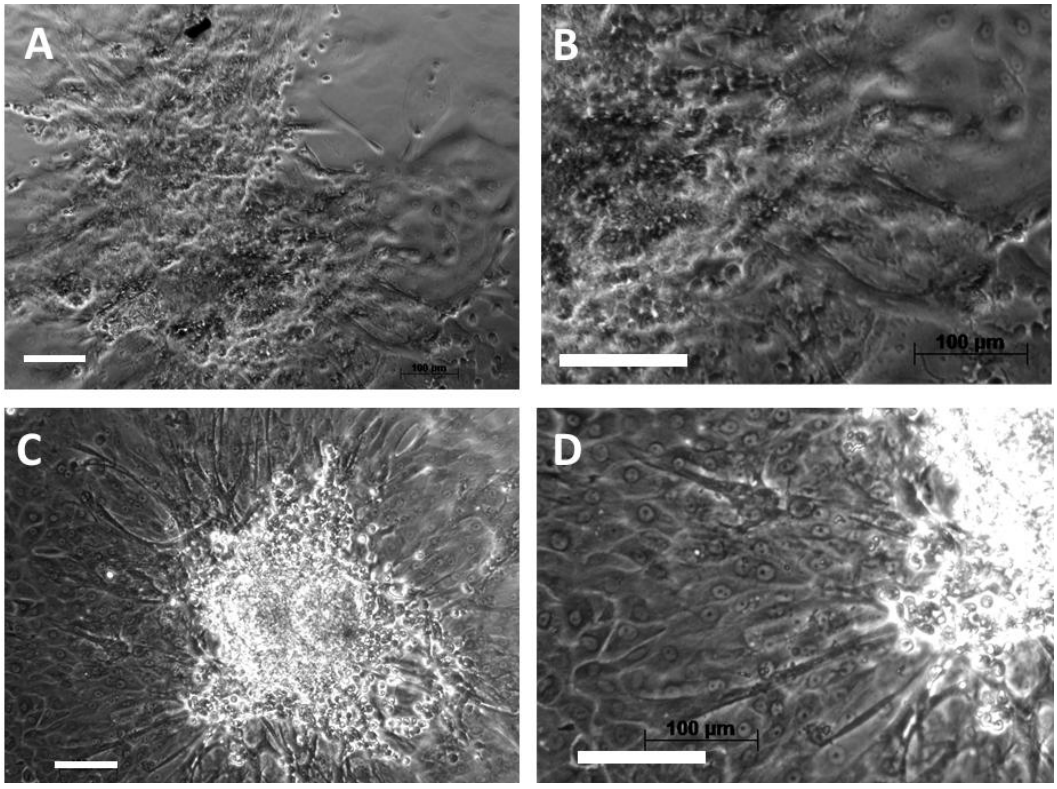

Figure 4.11 Colonies passaged onto collagen and laminin
Colonies on collagen (A, B) contained small round cells in the centre with larger cells present in a haphazard pattern at the periphery. Laminin wells also contained dense colonies of round loosely adherent cells with larger cells forming corded structures at the periphery. White scale bar represents 100µm.

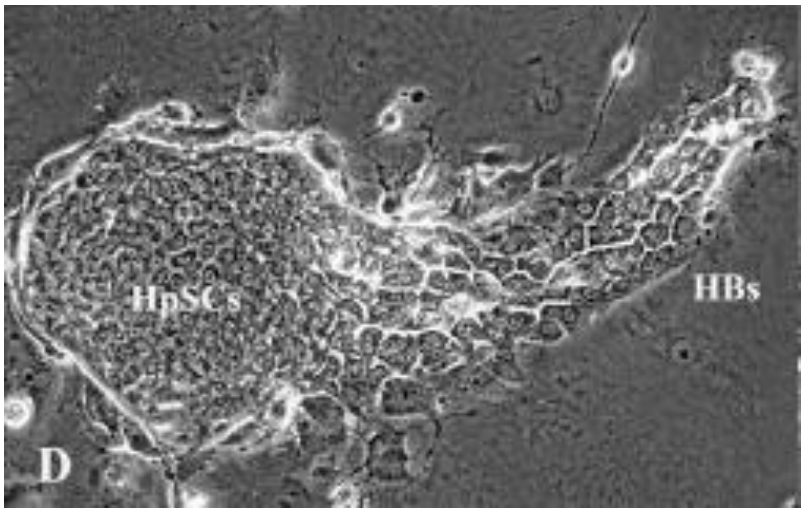

Figure 4.12 From Schmelzer et al. (2007) demonstrating human hepatic stem cells (HpSC) and hepatoblasts (HB)

4.5.5 Treatment with Accutase® reduces CD133 positive fraction

As only a very small percentage (0.5-2.5%) of the NPC fraction would be expected to be positive for CD133, and both positive and negative cell morphology appeared similar initially, it was suspected that cell-cell adhesions and clumping was falsely elevating the CD133 positive number (Schmelzer et al., 2007). This has been reported to be a problem with MACS of the NPC fraction and the addition of an Accutase step has been recommended to inhibit re-aggregation (Wauthier et al., 2008). Therefore the NPC fraction was incubated in Accutase for 5 minutes prior to sorting and starting number was reduced 10-fold.

Cells from D13912 were used for this experiment. Due to the small cell numbers retrieved, all cells were plated. After 24 hours in HCM, media was changed to Kubota's media to select for HpSCs.

4.5.5.1 Cell numbers

Of the 1.5 $x10^7$ cells sorted, a total of 1.1 $x10^7$ cells were retrieved. 101 $x10^5$ were in the negative fraction with 9 $x10^5$ in the positive fraction. This gave a positive percentage of 8.9%.

4.5.5.2 Cell morphology

There was a mix of morphologies in both fractions after 24 hours culture (Figure 4.13). Subjectively the positive fraction contained more small hepatocyte-like cells. Forty-eight hours' in Kubota's medium appeared to cause massive cell loss with only large macrophage-like cells remaining (Figure 4.14 A, B). Canine primary hepatocytes were also cultured in Kubota's media for 48 hours and became poorly adherent and changed morphology (Figure 4.14 C, D). After 72 hours, no viable cells were present in the CD133 positive wells.

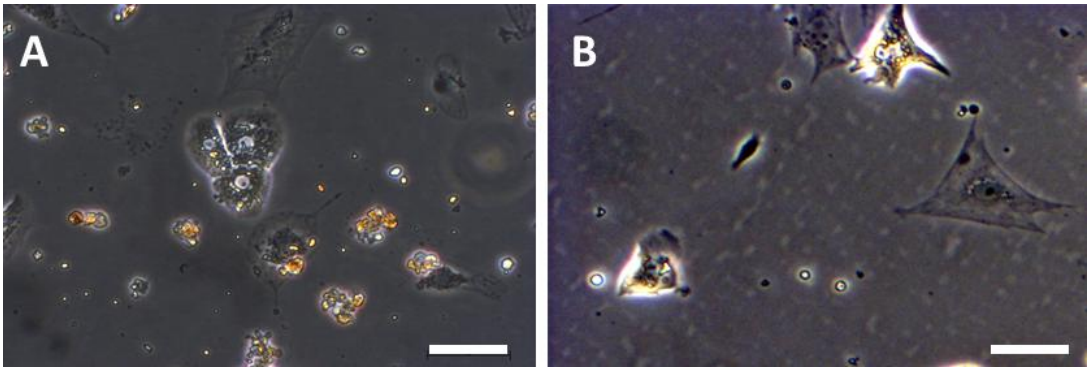

Figure 4.13 CD133 sorted cells after 24 hours culture
CD133 positive fraction (A) contained more small hepatocyte-like cells compared to the negative fractions (B) were morphology was more heterogeneous. Both fractions still contained a mix of cell morphologies. White scale bar represents 50µm.

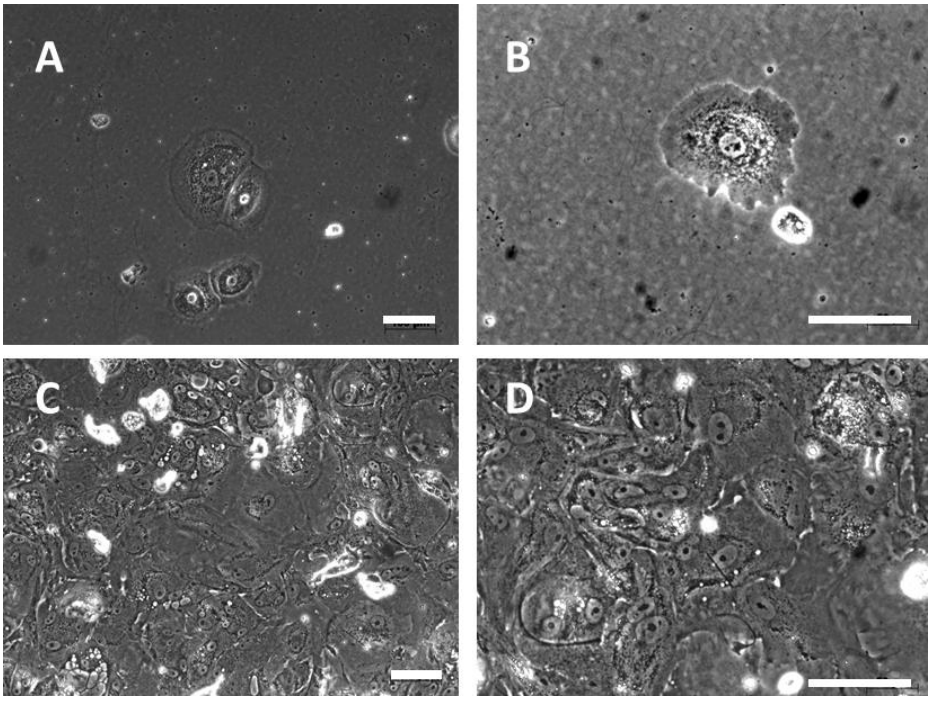

Figure 4.14 Cell culture of CD133 positive cells and primary hepatocytes after 48 hours in Kubota's media.
CD133 positive wells (A, B) contained only very few large cells of macrophage morphology with loss of small hepatocyte-like cells. Canine primary hepatocytes had a rolled appearance with detached edges (C, D). White scale bar represents 100µm.

4.6 Discussion

4.6.1 Isodensity centrifugation isolates low cell numbers which do not expand

Using Percoll, only a very small number of viable cells were isolated and large amounts of debris was also present in the fraction of interest. The cells isolated appeared small, round cells which are morphologically consistent with HpSC. These cells failed to expand in culture and were gradually lost. The Percoll experiments were performed during the period where hepatic perfusion was being optimized and it is likely that the low cell yield and large amounts of debris are, in part, reflected by this. Ficoll centrifugation appeared to isolate a much larger cell population but one that appeared heterogeneous with many fibroblastic and macrophage-like cells present. As Ficoll is primarily aimed at isolation of haemopoietic mononuclear cells and mesenchymal stem cells this is perhaps unsurprising. Characterisation of the resultant cells by immunocytochemistry for mesenchymal and macrophage markers would have further explored this likelihood. Insufficient cells were isolated for FACS analysis.

Schmelzer et al. (2007) stated that MACS sorting obtained the most satisfactory results and therefore this technique was pursued as an alternative. It is possible that with refined tissue processing and cell handling, the Percoll technique may have yielded reasonable quantities of viable HPC. The ability to vary Percoll density would also allow specific cell densities to be separated and may have further selected specifically for canine HPC.

4.6.2 MACS sorting for CD133 positive NPC selects for hepatic progenitor cells

The initial sort gave a much higher percentage of apparent CD133 positive cells than expected (38% versus 0.5-2.5% respectively). After 24 hours culture, both positive and negative fractions appeared morphologically similar with mainly small hepatocytes present. The most likely explanation for this is the continued presence of large numbers of hepatocytes in the “non-parenchymal cell fraction”. Wauthier et

al. (2008) noted that cell aggregation was a problem during MACS sorting resulting in an impure population of cells due to insufficient dissociation during tissue processing resulting in antigen negative cells remaining bound to antigen positive cells as well as re-aggregation during the isolation process. Despite this problem, CD133 positive cells demonstrated increased CD133 gene expression and also keratin 7 compared to CD133 negative cells, suggesting that MACS sorting was successful in enriching for CD133 positive cells. Although keratin 7 is expressed in HPC it is also expressed in cholangiocytes and is therefore not specific (Arends et al., 2009a; Wauthier et al., 2008). Treatment with cell dissociation agent has been recommended to reduce cell aggregation during sorting and this was performed during the next experiment (Wauthier et al., 2008). Repeated exposure of the cells to enzymes has the disadvantage of reducing viability of these fragile cells (Wauthier et al., 2008). Use of Accutase reduced the percentage of CD133 positive cells to nearer the expected percentage. Another option which has been described is to use serial MACS columns to further purify the cells expressing only the antigen of interest (Beier et al., 2007). This would have the disadvantage of subjecting the cells to longer periods in sub-optimal conditions, likely further reducing their viability.

4.6.3 Canine HPC can be expanded *in vitro* as primary culture

Morphologically, dense colonies of cells consistent with the description of human hepatoblasts *in vitro* appeared in culture. These appeared to arise at the edges of clusters of small bright round cells that appeared to be situated on top of the mono-layer. These cells may be consistent with hepatic stem cells as described by Wauthier et al. (2008). Although present in higher numbers, these two cell types were not exclusive to the CD133 positive population, possibly reflecting the impurity of the two populations. These cells, and particularly the HB expanded during culture. Examination of CD133 and keratin 7 gene expressions after 14 days culture revealed down-regulation of both. Human HpSC and HB are both reported to express CD133 but this is lost during differentiation towards hepatocytes (Wauthier et al., 2008). Arends et al. (2009a) noted that keratin 7 expression of canine HPC

was lost during culture. Therefore it is likely that cell differentiation was occurring during culture.

It appeared that Kubota's medium did not support the expansion of canine HPC although this would have to be confirmed as it is possible that other factors, for example, individual donor variation or the additional treatment with Accutase™ may also have contributed to reduced viability. The increased purity of CD133 positive cells i.e. reduce supporting cells, may also have affected viability of the HPC.

4.6.4 Mechanical picking allows passaging of viable HPC colonies

Enzymatic dissociation methods were unsuccessful in passaging the cells, however mechanical colony picking allowed viable colonies to be transferred. This is identical to what has been described with human HPC where mechanical picking was recommended (Wauthier et al., 2008). Passaging onto collagen-coated plastic allowed viable cells to adhere however the morphology appeared to change with random organization of cells and less obvious HpSC-morphology. A similar phenomenon has been reported by McClelland et al. (2008) where human HpSC became unstable on collagen type I. Laminin-coated tissue culture plastic appeared to give cell morphology most similar to that described for human HpSC with surrounding differentiated HB. Further expansion after culture was minimal which prevented further characterisation of the cells. Human HB colonies are reported not to expand to any great extend compared to HpSC (Schmelzer et al., 2007). Additionally, the isolated cells did not survive culture in Kubota's medium which has been described for the culture of human HpSC. It has been stated that Kubota's medium does not support HB growth without the presence of feeder cells (Schmelzer et al., 2007). In normal adult human hepatic tissue HpSC make up the overwhelming majority of HPC therefore, if this was the case in canine liver, expansion of cells would have been expected. It is possible that mainly canine HB were cultured either due to HB isolation or differentiation of HpSC to HB during the initial isolation and culture period.

It is notable that canine HPC did not expand under low seeding density and appeared to expand most readily in contact with many other cells of mixed morphology. Particularly the smaller HpSC-like cells appeared to expand into colonies admixed with other cell types. The hepatic stem cell niche has been described with HpSC partnered with angioblasts and hepatic stellate cells, both of which are also CD133 positive (Hristov and Weber, 2004; Kordes et al., 2007). It is likely that in some respects, the low purity of MACS sorting may be beneficial in the subsequent culture of HPC as a mixture of supporting cell types are required for HPC expansion *in vitro* (Wauthier et al., 2008). Despite the expansion, the cell numbers and colony sizes remained small. Interestingly, co-culture of HpSC with mature hepatocytes or media conditioned by mature hepatocytes prevents expansion on human HpSC (Wauthier et al., 2008). Therefore, the mixture of cells present may represent a double-edged sword; angioblasts, stellate and other mesenchymal cells supporting HPCs, whilst mature hepatocytes inhibit their expansion.

4.6.5 Methods of improving expansion

Further work at expanding these cells to a sufficient quantity to allow characterisation would be directed towards more tightly control culture conditions and utilizing co-cultures. The culture conditions for human HpSC and HB have been defined by Wauthier et al. (2008) who recommend co-culture with mitomycin-treated foetal mesenchymal feeder cells in a laminin coated Transwell™ system for HpSC. As the isolated canine cells appear to expand in concert with other cells, and laminin matrix allowed continued survival of passaged cells, this would appear to be a useful direction. Canine embryonic fibroblasts are available and these may be useful feeder cells.

4.6.6 Could HPCs arise from de-differentiated mature hepatocytes?

Finally, there are recent papers that describe highly purified mature hepatocytes in culture which de-differentiate to HPC with bipotential differentiation capacity (Chen et al., 2012a; Krause et al., 2013). This raises the possibility that HPC were not isolated but rather that they arose in culture from contaminating mature hepatocytes. This is especially a problem with heterogeneous populations as above and in the previously published paper describing canine hepatic progenitor cell culture (Arends et al., 2009a). Again, having a more precisely defined starting population and culture conditions would allow this possibility to be investigated. Performing a similar experiment to Chen et al. (2012a) where highly purified canine hepatocytes are cultured and examined for the appearance of hepatic progenitor cells would assess if this can occur in canine hepatocytes. Ultimately, as the aim is to culture a source of hepatic progenitor cells that could be expanded and differentiated to provide continual supply of mature hepatocytes *in vitro*, the source may be less important and culture of primary hepatocytes would provide a vastly more simple method of HPC production.

4.7 Summary

- Percoll density centrifugation produced a very small number of cells, which failed to expand in culture. The poor cell yield may improve with optimisation.
- Ficoll density centrifugation yielded a mixed cell population morphologically consistent with fibroblasts and macrophages.
- CD133 MACS produced colonies morphologically consistent with HpSC and HB.
- Mechanical passaging of colonies onto laminin-coated plastic was most successful
- Cells expanded in mixed cell cultures, therefore co-culture systems as described for human HPC should be investigated for further expansion after passaging.

Chapter 5: Mesenchymal stem cell isolation, characterisation and tri-lineage differentiation

5.1 Abstract

Mesenchymal stem cells (MSC) have been used to produce many tissue types *in vitro* and also appear to have profound immune-modulatory effects both *in vitro* and *vivo*. This chapter discusses progress made in isolating MSC and standardising characterisation of MSC in fundamental research. The standard protocols for osteogenic, adipogenic and chondrogenic differentiation along with known transcription factors and cell signalling pathways are also described. Canine-specific MSC research and clinical use of MSC to date are also defined.

This chapter describes the isolation and characterisation of both canine bone marrow-derived MSC and canine adipose tissue-derived MSC. Both cell types could be isolated and cultured with standard protocols, with a greater yield of Ad-MSC. Strong adherence to plastic was noted, a minimum characteristic of MSC. Both cell types demonstrated identical cell surface antigen characteristics i.e. positive CD44, CD105 and STRO-1 expression whilst lacking haematopoietic markers CD45, CD11b and CD19. Ad-MSC and BM-MSC were then differentiated along the standard mesodermal tri-lineage (i.e. osteogenic, adipogenic and chondrogenic differentiation) using published protocols. These differentiated cells were analysed with cytochemical staining and also gene expression using real-time PCR. Both Ad-MSC and BM-MSC demonstrated convincing differentiation by staining. Gene expression analysis demonstrated profound up-regulation of adipocyte genes in both cell types after the adipogenic protocol. After the osteogenic protocol, Ad-MSC demonstrated dramatic up-regulation of osteoblast markers however the BM-MSC despite having extremely strong staining for calcification, showed no up-regulation. Chondrogenic differentiation demonstrated strong up-regulation of aggrecan in both cell types but no *SOX9* up-regulation.

The study demonstrates reliable isolation and expansion of both Ad-MSC and BM-MSC cells in the dog. Both MSC cell types have been robustly characterised and can be utilised for further studies of differentiation including hepatocyte differentiation.

5.2 Introduction

5.2.1 Mesenchymal stem cell isolation

Mesenchymal stem cells and their properties were first described in the 1960's by Friedenstein et al. (1966) when they were isolated from bone marrow. Since then, it has been recognised that MSC can be isolated from almost any tissue in the body (Crisan et al., 2008). There is much debate about the origin of MSC, with one hypothesis that they are perivascular pericytes (Bianco et al., 2010; Crisan et al., 2011) or, as was originally termed by Friedenstein et al. (1966), simply a subset of fibroblasts (Haniffa et al., 2009; Hematti, 2012). Whichever their provenance, MSC have been demonstrated to have the ability to differentiate *in vitro* not only into mesodermal tissue types but also to trans-differentiate into other tissue types such as neurones and hepatocytes (Jeong et al., 2013; Lee et al., 2012).

5.2.2 Defining mesenchymal stem cells

One of the challenges in MSC research is the vast array of isolation methodologies and lack of standardization of what should define an MSC (Bourin et al., 2013; Shen, 2013). The cells which are isolated from tissues (e.g. adipose tissue) by digestion and centrifugation are termed the stromal vascular fraction (SVF). This fraction is a heterogeneous population, composed of stromal and haemopoietic stem and progenitor cells, endothelial cells, erythrocytes, fibroblasts, lymphocytes, monocyte/macrophages and pericytes (Bourin et al., 2013). Subsequent culture, washing and passaging selects for tissue-derived stromal cells or MSC by removing the majority of haemopoietic elements. Different isolation and culturing methodologies will produce populations of varying heterogeneity.

This challenge has been partially addressed by Dominici et al. (2006) who defined minimal criteria for human BM-MSC and Bourin et al. (2013) for human Ad-MSC. Table 5.1 highlights the antigen combination recommended by Dominici et al. (2006). Bourin et al. (2013) stated that in addition to these markers, CD13 and 36

positivity and CD106 negativity would distinguish cultured Ad-MSC from BM-MSC. Other markers which have been utilized to define MSC are CD44 and STRO-1 (Bourin et al., 2013; Kern et al., 2006; Ning et al., 2011).

Positive Marker	Negative Marker
CD105	CD45
CD73	CD34
CD90	CD14 or CD11b
	CD79α or CD19
	HLA-DR
	CD14 or CD11b

Table 5.1 Minimum cell antigen markers defined by the International Society for Cellular Therapy to characterise bone marrow MSC.

As well as these cell surface markers, the cells should readily adhere to tissue culture plastic and demonstrate the ability to produce osteoblastic, chondrocytic and adipocytic lineages (Figure 5.1). Dominici et al. (2006) stated that staining with Alizarin red/ Alcian blue and Oil Red O respectively would be sufficient to show differentiation; however, Bourin et al. (2013) recommended the addition of quantitative expression of lineage specific proteins or genes. The rational for this being that the compounds stained are not cell-type specific e.g. lipid may be present in hepatocytes and myocytes as well as adipocytes.

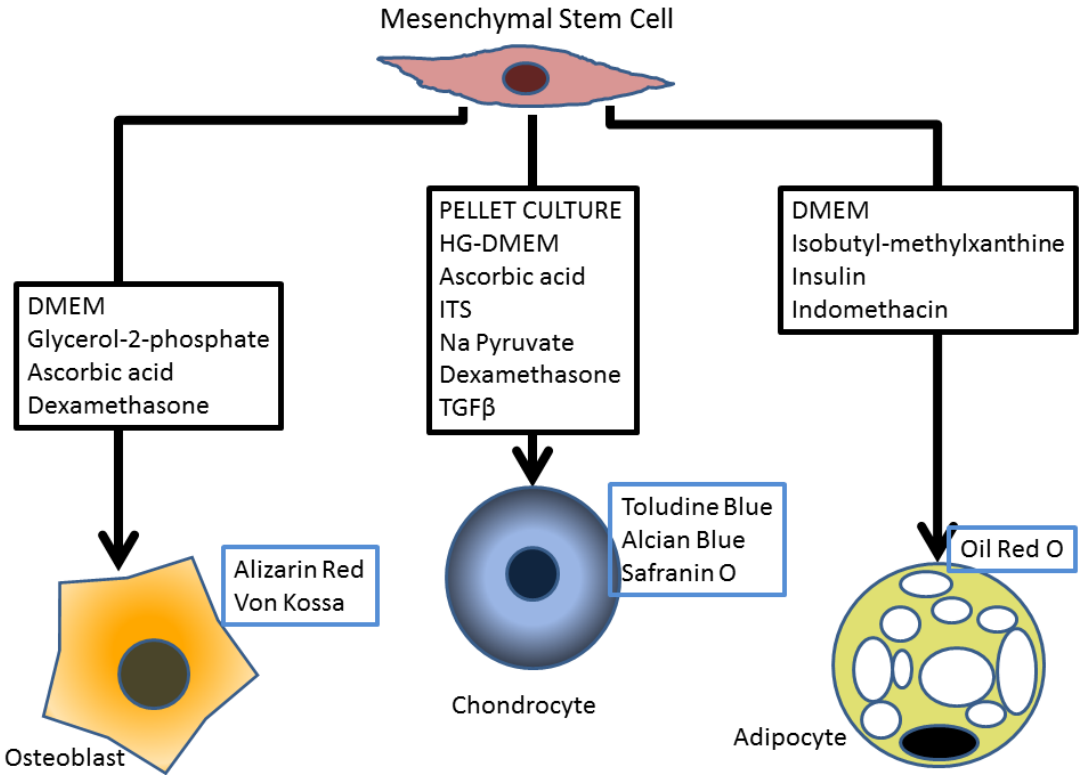

Figure 5.1 Common compounds used in MSC characterisation by differentiation Cytochemical stains commonly used are listed in blue boxes. DMEM – Dulbecco's modified Eagle's medium, HG – high glucose, ITS – insulin/transferrin/selenium premix.

5.2.3 Regulation of MSC differentiation

Cell signalling and gene expression to direct the fate of MSC either to remain as stem cells or towards differentiation is being elucidated. These studies will help inform optimum conditions to both expand undifferentiated MSC in vitro and allow directed, and optimum, differentiation.

5.2.3.1 Osteogenesis

Runx2 is the major controlling transcription factor in differentiation of MSC towards osteoblasts (Figure 5.2) (Cook and Genever, 2013). Experiments utilising overexpression demonstrated that Runx2 upregulates osteocalcin and collagen 1A1, causing osteogenesis both *in vitro* and *in vivo*. Conversely, in knockout mice

maturation arrest of osteoblasts was noted. Dexamethasone, included in MSC osteogenesis protocols, has been demonstrated to enhance Runx2 activity by causing post-translational modification of the protein (Phillips et al., 2006; Shui et al., 2003).

5.2.3.2 Adipogenesis

The major regulator is PPARγ, with forced expression in fibroblasts causing adipogenesis (Figure 5.2) (Tontonoz et al., 1994). PPARγ also inhibits osteogenic differentiation. Other regulators having a less marked effect include *C/EBPα*, thought to induce via a positive feedback loop with PPARγ and SREBP1 which enhances PPARγ expression (Cook and Genever, 2013).

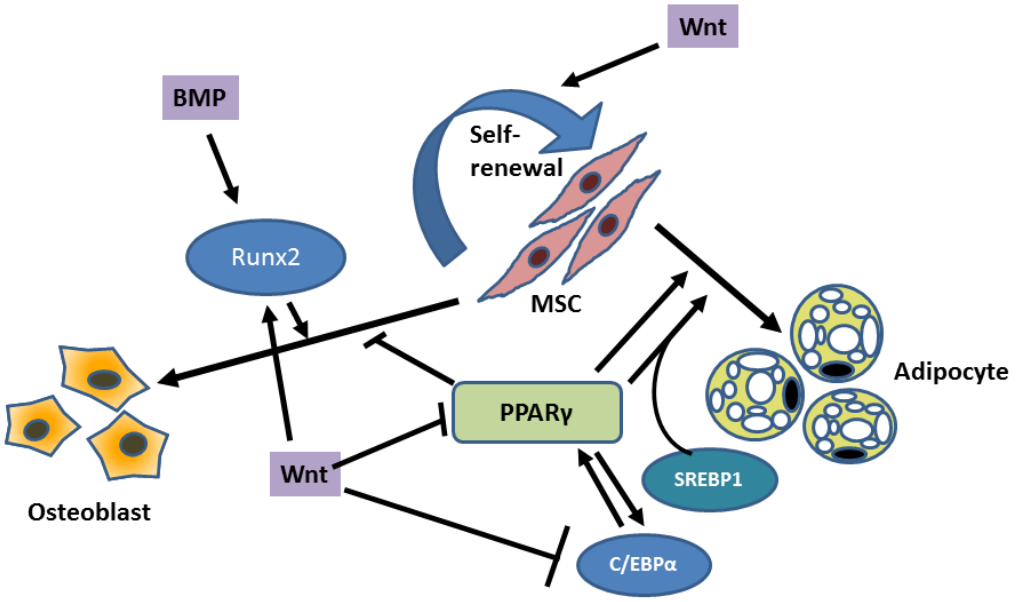

Figure 5.2 Major regulators and inhibitors of MSC osteoblastic and adipocytic differentiation
BMP – bone morphogenic protein, PPARɣ - Peroxisome proliferator-activated receptor gamma. Adapted from Cook and Genever (2013).

5.2.3.3 Chondrogenesis

The master regulator of chondrogenesis is *Sox9* where again knockout models demonstrate absence of chondrogenesis (Akiyama et al., 2002). This gene is expressed during chondrogenesis until the hypertrophic chondrocyte stage (the

terminal stage of chondrocyte differention), when transcription ceases. Two other Sox genes are involved, *L-Sox5* and *Sox6*. These are distinct from *Sox9* as they lack transactivation domains and appear to function by recruiting other regulators (Frith and Genever, 2008). *Runx2*, important in osteogenesis, also appears to be important in chondrogenic differentiation, specifically the step to produce terminally differentiated hypertrophic chondrocytes (Cook and Genever, 2013). Figure 5.3 demonstrates the major signaling pathways in chondrogenic differentiation of MSC.

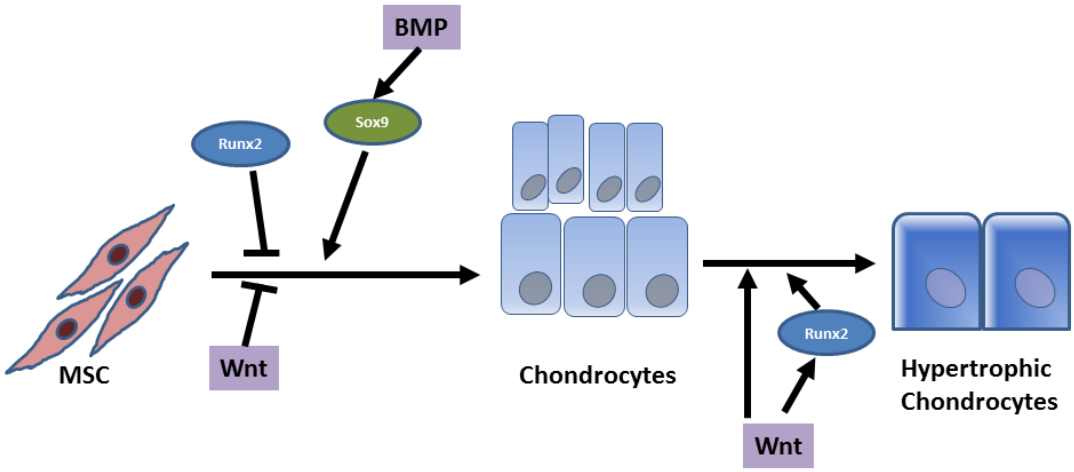

Figure 5.3 Major regulators and inhibitors of MSC chondrogenic differentiation
Adapted from Cook and Genever (2013).

Regulation of gene expression is thought to be largely controlled Wnt and the TGF-β superfamily pathways (Williams and Hare, 2011). Canonical Wnt maintains stem cell multipotency but stimulates differentiation of committed cells during osteogenesis (Figure 5.2). Wnt acts as an inhibitor of adipogenesis by blocking *C/EBPα* and *PPARγ* expression. In chondrogenesis, Wnt causes inhibition of initial differentiation from MSC to chondrocyte but again stimulates late differentiation to hypertrophic chondrocyte (Figure 5.3) (Cook and Genever, 2013).

As part of the TGFβ superfamily, both TGFβ and bone morphogenic protein (BMP) are involved in MSC differentiation. Both bind to their specific SMAD receptors. These then interact with SMAD4 and together translocate to the nucleus where they

activate transcription. TGFβ and BMP have different and specific effects in MSC differentiation. BMP upregulates *Runx2*, inducing osteoblast differentiation and also appears to upregulate *Sox9*, inducing chondroblast differentiation (Semba et al., 2000). TGFβ inhibits the osteogenic effect of BMP by suppressing *Runx2* transcription and also stimulates chondrogenesis via cascading through p38, ERK-1, and JNK MAP Kinase pathways (Alliston et al., 2001)

5.2.4 Canine mesenchymal stem cell fundamental research

There has also been a rapid expansion of laboratory research on canine MSC, from the first publication by Kadiyala et al. (1997) describing canine BM-MSC isolation and osteogenesis. Trilineage differentiation of this source was then described by Csaki et al. (2007). Other sources of canine MSC that have been described include umbilical cord blood (Lim et al., 2007), adipose tissue (Black et al., 2007), foetal adenexa (Filioli Uranio et al., 2011), muscle and periosteum (Kisiel et al., 2012). With many of the early reports, characterization was minimal and differentiation limited. The more recent reports have demonstrated trilineage differentiation of almost all of these MSC sources (Filioli Uranio et al., 2011; Kisiel et al., 2012).

Other cell types that have been derived from canine MSC include neuronal cells (Chung et al., 2013; Seo et al., 2009), and cells with some hepatocyte gene expression (Choi et al., 2013).

The recommendations of cell surface antigen selection by ISCT have been adopted by some researchers in the canine MSC field although it is recognized that these markers may not apply across species (Dominici et al., 2006). There are the additional challenges in the field of canine MSC where a lack of antibodies specific for, or cross-reacting with the dog, can limit characterisation and that different methods (e.g. immunocytochemistry v's FACS) and antibody selection differences between papers limits comparisons and may explain apparent differences in findings. Table 5.2 and Table 5.3 summarises markers and methods used in canine Ad-MSC and BM-MSC reports.

Paper	Markers positive/method of testing	Markers negative/method of testing
Takemitsu et al. (2012)	CD29,44, moderate CD90/FC	CD34,CD45/FC
Oh et al. (2011)	CD29,44,90/FC	CD31,34,73,105/FC
Requicha et al. (2012)	CD73,90/105/qPCR – rapid down regulation during passage	nil
Vieira et al., (2010)	CD29,44,90/FC	CD13,14,34,45,73,105,117/FC
Kisiel et al. (2012)	CD90- equivocal, CD44/ICC	CD34,45,146/ICC
Park et al. (2013)	CD44, D54,90/FC	CD3,18,34,45,49d,80/FC
Ock et al. (2012)	CD90,105/FC	CD45/FC
Kang et al. (2012)	CD44,73,90,105/FC	CD14,34,45/FC
Ryu et al. (2012)	CD44,73,90,105	CD14,3445
Reich et al. (2012)	CD90/FC	---
Csaki et al. (2007)	CD90,105/ICC	CD34/45/ICC

Table 5.2 Studies describing cell antigen characteristics of canine Ad-MSC
FC- flow cytometry, ICC – immunocytochemistry, qPCR – real-time PCR.

Paper	Markers positive/method of testing	Markers negative/method of testing
Takemitsu et al. (2012)	CD29,44, moderate CD90/FC	CD34,CD45/FC
Quintanilha et al. (2013)	CD29,44,90/FC	CD11b,45/FC
Reich et al. (2012)	CD90/FC	---
Hodgkiss-Geere et al. (2012)	CD44,STRO-1/ICC	CD34,45/PCR
Kisiel et al. (2012)	CD90- equivocal,CD45 weak positive CD44/ICC	CD34,45,146/ICC
Ock et al. (2012)	CD90,105/FC	CD45/FC
Kang et al. (2012)	CD44,73,90,105/FC	CD14,34,45/FC
Ryu et al. (2012)	CD44,73,90,105	CD14,3445

Table 5.3 Studies describing cell antigen characteristics of canine BM-MSC
FC- flow cytometry, ICC – immunocytochemistry, qPCR – real-time PCR.

5.2.5 Clinical trials and experimental use of MSC in the dog

As yet there is little information on clinical trials of MSC in the dog. Treatment of osteoarthritis has been the most studied with one randomized double-blinded control trial consisting of 18 dogs with coxo-femoral osteoarthritis which were treated with autologous Ad-MSC. Outcomes were subjective clinical scores which improved significantly over time and relative to control animals (Black et al., 2007). A subsequent study used the same cell type in 14 dogs with humero-radial OA without blinding or a control group. Subjective clinical scores significantly improved over time (Black et al., 2008). In both studies the primary author was employed by, and the study sponsored by, a commercial veterinary stem cell company offering treatment for canine OA. There have been two further studies utilising canine autologous Ad-MSC in naturally occurring osteoarthritis. Both were extremely small studies (n=4 and 8) with no similarly affected control group. One study had purely subjective outcomes which were reported to be positive (Guercio et al., 2012),whilst the other reported an improvement in force plate gait analysis, leading to the conclusion that MSC were an appropriate treatment for severe hip joint osteoarthritis (Vilar et al., 2013). Pogue et al. (2013) used allogeneic canine Ad-MSC in 15 Dobermans with dilated cardiomyopathy. Although the treatment appeared safe, there were no apparent beneficial effects.

Experimentally, more rapid dermal wound healing has been documented in wounds treated with allogenic canine BM-MSC compared to a vehicle control with a concomitant reduction in local inflammation (Kim et al., 2013). Beagles with induced spinal cord injury demonstrated improved functional recovery after treatment with allogenic Ad-MSC which had been neuronally differentiated compared with vehicle controls (Park et al., 2012). Healing of experimental cartilage defects has also been reported to be improved by intra-articular injection of autologous BM-MSC (Mokbel et al., 2011). Finally, autologous BM-MSC were used in a canine model of ischaemic heart disease, where an improvement in cardiac function compared to a control group was noted (Silva et al., 2005).

5.2.6 Clinical use of MSC

As MSC have been shown to have immunomodulatory effects in addition to their ability to differentiate, there has been a huge interest in using these cells therapeutically. This has been tempered by legislation in the human field which defines stem cell therapies as drugs, therefore requiring stringent conditions of culture, as well as proof of safety and efficacy (European Medicines Agency, 2011). As a result, clinical use of MSC stem cell treatments does not occur in the USA or Europe. The exception to this is as part of clinical trials and there are 39 human trials listed using MSC in the European Union clinical trials register as of December 2013 (www.clinicaltrialsregister.eu). This same interest has inevitably also occurred in veterinary medicine, however there are no such restrictions on the use of stem cell therapies in veterinary medicine (Cyrano ski, 2013). As a result, stem cell therapy is offered commercially by a number of companies and individuals as well as even basic equipment to produce autologous "stem cells" on-site in veterinary practices (in reality this isolates the VSF). In the UK, private veterinary practices are offering MSC treatment for conditions as diverse as arthritis, inflammatory bowel disease, renal disease, neurological disease and skin disease. Case reports are appearing in the literature, for example, Case et al. (2013) reports a dog with gastrocnemius tendon strain that was treated with autologous mesenchymal stem cells. These practices are of concern as there is minimal to no phenotyping of the cells, the treatments are as yet unproven for these conditions and the long-term safety of these procedures is unknown.

5.3 Aims

The aims were to isolation, culture, characterise and perform tri-lineage differentiation of canine bone marrow and adipose mesenchymal stem cells/stromal cells. This would then provide a stem cell source with which to produce hepatocyte-like cells.

5.4 Materials and methods

5.4.1 Isolation of canine bone marrow mesenchymal stem cells

The distal femoral epiphysis from recently euthanased dogs was removed using a hacksaw. A Jamshidi bone marrow biopsy needle (Baxter) was inserted into the medullary cavity via the trochanteric fossa and approximately 40mls of DMEM low glucose containing Glutamic-I (Invitrogen, UK), with 10% FBS (Invitrogen, UK) and 100 U/mL penicillin G and 100 μg/mL streptomycin (both Invitrogen, UK) injected with the resultant cell suspension collected from the distal segment. This was transported on ice to the laboratory.

The cell suspension was diluted 1:1 with PBS and 20mls layered onto 15mls Ficoll Piqué Premium (GE Life Sciences) in a 50ml Falcon tube. This was then centrifuged at 450g for 30 minutes without brake. The cell containing interface was removed to a fresh Falcon tube, PBS added and pelleted at 150g for 5 minutes. The cells were then re-suspended in 30mls of MSC media, transferred to a T150 and incubated at 37^{o}C and 5% $CO_{2.}$ After 48 hours, media was removed, the flask washed with warmed PBS and fresh media added. Media was changed every 2-3 days and cells passaged once confluent.

5.4.2 Isolation of canine adipose stromal cells

Approximately 10g of falciform fat was excised from dogs which had been recently euthanased and placed in chilled MSC media. After transport to the laboratory, this was finely chopped into 2-4mm pieces, placed in a 50ml Falcon tube and warmed PBS containing 100 U/mL penicillin G, 100 µg/mL streptomycin and 1mg/ml collagenase Type I (Sigma-Aldrich) added to the 45ml mark. This was then incubated with constant shaking at 37^{o}C for 2 hours. 10% FCS was then added to inactivate the enzymes and the tube centrifuged at 300g for 5 minutes. The cell pellet was re-suspended in MSC media and filtered with 70µm cell strainer (BD Biosciences). The cells were then re-pelleted, suspended in 30ml MSC media transferred to a T150 and incubated at 37^{o}C and 5% $CO_{2.}$ After 48 hours, media was removed, the flask washed with warmed PBS and fresh media added. Media was changed every 2-3 days and cells passaged once confluent.

5.4.3 Cryopreservation of MSC

At passage 2/3, cells were trypsinised and counted as previously described. Cells were centrifuged at 400g for 5 minutes and re-suspended in freezing medium: 10% dimethyl sulphoxide (DMSO) (Sigma-Aldrich), 40% FCS and 40% MSC media. Cells at a density of 2 x 10^{6}/ml were placed in 1ml cryovials (Nunc, UK) and these placed in an isopropanol chamber (Mr Frosty, Nalgene, USA) in a -70^{o}C freezer before being transferred to either -150^{o}C or liquid nitrogen storage for longer term archiving.

Cells were rapidly thawed in a 37^{o}C water bath before adding the liquid to pre-warmed media. Cells were then centrifuged at 150rpm for 5 minutes and re-suspended in MSC media. Cells were plated into a T75 and cultured as before.

5.4.4 Isolation of canine peripheral blood mononuclear cells

A volume of 9mls of blood was collected from the jugular vein of a recently euthanased dog into a 10ml syringe containing 1ml acid-citrate dextrose (Sigma-Aldrich). This was gently mixed for 20 seconds and transported on ice to the laboratory. After dilution 1:1 with PBS the blood was layered over 10ml of 15mls Ficoll Paque Premium (GE Life Sciences) in a 50ml Falcon tube. This was then centrifuged at 450g for 30 minutes without brake. The cell containing interface was removed to a fresh Falcon tube, PBS added and pelleted at 150g for 5 minutes. These cells were then counted and re-suspended in PBS with 1% bovine serum albumin (Sigma-Aldrich).

5.4.5 Immunofluorescence Analysis

Cells were cultured in four chambered slides (BD Biosciences) until they were approximately 50% confluent. Media was removed, the cells washed with PBS and then fixed with 4% paraformaldehyde for 30 minutes. The cells were washed with PBS three times, permeabilised with 100% ethanol for 5 minutes before repeating the wash step. Blocking buffer (PBS containing 10% goat serum (Invitrogen) and 0.1% Tween 20 (Sigma-Aldrich, UK) was added for 1 hour at room temperature. This was then aspirated and the appropriate dilution of antibody in PBS containing 1% goat serum and 0.1% Tween added (Table 5.4). Slides were incubated at 4^{o}C overnight and then washed three times in PBST. The secondary antibody, again diluted in PBS containing 1% goat serum and 0.1% Tween was added and incubated at room temperature in the dark for 1 hour. Slides were then rinsed three times with PBST and 4', 6-diamidino-2-phenylindole (DAPI) at a concentration of 200ng/ml for 30 minutes added. The slides were then washed with PBST and examined using fluorescent microscopy (Zeiss, Aviovert 40) and Zeiss Aviovision 4.7 software. Secondary only and no antibody controls were also performed for each cell type and antibody.

Marker	Primary antibody	Dilution	Secondary antibody	Dilution	Flurophore
STRO1	IgM mouse anti-human MAB1038 (R&D Systems)	1:100	Goat anti-mouse IgG A-11001 (Life technologies)	1:500	Alexa Fluor® 488
CD44	IgG rat anti-canine MCA1042G (AbD Serotec)	1:100	Goat anti-rat IgG A11006 (Invitrogen)	1:500	Alexa Fluor® 488
CD105	Polyclonal rabbit orb10285 (Biorbyt)	1:50	Goat anti-rabbit IgG A-11008 (Life technologies)	1:500	Alexa Fluor® 488

Table 5.4 Primary and secondary antibodies used for immunocytochemistry

5.4.6 Flow cytometry analysis

Cells were suspended in FACS buffer (PBS with 1% bovine serum albumin [BSA]) at a concentration of 1 x10^7 cells/ml and 100ul added to 5ml Falcon tubes (BD Biosciences). Primary antibodies and, where required, secondary antibodies are listed in Table 5.5. For CD11b staining 20µl blocking reagent: 2.4G2 (anti-Fc receptor [BD Pharmingen]) were added for 10 minutes at room temperature prior to antibody addition. After incubation at 4^{o}C in the dark with antibody for 30 minutes, cells were washed in FACS buffer by centrifugation at 4ºC, 250g, for 5 minutes three times. Samples were re-suspended in 500µl of FACS buffer and kept on ice in the dark for analysis. Samples were run on a FACSCalibur and results acquired with CellQuestPro (both BD Biosciences). Post-acquisition analysis was performed using FlowJo (Treestar, USA). No antibody and isotype controls were run for each cell type and experiment. Canine peripheral blood mononuclear cells were used as positive control for CD45 and CD19 and canine bone marrow-derived macrophages (donated by Breno Beirao) a positive control for CD11b.

Marker	Primary antibody	Dilution	Isotype	Flurophore /secondary
CD11b	MCA1777S, AbD Serotec	1:10	IgG1	Goat anti mouse Alexa Fluor 488 A-11001, Life technologies
CD19	ab24936, Abcam	1:100	IgA	FITC
CD45	MCA1042G, AbD Serotec	1:10	IgG2	Phycoerythrin

Table 5.5 Cell surface markers and antibodies used for flow cytometry

5.4.7 Adipogenic and osteogenic differentiation of MSC

MSC cells were passaged into 6 well and 12 well plates. Once 60-70% confluence was achieved, commercially available media was used for adipogenesis and osteogenesis (STEMPRO® Adipogenesis Differentiation Kit and STEMPRO® Osteogenesis Differentiation Kit, Invitrogen, respectively). Control cells were maintained in standard MSC media. After 14 days, RNA was extracted from the 6 well plate cells as previously described and cells in the 12 well plates were used for lineage specific staining described below.

5.4.8 Chondrogenic differentiation of MSC

A total of 2.5 x 10^5 MSC were aliquoted into 1.5ml polypropylene 1.5ml microcentrifuge tubes (Fischer Scientific, UK). These were then spun at 500g for 5 minutes to pellet the cells. MSC media was then aspirated and either fresh MSC media or chondrogenic media added. Five tubes of each cell and media type were run. After 12 hours the cell pellet was gently detached from the bottom to become free-floating by pipetting. Media was then changed every 2-3 days for 21 days. Pellets were then harvested and three fixed in 4% formaldehyde and Toluidine blue staining performed. RNA extraction was performed on the remaining 2 pellets in each experiment.

5.4.9 Oil Red O staining for lipid

Oil Red O power (300mg) (Thermo, UK) was dissolved in 100ml of isopropanol to give stock solution. Six mls of stock was mixed with 4mls of distilled water and incubated for 10 minutes. After this, the solution was passed through filter paper (Whatmann, UK) and used within 2 hours.

Media was aspirated from the wells and the cells rinsed in PBS before being fixed in 10% formaldehyde for 30 minutes. The wells were then gently rinsed with distilled water then 60% isopropanol added for 5 minutes. This was then aspirated and the Oil Red O solution added. The wells were then incubated for 5 minutes before the solution rinsed with distilled water until the rinse became clear. 1ml of distilled water was added to the wells and the cells imaged under phase contrast microscopy (Zeiss, Aviovert 40) and Zeiss Aviovision 4.7 software.

5.4.10 Alizarin red staining for calcification

2g of Alizarin red powder (Sigma Aldrich, UK) was added to 100ml of distilled water and the pH adjusted to 4.1-4.3 with 10% ammonium hydroxide. Media was aspirated from the wells and the cells rinsed with PBS. Absolute ethanol was added to the wells for 30 minutes then aspirated and the wells allowed to dry. The Alizarin red solution was then added for 5 minutes, removed and the wells carefully rinsed three times with distilled water. The wells were examined grossly for staining as well as under phase contrast as described above.

5.4.11 Toluidine Blue staining for chondrogenesis

Pellets were embedded in paraffin wax blocks and sections cut using a microtome. Toluidine blue staining was performed by Neil MacIntyre of the R(D)SVS pathology service. Dewaxing was performed using xylene for 15 minutes, descending concentrations of ethanol (100, 95, 90, 70, and 0%) for 10 minutes each. The sections were rinsed in distilled water and submerged in 1% aqueous Toluidine blue solution (Sigma Aldrich) for 30 minutes at room temperature. The slides were then rinsed in 1

part distilled water and 4 parts 1% HCl in 70% ethanol for 5 seconds. The slides were then rinsed in distilled water, dried and mounted using DPX mountant (VWR, UK).

5.4.12 Primer optimization to perform MSC differentiation analysis

Samples of adipose tissue, cartilage and trabecular bone <5mm ^{3} were taken from recently euthanased dog and submerged in RNALater. These samples were stored at 4^{o}C for 24 hours before being transferred to -20^{o}C for long-term storage. After thawing, 20mg of each tissue was placed 2ml plastic tubes containing 1.4mm ceramic beads (Fast Prep Lysing Matrix D tubes, MP Biomedical) with 600µl RLT Buffer (Qiagen) with the addition of 1:100 β Mercaptoethanol (Gibco). Tissue was disrupted using a Fast Prep 24 Instrument (MP Biomedical) for 30 seconds at level 5, placed on ice for 30 seconds then repeated until no tissue mass was visible. The tissue lysate was placed in a fresh Eppendorf tube and 1 volume of 70% ethanol added. RNA was extracted using RNA Easy Mini Kit (Qiagen). The solution was then mixed and 700µl transferred to an RNA Easy mini column. The column was centrifuged at 10,000g for 15 seconds, the flow-through discarded and this procedure repeated with any remaining solution. A volume of 350µl of RW1 was added to the column and centrifugation repeated at 10,000g for 15 seconds and flow-through discarded. DNA digestion was performed using 10µl of DNase solution in 70µl RDD which was pipetted onto the column membrane and incubated at room temperature for 15 minutes. A volume of 350µl of RW1 was again added to the column and centrifugation repeated at 10,000 for 15 seconds and flow-through discarded. 500µl of RPE buffer was added and the sample centrifuged at 10,000g for 2 minutes. The column was then placed into a new collection tube and centrifugation was repeated for 1 minute to ensure complete ethanol removal. The column was then placed in a 1.5ml Eppendorf, 30µl of nuclease free water added to the column and centrifugation performed at centrifuged at 10,000g for 1 minute. The resultant samples were chilled on ice and quantity and quality assessed by spectrophotometry using Thermo Nanodrop™ (Thermo, USA). RNA was reverse transcribed to cDNA using

Omniscript® reverse transcription kit (Qiagen, UK) and primer efficiency and specificity were tested as described in Chapter 2.

5.5 Results

5.5.1 Canine bone marrow and adipose-derived mesenchymal stem cells can be isolated from ischaemic tissue.

A total of 8 bone marrow and 7 adipose derived MSC cultures were undertaken (Table 5.6). All but one bone marrow culture produced viable MSC's which could be expanded.

Dog Id	Breed	Sex	Age (months)	Bone Marrow	Adipose	Culture Comments
D231112	Border Collie	ME	84	2.9 x 10^7 yield	1 x10^7 falciform	Both viable.
D10513	Labrador	ME	60	1 femur	≈ 5g falciform	Both viable
D17513	Labrador	ME	120	1 femur	≈ 10g falciform	Adipose viable, few BM - discarded
D19713	SBT	FE	72	2 femurs	≈ 10g falciform	Both viable
D16813	Rottweiler	MN	24	1 femur	≈ 10g falciform	Both viable
D19913	Beagle	FE	6	---	≈ 10g falciform	Viable
D20913	Mastiff	ME	48	1 femur	≈10g falciform	Both viable
D41013	JRT	ME	48	1 femur	≈10g falciform	Both viable

Table 5.6 Signalment of dogs and location of MSC collection

5.5.2 Canine adipose and bone marrow mesenchymal stem cells can be expanded *in vitro*

Both expanded at a similar rate with Ad-MSC requiring passaging earlier due to the higher plating density (Figure 5.4).

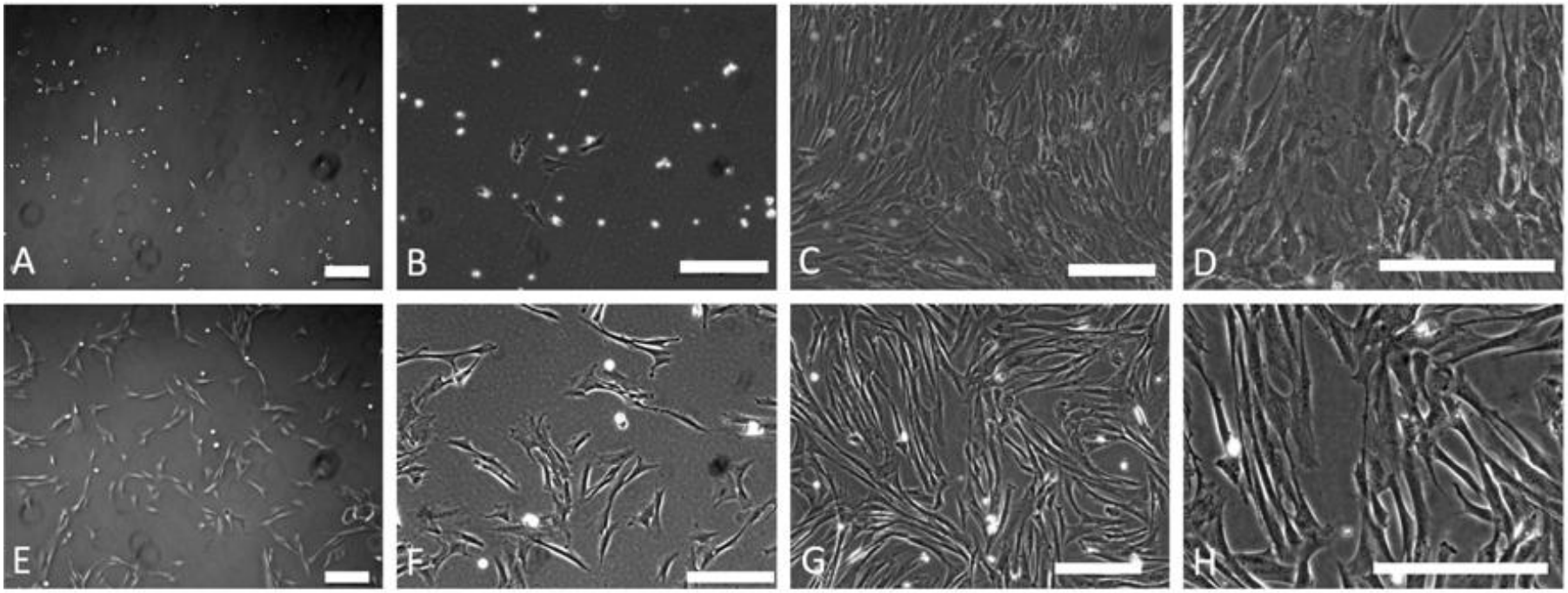

Figure 5.4 Cells derived from D231112 and cultured on plastic with MSC culture medium.
A&B Bone marrow-derived MSC 48 hours after plating, C&D BM-MSC after 14 days of culture. E&F Adipose-derived MSC 48 hours after plating, G&H Ad-MSC after 7 days of culture. White bar represents 100µm.

5.5.3 Ad-MSC and BM-MSCs express stem cell markers CD105, CD44 and STRO-1

Both Ad-MSC and BM-MSC were examined for CD105, CD44 and STRO-1 expression using immunofluorescence. Both MSC types had strong cytoplasmic staining for CD105 (endoglin) (Figure 5.5) and STRO-1 (Figure 5.6). CD44 staining was stronger on the Ad-MSC but both cell types were positive (Figure 5.7). All negative controls confirmed the specificity of antibody binding.

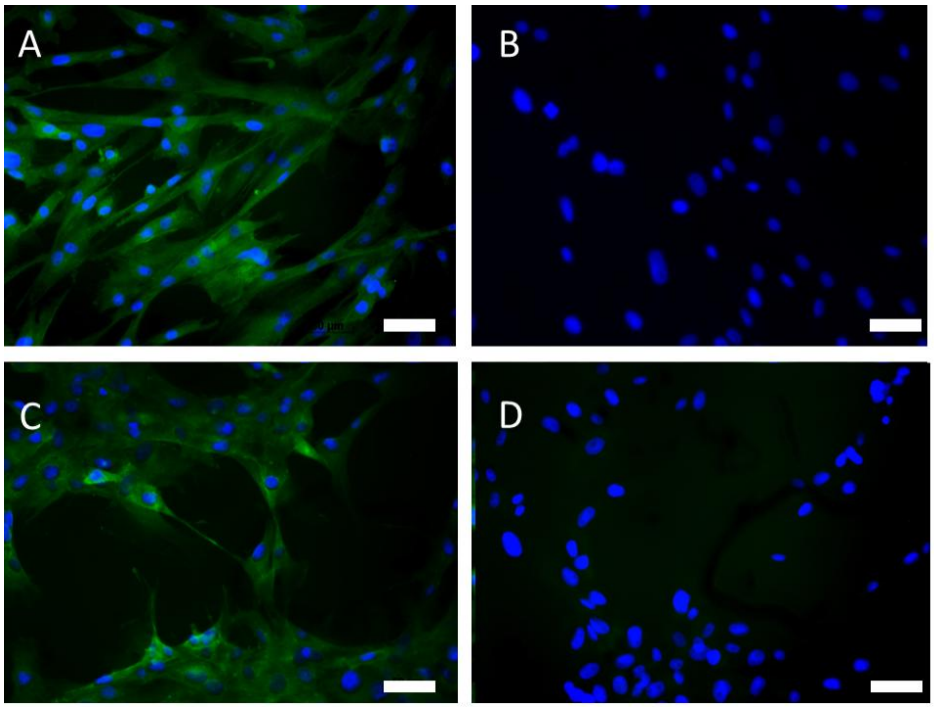

Figure 5.5 Immunofluorescence analysis for CD105 (Endoglin) expression of Ad-MSC and BM-MSC
Ad-MSC (A) and BM-MSC (C) were positive for CD105 (Alexa Fluor 488). Nuclei counterstained with DAPI. Negative controls Ad-MSC (B) and BM-MSC (D) with secondary antibody only and DAPI nuclear staining. White bars represent 50µM.

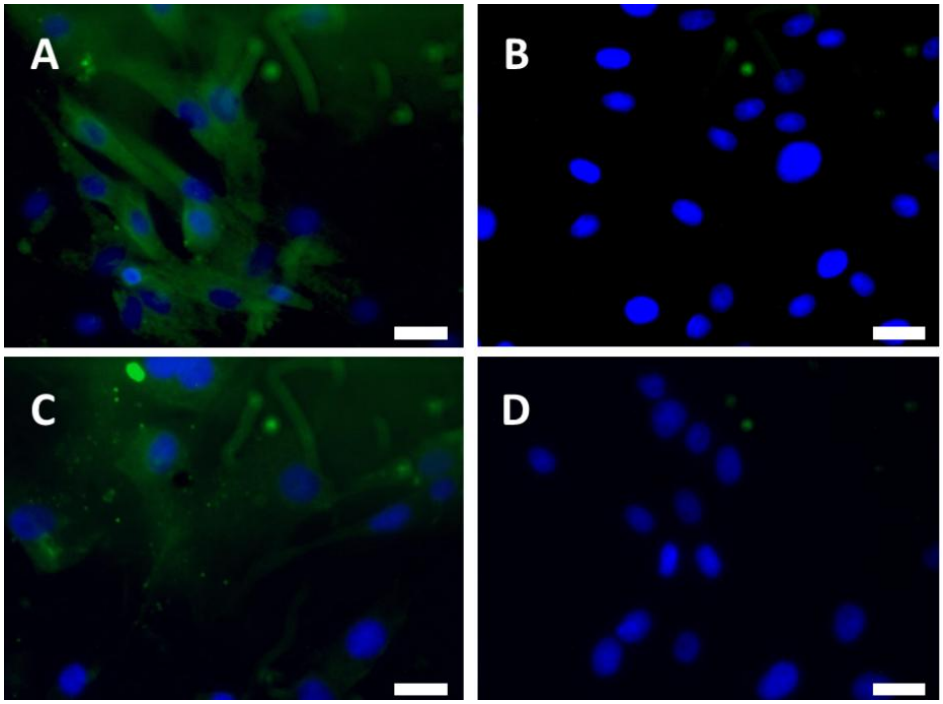

Figure 5.6 Immunofluorescence analysis for STRO-1 expression of Ad-MSC and BM-MSC

Ad-MSC (A) and BM-MSC (C) were positive for STRO-1 (Alexa Fluor 488). Nuclei counterstained with DAPI. Negative controls Ad-MSC (B) and BM-MSC (D) with secondary antibody only and DAPI nuclear staining. White bars represent 25µM.

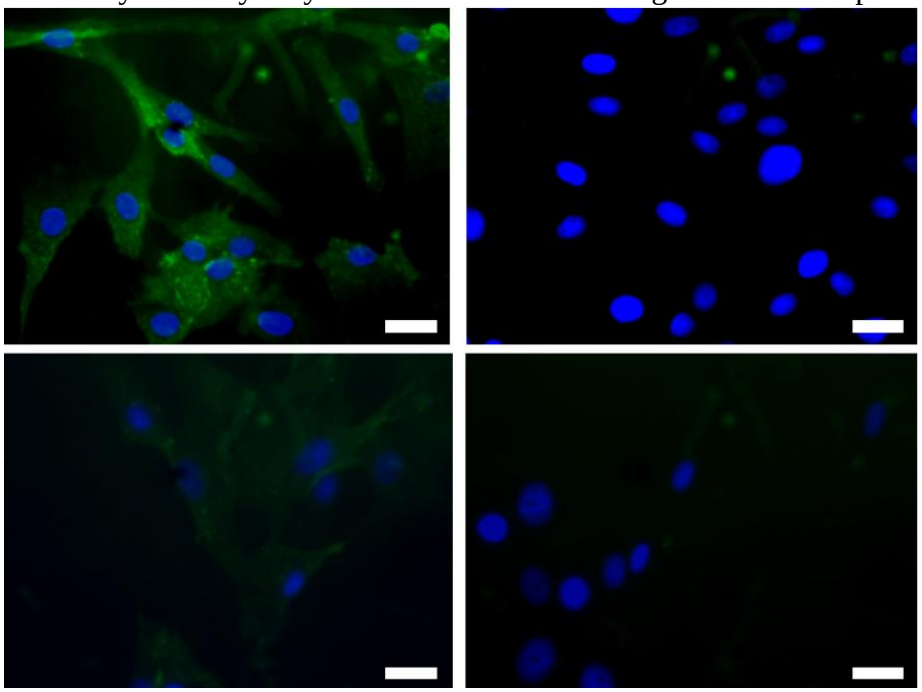

Figure 5.7 Immunofluorescence analysis for CD44 expression of Ad-MSC and BM-MSC

Ad-MSC (A) and BM-MSC (C) were positive for CD44 (Alexa Fluor 488). Nuclei counterstained with DAPI. Negative controls Ad-MSC (B) and BM-MSC (D) with secondary antibody only and DAPI nuclear staining. White bars represent 25µM.

5.5.4 Isolated cells lack haematopoietic markers

Adipose-derived MSC were uniformly negative for CD45 whilst only 3.42% of BM-MSC were positive (Figure 5.8). The population of freshly isolated canine white blood cells were 92.3% positive for CD45, as would be expected for a pan-leucocyte marker. This served as a positive control. The negative population in the leucocytes would most likely be contaminating erythrocytes. Both Ad-MSC and BM-MSC were uniformly negative for CD19. The positive control canine white blood cells had a positive population of 4.25% which would be within the range of B lymphocytes present in peripheral blood(Faldyna et al., 2001). For marker CD11b, 57.2% of the bone marrow-derived macrophages were positive. Neither Ad-MSC nor BM-MSC were positive for CD11b (Figure 5.10).

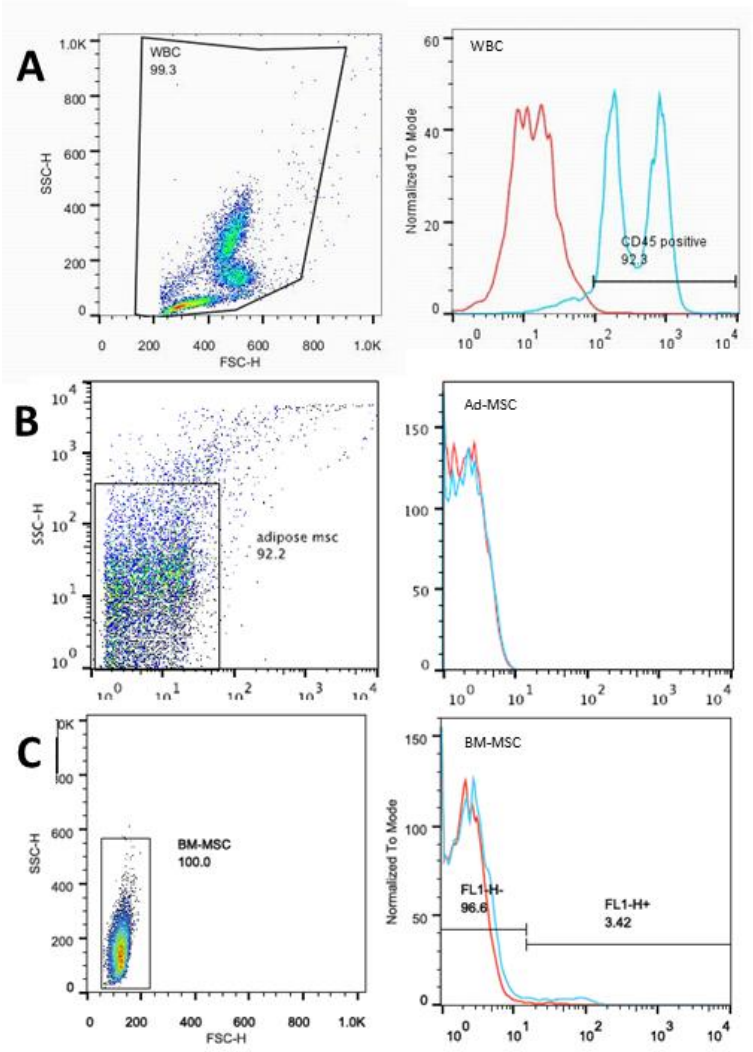

Figure 5.8 CD45 expression of canine white blood cells, Ad-MSC and BM-MSC by flow cytometry

Freshly isolated canine white blood cells as positive control (A). Canine Ad-MSC from D231113 (B) and BM-MSC from D231113 (C). CD45 stained cells in blue and isotype control in red.

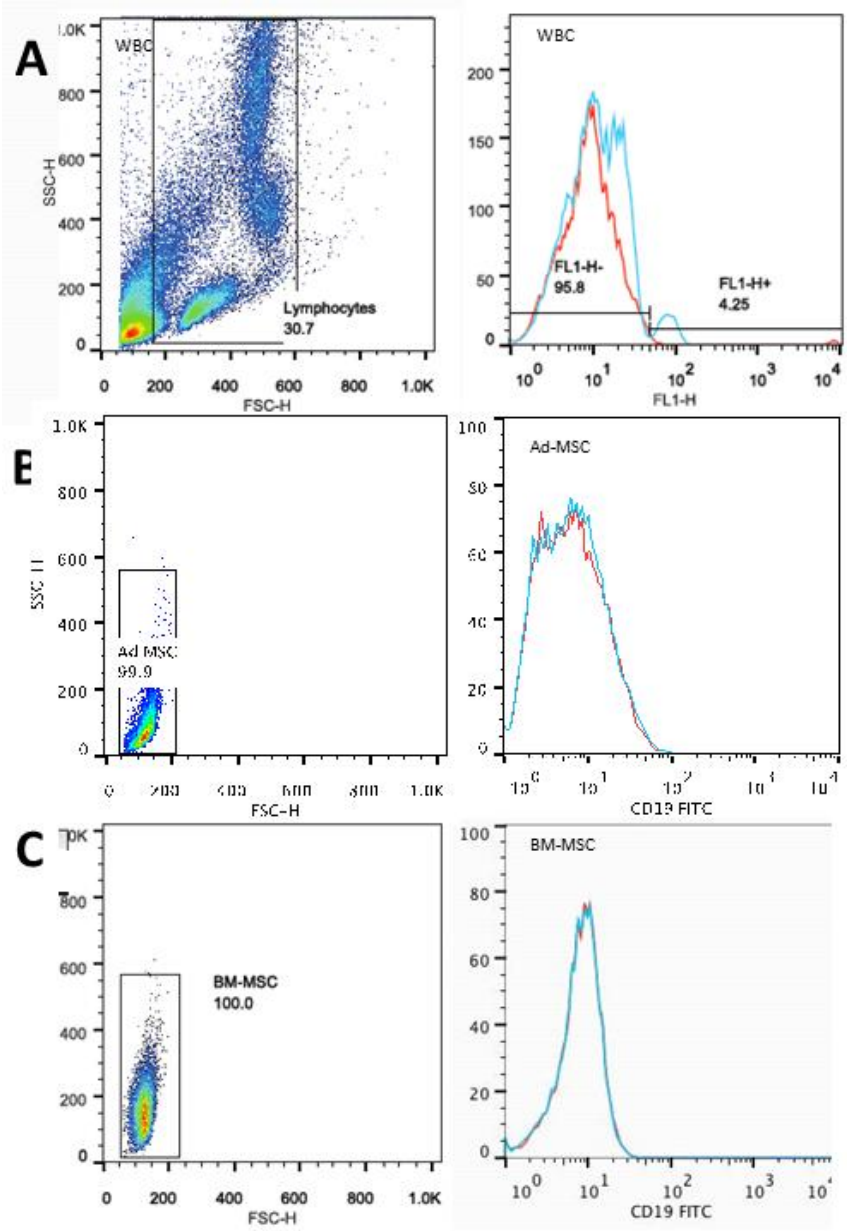

Figure 5.9 CD19 expression of canine white blood cells, Ad-MSC and BM-MSC by flow cytometry

Freshly isolated canine white blood cells as positive control (A). Canine Ad-MSC from D231113 (B) and BM-MSC from D231113 (C). CD19 stained cells in blue and isotype control in red.

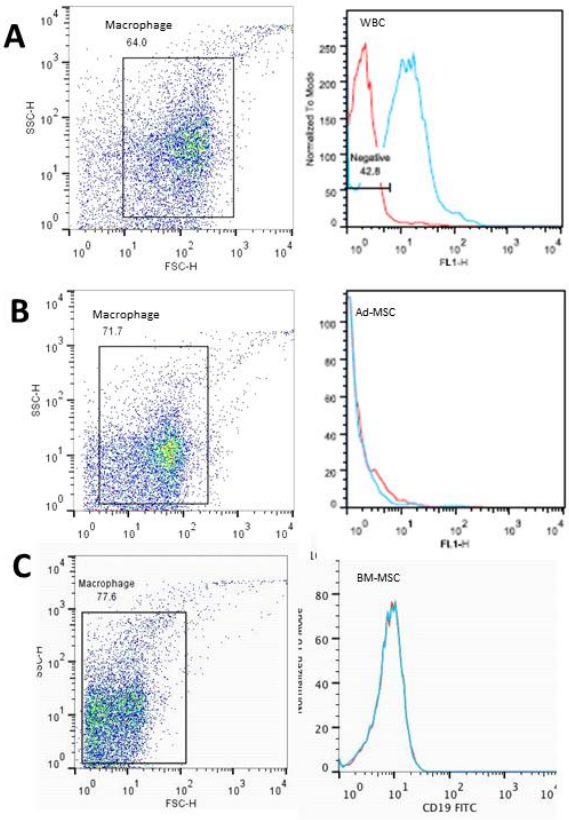

Figure 5.10 CD11b expression of canine white blood cells, Ad-MSC and BM-MSC by flow cytometry
Freshly isolated canine white blood cells as positive control (A). Canine Ad-MSC from D231113 (B) and BM-MSC from D231113 (C). CD11b stained cells in blue and isotype control in red.

5.5.5 Optimisation of adipocyte, osteoblast and chondrocyte primers

Two genes expressed by chondrocytes (*Sox9* and aggrecan), two expressed by osteoblasts (osteonectin [*SPARC*] and osteopontin) and three expressed by adipocytes (Fatty acid binding protein 4[*FAB4*], lipoprotein lipase [*LPL*] & leptin) as well as three reference genes (*MRPS7, MRPS25 & GAPDH*) had good efficiency, dissociation curve and were the expected size on gel electrophoresis (Table 5.7).

Gene	Sequence	Product size (bp)	Efficiency %	TM ^{o}C	Dissociation curve	Gel size
MRPS7 Ref	F– AGTGCAGGGAGAAGAAGCAC R - CAGCAGCTCGTGTGACAACT	62	97.6	58.33/58.33	√	√
MRPS25 Ref	F – TCTTGGGGAAGAACAAGGAA R - AGTGGGCTGGGTGAGAAAG	72	101.3	59/60	√	√
GAPDH Ref	F – GGGAAGATGTGGCGTGAC R - GAAGGCCATGCCAGTGAG	123	96.9	60/60	√	√
Aggrecan Cart	F – ATCAACAGTGCTTACCAAGACA R- ATAACCTCACAGCGATAGATCC	122	107.8	56.5/56.4	√	√
Sox9 Cart	F – GCTCGCAGTACGACTACACTGAC R - GTTCATGTAGGTGAAGGTGGAG	101	110	63/ 58.4	√	√
SPARC Osteo	F – CCACCCGCTTCTTTGAGAC R- TCACCAGATCCTTGTCAATATCC	111	104.3	60/60	√	√
Osteopontin Osteo	F – CATATGATGGCCGAGGT R - CAAGTGATGTGAAGTCCTCCTC	114	97.4	60.94/60.78	√	√
FAB4 Adipose	F– GACTTTTCTGTCATCCGC R - TCAACAGACCCTGAAATA	117	92.3	58.4/57.9	√	√
LPL Adipose	F – ACACATTCACAAGAGGGTCAC R - CTCTGCAATCACACGGATG	134	108.1	57.9/56.7	√	√
Leptin Adipose	F – CTATCTGTCCTGTGTTGAAGCTG R= GTGTGTGAAAATGTCATTGATCCTG	103	104.2	60.6/59.3	√	√

Table 5.7 Genes optimised to characterise adipogenic, osteogenic and chondrogenic differentiation of MSC

5.5.6 Canine Ad-MSC and BM-MSC can become adipocytes

After culture for 14 days in adipogenic media, both cell types had multiple small refractile intracytoplasmic vacuoles present. These stained with Oil Red O, demonstrating the presence of lipid. The BM-MSC had larger numbers of vacuoles per cell compared to the Ad-MSC. Undifferentiated Ad-MSC and BM-MSC were negative on Oil Red O staining (Figure 5.11). Both MSC types demonstrated significant gene expression increases in FAB4 and LPL. In both cases leptin was not increased with a significant, but small-fold decrease in Ad-MSC seen (Figure 5.12).

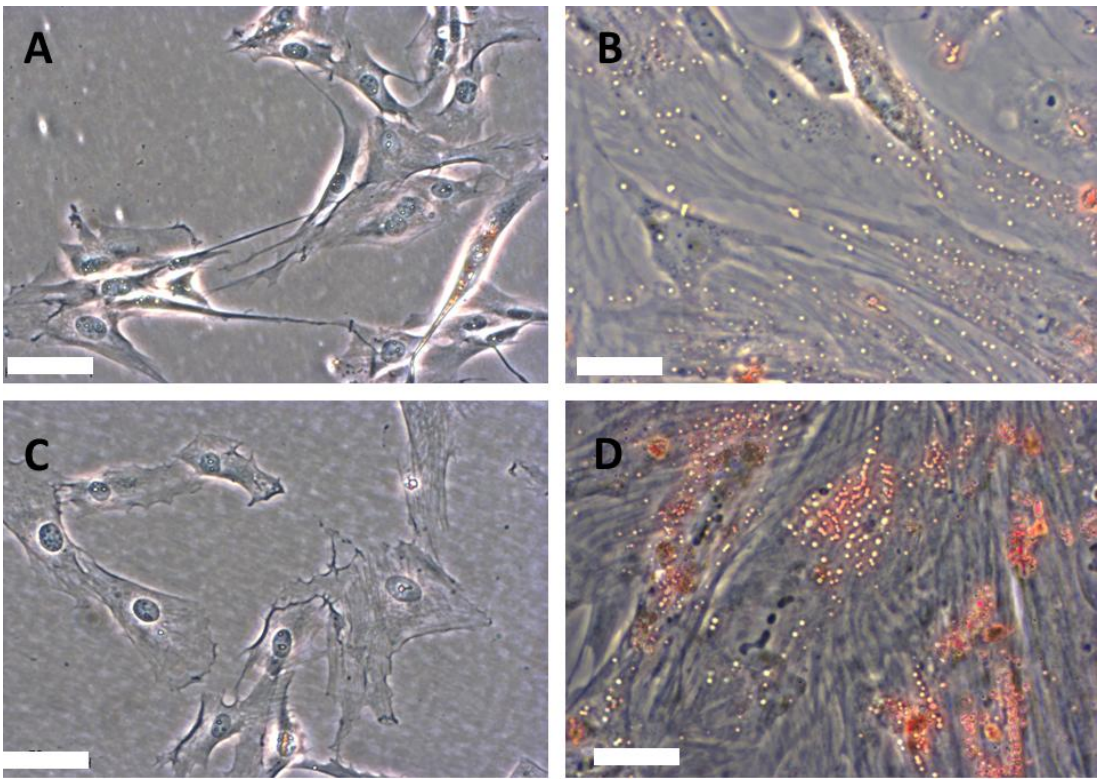

Figure 5.11 Oil Red O staining for lipid of Ad-MSC and BM-MSC
Undifferentiated Ad-MSC (A) and BM-MSC (C). Ad-MSC (B) and BM-MSC (D) after 14 days in adipogenic media. White bar represents 50µm.

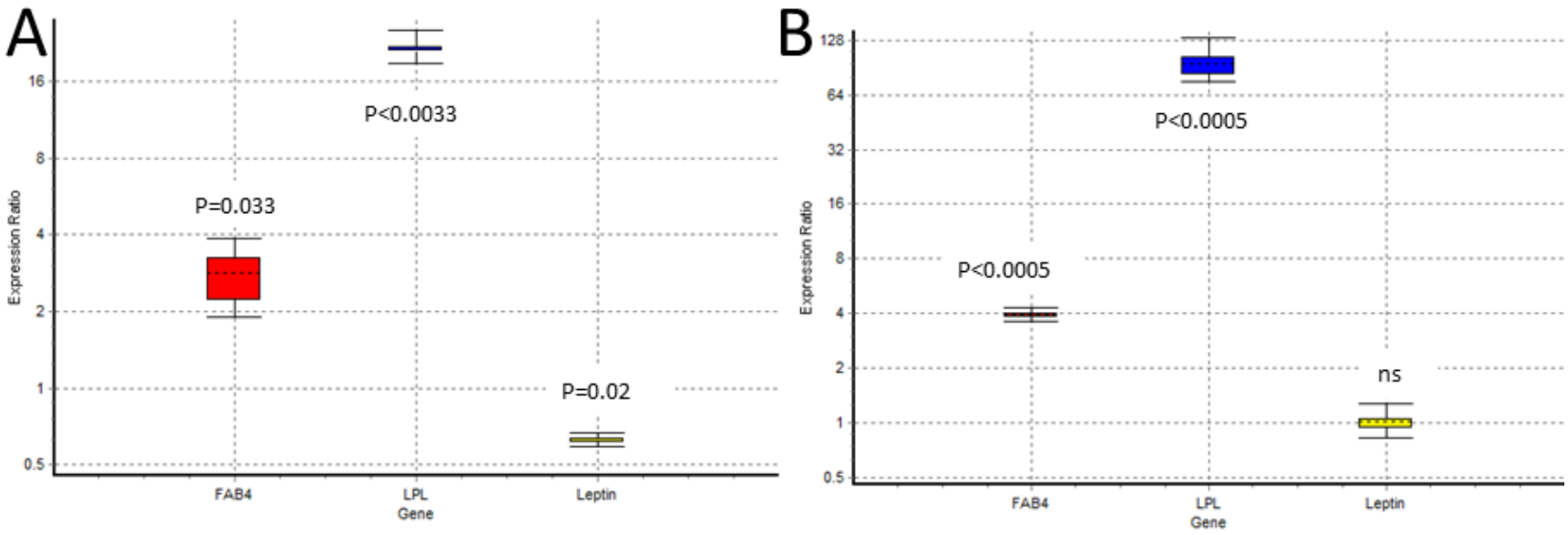

Figure 5.12 Fold increase of adipocyte gene expression.
Ad-MSC (A) and BM-MSC (B) cultured in adipogenic media compared with control MSC media. Boxes represent the interquartile range, or the middle 50% of observations. The dotted line represents the median gene expression. Whiskers represent the minimum and maximum observations. FAB4 – fatty-acid binding protein 4, LPL –lipoprotein lipase. ns = not significant.

5.5.7 Canine Ad-MSC and BM-MSC can differentiate into osteoblasts

Undifferentiated BM-MSC demonstrated slight staining with Alizarin red, both grossly and microscopically while undifferentiated Ad-MSC showed no staining (Figure 5.13 A, C). Both cell types, which had been cultured in osteogenic media for 14 days had obvious red spicules grossly, and microscopically (Figure 5.13 C/D, E/H). This was most pronounced in the BM-MSC. Examining gene expression for osteopontin and osteonectin, there was no large fold change in osteonectin and a small fold decrease in BM-MSC (Figure 5.14B). In the differentiated Ad-MSC both osteopontin and osteonectin demonstrated large fold increases, which were significant ($p=0.033$ for both, Figure 5.14A).

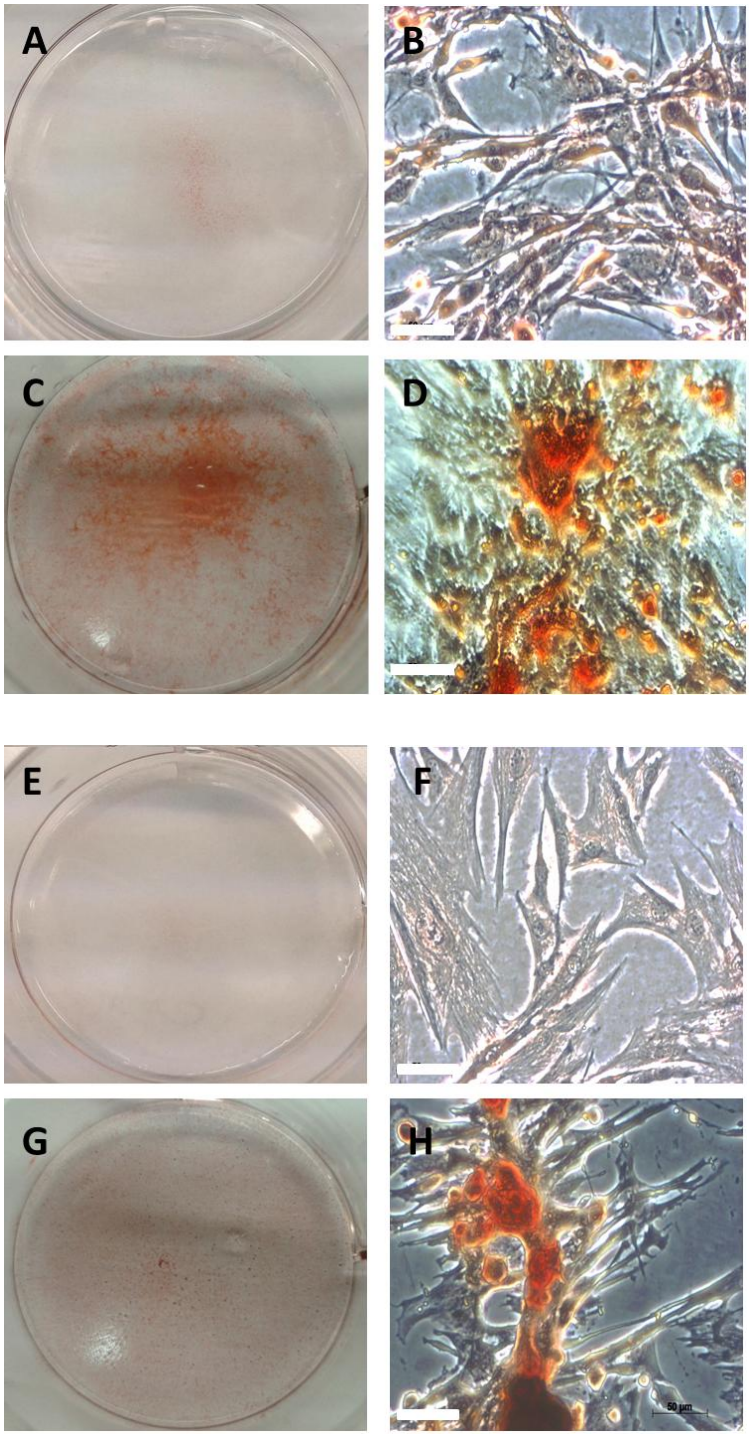

Figure 5.13 Alizarin Red staining for calcification of BM-MSC and Ad-MSC
Undifferentiated BM-MSC (A, B). BM-MSC after 14 days in osteogenic media (C, D). Undifferentiated Ad-MSC (E, F). Ad-MSC after 14 days in osteogenic media. White bar represents 50µm.

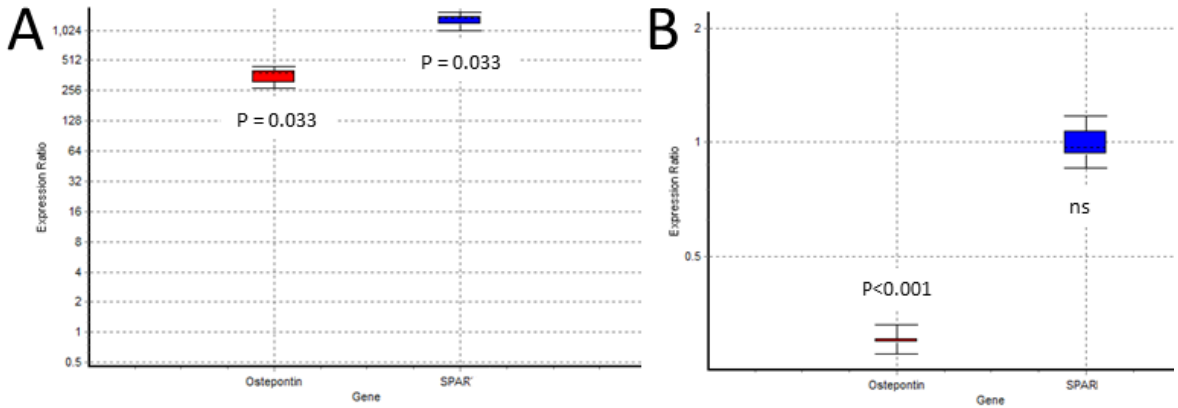

Figure 5.14 Fold increase of osteopontin and osteonectin expression
Ad-MSC (A) and BM-MSC (B) cultured in osteogenic media compared with control MSC media. Boxes represent the interquartile range, or the middle 50% of observations. The dotted line represents the median gene expression. Whiskers represent the minimum and maximum observations. SPAR – osteonectin. ns = not significant.

5.5.8 Canine Ad-MSC and BM-MSC can differentiate into chondrocytes

The positive control of mast cells demonstrated metachromatic purple staining, indicating the staining protocol was effective (Figure 5.15A). The Ad-MSC and to a lesser extent BM-MSC showed diffuse metachromatic staining throughout the pellet which was not present in the control pellets (Figure 5.15B, D). The BM-MSC control pellets were of much smaller diameter than the TGFβ pellets. Both cell types demonstrated large fold increases in aggrecan which was significant. Sox9 expression was no different between control MSC and MSC in chondrogenic media in both cell types (Figure 5.16).

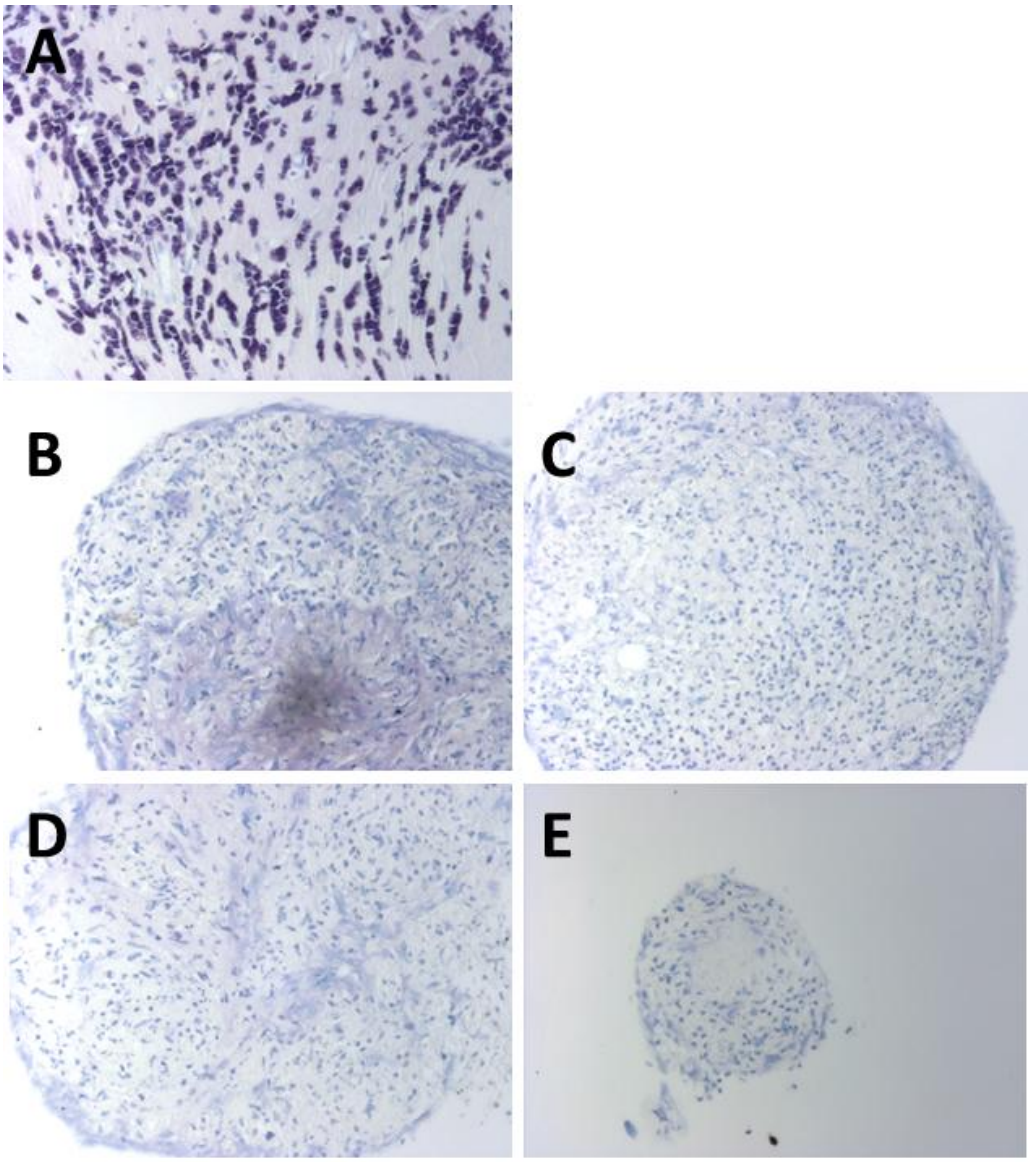

Figure 5.15 Toluidine blue staining of Ad-MSC and BM-MSC cell pellets
Positive control of dermal mast cell tumour (A). Ad-MSC (B) and BM-MSC (D) pellets cultured in chondrogenic media with TGF-β for 21 days. Ad-MSC (C) and BM-MSC (E) cultured in chondrogenic media without TGF-β for 21 days. All images x 200.

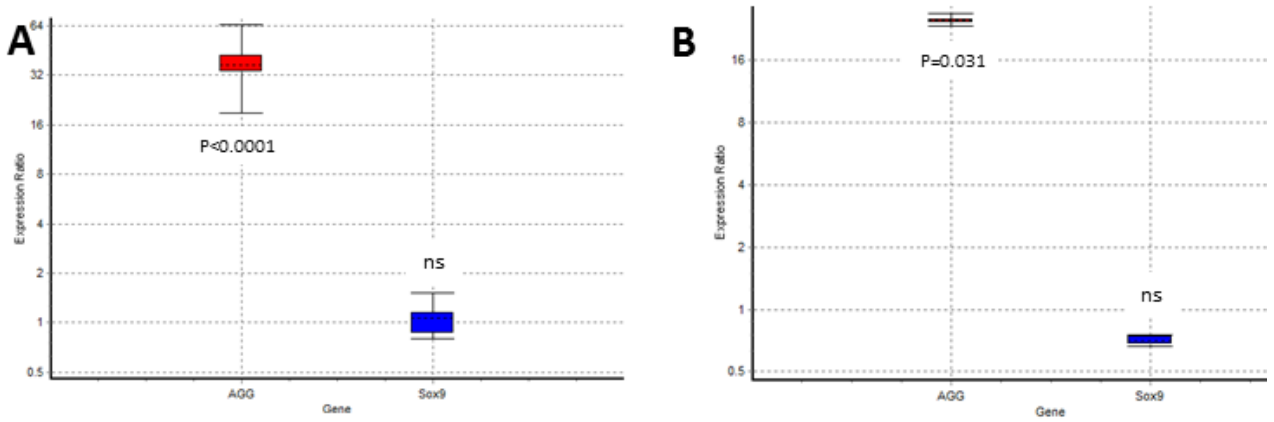

Figure 5.16 Fold increase of Aggrecan and Sox9 expression
Ad-MSC (A) and BM-MSC (B) cultured in chondrogenic media compared with control MSC media. Boxes represent the interquartile range, or the middle 50% of observations. The dotted line represents the median gene expression. Whiskers represent the minimum and maximum observations. AGG – aggrecan.

5.6 Discussion

5.6.1 Cells morphologically consistent with MSCs can be isolated from canine ischaemic bone marrow and adipose tissue

This study has demonstrated that canine MSC could be reliably isolated from both bone marrow and adipose tissue in a range of breeds, ages and sexes. The only poor yield was from bone marrow of a 10 year old, entire male, Labrador. It is possible that the age of the animal may have been the reason for the poorer yield, although good yields were obtained from other mature animals and adipose tissue from the same animal produced a successful culture. Morphologically, cells from both tissue types were consistent with descriptions of MSC in the literature, namely fibroblast-like cells with multiple projections, although Ad-MSC subjectively contained less cytoplasm (Hematti, 2012). After 48 hours, it was a consistent finding that many more cells were adhered to the culture plastic from the adipose tissue than bone marrow. This finding has been shown in many species, however there is debate as to whether this is purely a dilution effect of blood as when direct weight comparisons were made, no difference in yield was detected (De Ugarte et al., 2003; Kern et al., 2006; Strioga et al., 2012). In this case, the difference in yield may be purely a function of the different methods of collection with collagenase digestion of adipose tissue yielding more cells than simple flushing of the bone marrow medullary cavity. Collagenase digestion of bone marrow may yield a higher concentration of BM-MSC than flushing. Both MSC types readily adhered to tissue culture plastic therefore fulfilling one of the minimal criteria of mesenchymal stem cells (Dominici et al., 2006).

5.6.2 The isolated cells fulfil cell surface antigen criteria of MSC

Previously in our laboratory, BM-MSC have been isolated and demonstrated to express CD44 and STRO-1 by ICC (Hodgkiss-Geere et al., 2012). This present

study confirmed this finding in BM-MSC and also demonstrated that Ad-MSC also express these markers. In addition, both MSC types express CD105, one of the markers highlighted by Dominici et al. (2006). An important aspect of MSC phenotyping is to ensure that there is not significant contamination by haematopoietic cells. This is most convincingly performed by flow cytometry (Dominici et al., 2006). These would be most likely to be present in the BM-MSC due to cohabitation of the bone marrow niche. Using the pan-leucocyte marker CD45, a small percentage (3.4%) of the BM-MSC was positive, consistent with this hypothesis, whilst no CD45 positive Ad-MSC were detected. Neither Ad-MSC nor BM-MSC populations contained CD11b nor CD19 positive cells, demonstrating cultures were free of monocytes/macrophages and B cells.

5.6.3 Isolated canine Ad and BM-MSC are capable of tri-lineage mesenchymal differentiation

Using standard staining to demonstrate adipocyte, osteoblast and chondrocyte differentiation, both cell types were convincingly positive for all lineages. Toludine blue metachromatic staining of cartilage pellets, although present, was less dramatic than that demonstrated by Requicha et al. (2012). Both cell types also demonstrated significant increases in aggrecan gene expression, the major proteoglycan in articular cartilage produced by chondrocytes (Kiani et al., 2002). Interestingly, both cell types showed no increase in *Sox9*, which is the master-regulator of chondrogenesis. As one of the functions of *Sox9* is to bind to the aggrecan promoter and upregulate aggrecan expression, this appears an unusual result (Sekiya et al., 2000). One possible explanation for this apparent paradox is that gene expression during differentiation is dynamic and *Sox9* gene expression is shut-off during final maturation of chondrocytes into hypertrophic chondrocytes (Murakami et al., 2000). Therefore it is possible up-regulation of Sox9 was missed in these samples. Analysis at a range of time points would clarify this. Another possibility is that chondrogenesis is dysregulated and stimulation of gene expression is down-stream of Sox9 expression. From the literature there appears to be variation in Sox9 expression. Reich et al. (2012) detected an increase in Sox9 with BM-MSC but a

decrease with Ad-MSC. This was corroborated with more convincing cartilage formation in BM-MSC by histology and up-regulation of Collagen 2A1 only in BM-MSC. Other authors have demonstrated convincing chondrogenic differentiation of both canine Ad-MSC and BM-MSC with Sox9 expression and also convincing chondrogenic differentiation with no Sox9 up-regulation (Csaki et al., 2007; Requicha et al., 2012; Vieira et al., 2010). Innes et al. (2013) failed to get convincing differentiation of Ad-MSC using the same media formulation as the present study. These disparate results need to be viewed with knowledge that a donor age-related reduction in differentiation ability of MSCs has been demonstrated, along with variation in ability according to donor site and passage number (Guercio et al., 2013; Kanawa et al., 2013; Vieira et al., 2010; Volk et al., 2012).

The optimum conditions for chondrogenic differentiation are under constant refinement. The Requicha et al. (2012) chondrogenic media also contained sodium bicarbonate and L-proline which may improve differentiation. Also FGF has been demonstrated to up-regulate *Sox9* expression therefore addition of this growth factor to chondrogenic media may enhance chondrogenesis (Murakami et al., 2000). Ad-MSC, appear to lose sensitivity to TGFβ during culture by down regulation of the TGF-β receptor. Receptor expression can be restored by the addition of bone morphogenic protein (BMP), which also directly up-regulates *Sox9*; therefore this may be a useful addition to chondrogenic media (Hennig et al., 2007; Semba et al., 2000). Finally, temporal variation in growth factors may also be important. It has been shown that a specific protocol of sequential addition of TGFβ and BMP, importantly including a period without growth factors, improved chondrogenesis in human BM-MSC at least (Handorf and Li, 2014).

Both cell types produced nodules which stained strongly with Alizarin red, indicating calcification after 14 days culture in osteogenic media. Undifferentiated BM-MSC exhibited mild staining which became dramatic after differentiation. Interestingly, there was no up-regulation of the osteoblast markers osteopontin and osteonectin in these cells. This may be that these genes were sufficiently expressed in the basal state, consistent with the initial staining results or as osteoblast gene expression

during differentiation has been shown to be dynamic in BM-MSC and Ad-MSC, the period of up-regulation may have been missed in this experiment (Kulterer et al., 2007; Requicha et al., 2012).

Both cell types demonstrated the presence of lipid vacuoles after adipogenic induction as well as many fold significant increases in FAB4 and LPL. In both cell types there was no increase in leptin expression. In the studies of canine Ad-MSC by Vieira et al. (2010), and canine umbilical cord vein MSC by Zucconi et al. (2010), leptin expression was demonstrated in the undifferentiated cells. In the present study, leptin was also detectable by qPCR in the undifferentiated cells therefore this may explain the lack of increase in gene expression. Leptin is a hormone produced by adipocytes in proportion to their total mass *in vivo* (Maffei et al., 1995). It has been proposed that one of signalling triggers is physical distension of the adipocyte by fat vacuoles (Hamilton et al., 1995). Although multiple lipid vacuoles were present in the differentiated adipocytes, there was no evidence of cell membrane distention. This may be a factor in the lack of increase.

5.7 Summary

- Reproducibly isolated cells consistent with MSC from both adipose and bone marrow tissue
- Both cell types express CD44, CD105 and Stro-1
- Both cell types lack haematopoietic markers CD45, CD11b and CD19
- Cells can be readily expanded and differentiated to adipogenic, osteogenic and chondrogenic cells.
- Both adipose and bone marrow can provide a source of MSCs which can be used to perform differentiation protocols towards hepatocyte-like cells.

Chapter 6: Mesenchymal to hepatocyte differentiation

6.1 Abstract

Differentiation of mesenchymal stem cells (MSC) into hepatocyte-like cells has been demonstrated in many species. Canine adipose and bone marrow-derived mesenchymal stem cells isolated and characterised as described in chapter 5 were cultured in conditions described to produce hepatocyte-like cells in other species. The effect of DNA demethylation and preventing histone deacetylation, with 5AZA and valproic acid respectively, on differentiation capacity was also examined. Cells were assessed using the tests validated with primary canine hepatocytes.

Undifferentiated adipose and bone marrow-derived MSC were positive for LDL uptake. This was confirmed to be via the specific LDL receptor by lack of Ac-LDL uptake, Immunofluorescence demonstrating the presence of LDL receptor on the cell membrane and LDL-receptor gene expression at the same level as canine primary hepatocytes. Mouse and human bone marrow-derived MSC were also assessed for LDL receptor presence by LDL/Ac-LDL uptake and immunofluorescence. Both of these species MSC were also found to express the LDL receptor. Undifferentiated adipose and bone-marrow-derived MSC's also demonstrated albumin gene expression. Both these characteristics have been attributed to a hepatocyte-like phenotype.

During differentiation both cells types exhibited a dramatic change in morphology from fibroblastic to epithelial. A reduction in vimentin and fibronectin gene expression was noted, consistent with this. The only evidence of a hepatocyte-like phenotype was an increase in α1anti-trypsin in differentiated BM-MSC. Both DNA demethylation and histone deacetylator inhibitors did not improve hepatocyte differentiation.

Although differentiation capacity is donor and culture condition dependant, this data suggests that canine adipose and bone marrow-derived do not undergo differentiation to a hepatocyte-like phenotype using these differentiation protocols.

6.2 Introduction

Since the discovery that MSC have the ability to differentiate beyond cells of mesodermal lineage, termed transdifferentiation, there has been great interest in production of hepatocyte-like cells *in vitro* from MSC's (Seo et al., 2005). The first report of this was by Schwartz et al. (2002) utilising human, murine and rat BM-MSC. This paper provided robust analysis of the resultant cells. These cells became epithelioid and stained positively for albumin, keratin 18 and hepatocyte nuclear factor 3β. PCR analysis revealed increased gene expression of albumin, keratins 18 and 19, transthyretin and selected cytochrome enzymes. Albumin and urea release into the supernatant was demonstrated along with positive staining for glycogen. Seo et al. (2005) provided the first demonstration that adipose-derived MSC could also be differentiated into hepatocyte-like cells using human adipose tissue. This again was convincingly demonstrated with a change to epithelioid morphology, gene expression of α-foetal protein and albumin as well as urea production. Since these initial reports, there have been many subsequent papers detailing production of hepatocyte –like cells from MSC in a variety of species. In part, these studies have attempted to improve the degree and efficiency of differentiation as this, 10 years on since the first report, is still stated to be inadequate (Wu and Tao, 2012). Although similar basic protocols are utilised, differences in growth factor/chemical concentrations, culture times and confirmatory tests make comparisons between reports difficult. As stated in the previous chapter, age of donor, site of MSC harvest and passage number are significant factors in the efficiency of mesodermal lineage differentiation. It is likely that these also are important in transdifferentiation efficiency, further complicating the picture.

6.2.1 Growth factors and compounds used in hepatocyte differentiation

The majority of MSC to hepatocyte-like cell reports have based their differentiation protocols on what is known about key growth factors and chemicals required during foetal liver development as well as empirical evidence (Snykers et al., 2009a).

The three growth factors which are commonly used in MSC to hepatocyte differentiation are fibroblast growth factors (FGF), Oncostatin M (OSM) and hepatocyte growth factor (HGF).

6.2.1.1 Fibroblast growth factors

Fibroblast growth factors have diverse roles with main functions including angiogenesis, wound healing and neurogenesis (Ornitz and Itoh, 2001). As the name suggests are potent stimuli for fibroblastic proliferation. FGF appears to be an important stimulus at the endodermal specification stage of hepatogenesis (Wu and Tao, 2012). FGF-1, FGF-2 and FGF-8 are produced by the adjacent cardiac mesoderm during hepatic foregut endoderm specification. It has been shown that FGF-8 knockout is lethal prior to hepatogenesis and FGF-8 has only partial hepatogenic activity. Purified FGF1 & 2 efficiently specified hepatic differentiation. FGF-4 receptors are expressed in the endoderm during hepatogenesis (Wells and Melton, 1999; Zaret, 2001). In stem cell to hepatocyte differentiation, both FGF-2 and FGF-4 have been utilised in protocols (Al Battah et al., 2011).

6.2.1.2 Oncostatin M

OSM is a member of the IL-6 cytokines, originally isolated from lymphoma cells. In embryogenesis, the foetal liver is infiltrated by haematopoietic stem cells (HSC); thereby becoming a major site of haematopoiesis for a period of embryogenesis before the liver abruptly switches from haematopoiesis to further hepatic differentiation. This change is controlled in part by OSM which is released from the HSC and induces maturation of hepatocytes in mid to late foetal development (Kamiya et al., 2001; Kinoshita et al., 1999). For hepatocyte differentiation of stem cells, OSM concentrations range from 10-30ng/ml (Al Battah et al., 2011).

6.2.1.3 Hepatocyte growth factor

HGF was originally identified to be increased in the serum of partially hepatectomised rats and was able to cause *in vitro* hepatocyte proliferation (Matsumoto and Nakamura, 1997). Subsequently it has been identified that HGF is secreted by mesenchymal cells during embryonic development and binds to hepatocyte growth factor receptor (HGFR), which is encoded by c-Met, a proto-oncogene. HGFR is a tyrosine kinase receptor which upon activation initiates the invasive growth programme (Gentile et al., 2008). The interaction of HGF and HGFR regulates epithelial development and morphogenesis of various organs during embryogenesis including the kidney, mammary gland, lung and liver. During liver formation and maturation, HGF appears to play a role in in the early post-natal period (Nakamura et al., 2011). Concentrations of HFG used in MSC to hepatocyte differentiation range from 5-50ng/ml with 20ng/ml most commonly used (Schwartz et al., 2002; Talens-Visconti et al., 2007).

Both OSM and HGF therefore appear to induce hepatic maturation but act via different signalling pathways with OSM acting via STAT-3 and HGF acting via an as yet unknown STAT-3 independent means (Kamiya et al., 2001).

Other compounds commonly added to media during differentiation are dexamethasone, nicotinamide, insulin, transferrin and selenium (Wu and Tao, 2012). For many of these compounds, evidence of efficacy is empirical and the method of action is unknown. Steroids have been shown to up-regulate HGFR expression and also promote differentiation by suppression of cell division.

Addition of DMSO to primary hepatocyte cultures has been shown to improve function via "re-differentiation" of hepatocytes whereby they regain function which was lost during *in vitro* culture (Su and Waxman, 2004). As a result of this, DMSO has also been used during hepatocyte differentiation of mesenchymal stem cells (Snykers et al., 2009a). The mechanism of DMSO action has not been defined

although histone hyper-acetylation has been postulated (Snykers et al., 2007). Use of DMSO is not without risk, as although DMSO is commonly used for cryopreservation during cell culture, it has the potential to be toxic and has been shown to reduce stem cell viability, reduce stem cell markers and decrease functionality of ESC-generated hepatocyte-like cells (Pal et al., 2012).

6.2.2 Epigenetic modification

Gene expression can be regulated by modifications which do not change the DNA sequence. This has been termed epigenetic modification. Methylation of DNA i.e. the binding of a methyl group to cytosine-guanine dinucleotides (CpG) suppresses expression of those genes either by physically interfering with transcriptional binding proteins or also by binding of proteins containing a methyl-CpG-binding domain (MBD), which in turn attracts histone deacetylases modifying histone to produce a compact chromatin structure. This has the effect of reducing gene expression. After DNA replication and cell division, maintenance methylation by DNA methyltransferase 1 (DNMT1) acts transfer the methylation status down to the resultant 2 DNA "offspring".

In the production of induced pluripotent stem cells (iPSC), it has been shown that DNA methylation serves as an "epigenetic memory" in that iPSC produced from different cell types retain a memory affecting their ability to differentiate whereby the most efficient differentiation is towards a cell type related to the cell or origin (Kim et al., 2010). As an example of this, iPSC produced from pancreatic β cells had a methylation pattern that was unique, with increased histone acetylation of key genes including insulin. As stated above, acetylation of histone allows a more open structure, favoring gene expression. These β cell-derived iPSC differentiated more efficiently into β cell than iPSC from other tissues or embryonic stem cells (Bar-Nur et al., 2011).

There has been much interest in modifying the epigenetic memory of stem cells to enhance their pluripotent potential (Moschidou et al., 2013; Rajasingh et al., 2011).

Two main classes of compound have been used: DNA methylation inhibitors; 5Aza-2-deoxycytidine (5AZA), zebularine and histone deacetylase inhibitors; valproic acid, trichostatin A (TSA) and sodium butyrate.

6.2.2.1 5AZA and zebularine

These are analogues of cytidine for which they substitute during replication. These then covalently bind DNMT causing enzyme degradation. As they intercalate within genomic DNA, this may cause mutation and cytotoxicity (Christman, 2002; Yoo et al., 2004). These compounds have also been used to enhance the differentiation ability of MSC's (Naeem et al., 2013; Seeliger et al., 2013). Specifically, in differentiation towards hepatocyte-like cells, Seeliger et al. (2013) demonstrated that pre-treatment of human Ad-MSC with 5AZA improved the subsequent functional abilities of hepatocyte-like cells compared to untreated cells. Sgodda et al. (2007) utilized 5ASA prior to hepatocyte induction of rat Ad-MSC. No untreated cells were differentiated to assess the effect of 5AZA on efficiency or function of differentiation.

6.2.2.2 Valproic acid

Chen et al. (2009) showed that incubation with 2.5mM valproic acid for 72 hours prior to differentiation improved hepatocyte gene expression and function of mouse BM-MSC and Dong et al. (2013) demonstrated the same effect with 5mM valproic acid on human BM-MSC. Trichostatin A has also been used to improve hepatocyte differentiation of human BM-MSC (Snykers et al., 2007).

6.2.2.3 Sodium butyrate

This appears to improve primary hepatocyte culture function is also a histone deacetylase inhibitor. This has been used in embryonic stem cell and induced pluripotent stem cell to hepatocyte differentiation to improve efficiency of differentiation (Perry et al., 1979; Sharma et al., 2006; Zhang et al., 2011). There is one report of sodium butyrate use in MSC differentiation at present where pre-treatment decreased the efficiency of adipogenic and chondrogenic differentiations but enhance osteogenic differentiation (Lee et al., 2009).

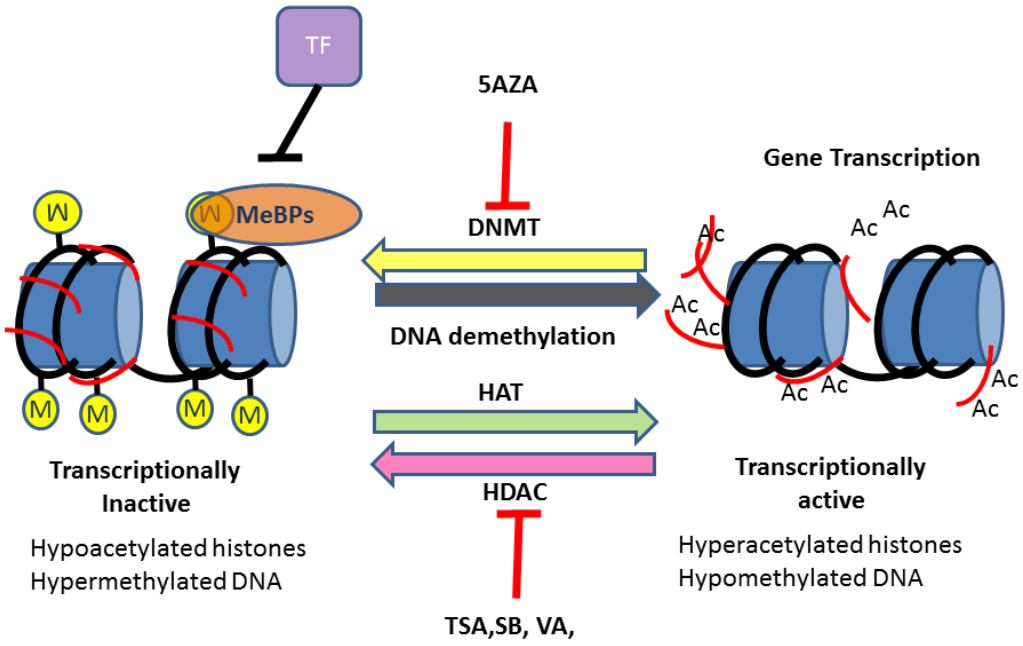

Figure 6.1 Epigenetic control of gene transcription
Hypermethylation of DNA and deacetylation of histones will tend to down-regulate gene expression. Binding of transcription factors (TF) is blocked by non-permissive chromatin resulting from methyl-binding proteins (MeBPs) binding to methylated cytosine and recruitment of HDAC co-repressor complexes. DNMT inhibitors such as 5AZA (5-AZA-C) and histone deacetylase (HDAC) inhibitors (valproic acid [VA], Trichostatin A[TSA], sodium butyrate [SB]) modify chromatin structure to produce an open and transcriptionally active configuration allowing transcription factor access and favouring gene expression. Modified from Snykers et al. (2009b).

6.2.3 Canine MSC to hepatocyte differentiation

There is one report in the literature describing canine MSC to hepatocyte differentiation. Choi et al. (2013) differentiated canine amniotic and BM-MSC's using a conditioning step of 20ng/ml EGF and 10ng/ml bFGF and then 2 step conditioning of; 20ng/ml HGF and 5ng/ml bFGF, finally 20ng/ml OSM, 1µM dexamethasone and 5mmol/l nicotinamide. Demonstration of hepatocyte function was restricted to gene expression using end-point PCR and gel electrophoresis. Amniotic cells expressed albumin, tyrosine aminotransferase and α1-anti-trypsin whilst BM-MSC only exhibited α1-anti-trypsin expression. No functional assays were performed.

6.3 Aims

The aims of this chapter were to produce functional canine hepatocyte-like cells from canine adipose and bone marrow-derived mesenchymal stem cells isolated and characterised in Chapter 5. Protocols published and proven to be successful in other species will be used. The effect of DNA demethylating compounds and histone deacetylase inhibitors will also be investigated. The success of attaining a hepatocyte-like phenotype will be judged on methods validated using canine primary hepatocyte cultures in Chapter 3. This includes gene expression, cytochrome activity, LDL uptake and PAS staining.

6.4 Materials and Methods

6.4.1 Primer efficiency

Primers for E-cadherin, fibronectin, vimentin and β-catenin were donated by Alexandro Cervantes. Efficiency was assessed using 10-fold dilutions of cDNA from canine hepatic tissue using the method described in Chapter 2.

6.4.2 Culture of mouse and human BM-MSC

6.4.2.1 Mouse

Murine bone marrow mesenchymal stem cells were purchased from Life technologies (Gibco Cat. No. S1502-100). These were thawed by swirling the cryopreservation vial in a 37^{o}C water bath before transferring to a 15ml falcon tube and slowly adding 10ml warm DMEM/F12 medium containing 10% foetal calf serum and 100 U/mL penicillin G and 100 μg/mL streptomycin (all Invitrogen, UK). This was centrifuged at 300g for 5 minutes and the cells re-suspended in 10 mLs of warmed media. These cells were counted and seeded at 5 x10^{3}/cm^{2}. Media was changed every 3 days and cells passaged when 80% confluent using the method detailed in Chapter 2.

6.4.2.2 Human

Human bone marrow derived mesenchymal stem cells were purchased from Life technologies (Gibco Cat. No. A15652). These were thawed and processed in the same manner as the mouse cells except for the fact that MesenPRO RS™ Medium (Invitrogen, UK) was used.

6.4.3 5-Aza-2′-deoxycytidine (5AZA) toxicity assay

Stock 5AZA solution was prepared by dissolving 5-Aza-2′-deoxycytidine (Sigma Aldrich, UK) in 50% acetic acid to a concentration of 50mg/ml. A total of 1.5 $x10^4$ cells/cm^2 of both Ad-MSC and BM-MSC were plated into 96 well plates in standard MSC media. After 24 hours, concentrations of 5, 10, 15,20,25,30 and 50µM of 5AZA were added to 3 wells of each cell type. Control cells had vehicle equivalent to the 50 µM concentration added. After 24 hours, media was replaced with fresh MSC media and cell viability was assessed using the MTT assay at time points 24 and 48 hours.

6.4.4 Hepatic differentiation of mesenchymal stem cells

Cells were plated at a concentration of 1 $x10^4$/cm^2 in 6 well plates (RNA extraction), 12 well plates (Periodic acid Schiff staining) and 96 well plates (Cytochrome activity) and cultured in standard MSC media for 48 hours prior to commencing experiments.

6.4.5 Experiment 1 - Differentiation according to Lee et al. (2004)

Canine BM-MSC from D231112 were used. A 2 day pre-induction step in serum-deprived Iscove's Modified Dulbecco's Media containing 20ng/ml of bFGF and epidermal growth factor was performed before the two step differentiation process performed (Figure 6.2). Cells were collected for real time PCR analysis on days 15 and 20.

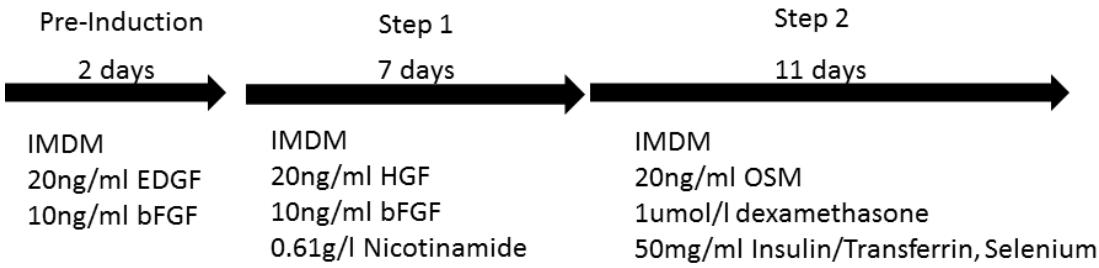

Figure 6.2 Protocol used during MSC to hepatocyte-like cell differentiation. Based on protocol described by Lee et al. (2004). EDGF – epidermal-derived growth factor, HGF – hepatocyte growth factor, bFGF – basic fibroblastic growth factor, OSM – oncostatin M.

6.4.6 Experiment 2 - Differentiation according to Talens-Visconti et al. (2007)

Both Ad-MSC and BM-MSC from D231113 were used. Figure 6.3 shows the protocol used.

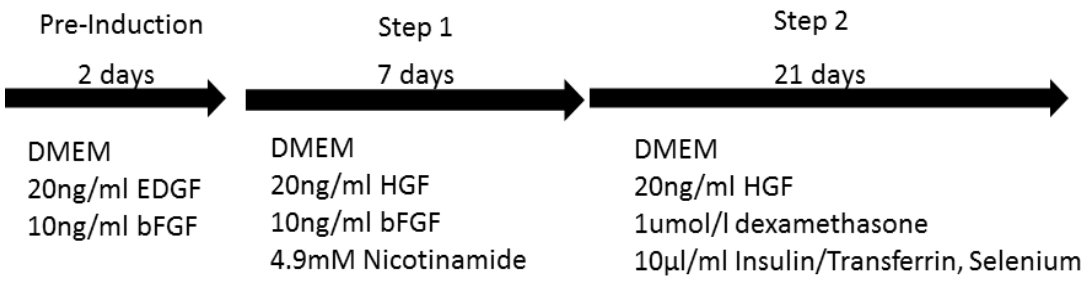

Figure 6.3 Protocol for MSC to hepatocyte differentiation modified from Talens-Visconti et al. (2007)
EDGF – epidermal-derived growth factor, HGF – hepatocyte growth factor, bFGF – basic fibroblastic growth factor.

Cells were photographed to assess morphology at time points 0,14 and 30 days. Cells from a 6 well plate were harvested at time points 0,14 and 30 days for PCR analysis. Undifferentiated Ad-MSC and BM-MSC which had been in culture for 30 days were also harvested as controls. DiI-LDL uptake was assessed at time points 0 and 14 days. Cytochrome P450 activity was assessed at time points 0, 14 and 30 days using the Promega Luciferin assay. At each time point, three wells had rifampicin added at a concentration of 50µM for 48 hours prior to cytochrome activity measurement in an attempt to induce cytochrome activity. PAS staining was performed at time points 0 and 30 days. AD23113 primary hepatocytes were used as a positive control.

6.4.7 Experiment 3 - Does a longer differentiation protocol allow transdifferentiation to hepatocyte-like phenotype?

A protocol based on both Lee et al. (2004) and Talens-Visconti et al. (2007) was used (Figure 6.4). Cells were plated onto collagen coated plates as before and photographed and harvested for PCR analysis at time points 0 and 50 days. Cytochrome activity was assessed as in experiment 1.

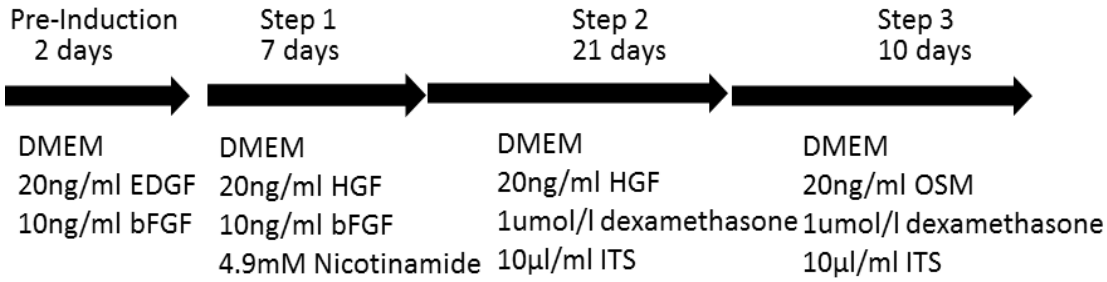

Figure 6.4 Experiment 3 protocol for MSC to hepatocyte differentiation
Modified from both Lee et al. (2004) and Talens-Visconti et al. (2007). EDGF – epidermal-derived growth factor, HGF – hepatocyte growth factor, bFGF – basic fibroblastic growth factor, OSM – oncostatin M. ITS – Insulin/transferrin/Selenium supplement (Sigma-Aldrich, UK).

6.4.8 Experiment 4 – Does prior 5AZA treatment allow transdifferentiation to hepatocyte-like phenotype?

A differentiation protocol according to Talens-Visconti et al. (2007) was again utilised using Ad-MSC and BM-MSC from D231113 after 24 hours' culture in MSC media with the addition of 20µM 5AZA . Cell morphology was photographed and real-time PCR was performed at time points 0 and 18 days.

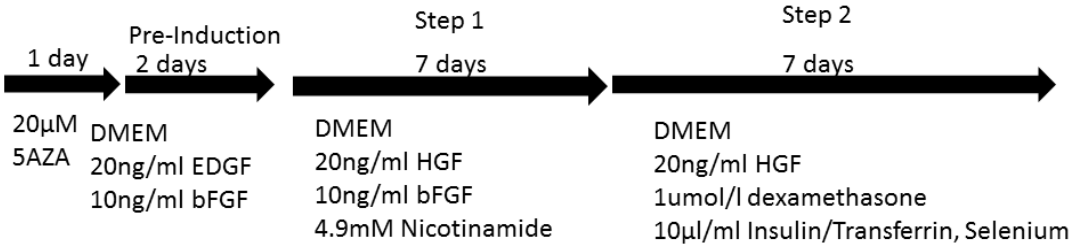

Figure 6.5 Protocol for experiment 4
5AZA - 5-Aza-2′-deoxycytidine, EDGF – epidermal-derived growth factor, HGF – hepatocyte growth factor, bFGF – basic fibroblastic growth factor.

6.4.9 Experiment 5 - Does prior valproic acid treatment allow transdifferentiation to hepatocyte-like phenotype?

Valproic acid sodium salt (Sigma Aldrich, UK) was dissolved at a concentration of 150mg/ml in standard MSC medium to provide stock solution. Cells Ad-MSc and BM-MSC from D19713 were treated with 5mM valproic acid for 72 hours in standard MSC media prior to repeating the protocol used in experiment 2.

6.5 Results

6.5.1 PCR efficiency of epithelial and mesenchymal genes

Primers for E-cadherin, fibronectin, vimentin and β-catenin had acceptable efficiency, dissociation curves and obtained the expected product size on gel electrophoresis tissue (Table 6.1).

Gene	Sequence	Product size (bp)	Efficiency %	TM ^{o}C	Dissociation curve	Gel size
E-cadherin	F – TGACAGCTACACGTTCACCG R- TGCATCCTTCAAAACTCACCCT	80	101.3	60.3/60.16	√	√
Fibronectin	F – GACCTAGAGGTCATCGCTGC R- CAGGGCTGTTTCCTCCTGTT	115	97.7	60/55.00	√	√
Vimentin	F – GGACCAGCTCACCAACGACA R - GCATCTCCTCTTGCAACTTCTC	99	98.3	62/60.62	√	√
β-catenin	F – GGAATGGCTACCCAAGCTGA R - AAGACTGTTGCTGCCAGTGA	91	96.3	59.74/59.8	√	√

Table 6.1 Primer details and efficiency obtained using 10-fold dilutions of hepatic tissue

6.5.2 Canine BM-MSC do not differentiate to hepatocyte-like cells with a 20 day protocol

6.5.2.1 Morphology

Compared to BM-MSc which had been maintained in standard MSC media, there was significant cell loss during the protocol with many cells detaching during media change. Only small pockets of cells remained (Figure 6.6). The cells subjectively had a higher cytoplasm to nucleus ratio and were more polygonal than undifferentiated MSC but had not assumed an epithelial morphology demonstrated by Lee et al. (2004) and other papers documenting hepatocyte differentiation.

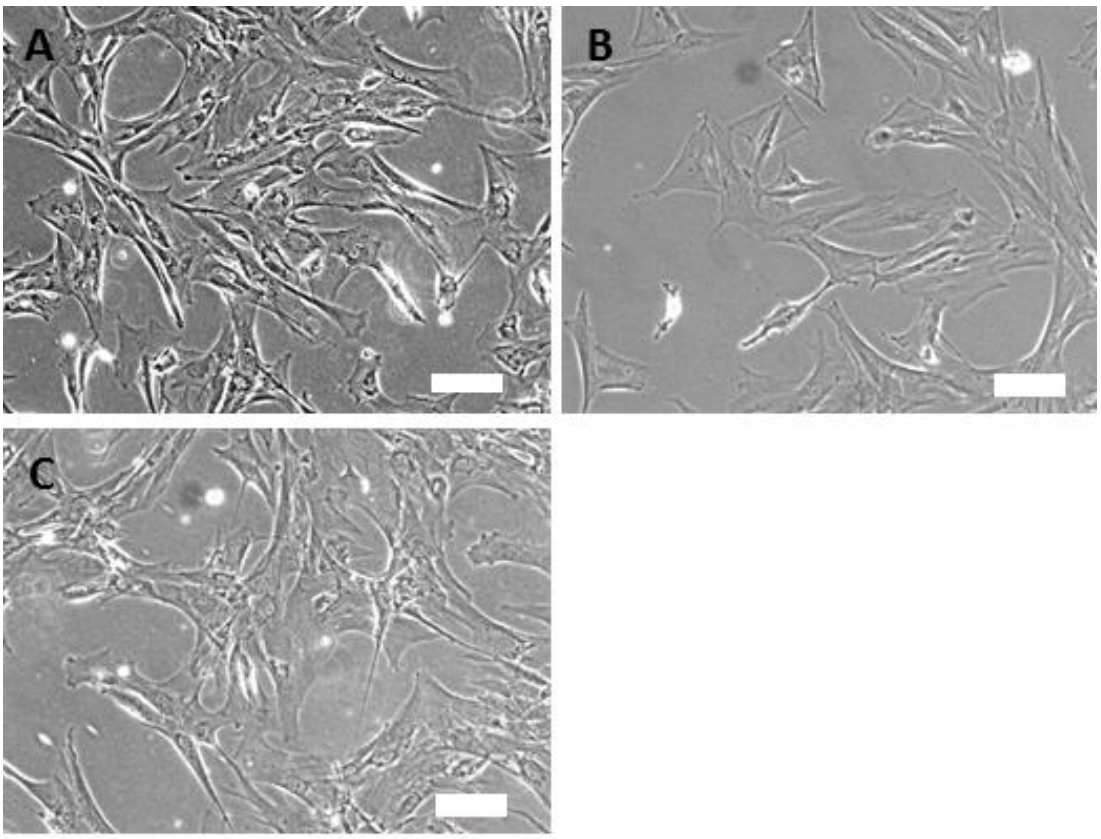

Figure 6.6 Morphology of D231112 BM-MSC before and after differentiation protocol

A- Day 0, undifferentiated BM-MSC, B- cells at day 20 after differentiation protocol, C – undifferentiated BM-MSC after 20 days in culture. White bar represents 50µm.

6.5.2.2 Gene expression

RNA yield from time point 20 days was inadequate for real-time PCR analysis due to the low cell numbers. Sufficient RNA was collected from day 15 for limited analysis. cDNA from fresh canine hepatocytes were used as a positive control. No increase in albumin, transthyretin, cytochrome 1A2 or keratin-18 gene expression was noted between day 0 and 15 (Figure 6.7).

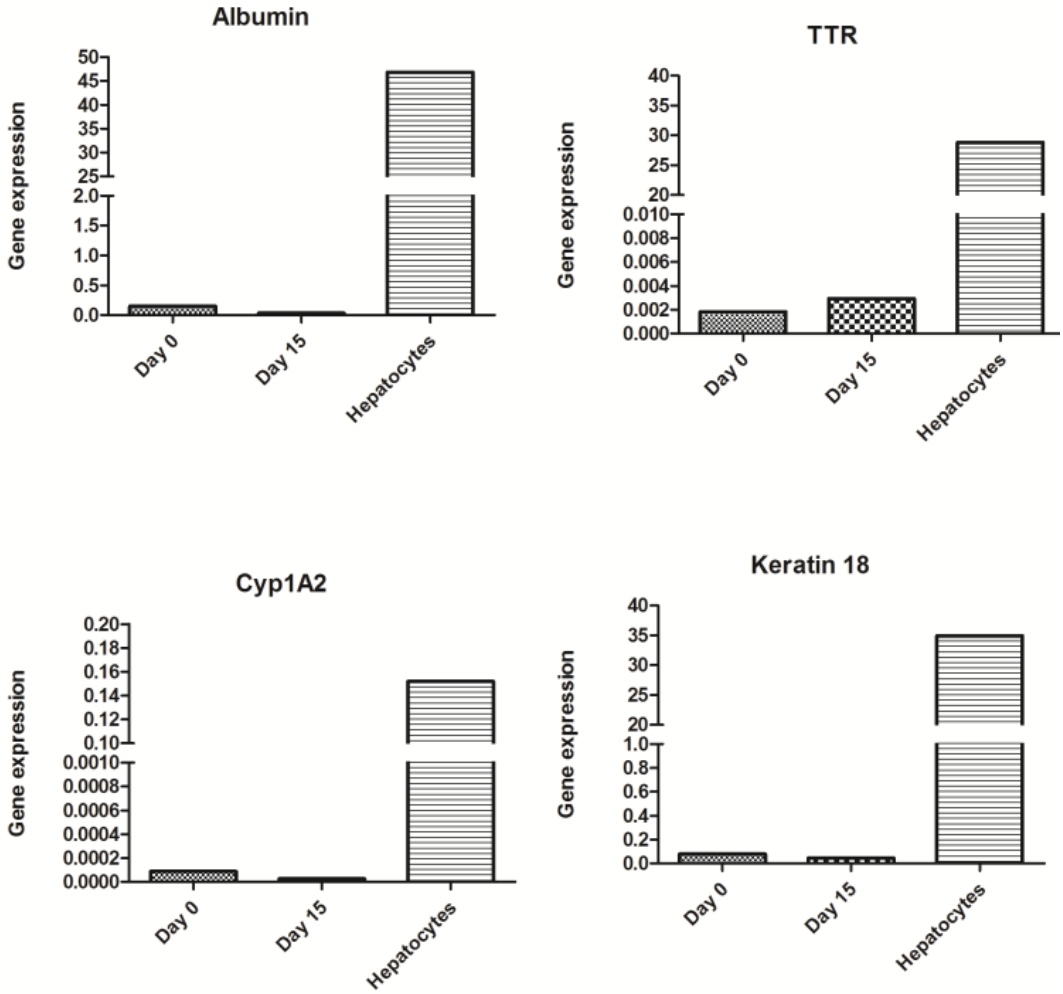

Figure 6.7 Real time PCR analysis of BM-MSC D231113 hepatocyte differentiation

Genes of interest compared against geometric mean of B2MG, HPRT and RPL8. TTR – transthyretin, Cyp1A2 – cytochrome 1A2.

6.5.3 Thirty day protocol causes change in morphology but not gene expression

In view of the apparent cell loss during differentiation, and the fact that cell density appears to be crucial to differentiation efficiency i.e. approaching confluence improves differentiation, MSC's were plated onto collagen-coated plates prior to differentiation which prevented cell loss (Snykers et al., 2009a).

6.5.3.1 Morphology

There was a gradual but dramatic change in morphology from fibroblastic mesenchymal morphology to cells, which had a much higher cytoplasm to nucleus ratio and appeared epithelioid with a cuboidal cobblestone appearance to the monolayer (Figure 6.8). This change in morphology was consistent with what had been described by Talens-Visconti et al. (2007) for Ad-MSC and Lee et al. (2004) for BM-MSC. No cell loss was evident on this occasion.

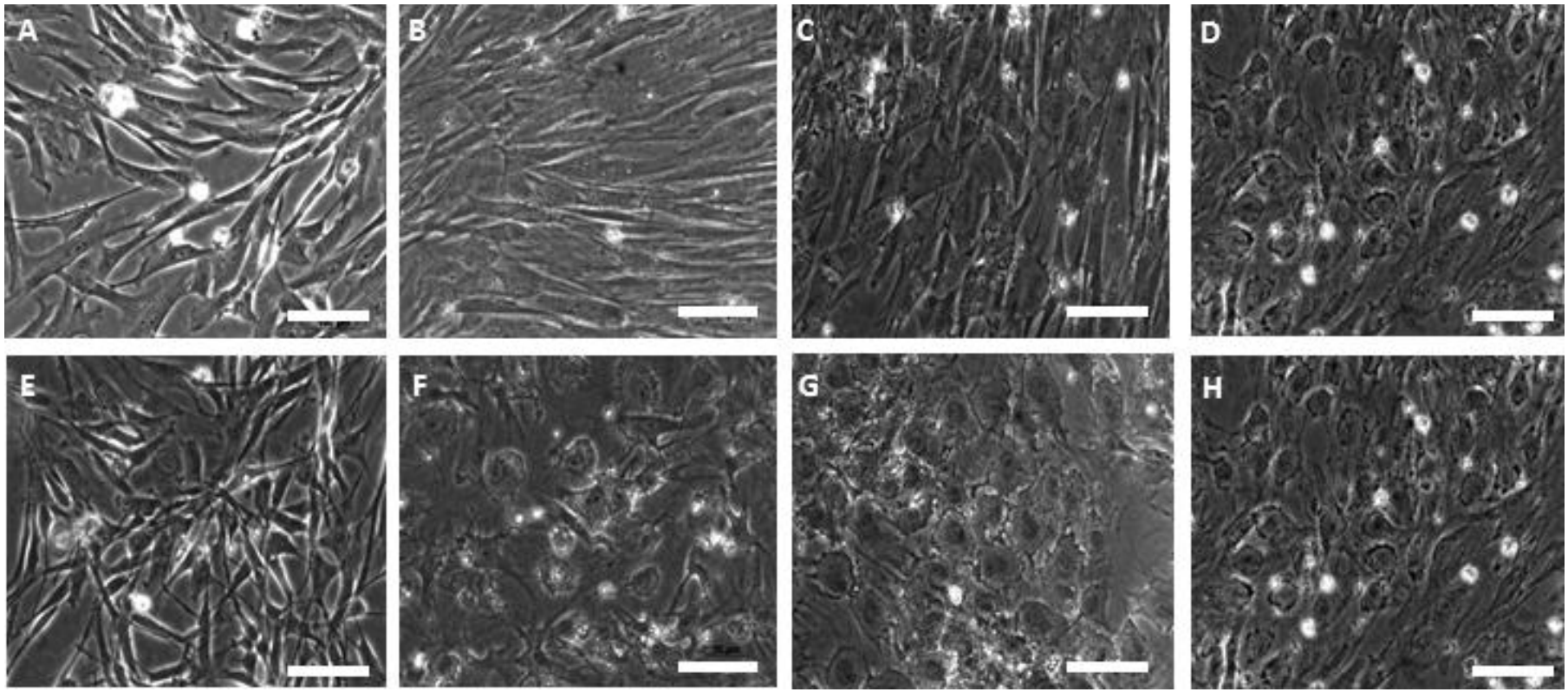

Figure 6.8 Morphology of Ad-MSC and BM-MSC that had hepatocyte differentiation based on Talens-Visconti et al. (2007).
A-D = Ad-MSC, E-H = BM-MSC. Time points from left to right, 0, 6, 14, 30 days. White bar represents 100µm.

6.5.3.2 PCR analysis

Analysis of the early markers of hepatocyte differentiation (αfoetal protein and keratin 7), demonstrated that expression actually decreased during differentiation of both Ad-MSC and BM-MSC (Figure 6.9 and Figure 6.11). Compared to the primary hepatocytes used as a positive control, gene expression of cytochrome P450 enzymes and mature hepatocyte markers albumin and keratin 18 was many magnitudes smaller in all stages of the Ad-MSC's (Figure 6.9, Figure 6.10, Figure 6.11 & Figure 6.12). Only Cyp3A12 expression was increased in the day 30 Ad-MSC cells compared to day 0 and the undifferentiated controls. From the BM-MSC differentiation, Cyp1A2 and 2D15 increased during differentiation. For all cytochrome genes, expression was several orders of magnitude below the positive controls. Of note was that undifferentiated Ad-MSC and BM-MSC expressed albumin. In view of the lack of increase in early hepatocyte markers and lack of other hepatocyte gene expression increase, there was no convincing progression of differentiation towards a hepatocyte phenotype based on gene expression.

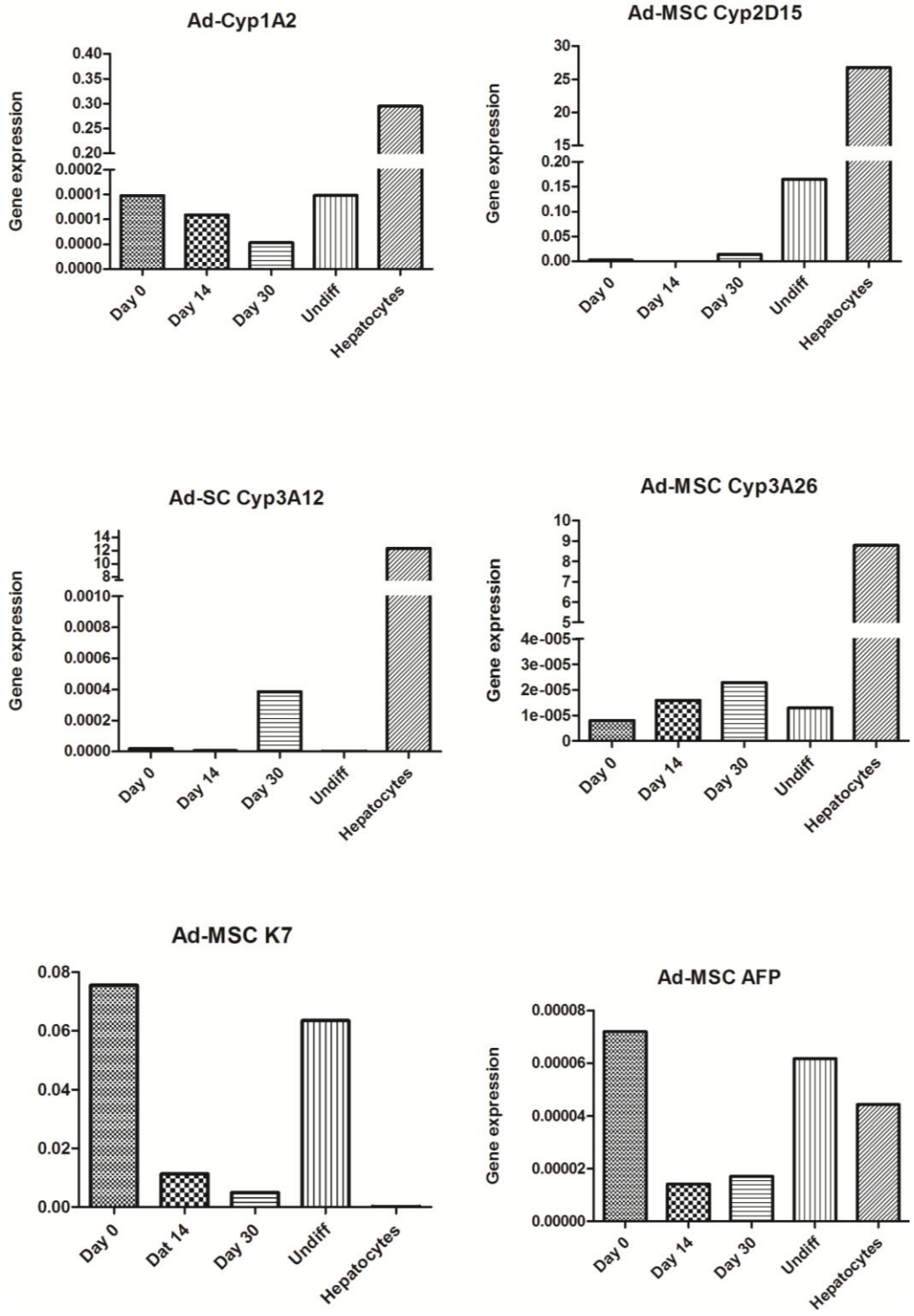

Figure 6.9 Real time PCR analysis of Ad-MSC D231113 hepatocyte differentiation
K7- Keratin 7, AFP - αfoetal protein.
Hepatocytes – D231113 primary hepatocytes used as positive control. Undiff – undifferentiated Ad-MSC maintained in MSC media for 30 days.

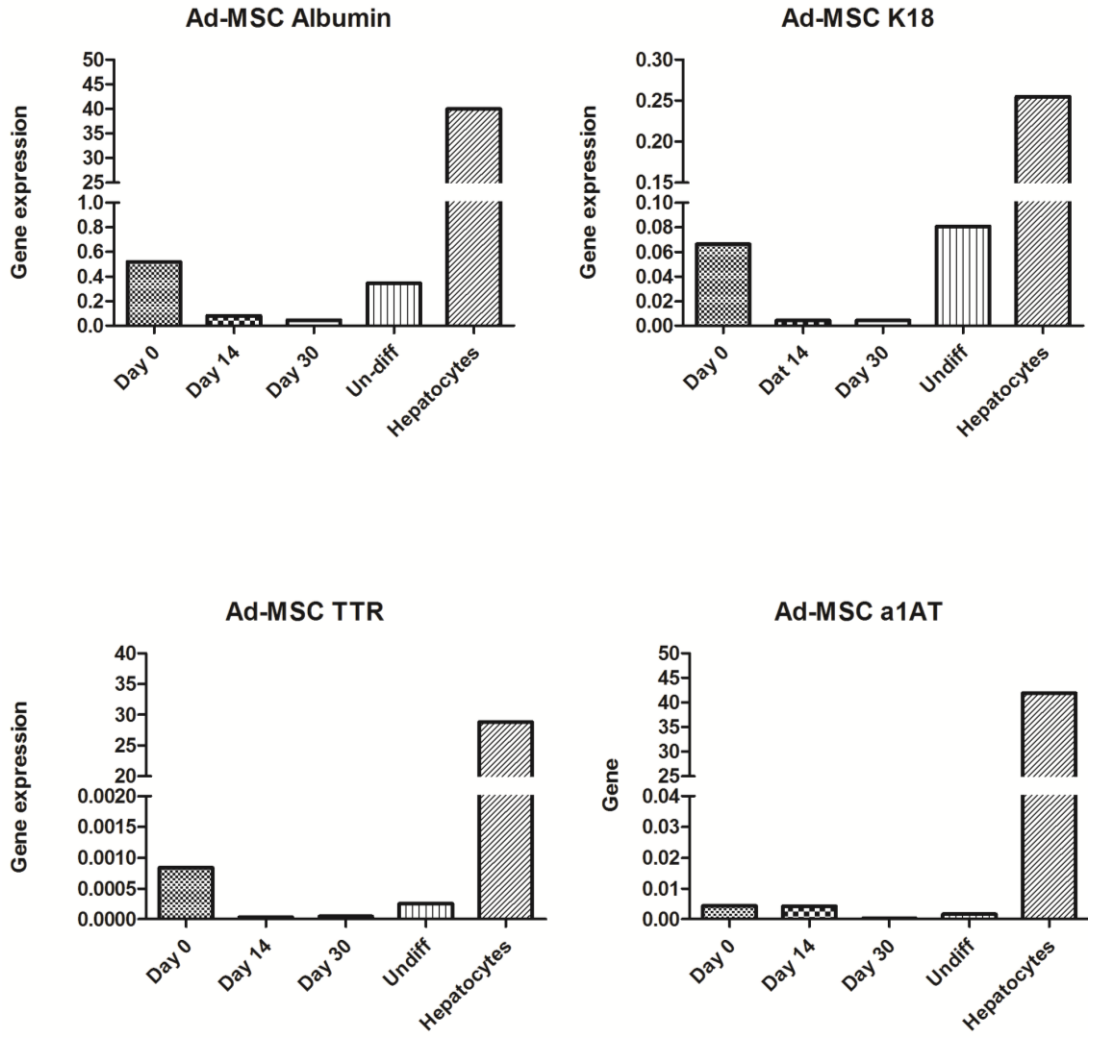

Figure 6.10 Real time PCR analysis of Ad-MSC D231113 hepatocyte differentiation

K18 – keratin 18, TTR – transthyretin, a1AT – α1-antitrypsin. Hepatocytes – D231113 primary hepatocytes used as positive control. Undiff – undifferentiated Ad-MSC maintained in MSC media for 30 days.

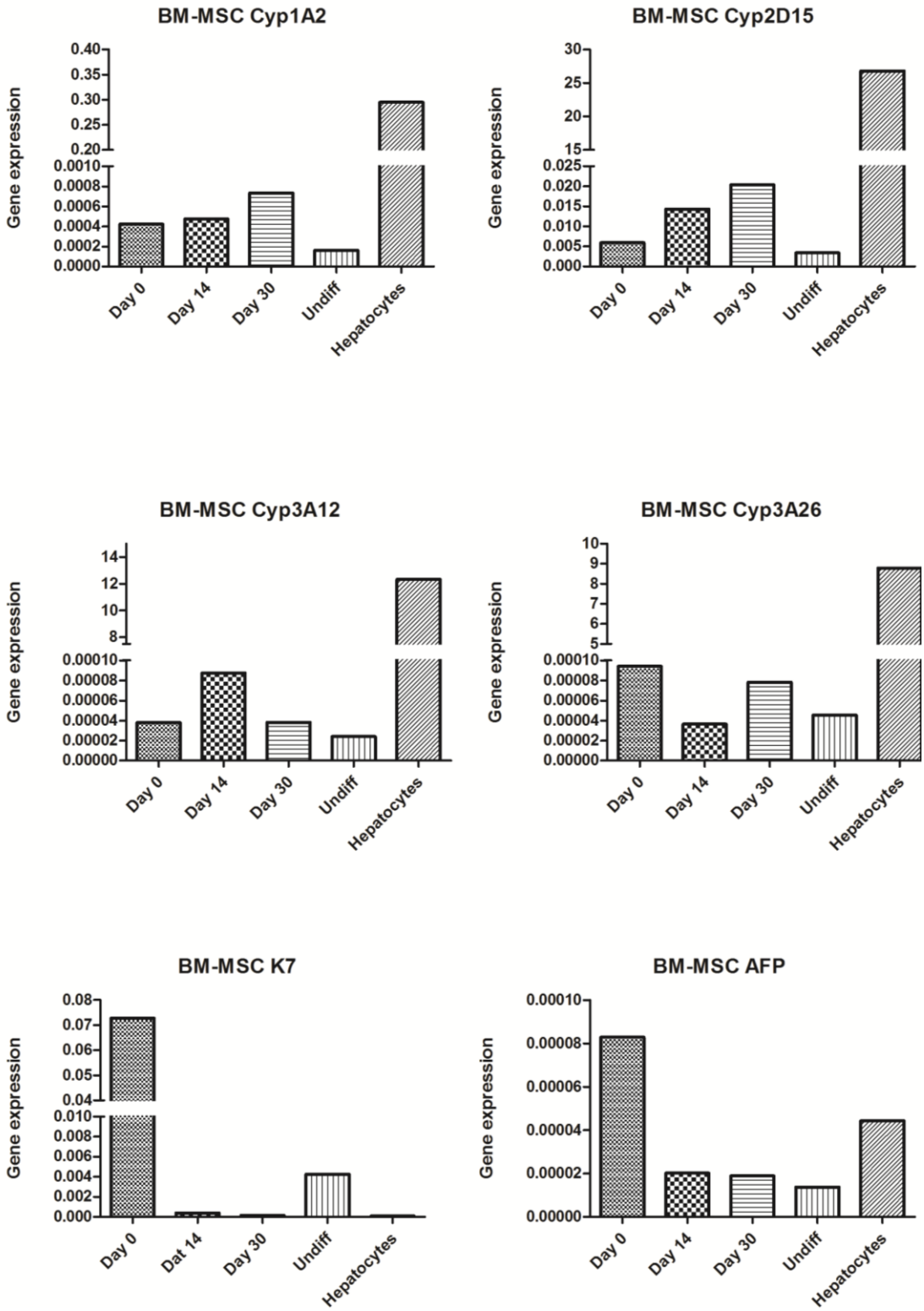

Figure 6.11 Real time PCR analysis of BM-MSC D231113 hepatocyte differentiation

K7- Keratin 7, AFP - αfoetal protein.

Hepatocytes – D231113 primary hepatocytes used as positive control. Undiff – undifferentiated BM-MSC maintained in MSC media for 30 days.

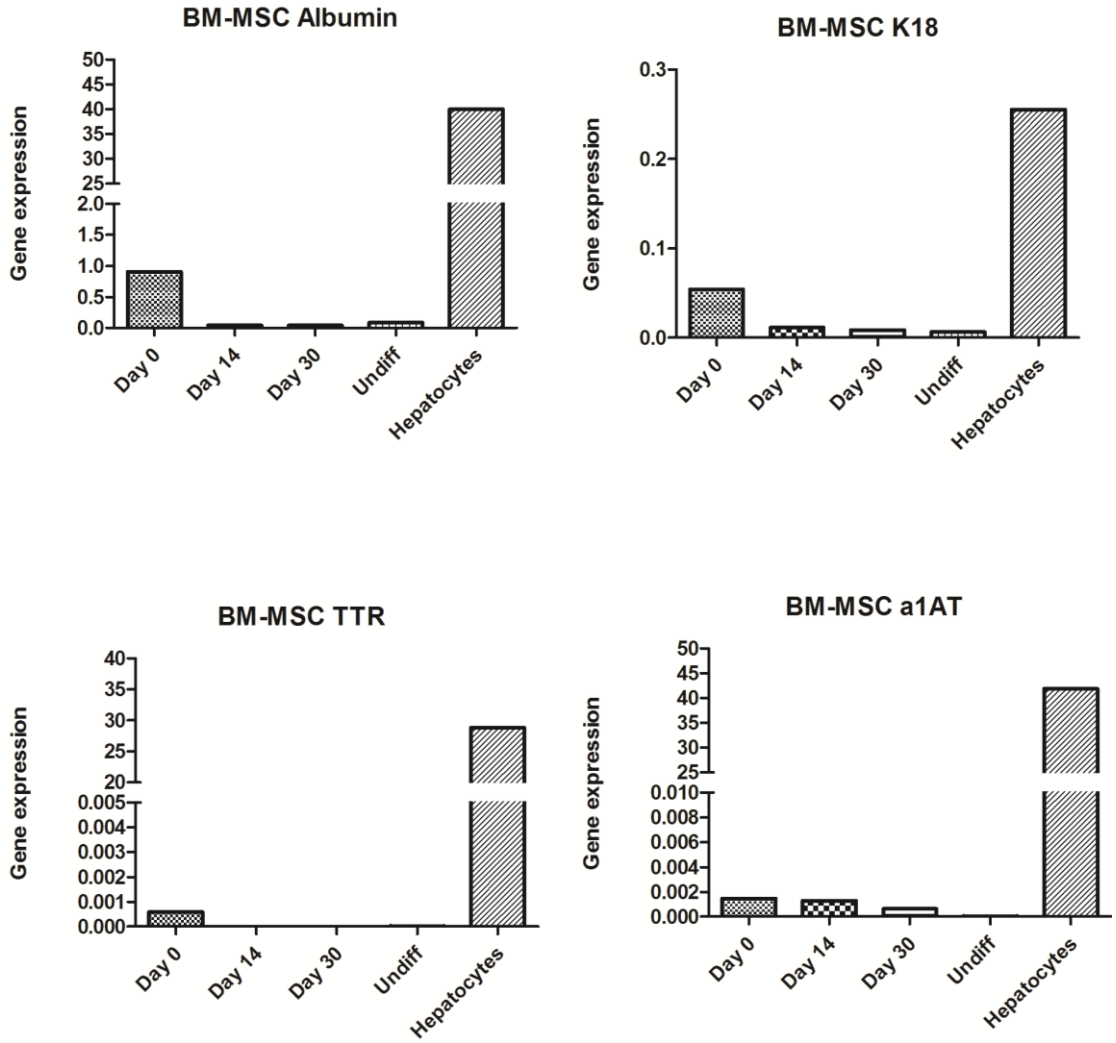

Figure 6.12 Real time PCR analysis of BM-MSC D231113 hepatocyte differentiation

K18 – keratin 18, TTR – transthyretin, a1AT – α1-antitrypsin. Hepatocytes – D231113 primary hepatocytes used as positive control. Undiff – undifferentiated BM-MSC maintained in MSC media for 30 days.

6.5.3.3 Undifferentiated Ad-MSC and BM-MSC take up LDL

Surprisingly, both undifferentiated Ad-MSC and BM-MSC strongly took up LDL after 3 hours' incubation (Figure 6.13). Identical results were also observed at days 14 and 30.

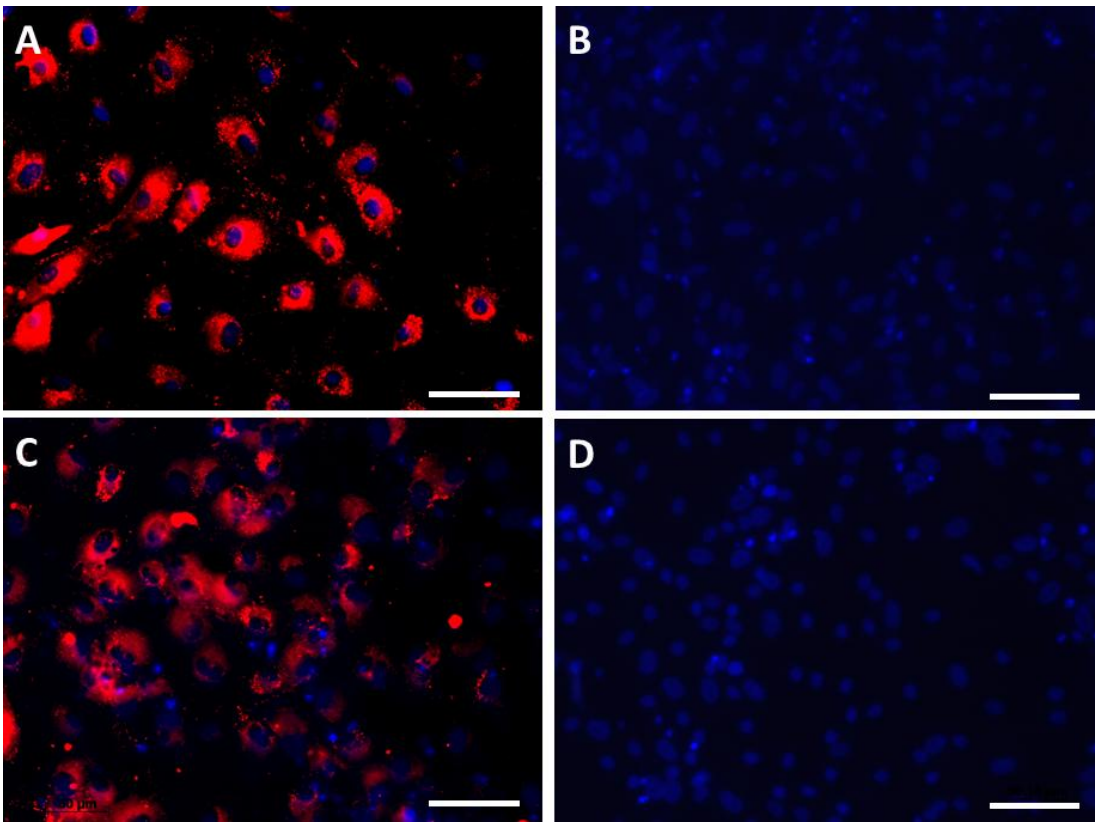

Figure 6.13 DiI-LDL uptake of undifferentiated D231113 Ad-MSC and BM-MSC.
A – Ad-MSC after culture in DiI-LDL, B – Ad-MSC negative control
C – BM-MSC after culture in DiI-LDL, D – BM_MSC negative control.
DAPI as nuclear stain. White bar represents 100µm.

6.5.3.4 Undifferentiated Ad-MSC and BM-MSC demonstrate non-specific Periodic acid Schiff staining

Faint but distinct staining was present at days 0, 14 and 30 in both Ad-MSC and BM-MSC, suggestive of glycogen storage. Figure 6.14 shows representative staining at days 0 and 14 along with PAS staining of primary hepatocytes during culture.

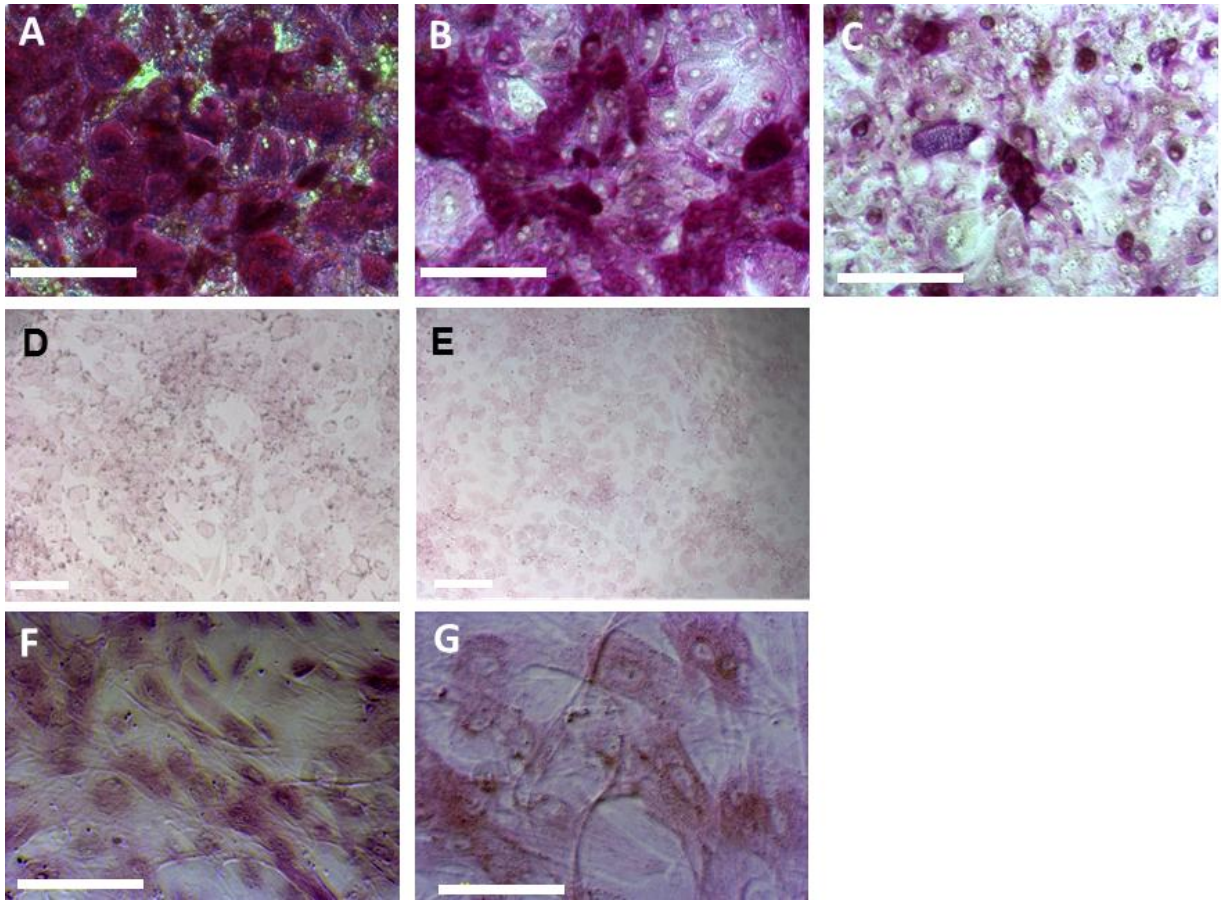

Figure 6.14 Periodic acid Schiff staining of canine primary hepatocytes, Ad-MSC and BM-MSC during differentiation
A- primary hepatocytes in culture 24 hours, B – primary hepatocytes in culture 72 hours, C – primary hepatocytes in culture 6 days, D – Ad-MSC undifferentiated, E – BM-MSC undifferentiated, F - Ad-MSC after 14 days on differentiation protocol, G - BM-MSC after 14 days on differentiation protocol. White scale bar represents 100µm.

In view of this positive PAS staining which was present in undifferentiated cells and differentiated cells with no other demonstration a hepatocyte phenotype; this was further investigated with examination of glycogen synthase gene expression. Glycogen synthase expression was measured at time points 0,14 and 30 days as well as in canine primary hepatocytes after culture for 1,3 and 6 days as a positive control. Glycogen synthase expression was normalised to three reference genes (HPRT, B2MG and RPL8).

This demonstrated no, or minimal expression of glycogen synthase at any time points of differentiation (Figure 6.15). As glycogen synthase activity is integral to glycogen accumulation this lack of gene expression would suggest that PAS staining was non-specific.

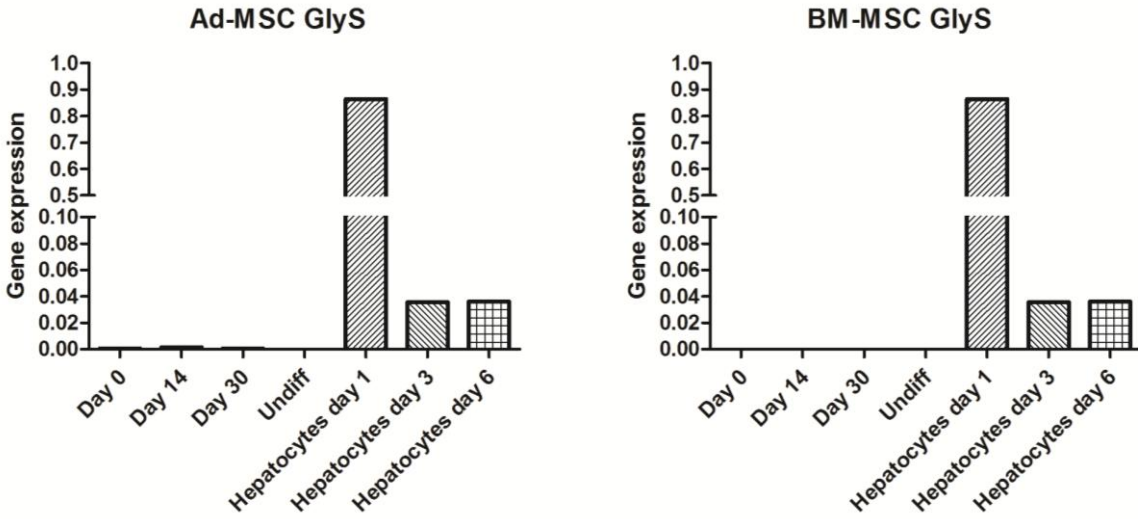

Figure 6.15 Glycogen synthase gene expression of Ad-MSC, BM-MSC and primary hepatocytes
Undiff – undifferentiated MSCs cultured for 30 days.

6.5.3.5 No CYP activity can be demonstrated during differentiation

Using the luciferase assay, there was no appreciable cytochrome activity at any of the time points, either basal activity or after induction with rifampicin (Figure 6.16). Some cell containing wells had lower luminescence than the cell free control wells, hence the negative values for some results.

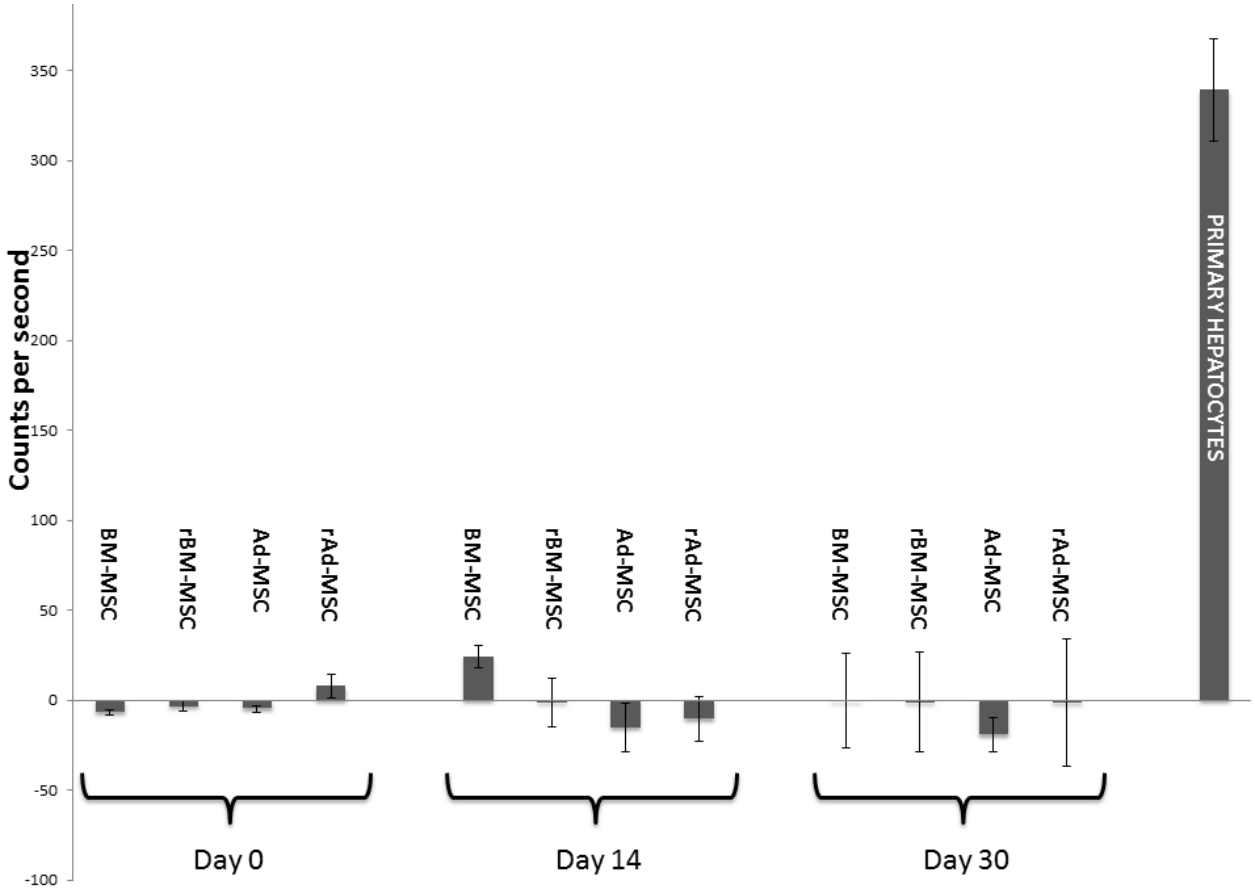

Figure 6.16 Cytochrome activity of Ad-MSC and BM-MSC at days 0, 14 and 30
CYP activity was measured using Promega Pro-Glo Luciferase-PFBE which was added to culture media for 3 hours. Media removed, detection buffer added and luminescence measured using a luminometer. Background values from cell-free wells were subtracted from result. Experiments were performed in triplicate. r – rifampicin treatment for 48 hours.

6.5.4 Extending to day 50 with a maturation step increases gene expression of α1anti-trypsin and transthyretin

As Lee et al. (2004) had continued their differentiation protocol for up to 6 weeks; a final maturation step was added.

6.5.4.1 Morphology

As with the previous experiment, there was a dramatic change in morphology, most evident in the BM-MSC cells to a more epithelioid pattern (Figure 6.17). The Ad-MSC morphology after 50 days was more heterogeneous with some cells still assuming a fibroblastic appearance.

6.5.4.2 PCR Analysis

The results after 50 days of differentiation demonstrated increases in α1 anti-trypsin, and transthyretin in both cell types (Figure 6.18 & Figure 6.19). No other hepatocyte genes demonstrated increased expression however.

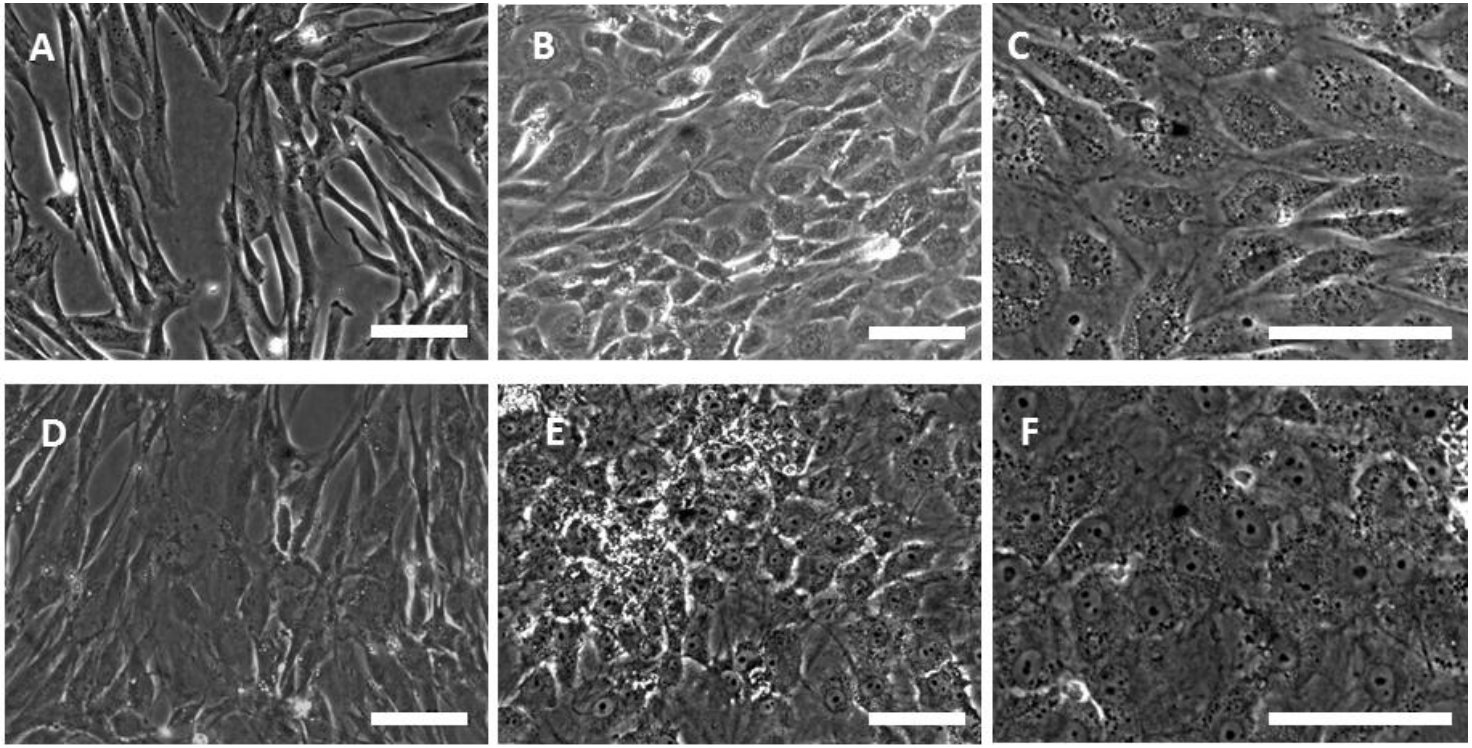

Figure 6.17 Morphology of Ad-MSC and BM-MSC during hepatocyte differentiation during experiment 3
A-C – Ad-MSC, D-F – BM-MSC. A - D day 0, B, C, E & F day 50. White bar represents 50µm.

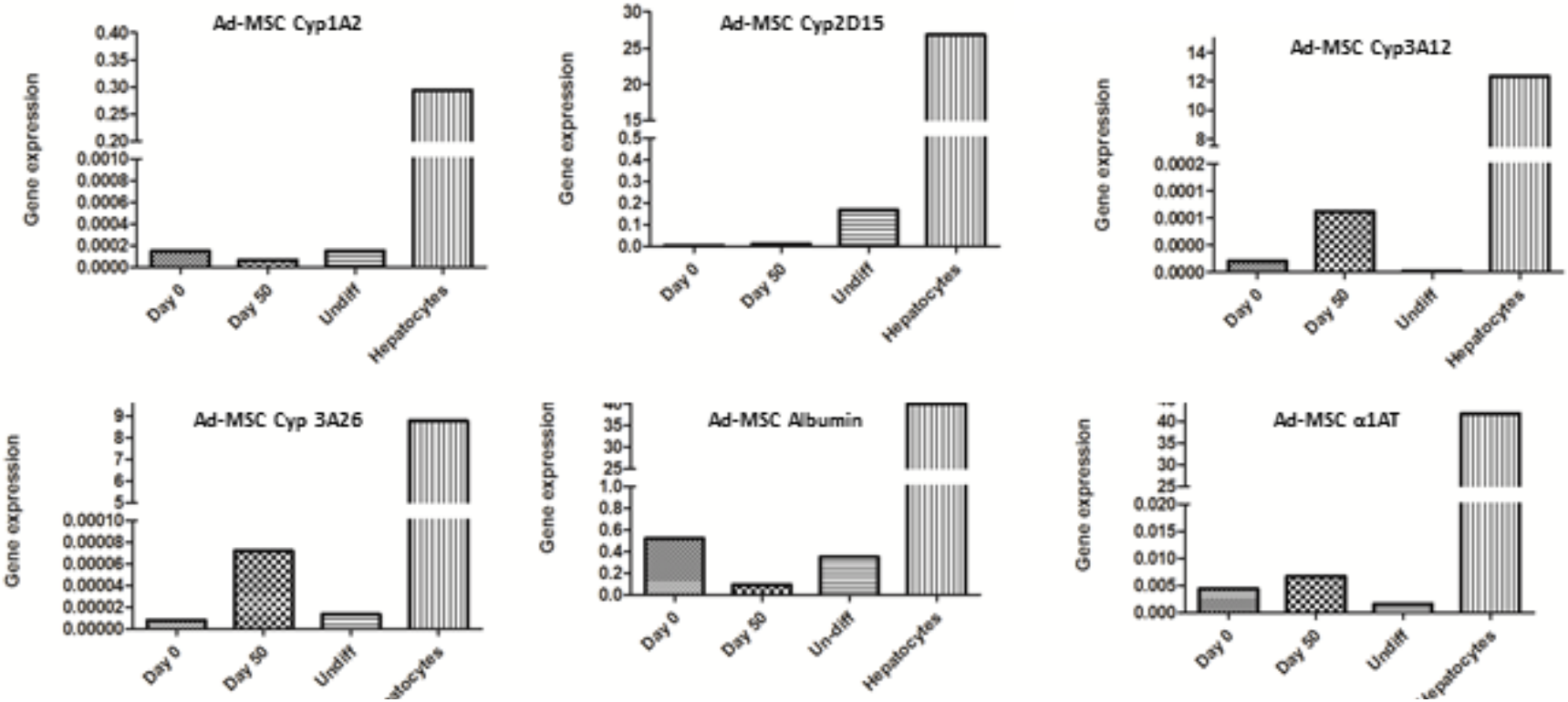
Ad-MSC Cyp1A2
Gene expression
0.40
0.35
0.30
0.25
0.20
0.0010
0.0008
0.0006
0.0004
0.0002
0.0000
Day 0
Day 50
Undiff
Hepatocytes
Ad-MSC Cyp2D15
Gene expression
30
25
20
15
0.5
0.4
0.3
0.2
0.1
0.0
Day 0
Day 50
Undiff
Hepatocytes
Ad-MSC Cyp3A12
Gene expression
14
12
10
8
0.0002
0.0001
0.0001
0.0000
0.0000
Day 0
Day 50
Undiff
Hepatocytes
Ad-MSC Cyp 3A26
Gene expression
9
8
7
6
5
0.00010
0.00008
0.00006
0.00004
0.00002
0.00000
Day 0
Day 50
Undiff
Ad-MSC Albumin
Gene expression
35
30
25
1.0
0.8
0.6
0.4
0.2
0.0
Day 0
Day 50
Un-diff
Hepatocytes
Ad-MSC α1AT
Gene expression
40
35
30
25
0.020
0.015
0.010
0.005
0.000
Day 0
Day 50
Undiff

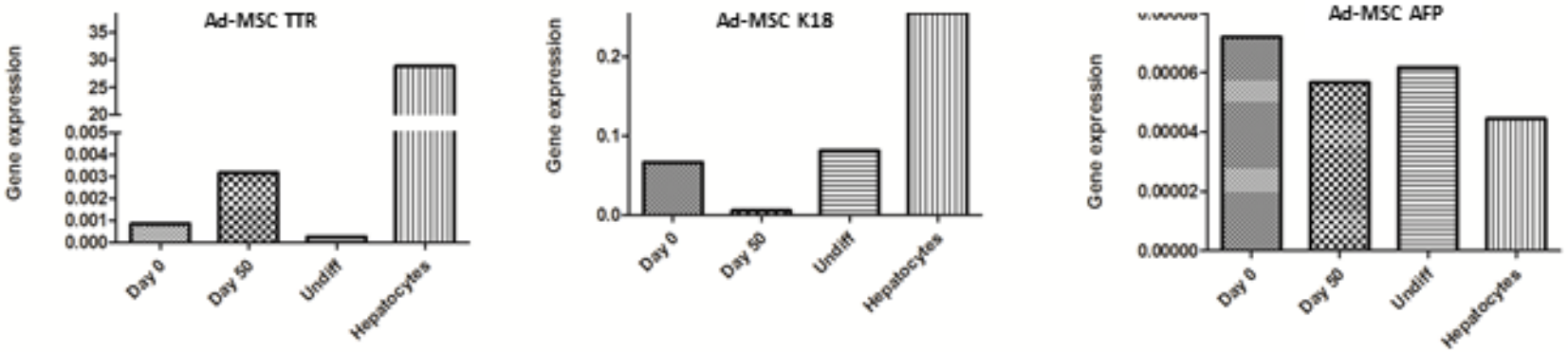

Figure 6.18 Ad-MSC hepatocyte differentiation relative gene expression 50 day experiment.

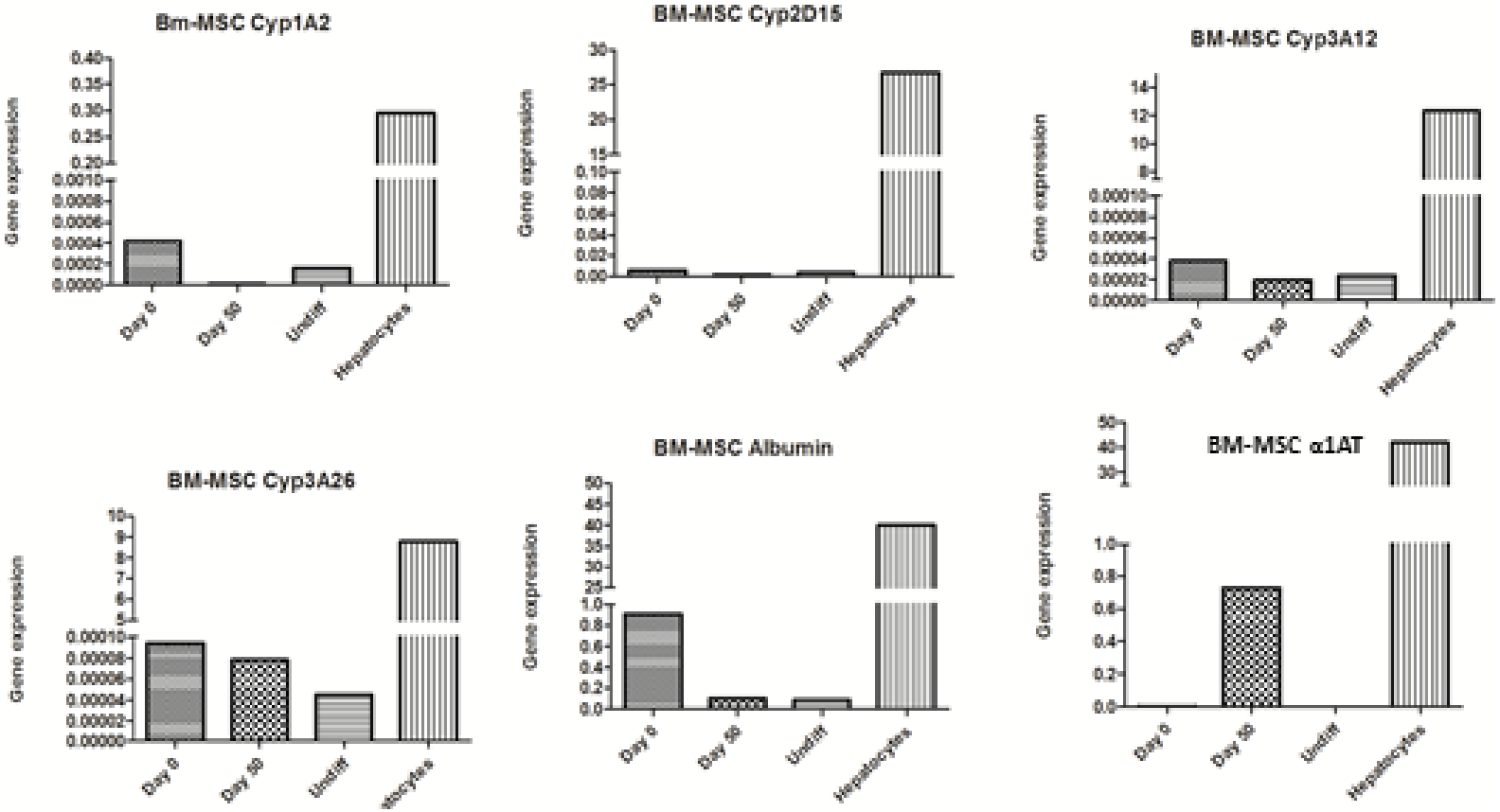
Bm-MSC Cyp1A2
Gene expression
Day 0
Day 30
Undiff
Hepatocytes
BM-MSC Cyp2D15
Gene expression
Day 0
Day 30
Undiff
Hepatocytes
BM-MSC Cyp3A12
Gene expression
Day 0
Day 30
Undiff
Hepatocytes
BM-MSC Cyp3A26
Gene expression
Day 0
Day 30
Undiff
BM-MSC Albumin
Gene expression
Day 0
Day 30
Undiff
Hepatocytes
BM-MSC α1AT
Gene expression
Day 0
Day 30
Undiff
Hepatocytes

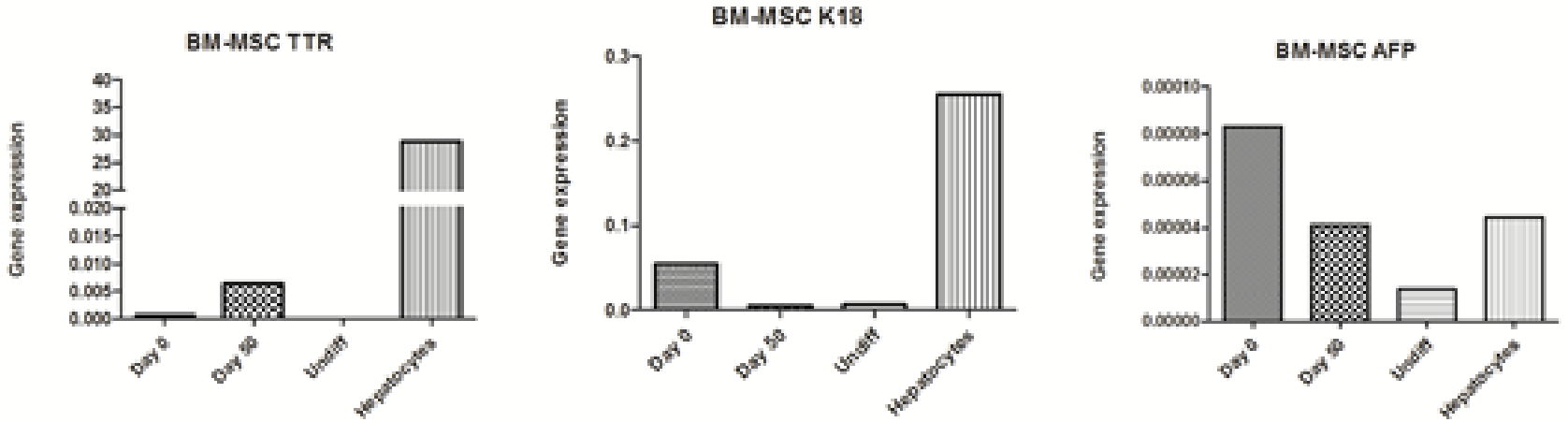

Figure 6.19 BM-MSC hepatocyte differentiation relative gene expression experiment 3

K18 – keratin 18, TTR – transthyretin, a1AT – α1-antitrypsin. Hepatocytes – D231113 primary hepatocytes used as positive control. Undiff – undifferentiated BM-MSC maintained in MSC media for 30 days.

6.5.4.3 Cytochrome activity, basal and rifampicin

No activity was detected either basal or after 48 hours treatment with rifampicin (***Figure 6.20***)

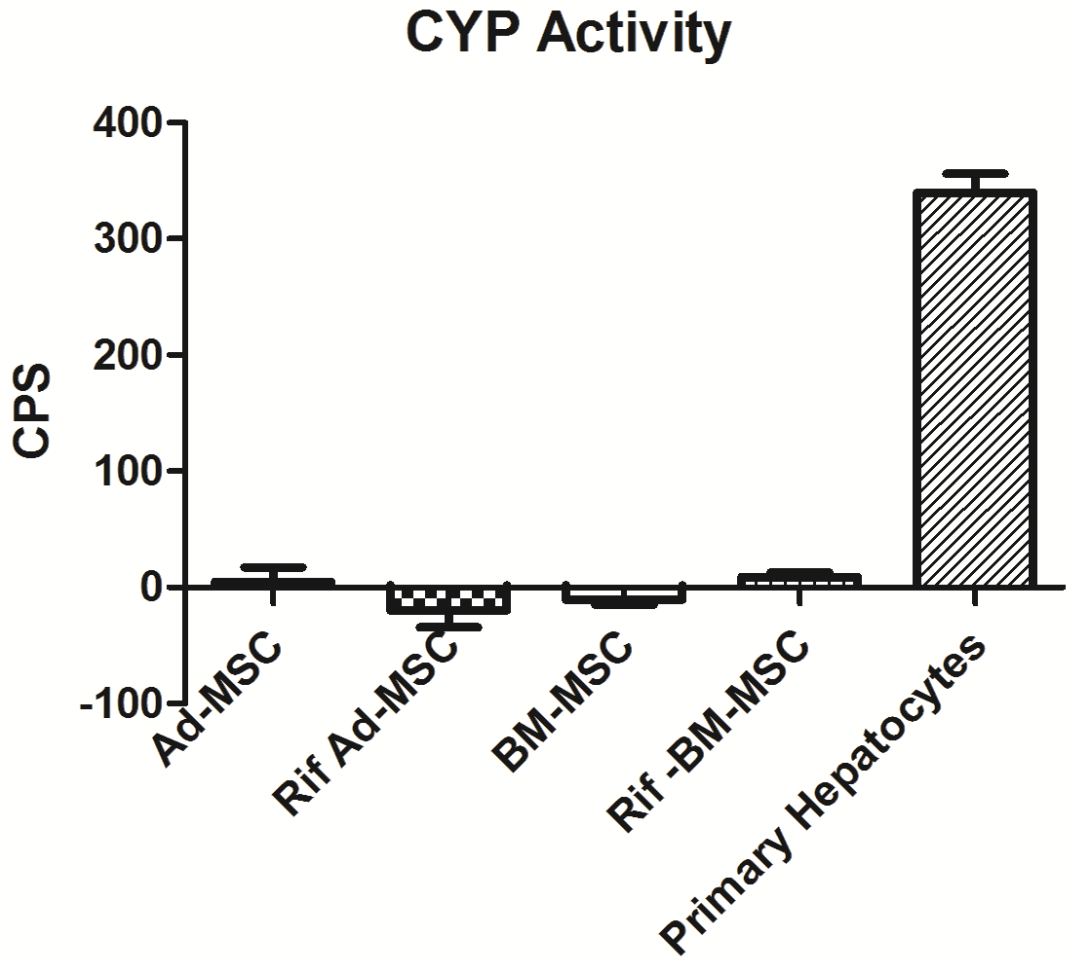

Figure 6.20 CYP activity at day 50 of experiment 3.
CPS – counts per second of luminescence after subtraction of luminescence from no cell control wells. Rif – cells treated with rifampicin at 25µM for 48 hours prior to experiment.

6.5.5 Pretreatment with 5AZA does not enhance transdifferentiation

6.5.5.1 5AZA cell viability assay

As 5AZA can be cytotoxic, a viability assay was performed at a range of concentrations (Juttermann et al., 1994). At 24 hours, all concentrations of 5AZA had caused a decrease in Ad-MSC viability compared to the control. There was no effect on BM-MSC at 24 hours. An obvious dose response in both Ad-MSC and BM-MSC was noted 48 hours after treatment with 5AZA. As 20µM had been used in previously published papers and caused an approximately 50% reduction in viability, this concentration was selected for the subsequent experiment (Seeliger et al., 2013; Sgodda et al., 2007).

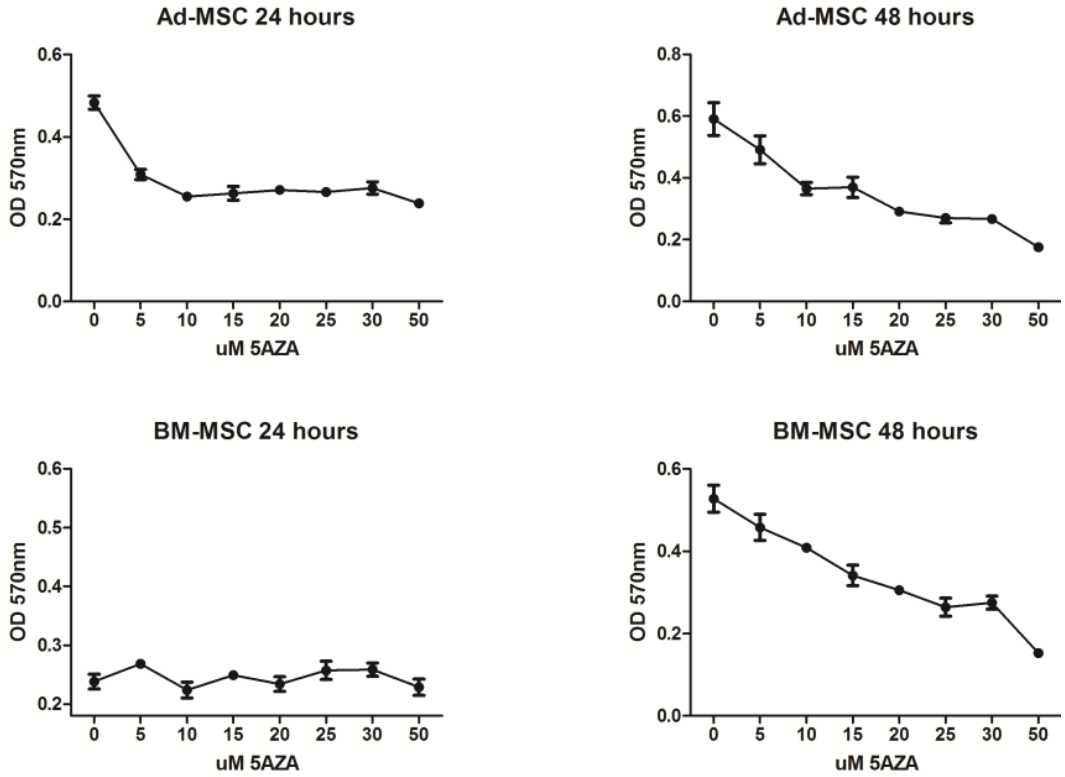

Figure 6.21 Cell viability assays at 24 and 48 hours after exposure to 5AZA for 24 hours
OD 570nm – value after subtraction of no cell control optical density. Each concentration was performed in triplicate. Error bars represent standard error of mean.

6.5.5.2 Cell morphology

The largest change in morphology appeared to be in the BM-MSC where they assumed epithelial-type morphology however little change in morphology was noted in the Ad-MSC (Figure 6.22).

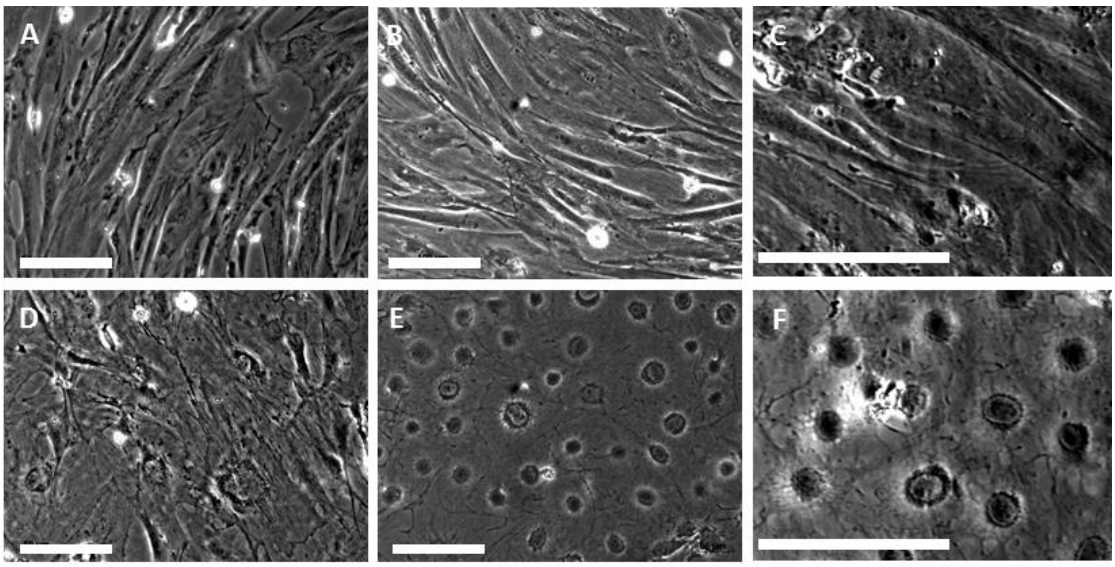

Figure 6.22 Morphology of Ad-MSC and BM-MSC during hepatocyte differentiation during experiment 4
A – Undifferentiated Ad-MSC; D – undifferentiated BM-MSC; C&D Differentiated Ad-MSC; E&F Differentiated BM-MSC. White bar represents 100µm.

6.5.5.3 PCR analysis

6.5.5.3.1 Hepatocyte and hepatocyte pre-cursor genes

Compared to time point 0 and undifferentiated cells, aside from a small increase in α1 antitrypsin in the BM-MSC, there was no increase in any of the hepatocyte/ hepatocyte pre-cursor genes analysed after 18 days in the differentiation media.

6.5.5.3.2 Mesenchymal and epithelial gene expression

Examination of genes expressed by mesenchymal cells demonstrated a reduction in vimentin, β catenin and fibronectin expression after differentiation by Ad-MSC (Figure 6.25). This was mirrored by the BM-MSC apart from β catenin which increased (Figure 6.26).

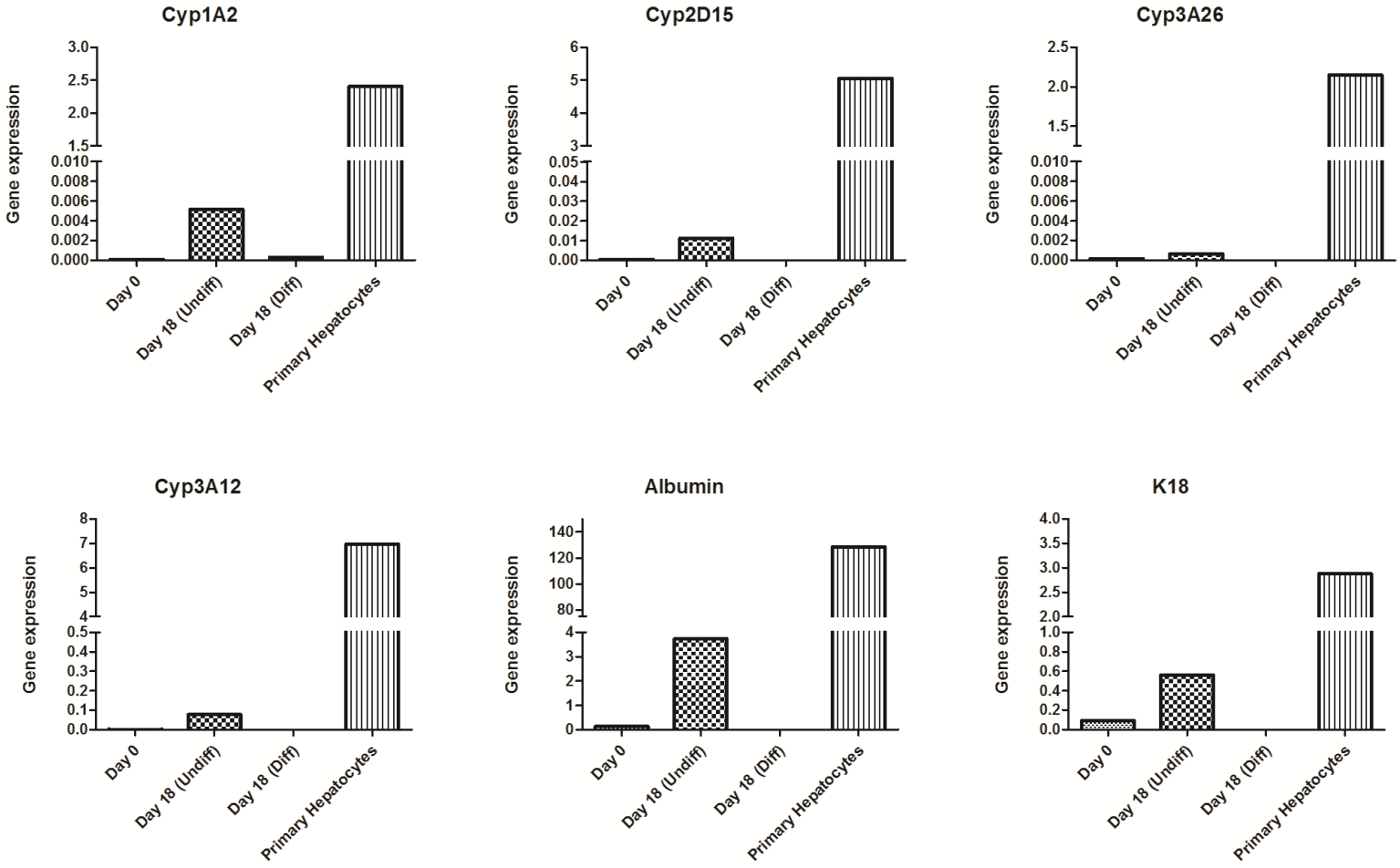
Cyp1A2
Gene expression
3.0
2.5
2.0
1.5
0.010
0.008
0.006
0.004
0.002
0.000
Day 0
Day 18 (Undiff)
Day 18 (Diff)
Primary Hepatocytes
Cyp2D15
Gene expression
6
5
4
3
0.05
0.04
0.03
0.02
0.01
0.00
Day 0
Day 18 (Undiff)
Day 18 (Diff)
Primary Hepatocytes
Cyp3A26
Gene expression
2.5
2.0
1.5
0.010
0.008
0.006
0.004
0.002
0.000
Day 0
Day 18 (Undiff)
Day 18 (Diff)
Primary Hepatocytes
Cyp3A12
Gene expression
8
7
6
5
4
0.5
0.4
0.3
0.2
0.1
0.0
Day 0
Day 18 (Undiff)
Day 18 (Diff)
Primary Hepatocytes
Albumin
Gene expression
140
120
100
80
4
3
2
1
0
Day 0
Day 18 (Undiff)
Day 18 (Diff)
Primary Hepatocytes
K18
Gene expression
4.0
3.5
3.0
2.5
2.0
1.0
0.8
0.6
0.4
0.2
0.0
Day 0
Day 18 (Undiff)
Day 18 (Diff)
Primary Hepatocytes

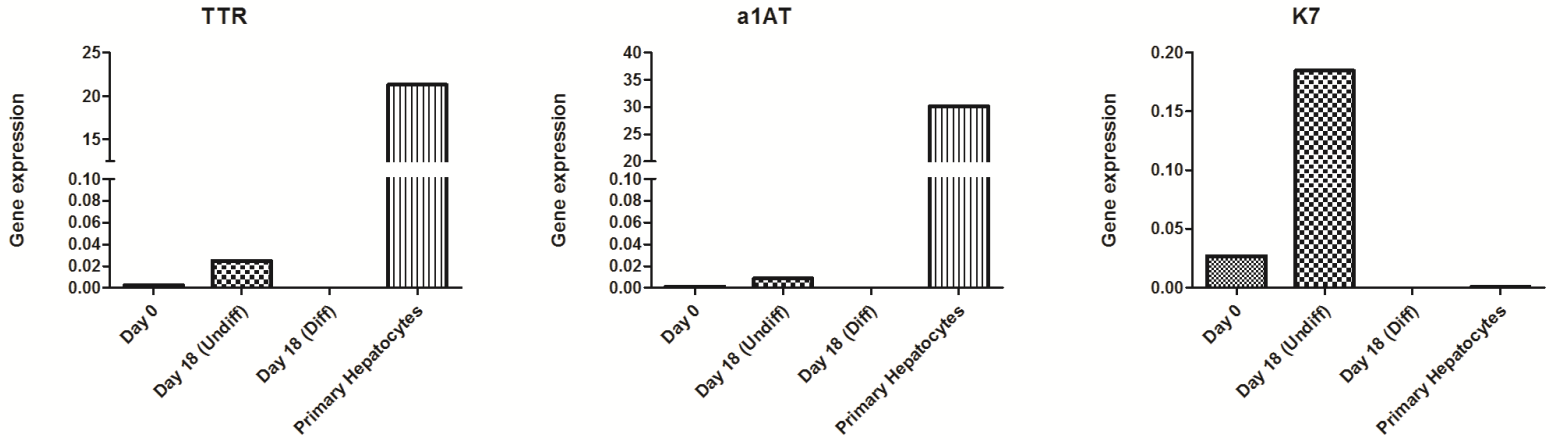

Figure 6.23 Ad-MSC hepatocyte differentiation relative gene expression after 5AZA pre-treatment

K18 – keratin 18, TTR – transthyretin, a1AT – α1-antitrypsin. Hepatocytes – D231113 primary hepatocytes used as positive control. Diff – BM-MSc after differentiation protocol. Undiff – undifferentiated BM-MSC maintained in MSC media for 18days.

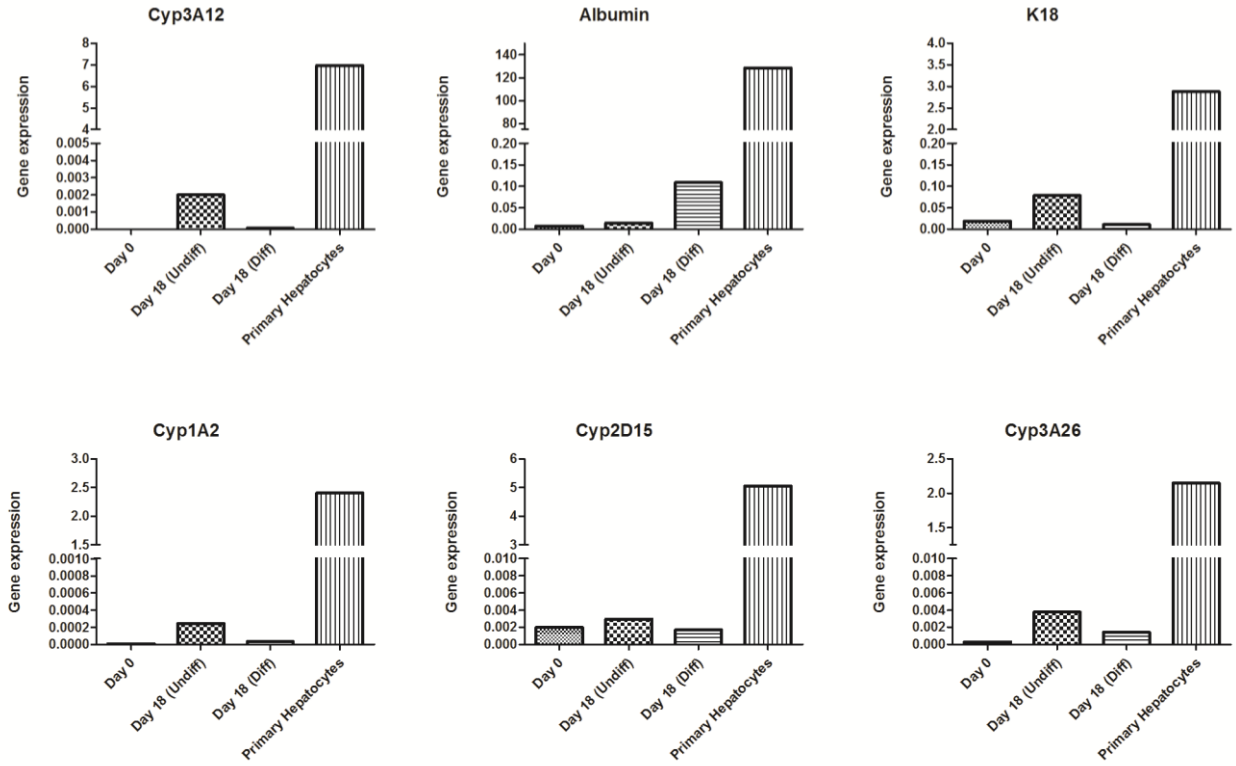
Cyp3A12
Albumin
K18
Cyp1A2
Cyp2D15
Cyp3A26
Gene expression
Day 0
Day 18 (Undiff)
Day 18 (Diff)
Primary Hepatocytes

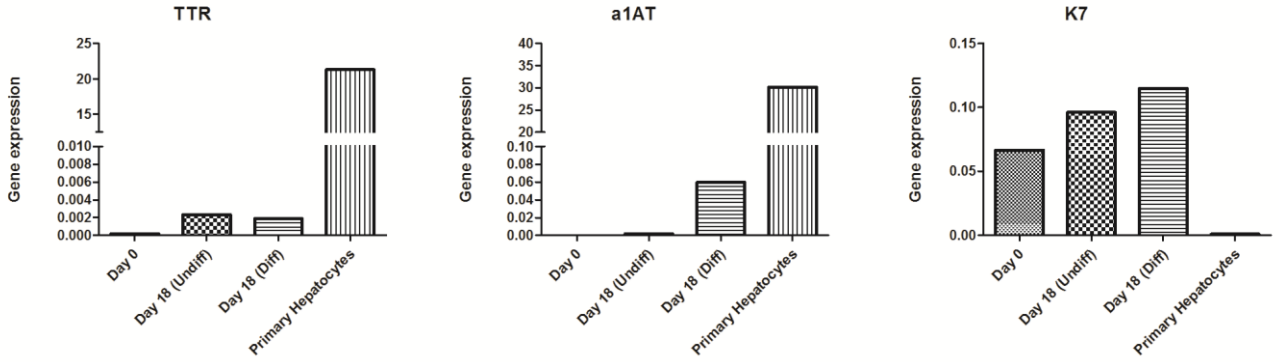

Figure 6.24 BM-MSC hepatocyte differentiation relative gene expression after 5AZA pre-treatment
K18 – keratin 18, TTR – transthyretin, a1AT – α1-antitrypsin. Hepatocytes – D231113 primary hepatocytes used as positive control. Diff – BM-MSc after differentiation protocol. Undiff – undifferentiated BM-MSC maintained in MSC media for 18days.

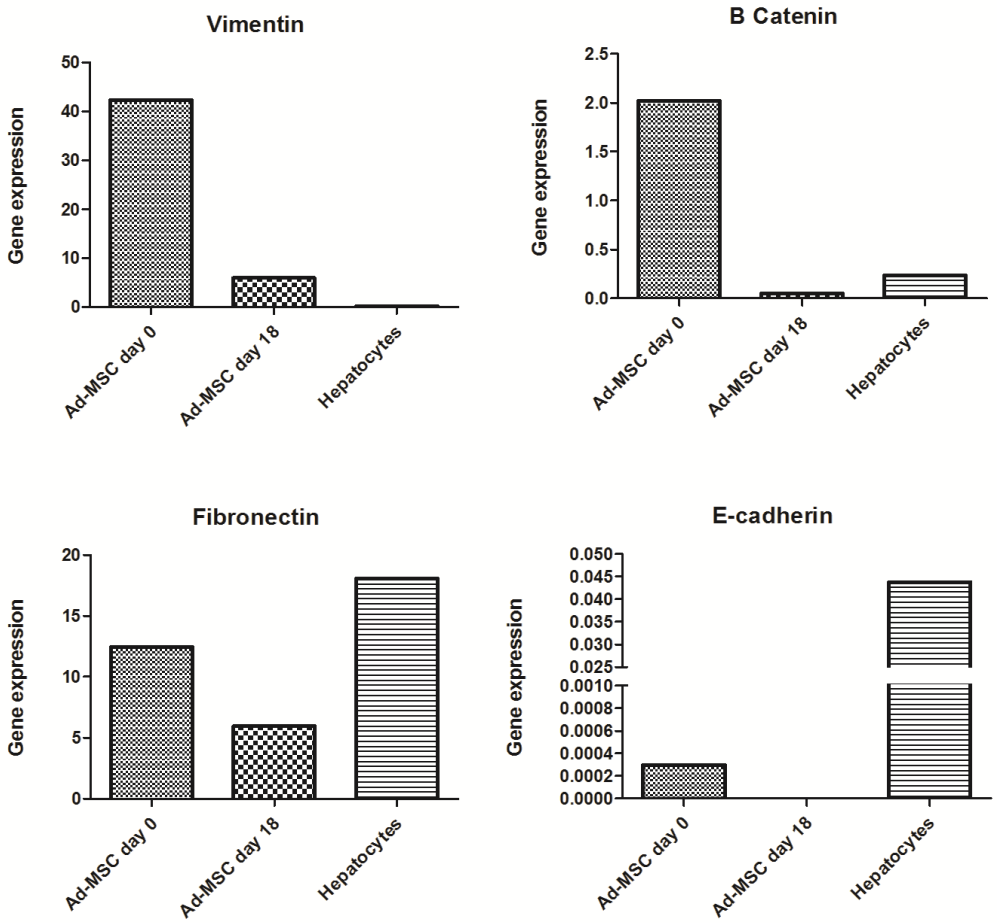

Figure 6.25 Mesenchymal and epithelial markers of Ad-MSc before and after differentiation and 5AZA pre-treatment

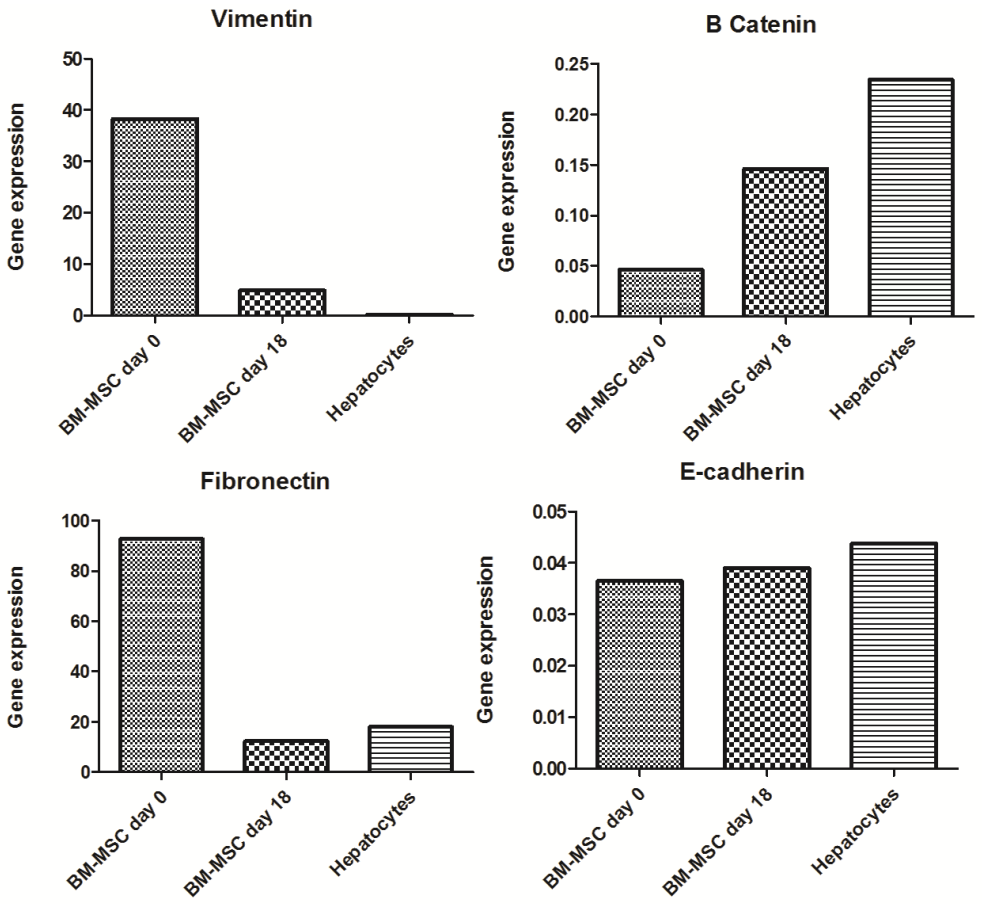

Figure 6.26 Mesenchymal and epithelial markers of BM-MSc before and after differentiation and 5AZA pre-treatment

6.5.6 Treatment with valproic acid (a histone deacetylase inhibitor) does not enhance hepatocyte-like differentiation

6.5.6.1 Morphology

Again a dramatic change in morphology occurred with both cells types taking on a more epithelioid morphology (Figure 6.27).

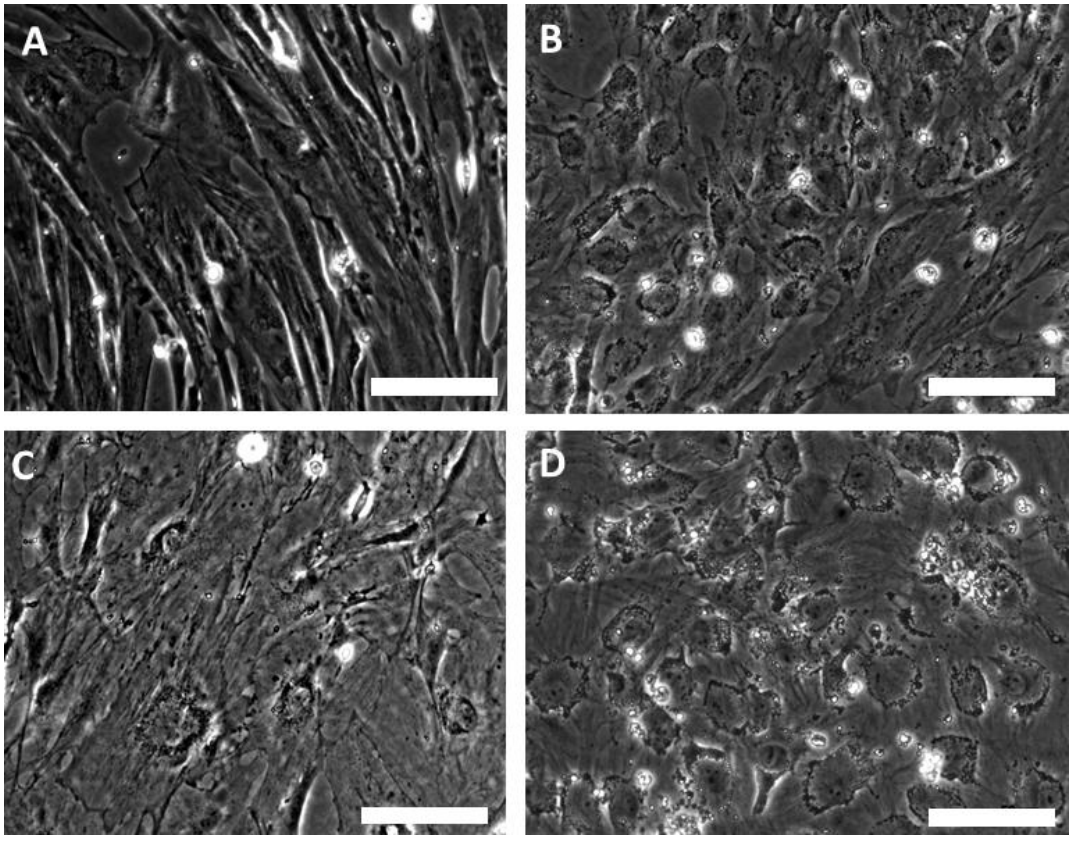

Figure 6.27 Morphology of Ad-MSC and BM-MSC after valproic acid treatment and hepatocyte differentiation
A – undifferentiated Ad-MSC, B – Ad-MSc after differentiation protocol. C-undifferentiated BM-MSC, D – BM-MSC after differentiation protocol. White bar represents 100µm.

6.5.6.2 Gene expression analysis

A reduction in vimentin expression was again demonstrated in both the Ad-MSC and BM-MSC, consistent with the change from a mesenchymal morphology. No increase in hepatocyte/hepatocyte precursor gene expression was noted after pre-treatment with valproic acid. An increase in α1 antitrypsin was again present in BM-MSC.

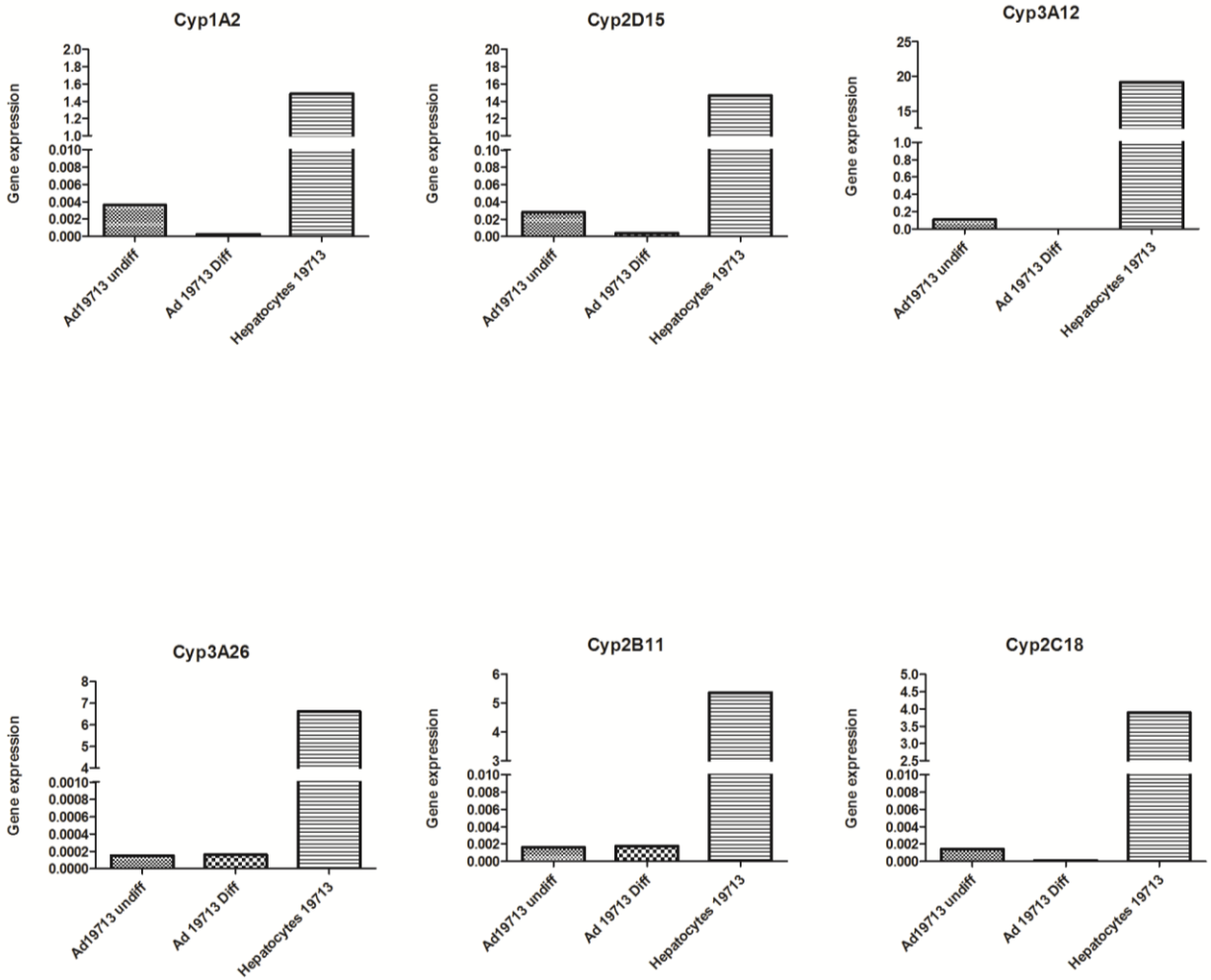
Cyp1A2
Gene expression
Ad19713 undiff
Ad 19713 Diff
Hepatocytes 19713
Cyp2D15
Gene expression
Ad19713 undiff
Ad 19713 Diff
Hepatocytes 19713
Cyp3A12
Gene expression
Ad19713 undiff
Ad 19713 Diff
Hepatocytes 19713
Cyp3A26
Gene expression
Ad19713 undiff
Ad 19713 Diff
Hepatocytes 19713
Cyp2B11
Gene expression
Ad19713 undiff
Ad 19713 Diff
Hepatocytes 19713
Cyp2C18
Gene expression
Ad19713 undiff
Ad 19713 Diff
Hepatocytes 19713

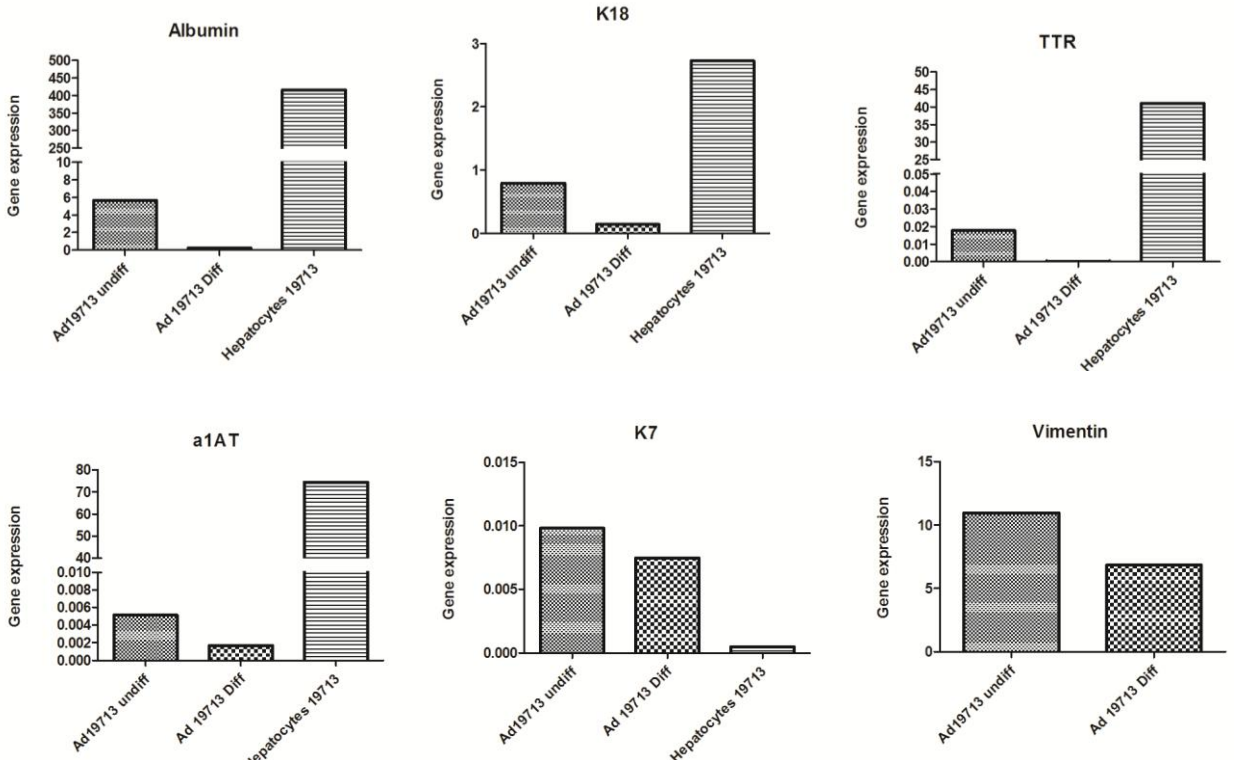

Figure 6.28 D19713 Ad- MSC hepatocyte differentiation relative gene expression after valproic acid treatment
K18 – keratin 18, TTR – transthyretin, a1AT – α1-antitrypsin.

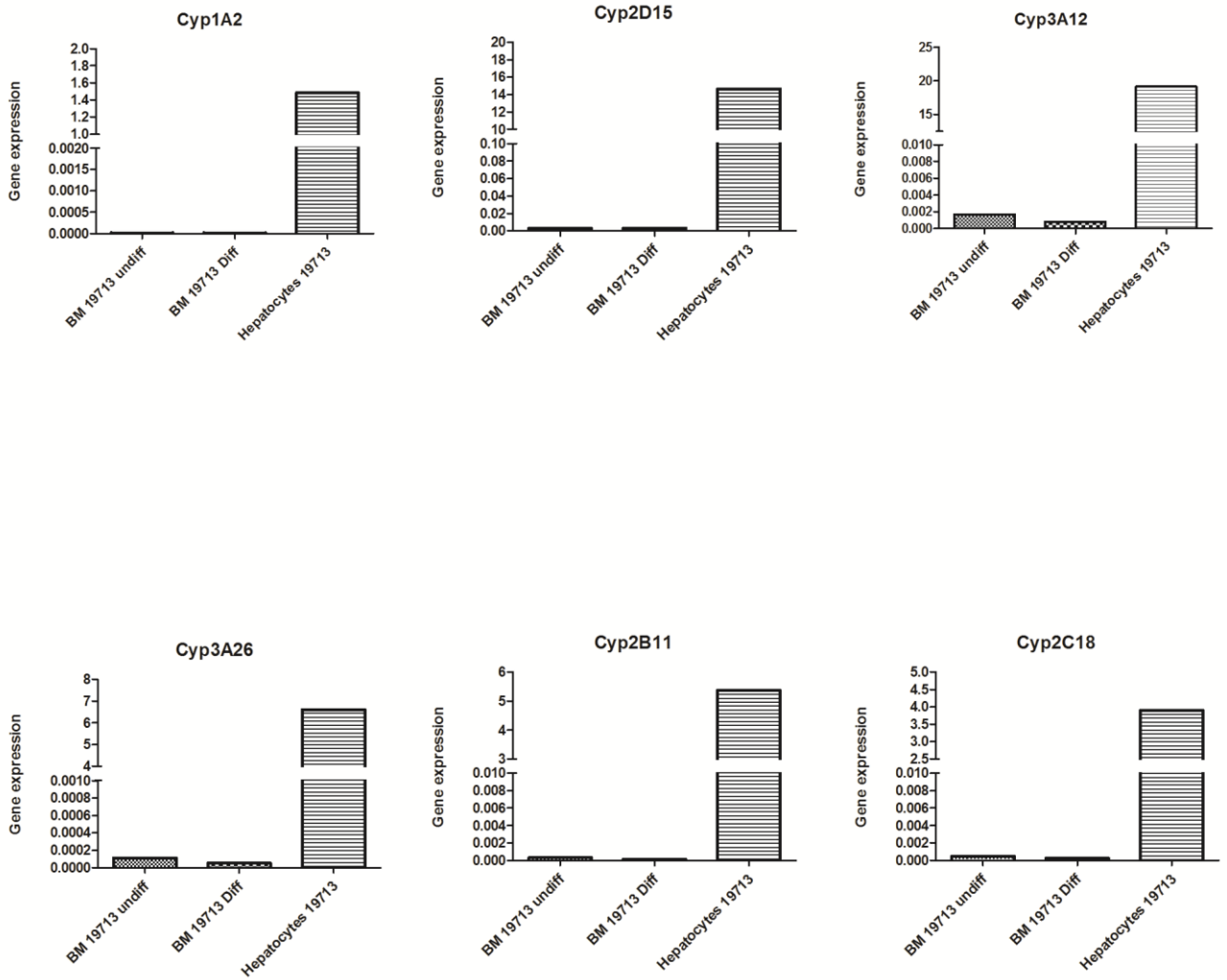
Cyp1A2
Gene expression
BM 19713 undiff
BM 19713 Diff
Hepatocytes 19713
Cyp2D15
Gene expression
BM 19713 undiff
BM 19713 Diff
Hepatocytes 19713
Cyp3A12
Gene expression
BM 19713 undiff
BM 19713 Diff
Hepatocytes 19713
Cyp3A26
Gene expression
BM 19713 undiff
BM 19713 Diff
Hepatocytes 19713
Cyp2B11
Gene expression
BM 19713 undiff
BM 19713 Diff
Hepatocytes 19713
Cyp2C18
Gene expression
BM 19713 undiff
BM 19713 Diff
Hepatocytes 19713

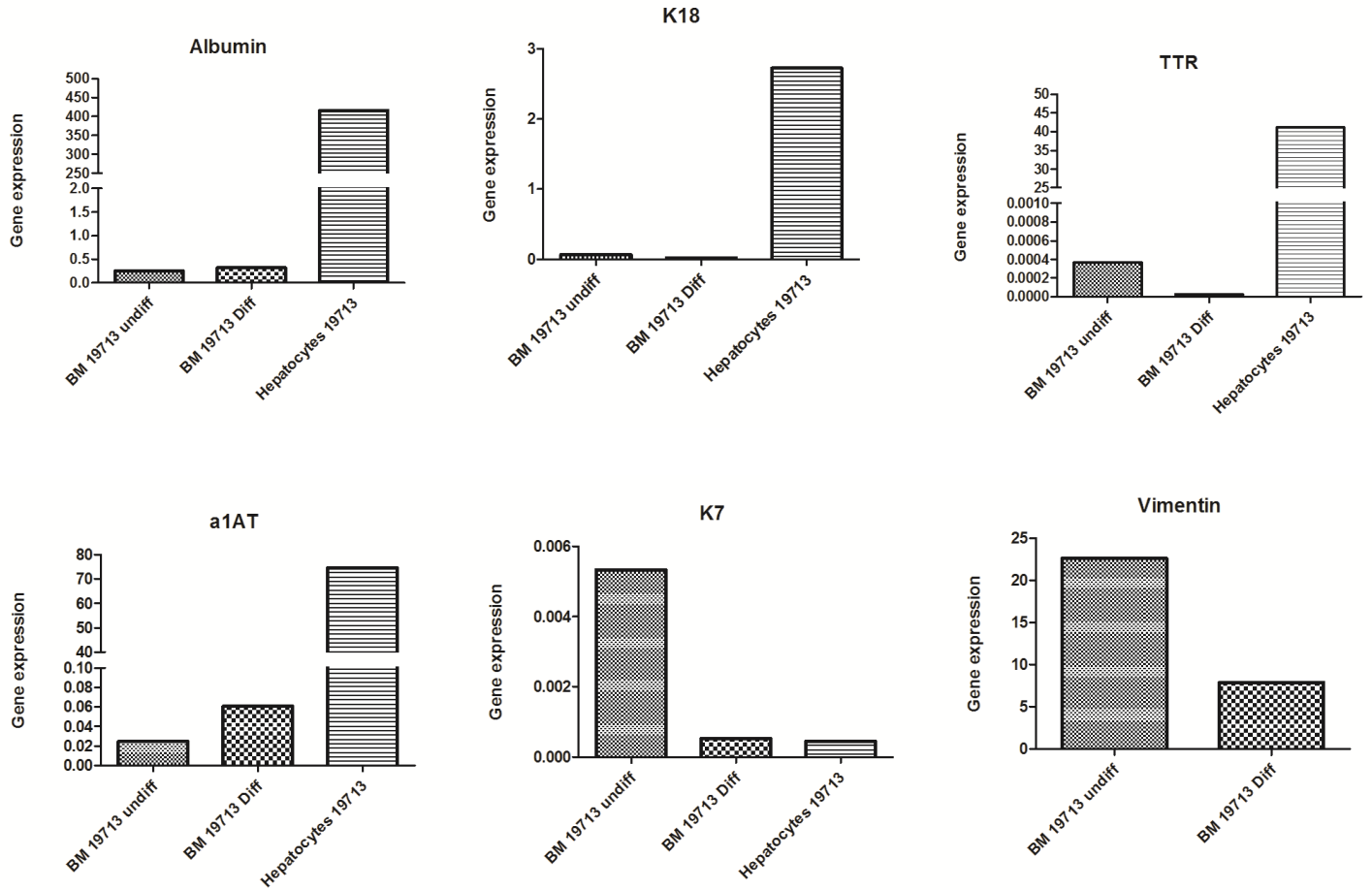

Figure 6.29 D19713 BM- MSC hepatocyte differentiation relative gene expression after valproic acid treatment
K18 – keratin 18, TTR – transthyretin, a1AT – α1-antitrypsin.

6.5.7 DiI-LDL uptake is specific for the LDL receptor in canine Ad-MSC and BM-MSC

To assess if LDL uptake was consistent in MSC, LDL and Ac-LDL uptake was performed with canine Ad-MSC and BM-MSC from 3 animals (D231113,D17513, D19713) and three canine primary hepatocyte culture (D231113, D19713, D20913). LDL-receptor gene expression relative to three reference genes was also performed on three canine primary hepatocyte cultures and two each of Ad-MSC and BM-MSC. Finally, immunocytochemistry using an anti-LDL receptor antibody was undertaken using hepatocytes, Ad-MSC and BM-MSC from D19713.

6.5.7.1 Ad-MSC and BM-MSC do not take up DiI-Ac-LDL

All MSC's and primary hepatocytes took up DiI-LDL strongly as was previously demonstrated (Figure 6.30). Isolated cells in all cultures avidly took up DiI-Ac-LDL however the majority were negative. These cells would be consistent with contaminating endothelial or macrophage cells. The lack of uptake of Ac-LDL suggests that LDL uptake is via the specific LDL receptor rather than scavenging receptors.

6.5.7.2 Ad-MSC and BM-MSC express the LDL receptor

Gene expression in all Ad-MSC and BM-MSC was within the range demonstrated by canine primary hepatocytes (Figure 6.31).

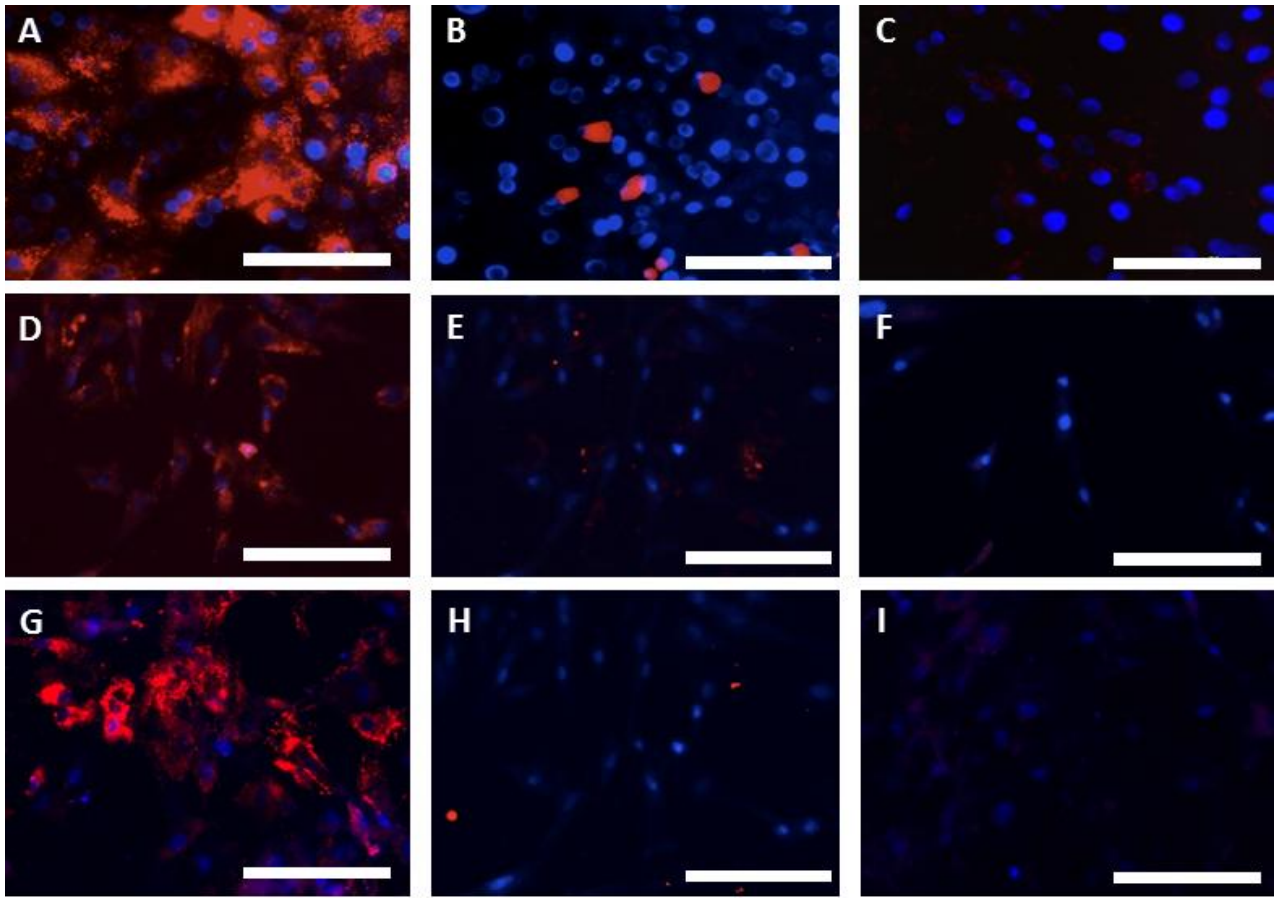

Figu***re 6.30 DiI-LDL and DiI-Ac-LDL uptake of primary hepatocytes, Ad-MSc and BM-MSC from D17913.***
A-C Primary hepatocytes, D-F Ad-MSC, G-I BM-MSC. A, D, G – DiI-LDL, B, E, H – Dil-Ac-LDL, CFI – control. Nuclei counterstained with DAPI. White scale bar represents 100µm.

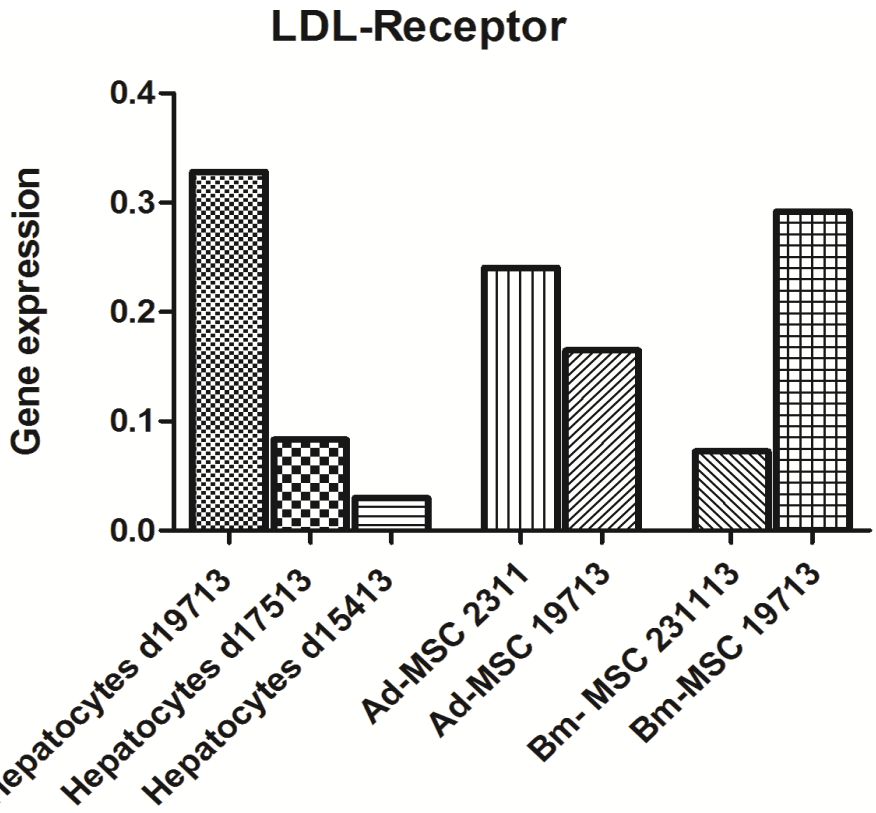

Figure 6.31 Relative gene expression of LDL-receptor on canine primary hepatocytes, Ad-MSC and BM-MSC.
Gene expression was normalised to three reference genes.

6.5.7.3 LDL receptor expression

Using an anti-LDL receptor antibody, immunocytochemistry demonstrated the presence of the receptor on all three cell types (Figure 6.32).

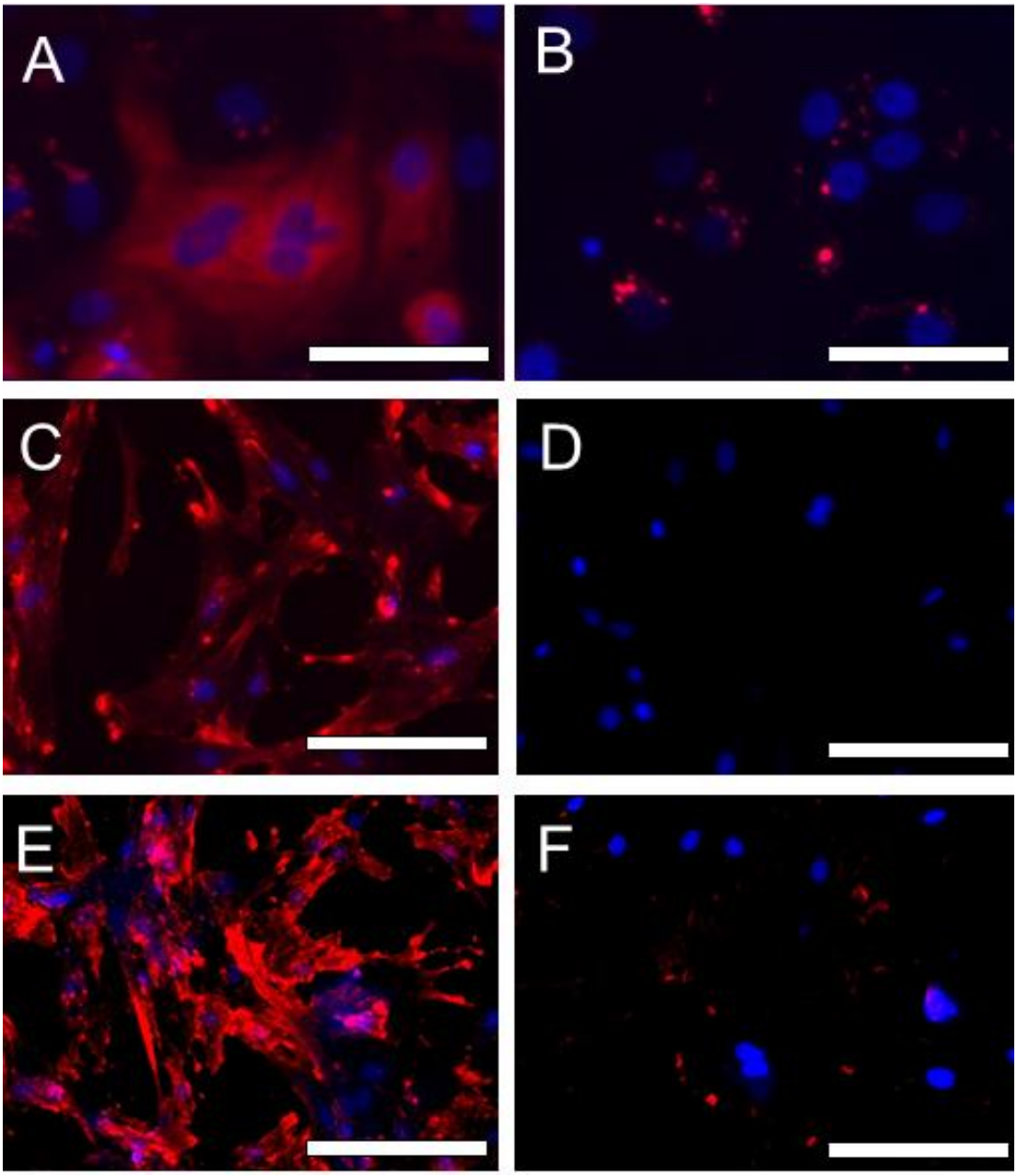

Figure 6.32 Immunocytochemistry using LDL-receptor antibody on D17913 primary hepatocytes, Ad-MSc and BM-MSC.
Strong positive staining was seen in primary hepatocytes (A), Ad-MSC (C) and BM-MSC (E). Negative controls were performed with the secondary antibody only (B,D,F) and no antibody controls (not shown). Nuclei were labelled with DAPI. White scale bar represents 100µm.

6.5.8 Human and mouse bone marrow MSC also demonstrate LDL uptake and LDL receptor expression

To assess if this finding was a species-specific response, mouse and human BM-MSC's were tested for LDL uptake and LDL receptor expression.

6.5.8.1 Mouse and Human BM-MSC LDL and AcLDL uptake

As with the canine BM-MSC, both mouse and human MSC's avidly took up DiI-LDL but not DiI-Ac-LDL, suggesting the presence of the specific LDL receptor (Figure 6.33). Unlike the canine Ad-MSC and BM-MSC, no isolated cells took up DiI-Ac-LDL, likely reflecting that the higher passage number (8 for mouse and 4 for human) than the canine MSC's and therefore loss of other contaminating cell types

.

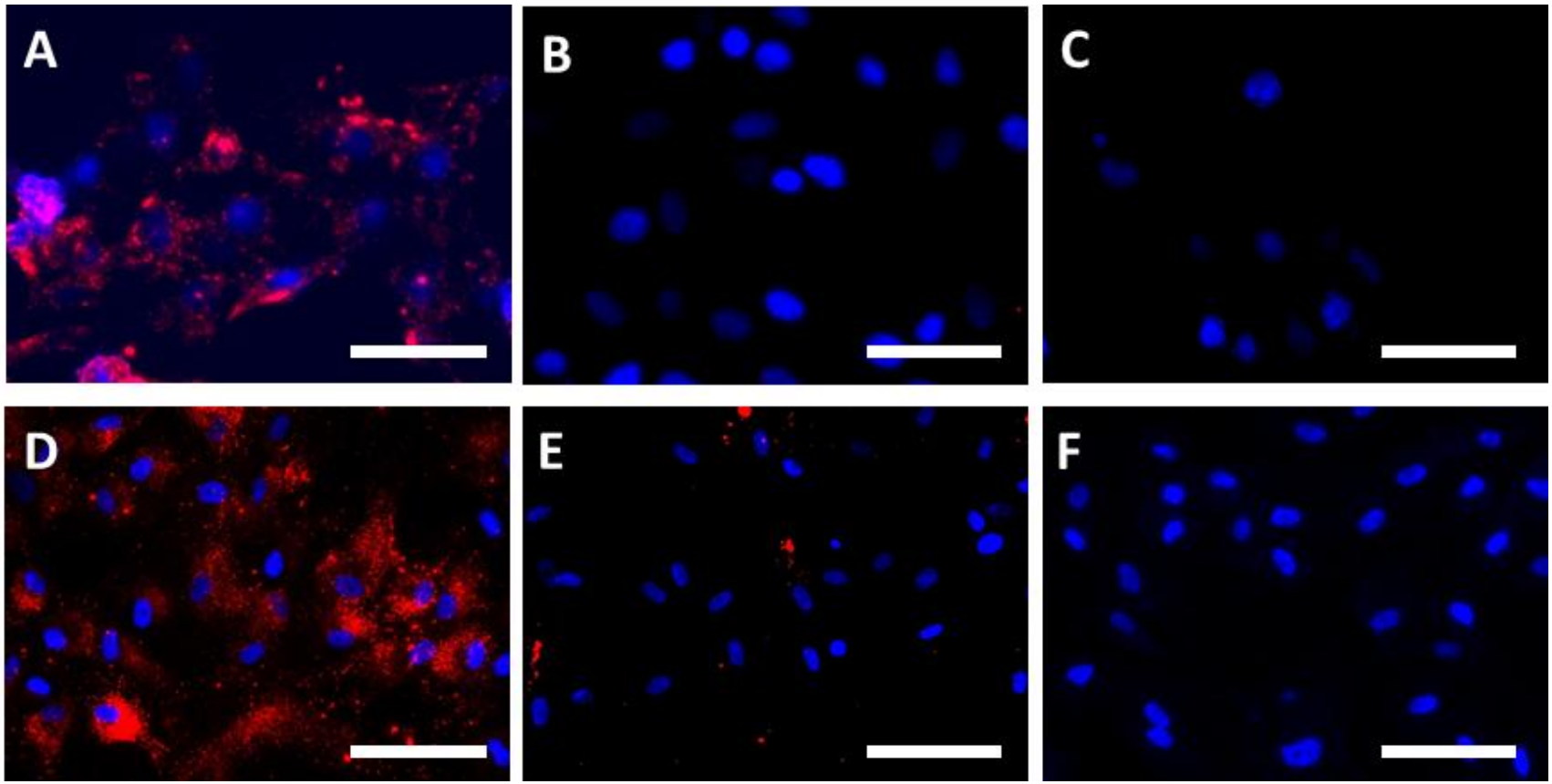

Figure 6.33 DiI-LDL and DiI-Ac-LDL uptake of mouse and human MSC
A-C mouse MSC, D-F human MSC. Cells were cultured in 20µg/ml of DiI-LDL (A, D), DiI-Ac-LDL (B, E) or standard MSC media for 3 hours. Nuclei were labelled with DAPI. White scale bar represents 100µm.

6.5.8.2 Mouse and human BM-MSC LDL receptor expression

Immunocytochemistry using anti-LDL receptor antibody confirmed the presence of the receptor on the cell membrane of both mouse and human MSC's (Figure 6.34).

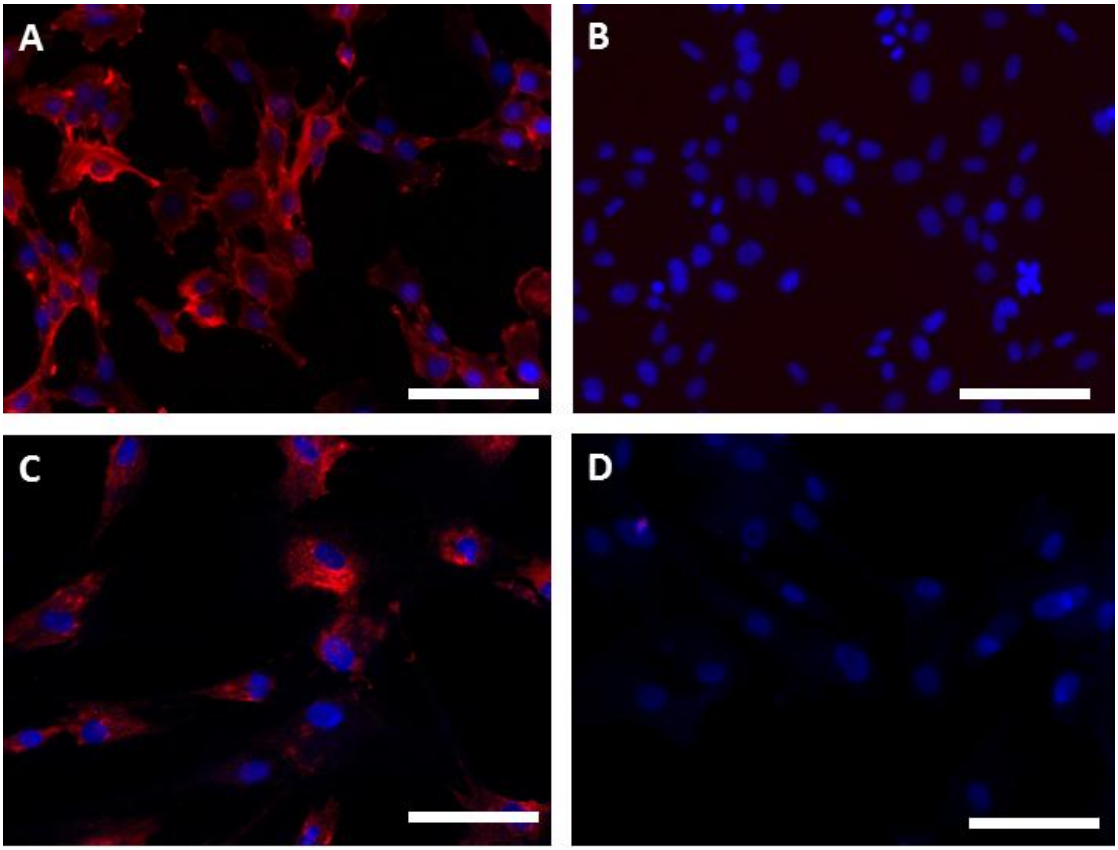

Figure 6.34 Immunocytochemistry using LDL-receptor antibody on mouse and human BM-MSC
Strong positive staining was seen in mouse BM-MSC (A), and human BM-MSC (C). Negative controls were performed with the secondary antibody only (B, D) and no antibody controls (not shown). Nuclei were labelled with DAPI. White scale bar represents 100µm.

6.6 Discussion

6.6.1 Hepatic gene expression and function in undifferentiated canine mesenchymal stem cells

Surprisingly, undifferentiated exhibited some of the characteristics which were anticipated to only be present in hepatocytes or differentiated hepatocyte-like cells. Specifically, albumin gene expression, LDL uptake and faintly positive PAS staining were demonstrated.

6.6.1.1 Albumin gene expression

Albumin gene expression is often used as one of the methods of demonstrating achieving of hepatocyte-like cells (Snykers et al., 2009a). During this study, albumin gene expression was demonstrated in both undifferentiated canine Ad-MSc and BM-MSC's. Albumin gene expression has been demonstrated in the pancreas, kidney, bone and microglial cells and is therefore not specific to hepatocytes (Beerheide et al., 2002). Albumin synthesis has been documented from bone and microglia (Fanali et al., 2012). Furthermore, PCR and immunofluorescence has demonstrated albumin gene and protein expression in human umbilical cord matrix cells, human BM-MSC and human Ad-MSC (Campard et al., 2008; Lee et al., 2004; Zemel et al., 2009).

6.6.1.2 LDL uptake

Uptake of LDL by both undifferentiated Ad-MSC and BM-MSc was another finding which was anticipated only to occur after successful hepatocyte differentiation as again it is commonly used to demonstrate hepatocyte differentiation. This was then confirmed by demonstrating gene expression of the LDL receptor and also presence of the receptor on the cell membrane by immunocytochemistry. This then necessitated removing this test from the assessment of resultant hepatocyte-like cells. To assess if this was a species-specific phenomenon, mouse and human MSC's were tested with LDL uptake and anti-LDL receptor antibodies and found to also be positive.

It has been demonstrated that mouse BM-MSC express LDL-oxidised receptors (LOX-1) and take up DiI-oxidised-LDL (the biological analogue to acetylated-LDL) and also express LOX-1 by gene expression and Western blot (Zhang et al., 2013a; Zhang et al., 2013b). In the present study, canine Ad-MSC and BM-MSC were found not to take up Ac-LDL. Liesveld et al. (1989) showed that human BM-MSC took up DiI-LDL in standard McCoy's media with 10% FCS, whilst culture in McCoy's' with 25% serum and 1μmol/L hydrocortisone, this reduced and DiI-Ac-LDL uptake increased. Therefore these apparent differences may be an artefact of culture conditions rather than a fundamental cellular difference. Both the mouse and human BM-MSC's were cultured under the conditions recommended by the supplier and produced identical results to the canine MSC's i.e. no DiI-Ac-LDL uptake but avid DiI-LDL uptake.

Finally, in line with the theory that MSC are fibroblast populations, it has been demonstrated that fibroblasts express the LDL receptor, take up LDL but not modified LDL (Drevon et al., 1981; Gross and Webb, 1986; Haniffa et al., 2009; Quaschning et al., 1997; Sasaki and Cottam, 1982). Therefore in this respect, the presence of LDL receptors and specific uptake of LDL on MSC's is not surprising.

Assessing the effect of culture conditions on LDL receptor expression and the cells ability to take up LDL and Ac-LDL would be useful to assess if canine MSC demonstrate the same plasticity as human BM-MSC in regard to LDL and Ac-LDL uptake.

The presence of albumin gene expression and LDL uptake in MSC's serves to highlight the fact that no one single test or even limited range of tests is adequate to demonstrate successful differentiation of cells to a hepatocyte-like state (Hengstler et al., 2005).

6.6.1.3 Periodic acid-Schiff staining

Undifferentiated Ad-MSC and BM-MSC appeared to stain with PAS to a similar intensity as primary hepatocytes in culture, although no increased expression of glycogen synthase was detected by real-time PCR. It is most likely that staining was not specific for glycogen as other polysaccharides and proteoglycans which may be produced by mesenchymal stem cells will also stain positive (Rajan and Klein, 1982). Indeed although it is uncommon that PAS staining of undifferentiated MSC's are documented, there are previous reports of MSC to hepatocyte differentiation where undifferentiated MSC's are PAS positive (Prasajak and Leeanansaksiri, 2013). To improve the specificity of this stain, pre-treatment of one sample with diastase which would depolymerise glycogen and should then give a negative result would help guard against non-specific staining (Lee et al., 2004).

6.6.2 Gene expression evidence of transdifferentiation

Morphologically, both Ad-MSC and BM-MSC demonstrated a change from fibroblastic to epithelial in all culture conditions tested. This was most pronounced in the BM-MSC's. Examination of gene expression markers for mesenchymal and epithelial cells showed a down-regulation of vimentin and fibronectin (mesenchymal markers) but no corresponding increase in E-cadherin and β-catenin (epithelial and hepatocyte markers), suggesting that transdifferentiation was not complete (Schmelz et al., 2001).

6.6.2.1 Gene expression evidence of hepatocyte-like cells

Examination of hepatocyte gene expression also yielded no evidence of up-regulation after differentiation, the exception being α1 anti-trypsin which was increased in BM-MSc after the protocol used in experiment 3. Interestingly, Choi et al. (2013), who demonstrated canine amniotic MSC's ability to express tyrosine aminotransferase, α1 anti-trypsin and albumin after hepatocyte differentiation, also differentiated canine BM-MSC which only expressed α1 anti-trypsin. For both cell

types, α1 anti-trypsin is the most convincing band on the documented gel electrophoresis. To temper enthusiasm that the increase in α1 anti-trypsin may be the first sign that a hepatocyte-like state may be achieved, Beerheide et al. (2002) demonstrated α1 anti-trypsin expression in undifferentiated stem cells.

Therefore, at present, only canine amniotic fluid mesenchymal stem cells have been described as demonstrating limited gene expression of hepatocytes after differentiation (Choi et al., 2013). This would be consistent with the hypothesis that these stem cell sources have a greater differentiation potential than adult stem cell sources (Lee et al., 2004). Amniotic MSC's have been shown to have a higher self-renewal capacity than adult MSC's (>300 population doublings versus <25 respectively) as well as expressing more of an embryonic stem cell phenotype compared to adult MSC's (Joo et al., 2012; Wagner et al., 2008).

Although successful production of hepatocyte-like cells from MSC's has been described in many species including human, mouse, rat, pig and horse, there are also reports of failed transdifferentiation from healthy human and rat BM-MSC's (Bruckner et al., 2013; Lange et al., 2005a; Snykers et al., 2009a; Snykers et al., 2007).

6.6.3 Effect of epigenetic modification on hepatocyte differentiation

Two methods were used to try and improve the pluripotent potential of the MSC; DNA demethylation using 5AZA and histone hyperacetylation using valproic acid. Neither compound appeared to allow hepatic differentiation.

5AZA concentrations described in MSC to hepatocyte differentiations range from 1-20μM therefore the concentration utilised (20μM) was at the top of this range (Snykers et al., 2009a). Performance of a DNA methylation assay would have been useful to confirm efficacy of 5AZA incubation in these cells (Seeliger et al., 2013).

Similarly, although the valproic acid concentration was at the high end of published concentrations (2- 5mM), the efficacy may have been documented by Western blot or immunofluorescence analysis (Chen et al., 2009; Dong et al., 2013; Kisseberth et al., 2008).

6.6.4 Further options to improve transdifferentiation efficiency

6.6.4.1 Epigenetic modification

Other compounds which should be tested include: trichostatin A (a DNA methytransferase inhibitor) which has been demonstrated to dramatically improve hepatic differentiation of human BM-MSC's and also DMSO (a histone deacetylase inhibitor) which added towards the end of differentiation enhanced differentiation (Seo et al., 2005; Snykers et al., 2007). Finally, it has been suggested that utilising both types of compound may improve differentiation efficiency dramatically (Snykers et al., 2009b).

6.6.4.2 Culture conditions

At present, the majority of stem cell to hepatocyte differentiation protocols uses a 2D culture system on simple basal substrates (e.g. collagen type I) with solely the stem cell to be differentiated present. *In vivo*, hepatocytes are in a complex environment with diverse surrounding cell types and extracellular matrix (Palakkan et al., 2013). Beginning to reconstruct this *in vitro* improves primary hepatocyte function and transferring this same rationale to hepatocyte differentiation of stem cells has proven successful (Snykers et al., 2009a). Options for improving differentiation with modified culture conditions include the following stratagies;

6.6.4.3 Co-culture

Culturing MSC with primary hepatocytes was initially performed to enhance the longevity and function of the primary hepatocytes; however, it has since been demonstrated that this also improves the differentiation of MSC's towards a

hepatocyte phenotype therefore this may be a useful method (Lange et al., 2005b; Mizuguchi et al., 2001; Qihao et al., 2007).

6.6.4.4 Modification of basal substrate

Although collagen was used to reduce cell loss during differentiation and is also the standard substrate on which primary hepatocytes are cultured, there has been much research into different culture substrates with various synthetic and natural substrates shown to improve resultant function of stem cell differentiated hepatocyte-like cells (Hay et al., 2011; He et al., 2013; Yamazoe et al., 2013). Culture of cells in a 3D system or artificial bioreactor has also been shown to improve the efficiency of differentiation of stem cells (Nagamoto et al., 2012)

6.6.4.5 Direct induction

Introduction of specific transcription factors has been used to directly produce hepatocyte-like cells from mesenchymal cells. Huang et al. (2011) demonstrated that mouse fibroblasts could be directly transduced into functional hepatocyte-like cells by lentiviral introduction and over-expression of Gata4, Hnf1α, Foxa3 and inactivation of p19, which mimics expression during embryogenesis. These genes have been shown to increase during Ad-MSc to hepatocyte differentiation, therefore this may be a useful method in the dog (Li et al., 2013a). Manipulation of gene expression via over-expression of microRNA (miRNA) has also been utilised in hepatocyte production from stem cells (Cui et al., 2013). As miRNA are highly conserved between species, an identical protocol may be used in canine MSC.

Chapter 7: Production of canine induced pluripotent stem cells and hepatocyte differentiation

7.1 Abstract

Induced pluripotent stem cells (iPSC) are adult cells that have been re-programmed to return to an embryonic stem cell-like state. These can then be differentiated into all cell types and are therefore another potential source of hepatocyte-like cells. This chapter discusses the common methods of inducing pluripotency, characterisation of the resultant cells and methods of hepatocyte differentiation. Insertion of a polycistronic plasmid containing Yamanaka transcription factors into canine epidermal keratinocyte progenitor (CPEK) cells and attempted production of canine iPSC is described. Colonies with iPSC compatible morphology, expressing the fluorescent protein tag coded by the plasmid, were produced and demonstrated to be alkaline phosphatase positive. The presence of plasmid DNA in the cells' genomic DNA was confirmed. After colony picking, alkaline phosphatase activity was reduced, and integration of the plasmid into the genome appeared to be lost. Using real time PCR, no difference in Nanog or Sox9 expression compared to non-induced CPEK was found.

Canine iPSC from parental sources - canine embryonic fibroblasts, bone marrow mesenchymal stem cell and adipose-derived mesenchymal stem cells, were then differentiated towards hepatocyte-like cells using a published protocol. The resultant cells demonstrated a hepatocyte-like phenotype based on gene expression and morphology.

7.2 Introduction

7.2.1 Induced pluripotent stem cell production

The first production of induced pluripotent stem cells (iPSC) was described by Takahashi and Yamanaka (2006) where four factors, *OCT4*, *Sox2*, *c-Myc* and *KLF4* were inserted into mouse embryonic stem cells and fibroblasts using a lentiviral vector. Overexpression of these factors produced an embryonic stem cell like state. One drawback is the very low efficiency of conversion achieved, ~0.1% or below.

Exogenous gene expression only appears to be required for initial activation of self-renewal and then is dispensable. This has been demonstrated by using doxycycline inducible transgenes confirming that only 10-14 days of expression was required (Stadtfeld et al., 2008a). To be truly fully reprogrammed to a pluripotent state, the exogenous factors should be silenced and cells maintain pluripotency by endogenous gene expression. iPSC which still have transgene expression are classed as Class I iPSC and are partially reprogrammed, whilst those which are maintained by endogenous gene expression with silencing of exogenous genes are defined as Class II. Reprogramming is a gradual process and key markers along the process appear to be; alkaline phosphatase activation and fibroblast gene silencing, expression of SEA-1, then silencing of exogenous genes and upregulation of endogenous *Oct-4* and *Nanog* (Stadtfeld et al., 2008a). The method of gene delivery affects the probability of transgene silencing. Using retrovirus, exogenous gene silencing occurs via methylation of DNA whereas constitutively active lentivirus is more likely to produce incompletely silenced transgenes, and as a result may prevent differentiation (Sommer et al., 2010; Takahashi and Yamanaka, 2006).

Production of iPSC by the lentiviral methods and Yamanaka factors has since been described in a wide variety of species - human, pig, rabbit, horse, dog and snow leopard (Breton et al., 2013; Cheng et al., 2012; Takahashi et al., 2007; Tancos et al., 2012; Verma et al., 2012; Whitworth et al., 2012).

There are two major concerns in using this method to induce pluripotency aside from low efficiency:

- *c-Myc* is an oncogene and teratoma formation is common (Okita et al., 2007)
- Random integration of multiple transgenes may activate endogenous oncogenes and/or cause mutation

As a result, there has been a concerted effort to refine the induction of pluripotency. *c-Myc* was found to be dispensable, but at the cost of reduced efficiency (Wernig et al., 2008). Subsequently, many other factors were discovered which, in combination can induce pluripotency; *Lin28, Glis1, Esrrb,Tbx3, Utf1*(Wang et al., 2013a). Substitutes for Oct4 have also been discovered; *Cebpa, Hnf4a, Gata3, Gata4, Gata6, Grb2, Pax1,* and *Sox7* (Shu et al., 2013).

Two main methods of alleviating the problem of insertion of exogenes into the genome have been developed – non-integrating methods and developing the ability to excise the integrated gene.

7.2.1.1 Non-integrating methods

Vector based

Delivery of the factors via adenovirus allowed induction of pluripotency without genomic integration, again with greatly reduced efficiency (Stadtfeld et al., 2008b). Circular polycistronic plasmids (containing all four factors on one plasmid) have also been used as non-integrating methods of induction. Repetitive transient transfection is used to allow expression of the factors for the requisite length of time without genomic integration (Gonzalez et al., 2009). Vectors based on oriP/Epstein-Barr nuclear antigen-1(EBNA1) can be maintained in the nucleus under drug selection without integrating (Yu et al., 2009). With these methods, there is still concern that vector fragments may still integrate with the host genome (O'Malley et al., 2009).

Protein delivery

A further method of avoiding genomic integration which has been pursued is by replacing gene delivery with the resultant proteins. Purification of Oct4, Sox2, Klf4 and C-Myc protein and addition to culture media with valproic acid has been used to produce iPSC (Zhou et al., 2009).

Micro RNAs

microRNAs (miRNAs) are non-coding RNAs that bind complementary messenger RNA causing degradation or translational silencing. These were initially used to enhance efficiency of iPSC production; however, miRNAs have been used alone to produce mouse and human iPSC (Anokye-Danso et al., 2011; Miyoshi et al., 2011).

Chemical -induced pluripotency

Hou et al. (2013) developed a cocktail of small molecules which acted to re-programme mouse cells to a pluripotent state thus completely avoiding the need for transgene expression. The combination of molecules, which includes valproic acid, was found to activate *Oct4* and *Sox2*. These are thought to be "master" pluripotency genes in that they activate other down-stream pluripotency genes.

Stimulus-triggered acquisition of pluripotency (STAP)

Obokata et al. (2014b) have demonstrated a radical new method of iPSC production that did not require exogenous factors. Exposure of neonatal murine lymphocytes to pH 5.4-5.8 for 30 seconds caused Oct-4 expression, subsequent expression of pluripotency markers, and the ability to differentiate to the three germ layers and produce teratomas in NOD SCID mice. This conversion was also demonstrated in multiple types of differentiated cells. These cells were non-proliferative in standard

iPSC media but culture in adrenocorticotropic hormone (ACTH) and LIF allowed expansion. One unique characteristic of these STAP cells compared to ESC and iPSC was the ability to differentiate into trophoblast, thus demonstrating pluripotency broader than ESC and iPSC (Obokata et al., 2014a). This method would avoid genetic manipulation and appears very straightforward. At present, the method has only been proven in immature murine cells therefore it is unknown if the method is applicable in adult cells or other species (Smith, 2014).

7.2.1.2 Excisable transgenes

An alternative route rather than avoiding integration is to have an excisable integration site. To this end, two main vectors have been developed: the Cre/Lox and piggy/Bac system (Figure 7.1).

Cre/Lox system

LoxP is a 34-base pair which, if present as a pair in a specific orientation on the genome, will allow the enzyme cre-recombinase to excise DNA between the two LoxP sites. Kaji et al. (2009) utilised this system in designing a plasmid containing all four factors which, after successful re-programming could be excised with a separate Cre-recombinase plasmid transfection. This method was successfully used to re-programme mouse and human cells. One disadvantage of this system is that excision of the vector is not complete - one LoxP site and DNA external to the LoxP sites remain which may act as mutagens.

Piggy/Bac

This is a transposon/transposase system which is completely excised leaving no residual footprint. These have been used to produce mouse and human iPSC (Kaji et al., 2009; Woltjen et al., 2009).

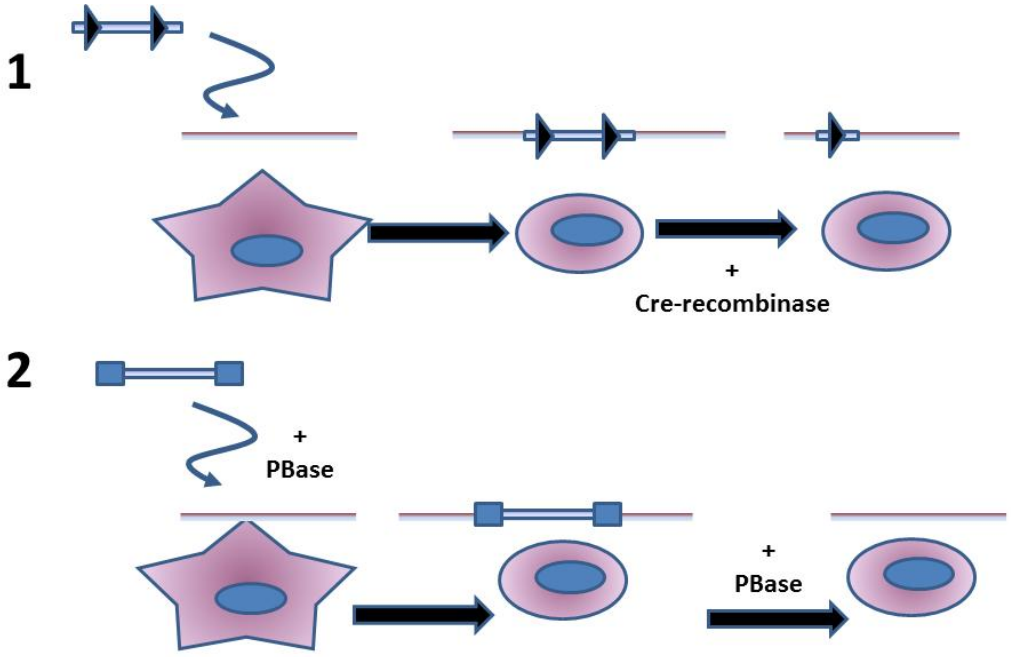

Figure 7.1 Methods of factor removal
Vector with LoxP sits (Black triangles), transient Cre expression removes the reprogramming factors with one LoxP and exogenous DNA remaining. (b) piggyBac transposons (blue squares) capable of being completely removed with transient piggyBac transposase (PBase) expression. Modified from O'Malley et al. (2009).

With both of these systems, cells with minimal copies of the vector need to be identified, integration sites mapped, the vector excised and validation of clones being factor-free. This is time consuming and, as a result, the newer non-integration methods may be more useful.

7.2.1.3 Methods of DNA delivery (Transfection)

The three main methods of nucleic acid delivery which avoid the use of viral vectors can be divided into chemical, non-chemical and particle based methods of transfection.

Particle-based methods

These methods include the "gene gun" where DNA is attached to gold nanoparticles and delivered to the cell nucleus but also magnetic assisted transfection and impalefection using nanostructures which are inserted into cells. Particle-based methods are not commonly used in iPSC production.

Chemical-based methods

These methods include calcium phosphate precipitation of DNA which then allows DNA entry to the cell nucleus, branched organic compounds and dextran-bound endocytosis of the DNA (Friedmann and Rossi, 2007). The most commonly employed chemical-based method is using liposomes, known as lipofection. DNA is carried in lipid vesicles which merge with cell membranes. This method is relatively highly efficient compared to the others (Felgner et al., 1994).

Non-chemical methods

The majority of these methods result in pores developing in the cell membrane allowing DNA entry. This can be achieved using laser, sonic waves, water, or electroporation. Of these, electroporation is most commonly employed. This involves subjecting cells to a high voltage pulse in suspension with the plasmid which results in transient cell membrane permeability via pore development, allowing the plasmid to enter the cells (Potter, 2001).

7.2.1.4 Transient and stable transfection

Once plasmid DNA has been delivered into the cell, the majority of it does not become integrated into the host cell's genomic DNA and is only transiently expressed whilst the plasmid DNA is present (generally days). Plasmid DNA is lost by degradation or a dilutional effect during mitosis (Kim and Eberwine, 2010). One method of allowing expression for the required length of time is repeated transfection

with the exogenous DNA (Gonzalez et al., 2009). Stable transfection occurs when the exogenous DNA integrates with the genomic DNA (Figure 7.2). As a result, exogenous integrated DNA is replicated along with genomic DNA during mitosis. Selection of the cells can occur if the exogenous DNA contains a resistance gene e.g. neomycin resistance which confers geneticin (G418) resistance to plasmid containing cells (Southern and Berg, 1982).

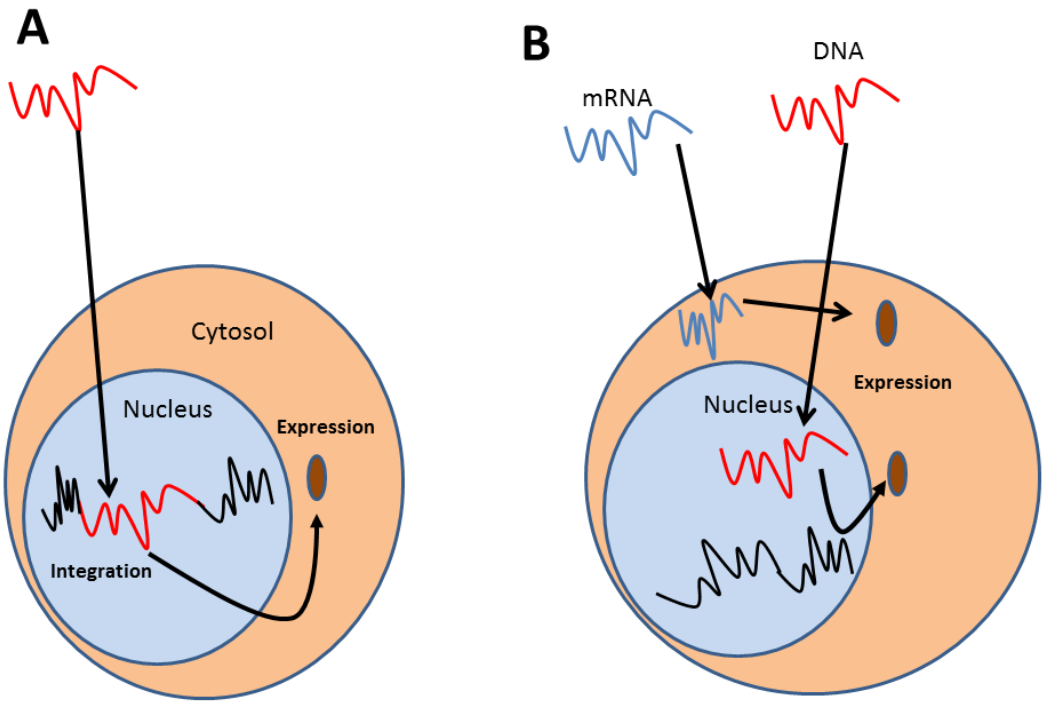

Figure 7.2 Transient and stable transfection
A – Exogenous DNA is integrated into the host cell genome allowing gene expression and transfer after mitosis. B – Transient transfection can be carried out with either RNA or DNA. This allows gene expression; however, the exogenous nucleotides are either degraded or diluted during mitosis.

7.2.2 Canine induced pluripotent stem cells

The first report of canine iPSC production was by Shimada et al. (2010), using lentiviral transfection with the Yamanaka factors to transfect canine embryonic fibroblasts. Post-transfection, cells were cultured on mouse embryonic fibroblasts (MEF) in LIF, valproic acid and bFGF containing media. Additionally, inhibitors of mitogen-activated protein kinase (MEK), glycogen synthase kinase 3β (GSK3β) and

TGF-β were used. The resultant cells were shown to differentiate to endoderm, mesoderm and ectoderm.

Luo et al. (2011) reported production of iPSC from canine adult fibroblasts, again using lentiviral transfection of the four Yamanaka factors and subsequent culture on MEF. Only LIF and bFGF was required to maintain pluripotency. These cells were also shown to have the ability to differentiate towards the three germ layers. A comparison between adipose stromal cell and fibroblast derived canine iPSC using the same method was also described (Lee et al., 2011). Canine adipose stromal cells were found to have double the reprogramming efficiency of fibroblasts.

A further report of canine iPSC from adult fibroblasts using lentiviral transfection of the Yamanaka factors has been published (Koh et al., 2013). These cells were both LIF and bFGF dependent, along with a requirement for MEK and GSK3β inhibition.

Whitworth et al. (2012) reported lentiviral production of canine iPSC using the Yamanaka factors as well as Lin28 and Nanog. Interestingly, unlike the previous three studies, these cells could be maintained without b-FGF and required only LIF. It was hypothesised that this difference was that the solely LIF dependent cells had been reprogrammed to an inner cell mass-like ground state.

One key criticism of the studies describing canine iPSC formation is that teratoma formation has been a stumbling block. Teratoma formation is considered to be the gold standard in assessing pluripotency (Zang et al., 2012). Of the studies so far, only Lee et al. (2011) has successfully demonstrated teratoma formation, whilst Whitworth et al. (2012) documented occasional tumour formation resembling germ cell tumours.

Another point of note is the paucity of reports on directed differentiation of canine iPSC to terminally differentiated cells. At present, there is only one report, utilising the protocol of Luo et al. (2011) to produce iPSC which were then differentiated into megakaryocytes, producing platelets using a co-culture system (Nishimura et al.,

2013). This may reflect instability in maintaining pluripotency once the exogenous transgenes have been silenced or continued expression of transgenes blocking differentiation.

7.2.3 Differentiation of iPSC to hepatocyte-like cells

The majority of differentiation protocols follow the main stages of embryonic development from pluripotency, to definitive endoderm (DE), foregut endoderm (FE), hepatic progenitors and finally mature hepatocytes. The majority of protocols utilize RMPI 1640 and activin A, often with B27 supplement to induce the step to DE. Further differentiation to hepatocytes has been achieved using either RMPI or knock-out serum replacement media. Growth factors used for DE to hepatocytes include FGF and bone morphogenic protein. Finally, a maturation step with oncostatin M and hepatocyte growth factor is used. Refinement of protocols has achieved up to 90% of cells expressing αfoetal protein (a hepatoblast marker) prior to the maturation step. Although iPSC can be efficiently differentiated towards a hepatocyte-like state, the cells are characterised as intermediate between foetal/adult rather than mature hepatocytes, with expression of albumin, hepatocyte nuclear factor 4a,α1 anti-trypsin, transthyretin, transaminotyrosine and cytochrome P450 (Gerbal-Chaloin et al., 2014). Functionality demonstrated after differentiation includes glycogen storage, ammonia to urea conversion, cholesterol uptake, albumin production, LDL uptake and cytochrome enzyme activity. In concert with differentiation halting at a foetal phenotype, functionality compared to primary hepatocytes is greatly reduced (Hannan et al., 2012). Recently, a 3-dimensional collagen matrix was used to produce iPSC-derived hepatocytes which were functionally closer to mature hepatocytes than those in 2D culture; therefore, improving culture conditions may assist in the final maturation step (Gieseck Iii et al., 2014).

The addition of Wnt3a at the induction step to DE has also been reported in iPSC to hepatocyte differentiation (Chen et al., 2012b). Wnt signaling during embryogenesis is complex. It has been demonstrated that Wnt is required for mesoderm specification and that both Wnt and activin are required for primitive streak induction and activin for hepatic commitment (Gadue et al., 2006). Activin and Wnt3a have both been shown to be important in hepatic differentiation of both human embryonic and induced pluripotent stem cells (Hay et al., 2008; Sullivan et al., 2010).

At present, there are no reports of hepatocyte-like cell production from canine iPSC.

7.3 Aims

The aims of this chapter were to produce canine induced pluripotent stem cells using the Cre/Lox vector containing *Oct4, Sox2, Klf4* and *C-Myc* created by Kaji et al. (2009). This would enable the transgenes to be excised once pluripotency had been achieved. Canine iPSC would then be differentiated towards a hepatocyte-like phenotype using a published protocol for human iPSC, and the success measured using tests validated in Chapter 3 (Chen et al., 2012b).

7.4 Methods

7.4.1 Plasmid expansion

The plasmid pCAG2LMKOSimO (Figure 7.1) was gifted by Keisuke Kaji (Kaji et al., 2009). DH5α bacteria (18258-012, Invitrogen) were thawed on wet ice. After mixing, 100µl was placed into a chilled 1.5ml polypropylene tube. A volume of 5ul of pCAG2LMKOSimO plasmid was added and the contents gently mixed. The tube was then held on ice for 30 minutes, at 42^{o}C for 45 seconds, then in ice for 2 minutes. One ml of Lysogeny broth (LB) was added and the tube shaken at 225rpm for 1 hour at 37^{o}C. This was then diluted 1:100 with LB also at 37^{o}C and 100µl spread onto LB agar with ampicillin at 100µg/ml. Agar plates were cultured overnight at 37^{o}C. Plates were examined and single colonies were picked with a

200µl pipette tip, transferred to 5ml of LB with 100µg/ml ampicillin and incubated for 10 hours before being transferred to 200ml of the same broth, and again incubated overnight at 37°C. Plasmid stocks were archived by mixing 800µl of bacterial broth and 200µl of glycerol and storing at -80°C.

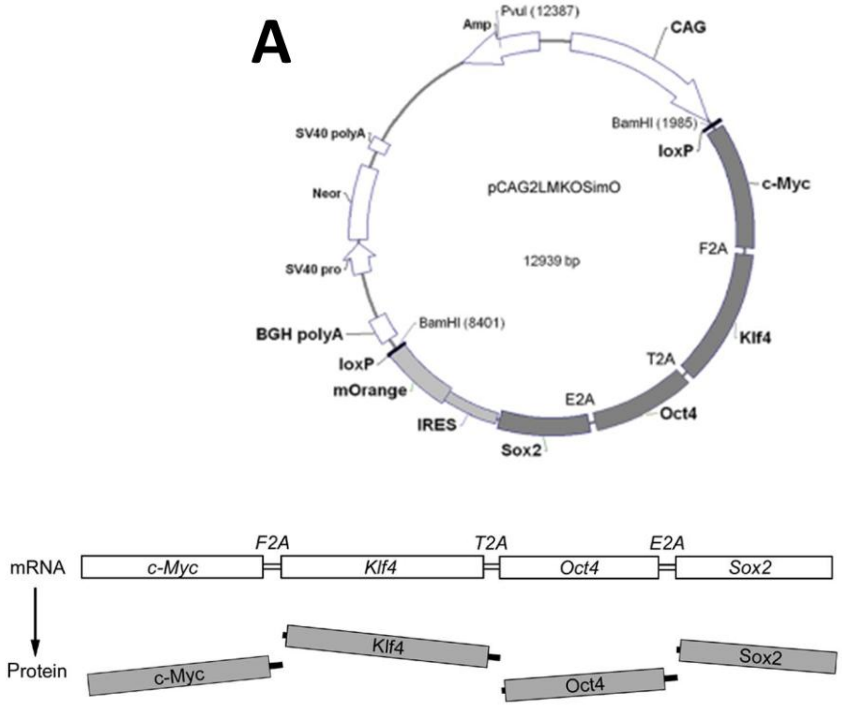

Figure 7.3 A - Plasmid map of pCAG2LMKOSimO designed by Keisuke Kaji. B – Demonstrating cleavage of protein at 2A linkages.
Plasmid contains both ampicillin (Amp) and neomycin (Neor) resistance genes. The 4 pluripotent expression factors are linked by 2A peptides which skip on protein translation allowing separation of proteins. mOrange is a fluorescent protein. LoxP sites flank the transgenes allowing subsequent excision using crea-recombinase.

7.4.2 Plasmid purification

The LB broth was centrifuged at 4000g for 10 minutes and supernatant removed. Plasmid purification from the bacterial cell pellet was carried out using an anion-exchange column (HiPure plasmid purification kit, Invitrogen) according to the manufacturer's instructions. Eluted DNA was suspended in 500µl of nuclease-free water. Yield and purity were measured using spectrophotometry (NanoDrop 1000, Thermoscientific).

7.4.3 Culture of canine epidermal keratinocyte progenitors (CPEK)

CPEK were purchased and expanded in in proprietary media (CellnTech advanced cell systems, Switzerland). These were initially seeded at a density of 4 x103/cm^2. These were expanded and passaged at 80% confluence using 0.25% trypsin-EDTA (Life Technologies).

7.4.4 Optimisation of CPEK transfection by electroporation

An Amaxa Nucleofector 2b (Lonza) was used with the corresponding keratinocyte nucleofection kit (Lonza). CPEK were trypsinised and trypsin neutralised with media containing 10% foetal bovine serum. Cells were counted and suspended in nucleofector solution at a concentration of 1 x10^7/ml. Two µg of pmaxGFP per 100µl of cell suspension was added and gently mixed. 100µl of suspension was added to each electroporation cuvette. Each cuvette was inserted into the nucleofector device and programs used were S1, U12, W1, T20, T13 and no program control. 500µl of warm culture media was added to each cuvette and each transfection transferred to one well of a 6 well plate. Cells were incubated for 24 hours at 37^{o}C and 5% CO_2 before being viewed under phase contrast and fluorescent microscopy.

7.4.5 Linearisation of pCAG2LMKOSimO

Restriction endonuclease PuvI (New England Biolabs Inc.) was used to linearise the plasmid. The solution (Table 7.1) was incubated at 37^{o}C for 1 hour.

Item	Volume/Amount
pCAG2LMKOSimO	25µl/75ng
Bovine Serum Albumin	0.5µl
NEB Buffer	5µl
H_2O	15µl
PvuI	5 µl

Table 7.1 Restriction endonuclease incubation conditions

7.4.6 Gel electrophoresis to confirm linearisation of plasmid

1.5µl each of linearized and circular plasmid were run in a 0.8% agarose gel with a 1Kb ladder (1Kb Plus DNA Ladder, Invitrogen) and Gel Red (Biotium) at 80 volts for 2 hours. The gel was imaged under UV (Gel Doc XR+ System, BioRad).

7.4.7 Inactivation of SNL feeder cells

Confluent SNL feeder cells (Cambridge Biosciences) were inactivated with Mitomycin C (Sigma) at a concentration of 10µg/ml for 2 hours at 37^{o}C. Cells were then washed three times with PBS and dissociated with 0.25% Trypsin-EDTA before being re-plated at 7.5 x10^4/cm^2 on gelatine-coated tissue culture dishes as feeder cells.

7.4.8 G418 kill curve

CPEK were cultured in 24 well plates and 0, 50,100 µg/ml, then increasing concentrations by 100 µg/ml to a maximum concentration of 2000µg/ml of G418 was added to the culture media. Media was changed every 3 days and wells examined daily to assess cell viability.

7.4.9 Transfection of CPEK with pCAG2LMKOSimO

1 x10^6 were transfected with 2µg of pCAG2LMKOSimO vector using program U17 and W1. No plasmid and also GFP plasmid sample were used as controls. After transfection, cells were plated onto SNL feeders and after 10 days G418 at the lowest concentration which caused complete cell death of untransfected CPEKs was added.

7.4.10 Alkaline phosphatase staining

Alkaline phosphatase staining was performed using an alkaline phosphatase leucocyte kit (Sigma-Aldrich). Cells were fixed in citrate-acetone-formaldehyde solution for 30 seconds at room temperature then rinsed in distilled water. Freshly prepared alkaline dye solution was added for 15 minutes and the wells protected from light. A final rinse was performed for 2 minutes using distilled water and well examined grossly and microscopically for red/pink positive staining.

7.4.11 Genomic DNA extraction

Cells were collected by removing media, rinsing in PBS and then using a cell scraper to collect cells in 1ml of PBS. This was transferred to a 1.5ml polypropylene tube and centrifuged at 1500rpm for 5 minutes to pellet the cells. Genomic DNA was extracted from cells using DNeasy blood and tissue kit (Qiagen). Genomic DNA extraction was carried out according to the manufacturer's instructions. Yield and purity were measured using spectrophotometry (NanoDrop 1000, Thermoscientific).

7.4.12 PCR to confirm presence of plasmid pCAG2LMKOSimO

Primers described by Kaji et al. (2009) were used to confirm the presence of plasmid DNA in transfected CPEK genomic DNA (Figure 7.4 and Table 7.2).

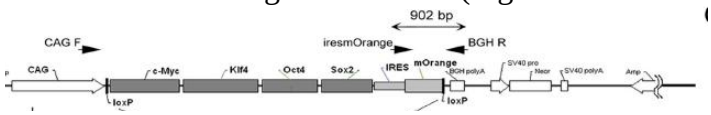

Figure 7.4 Diagram of vector demonstrating location of primer annealing locations and product size From Kaji et al. (2009).

Primer	Sequence
IRESmOrange	GGCCACAACCATGGTGAGCAAGGGCGAGGA
BGH R	TAGAAGGCACAGTCGAGG

Table 7.2 Primer sequence used for plasmid presence in cell genomic DNA

End point PCR was performed using Qiagen HotStarTaq DNA polymerase and Bio-Rad iCycler. Table 7.3 shows reaction components. An initial denaturation step of 95^{o}C for 5 minutes was followed by 35 cycles of 95^{o}C for 1 minute, annealing at 54^{o}C for 1 minute and extension at 72^{o}C for 1 minute. A final extension at 72^{o}C for 5 minutes was performed. No template controls using distilled water were also run. The final reaction solution was run on a 1.5% agarose gel at 80 volts with a 1Kb ladder (Invitrogen). The gel was visualized with UV and the Gel Doc XR+ System (BioRad).

Component	Volume per reaction
PCR buffer	10 µl
dNTP mix	2 µl
IRESmOrange	1 µl
BGH R	1 µl
HotStarTaq DNA Polymerase	0.5 µl
Template DNA	500ng
Distilled water	to make 100 µl total

Table 7.3 PCR mix components

7.4.13 Real Time PCR primers optimisation

Total Sox2 and canine Nanog primers as used by Kaji et al. (2009) and Vaags et al. (2009), respectively were used. Efficiency, dissociation curve and product size was assessed using transfected CPEK cDNA.

7.4.14 Relative expression of Sox2 and Nanog in transfected CPEK clones

cDNA from transfected CPEK clones and untransfected CPEK was diluted 1:20 and qPCR performed as previously described. Fold increase of Sox2 and Nanog compared to untransfected CPEK was calculated using MXPro QPCR software (Agilent Technologies, USA).

7.4.15 SNF conditioned iPSC media

10mls of incomplete iPSC media (Knockout DMEM, 10% ES-grade FBS, L-glutamine, 100 U/mL Penicillin G and 100 µg/mL Streptomycin, 0.1mM β-Mercaptoethanol, 1 x non-essential amino acids) was incubated with confluent, inactivated SNL cells for 24 hours before removal, filtration with 0.2µ filter and the addition of 10ng/ml of human recombinant leukemia inhibitory factor (Millipore, USA) and human basic fibroblast growth factor.

7.4.16 Matrigel-coated tissue culture plates

Reduced growth factor Matrigel (BD Biosciences) was thawed overnight on ice and diluted 1:20 in SNL conditioned iPSC media. Tissue culture plates were coated with a volume of 160µl/cm^2. Plates were then incubated at 37^oC for 1 hour and media aspirated.

7.4.17 Hepatocyte differentiation of iPSC

Canine iPSC produced by Alison Thompson using a lentiviral polycistronic Cre-excisable system (SCR511, Millipore) were used for this stage. Cell lines, Ad-MSC 4f and BM-MSC 4f were derived from mesenchymal stem cells from d231113 which failed to transdifferentiation into hepatocyte-like cells from their mesenchymal state (Chapter 6: Mesenchymal to hepatocyte differentiation). iPSC derived from canine embryonic fibroblasts (CEF) using the same system were also differentiated.

The protocol described by Chen et al. (2012b), based on Hay et al. (2008), was used for hepatocyte differentiation (Figure 7.5). Induced pluripotent stem cells (iPSC) were passaged from SNL feeder cells at 70% confluence onto Matrigel-coated plates using a 1:3 split. SNL conditioned-media was replaced daily until 60% confluence was achieved, upon which the protocol was followed. At time points 0 and 10days, cells were harvested for RNA extraction, supernatant in contact with the cells for 24 hours harvested for albumin and urea quantification, PAS staining and CYP activity performed as previously described. For PAS staining, one well was incubated with 0.1% w/v diastase for 30 minutes at room temperature to assess specificity for glycogen. Cells were photographed prior to removal from SNL feeders, and at time points 0, 3, 6 and 10 days.

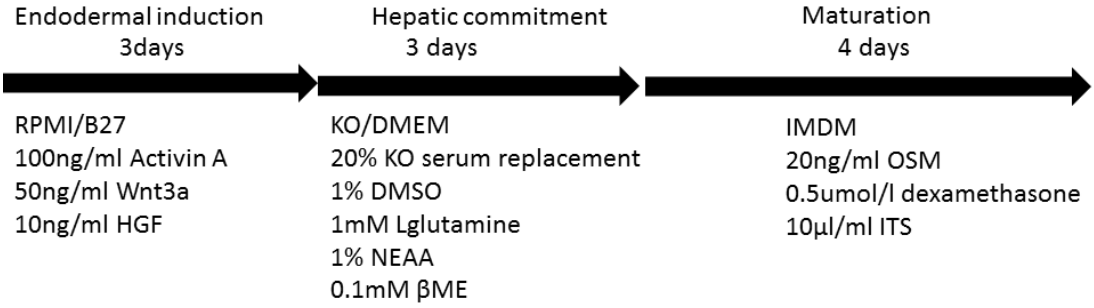

Figure 7.5 Protocol for iPSC differentiation to hepatocyte-like cells
RMPI – Roswell Park Memorial medium, HGF – hepatocyte growth factor, KO/DMEM – Knock-out DMEM, NEAA – Non-essential amino acids, βME – βMercaptoethanol, IMDM – Iscove's modified Dulbecco's medium, OSM – Oncostatin M, ITS – Insulin/transferrin/selenium pre-mix.

7.5 Results

7.5.1 Plasmid expansion

After DNA purification a total yield of 1.4mg of plasmid with a 260/280 absorbance ratio of 1.99 was produced.

7.5.2 Plasmid linearisation

To increase the chances of a stable transfection and also produce a predictable break-site in the plasmid (which would not disrupt the genes of interest) the plasmid was linearised. After incubation with PuvI restriction enzyme for 1 hour to linearise the plasmid (Figure 7.6A), equal concentrations of plasmid were electrophoresed on a 0.8% agarose gel. This demonstrated almost complete linearisation after digestion with a sharp band just above 12Kbp consistent with the plasmid size of 12.9Kbp (Figure 7.6B). The circular plasmid band is less well defined likely due to a combination of super-coiling and nicks.

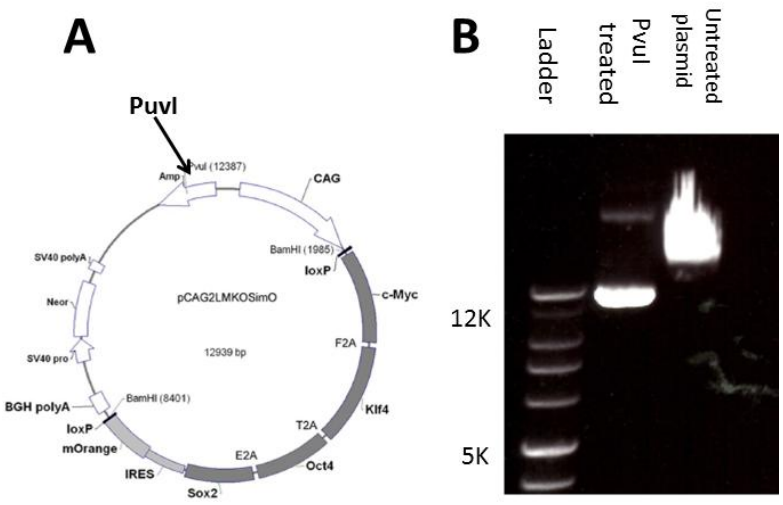

Figure 7.6 pCAG2LMKOSimO plasmid map and gel demonstrating ligation
A – plasmid map indicating single ligation site with PuvI enzyme.
B - Electrophoresis of untreated and ligated plasmid. Linearisation is almost complete with band at 12Kbp size.

7.5.3 Optimisation of electroporation

Twenty-four hours after GFP plasmid electroporation, the cells were imaged under fluorescent microscopy (Figure 7.7). A variation in transfection efficiency was noted between the different electroporation with programs U17 and W1 giving the most GFP positive cells. Both U17 and W1 were then selected to perform transfection with the pCAG2LMKOSimO plasmid containing the 4 Yamanaka factors.

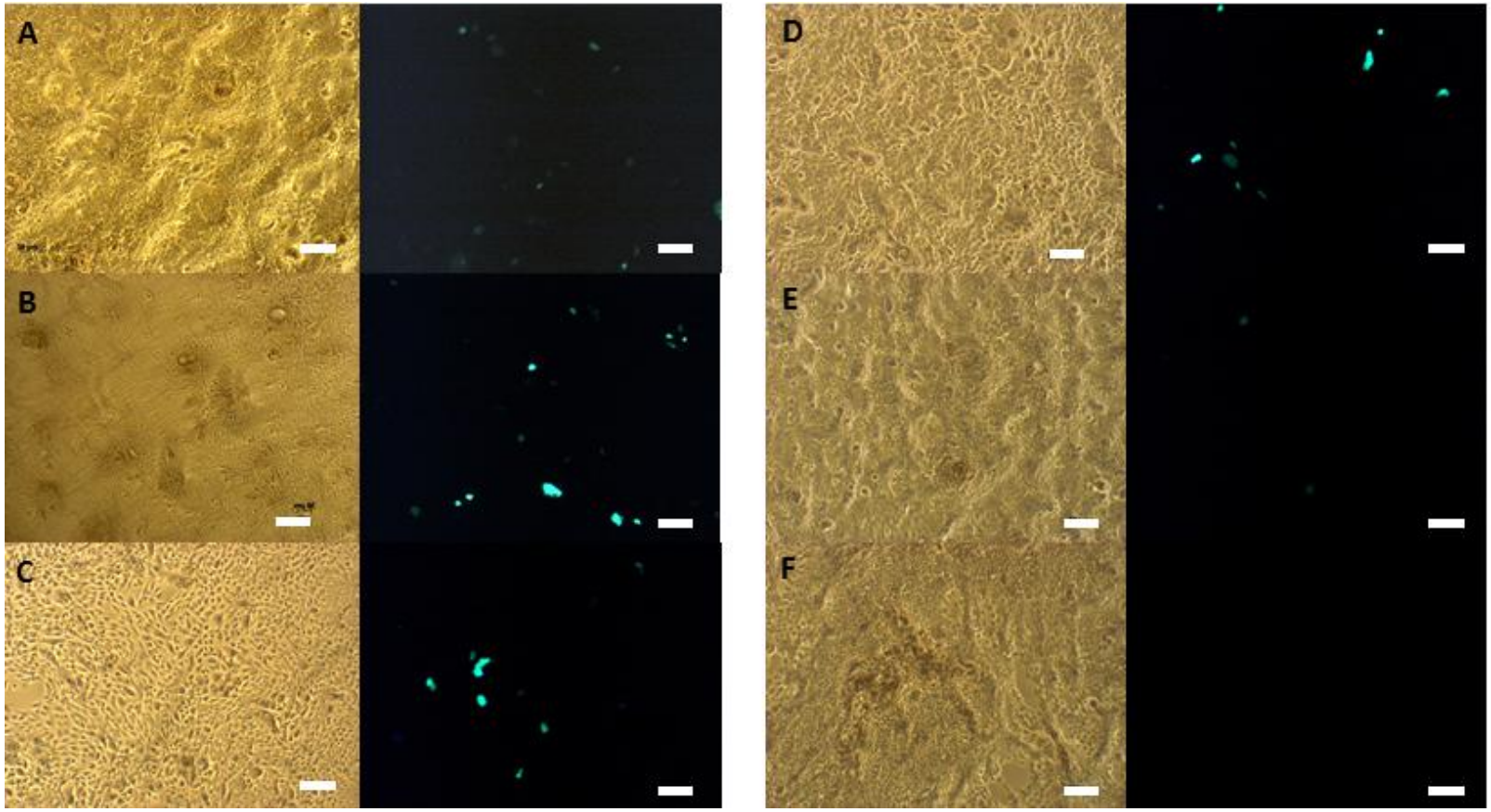

Figure 7.7 Optimisation of electroporation with GFP plasmid into CPEK cells.
CPEK cells imaged 24 hours after electroporation. Specific programmess are; A-S1, B-U12, C-W1, D-T20, E-T13. F – no electroporation control. U12 and W1 appeared to give the best transfection efficiency. Experiments performed in triplicates. White bar represents 200µm.

7.5.4 G418 kill curve

After 3 days, no viable cells were present at concentration of 800µg/ml and above. 800µg/ml was then chosen as the effective concentration to select for transfected cells.

7.5.5 CPEK can be successfully transfected with the pCAG2LMKOSimO plasmid

Examination of the cells after electroporation with the pCAG2LMKOSimO plasmid and also GFP control plasmid demonstrated lower transfection efficiency compared to the GFP control. Figure 7.8 shows cells 24 hours after U17 program electroporation however this was identical to the W1 program.

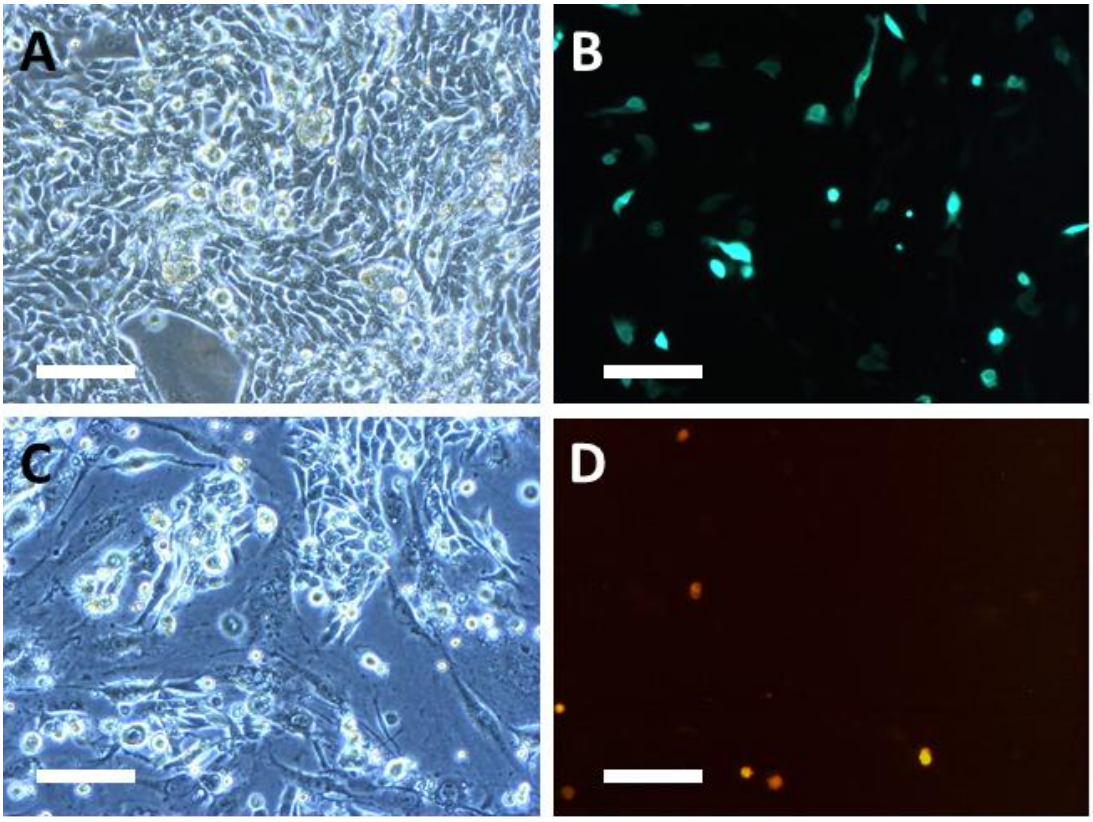

Figure 7.8 Transfection of CPEK with program U17
A/B – CPEK 24 hours after transfection with GFP plasmid. C/D CPEK 24 hours after transfection with pCAG2LMKOSimO plasmid. Both are demonstrating production of their respective fluorescent proteins GFP and mOrange. White bar represents 100µm.

Ten days after transfection, sparse dense colonies with a three dimensional structure were visible only in the cells which underwent U17. These contained cells which contained orange/red fluorescence (Figure 7.9).

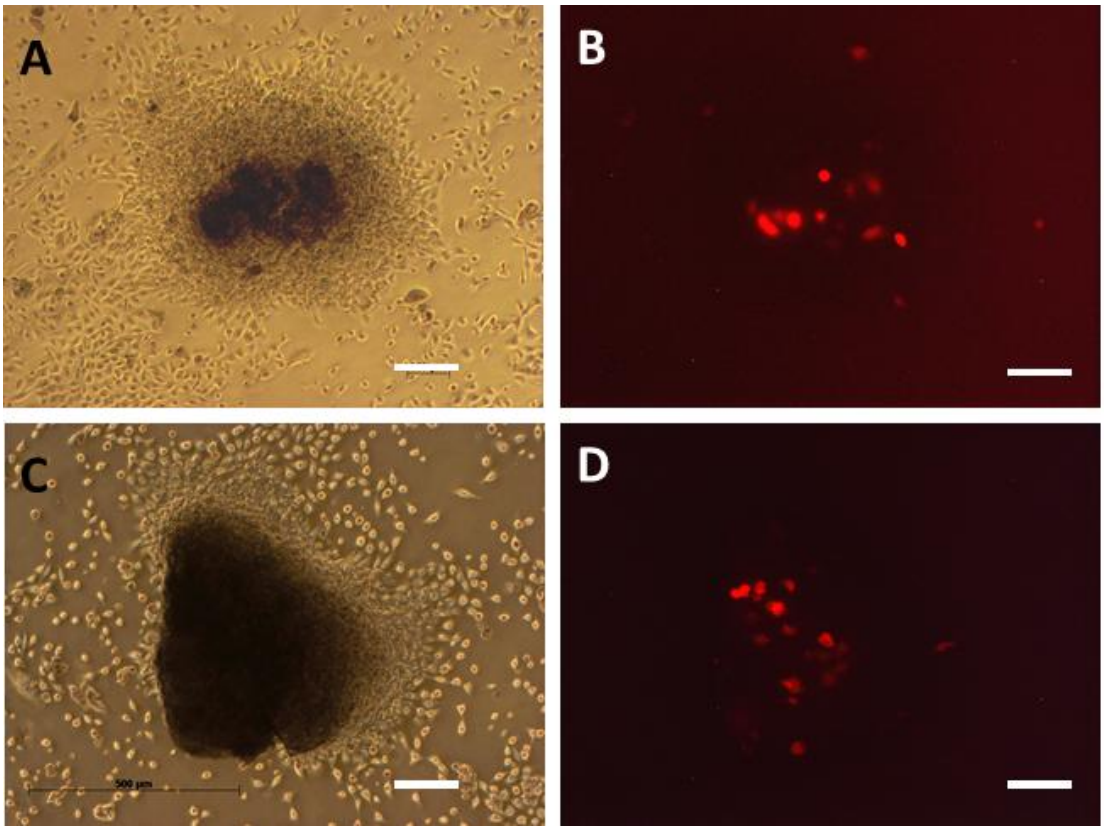

Figure 7.9 CPEK transfected cells after 10 days culture on feeders
Representative colonies 10 days after transfection. A&C – phase contrast images, B&D – Fluorescent microscopy. White bar represents 200µm.

G418 was added to the transfected cells at a concentration of 800µg/ml from day 10. Untransfected CPEKs were used as a control. By day 20, dense colonies were still present and fluorescent in U17 (Figure 7.10A/B). Some colonies of cells were present in W1. No viable cells were present in the control CPEK wells demonstrating CPEK susceptibility to this concentration of G418 and resistance of the plasmid-containing cells (Figure 7.10C).

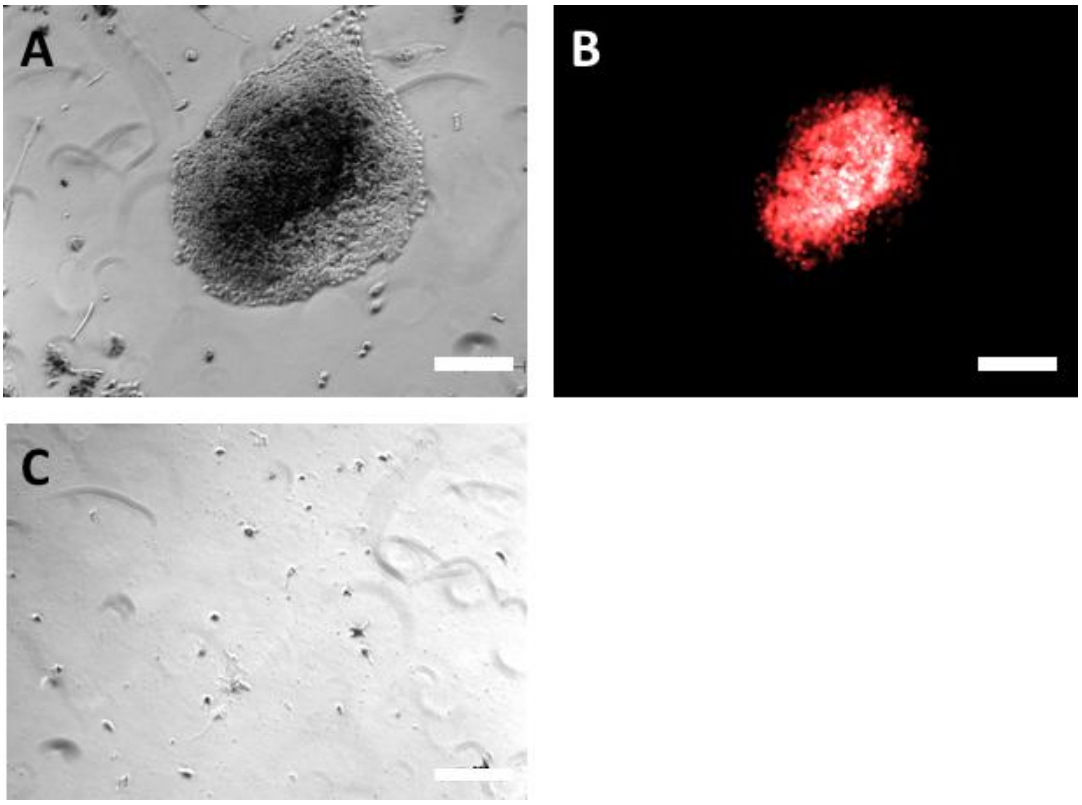

Figure 7.10 CPEK 20 days after transfection and 10 days after G418 addition
A/B – Transfected CPEK phase contrast and fluorescent microscopy.
C – untransfected CPEK after 10 days in G418, no viable cells present. White bar represents 200µm.

7.5.6 Is there evidence of plasmid integration into the genome?

This was performed at day 20. The presence of plasmid DNA was detected by PCR analysis in U17 cells and not W1 cells (Figure 7.11)

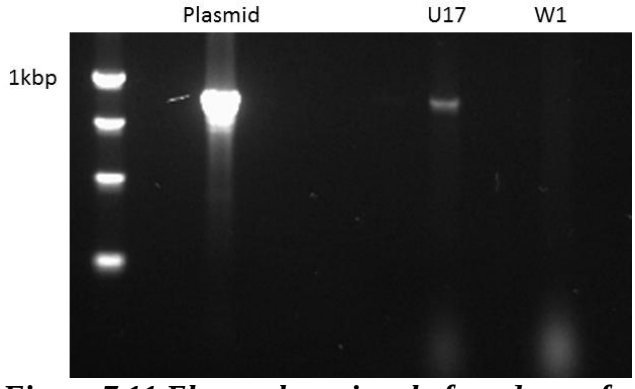

Figure 7.11 Electrophoresis gel of products after PCR of genomic DNA from cells 10 days after undergoing U17 and W1 transfection
Plasmid was used as positive control (plasmid). Presence of plasmid DNA in U17 cells and not in W1 cells.

7.5.7 Colonies demonstrate alkaline phosphatase activity

CPEK cells transfected using the U17 program (day 10) demonstrated strong alkaline phosphatase staining of the colonies whilst W1 transfected cells were uniformly negative. Mouse embryonic stem cells, used as a positive control, were strongly positive.

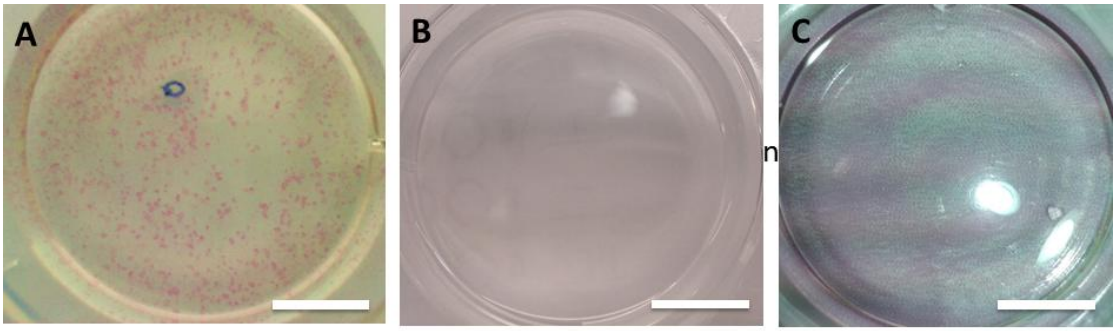

Figure 7.12 Alkaline phosphatase staining of CPEK and mouse embryonic stem cells
A- U17 transfected CPEK demonstrating strongly positive colonies. B- W1 transfected CPEK, alkaline phosphatase negative. C- Mouse embryonic stem cells (IOUD2) uniformly positive. White bar represents 10mm.

Twenty individual colonies were picked from the U17 plate and transferred to one well each of a 96 well plate. These were then cultured, expanded and passaged to a 24 well then a 12 well plate. 6 clones were viable and passaged to this stage. Alkaline phosphatase staining was then repeated (Figure 7.13). This demonstrated intense staining of the positive control and a lack of staining of untransfected CPEK as a negative control. The 6 clones showed only very weak staining which occurred in the centre of the colonies.

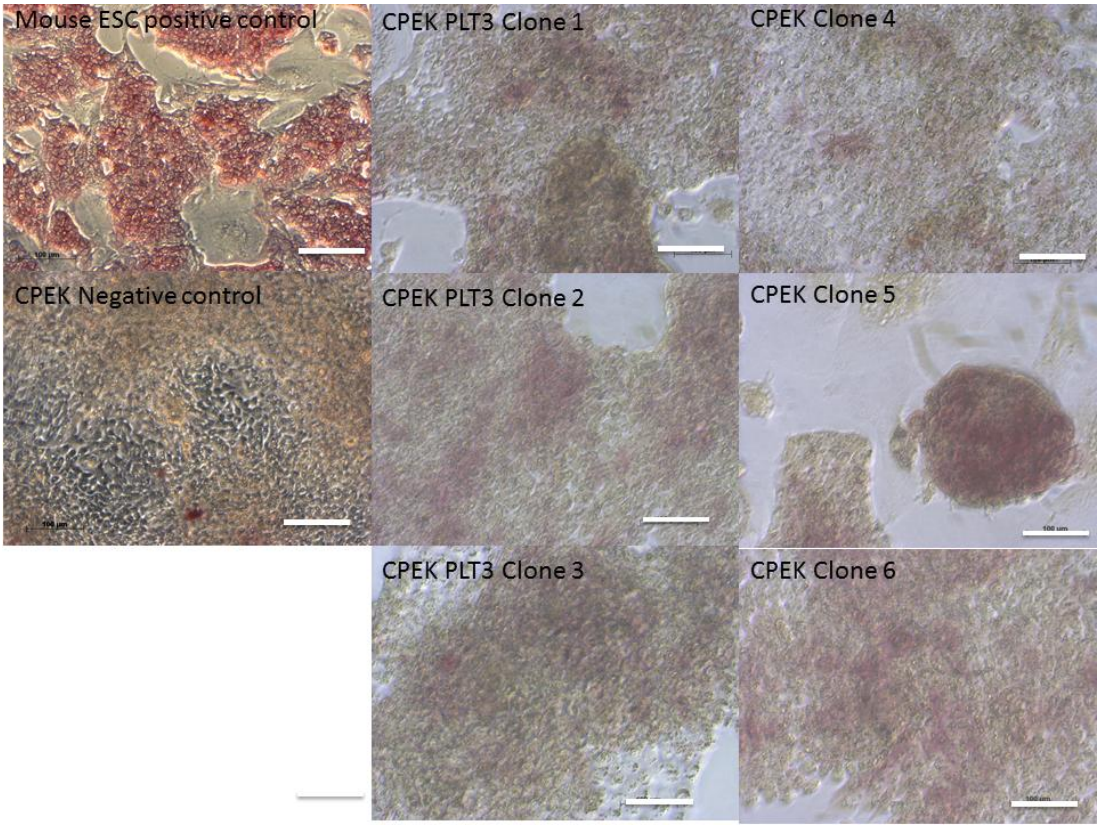

Figure 7.13 Alkaline phosphatase staining on mouse embryonic stem cells and picked transfected CPEK clones.
Alkaline phosphatase staining highly positive in mouse ESC (positive control) and negative in untransfected CPEKs (negative control).

The clones were further expanded and transferred to 6 well plates. Clones1-3 and 6 reached this stage whilst clones 4 and 5 failed to continue expanding.

7.5.8 Nanog and Sox 2 primer efficiency

Primer efficiency, dissociation curve and gel size was acceptable (Table 7.4).

Gene	Sequence	Product size (bp)	Efficiency %	TM ^{o}C	Dissociation curve	Gel size
Sox2	F- ACAGCTACGCGCACATGA R- GGTAGCCCAGCTGCTCCT	69	95.5	59.7/61.09	√	√
Nanog	F- CCTGCATCCTTGCCAATGTC R- TCCGGGCTGTCCTGAGTAAG	98	99.6	59.54/60.9	√	√

Table 7.4 Sox2 and Nanog primer sequence and characteristics

7.5.9 Picked colonies do not exhibit Nanog and Sox2 expression or have genomic plasmid integration

Real time PCR was performed to assess Nanog and total Sox2 expression compared to untransfected CPEK cells (Figure 7.14).

No difference in Sox2 (plasmid or endogenously expressed) or endogenous Nanog expression was noted in the remaining clones. Furthermore, no evidence of plasmid integration was detected in the genomic DNA of the remaining clones. Examination of the clones under fluorescent microscopy could not detect any orange fluorescence (images not shown).

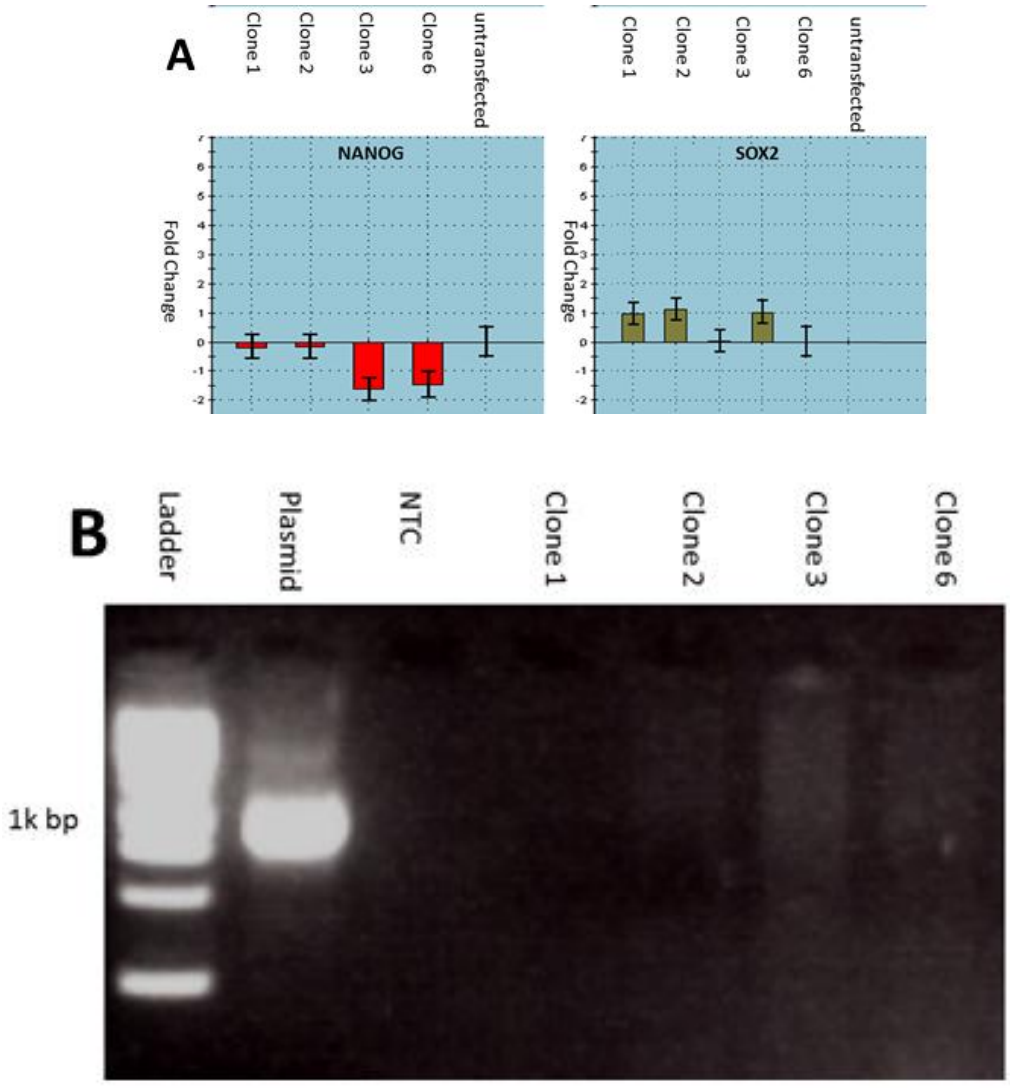

Figure 7.14 Fold change of relative gene expression compared to untransfected CPEK cells and plasmid integration in picked colonies.
A - Nanog and Sox2 gene expression normalized to two reference genes (B2MG, RPL8). B – PCR of genomic DNA with plasmid as positive control.

As alkaline phosphatase activity and plasmid integration appeared to have been lost, induced pluripotent stem cells derived using lentiviral transfection with a 4 factor plasmid, produced and characterised by Alison Thompson and Ruchi Sharma in the

group were used for the hepatocyte differentiation experiments. Cre excision of the transcription factors had not been performed.

7.5.10 Canine iPSCs can be differentiated into hepatocyte-like cells

7.5.10.1 There is morphologic evidence of hepatocyte-like cells

After dissociation from feeder cells and plating onto Matrigel, all three cell types assumed a mono-layer formation (Figure 7.15 B, F, and J). Cell attachment on the feeders was weak and this continued on Matrigel, leading to cell loss during media change. At the final day of maturation, the Ad-MSC iPSC had assumed compact round cell morphology, with BM-MSC iPSC exhibiting morphology most consistent with a hepatoblast, namely epithelioid polygonal cells with a moderate cytoplasm to nucleus ratio and obvious demarcations between cells (Figure 7.16). The CEF iPSC morphology appeared midway between the other two cell types.

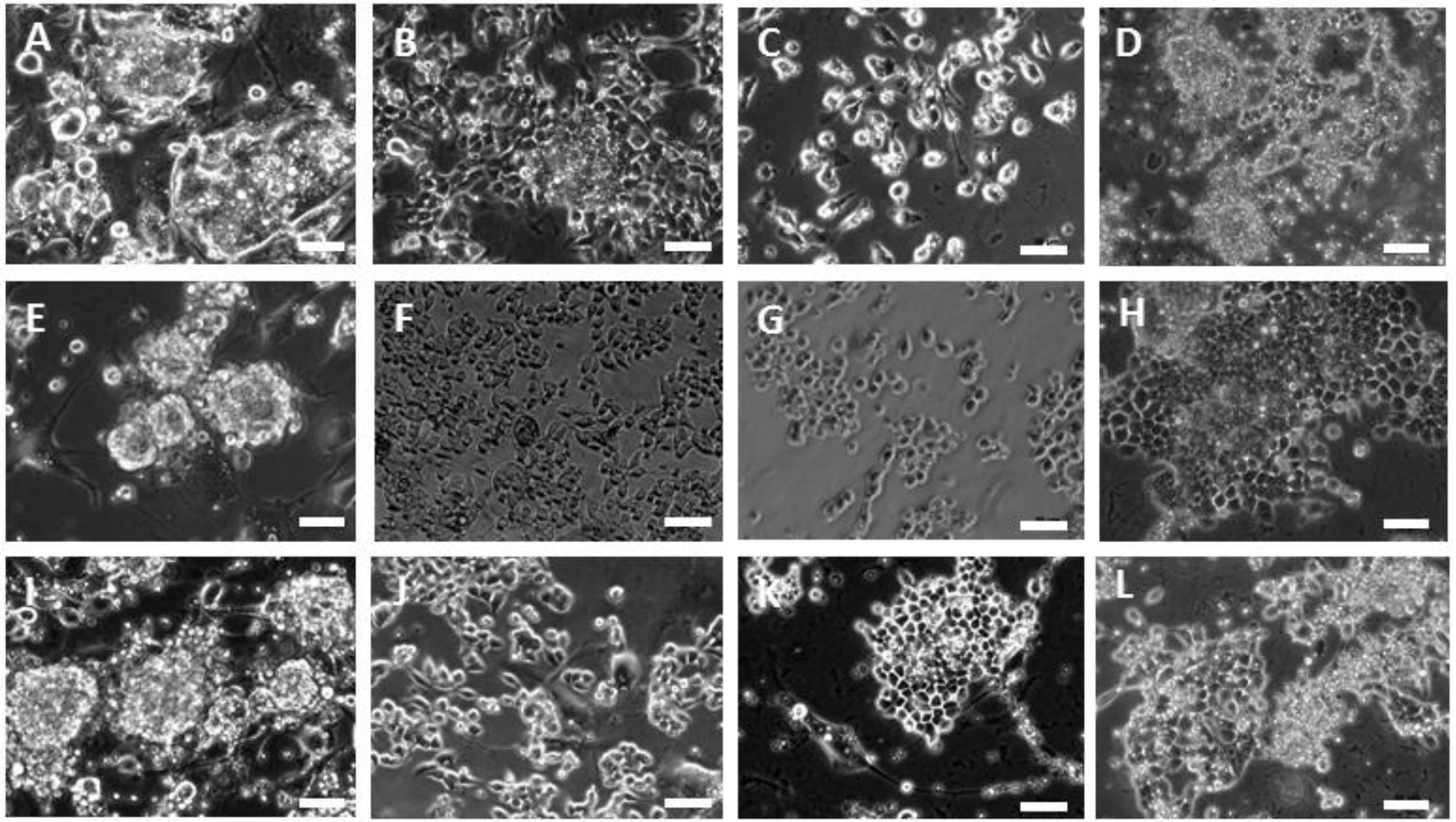

Figure 7.15 Morphology of iPSC to hepatocyte differentiation
Time points from left to right – Colonies on SNL feeder cells prior to differentiation, 24 hours after dissociation and plating on Matrigel, Day 3 of differentiation, Day 10 – final time point. A-D Ad-MSC iPSC, E-H BM-MSC iPSC, I-L CEF iPSC. White bar represents 50µm.

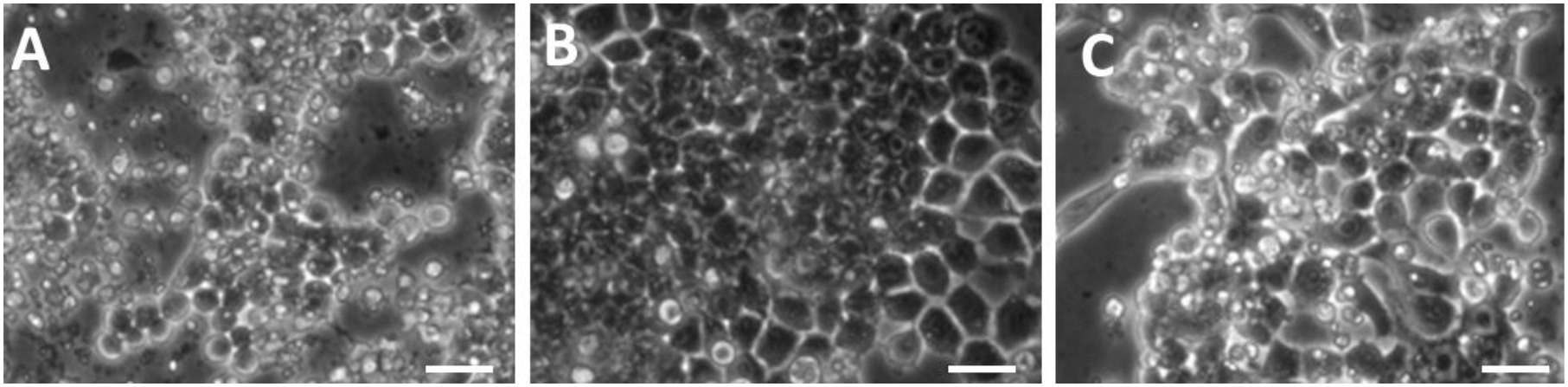

Figure 7.16 Higher magnification of iPSC to hepatocyte differentiated cell morphology at day 10
A- Ad-MSC iPSC, B –BM-MSC iPSC, C- CEF iPSC. White scale bar represents 50µm.

7.5.10.2 All cells exhibit increased hepatocyte gene expression after differentiation

An increase in cytochrome gene expression was noted in all three cell types after differentiation (Figure 7.17). Increases were also noted in albumin, keratin 18, glycogen synthase, LDL receptor, transthyretin and α1 anti-trypsin. αfoetal protein was increased in CEF and Ad-MSC4f cells. When analysed for significance, a broad range of genes were significantly increased by the differentiation protocol in all cell types (Table 7.5).

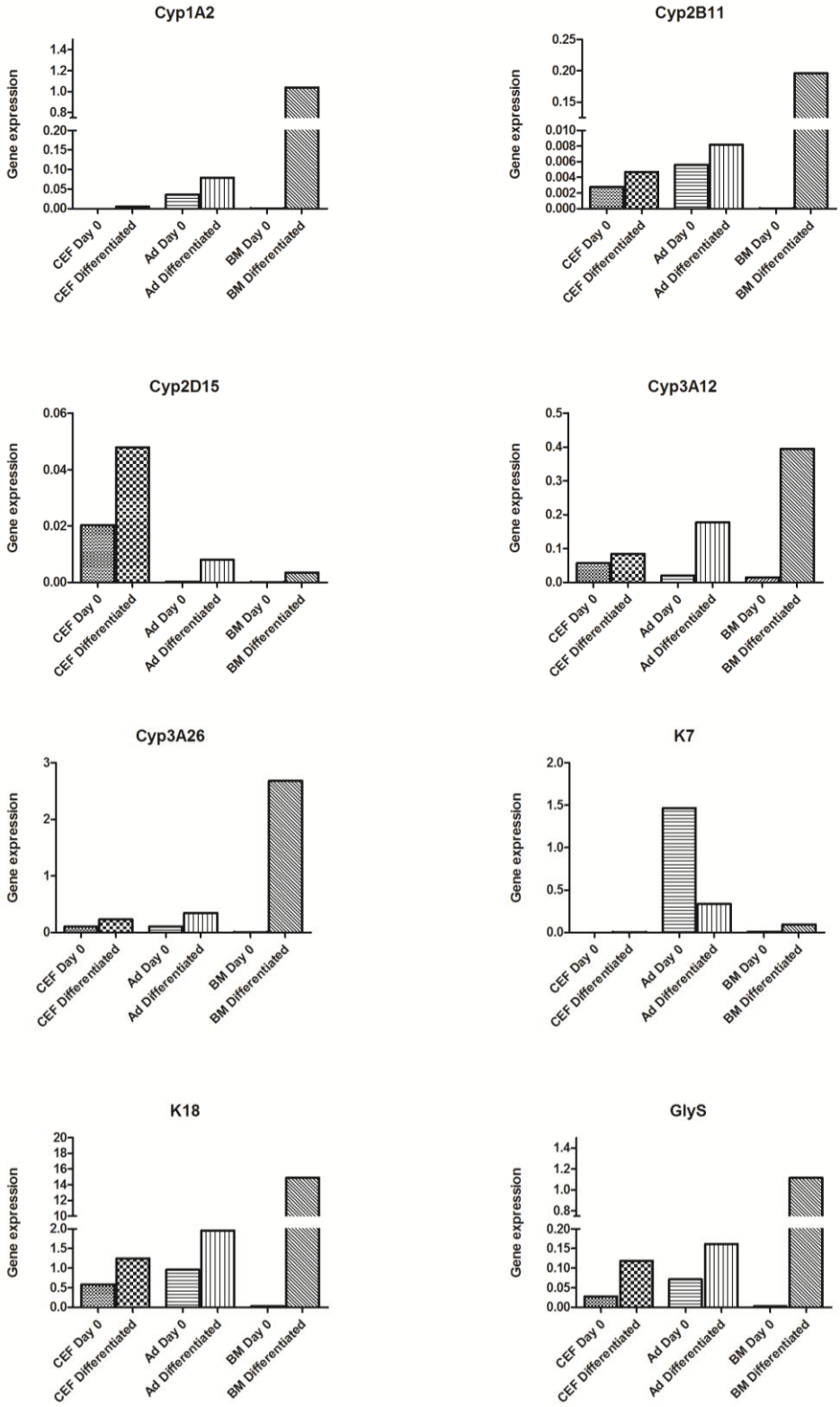

Figure 7.17 qPCR analysis of iPSC to hepatocyte differentiation
K7 – Keratin 7, K18 – Keratin 18, GlyS – Glycogen synthase.

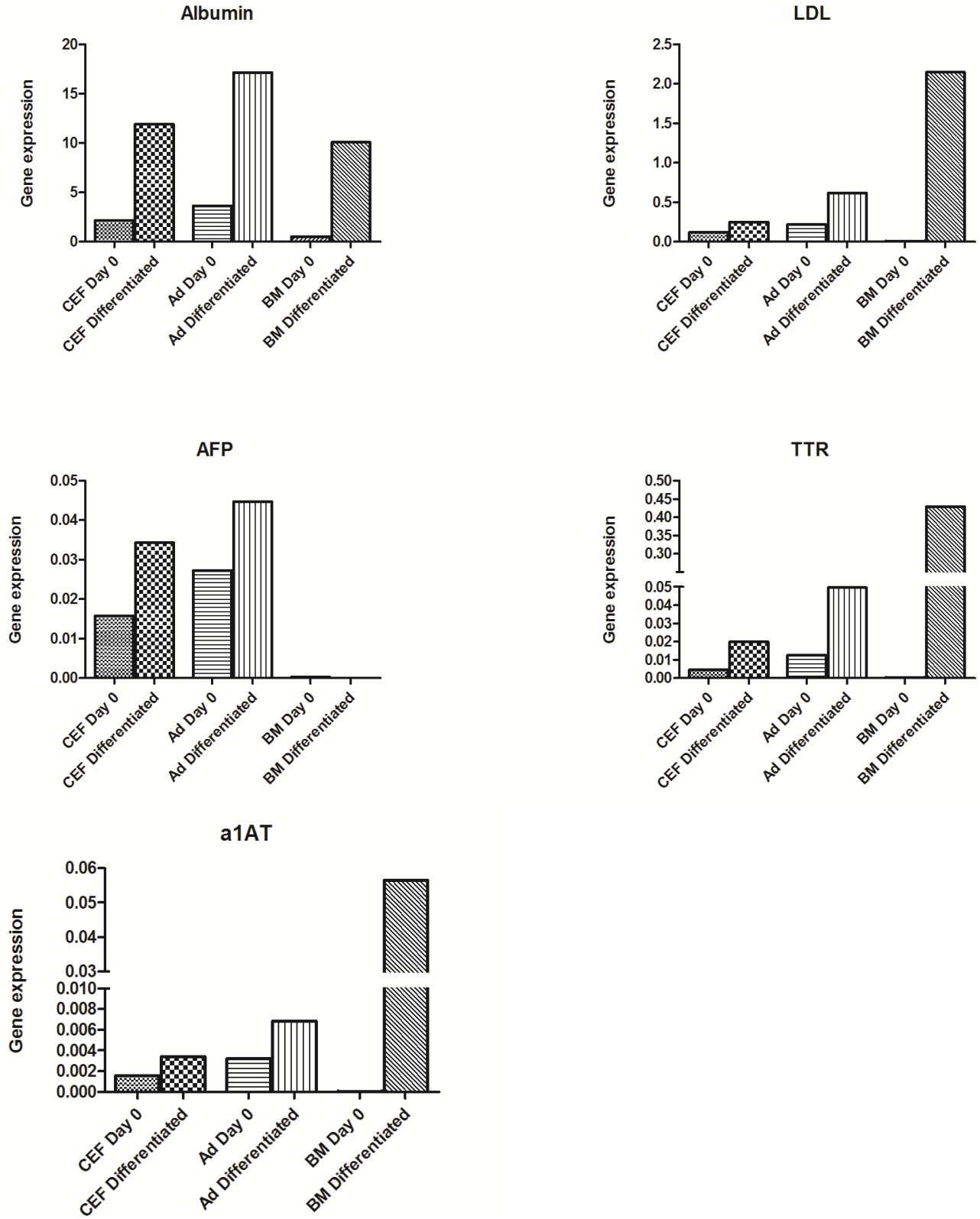

Figure 7.18 PCR analysis of iPSC to hepatocyte differentiation
LDL – Low density lipoprotein receptor, AFP – α Foetal protein, TTR – transthyretin, a1AT – α1 anti-trypsin

Cell Type	Gene	p value
Ad-MSC iPSC	albumin	0.019
	Keratin 18	0.028
	α1AT	0.019
	Glycogen synthase	0.019
	Low density lipoprotein receptor	0.019
BM-MSC iPSC		
	Cyp3A12	0.003
	Cyp3A26	0.05
	Cyp2D15	0.011
	Albumin	0.036
	Keratin 18	<0.0001
	TTR	0.036
	Glycogen synthase	<0.0001
	Low density lipoprotein receptor	0.036
CEF iPSC		
	Cyp1A2	0.024
	Cyp2B11	0.034
	Cyp2D15	0.034
	Albumin	0.013
	Keratin 18	<0.0001
	α1AT	0.013
	Glycogen synthase	0.037
	Low density lipoprotein receptor	0.037

Table 7.5 Significant gene increases after hepatocyte differentiation

7.5.10.3 Cells only demonstrate non-specific PAS staining

In the undifferentiated cells, both diastase and non-diastase cells demonstrated the same level of mild staining, indicating that this was non-specific (Figure 7.19). On staining the differentiated cells, cell loss during the staining made examination of cells difficult; however, no obvious difference in staining intensity was noted between diastase treated/untreated cells.

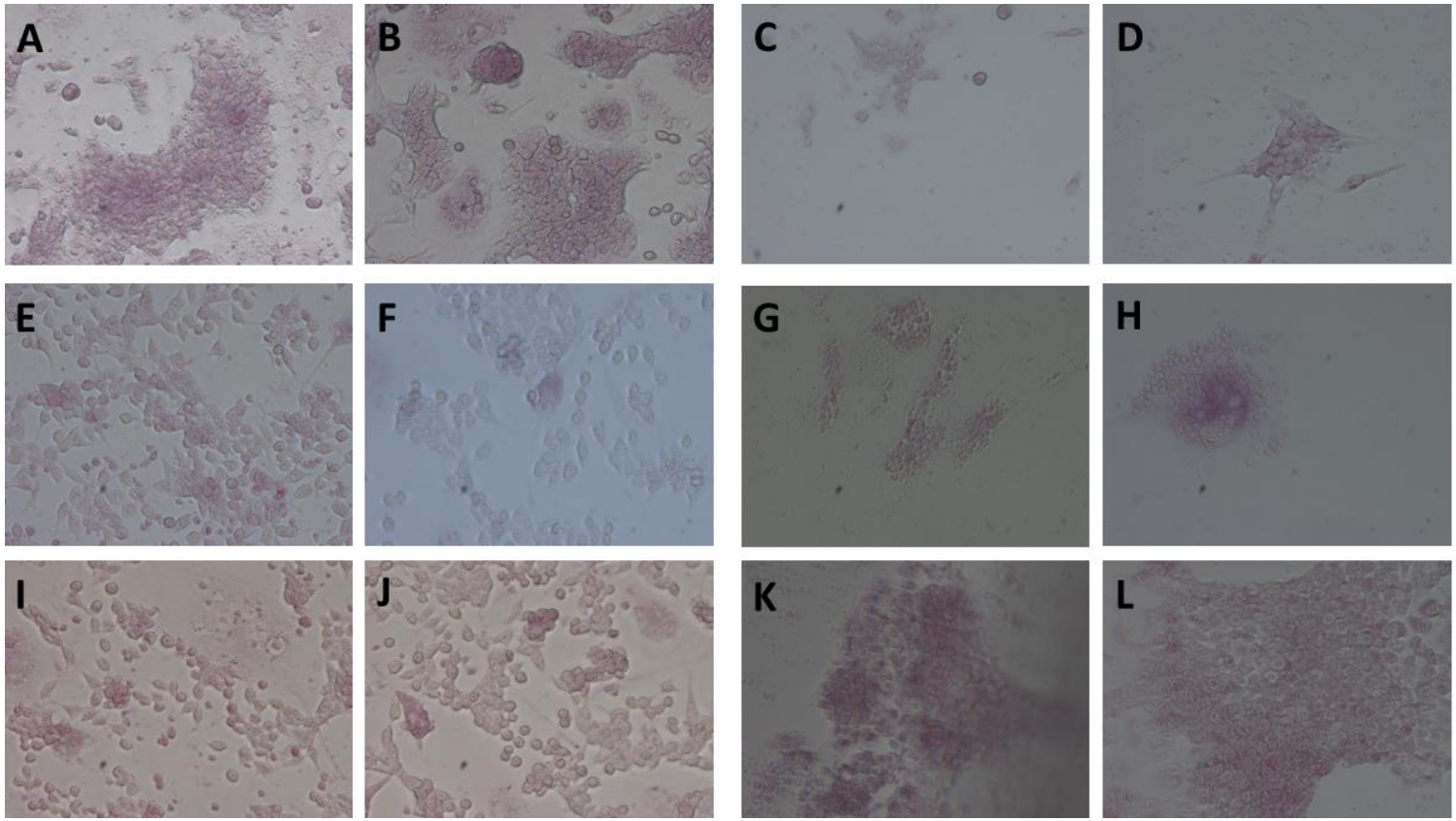

Figure 7.19 Periodic acid Schiff staining of iPSC before and after hepatocyte differentiation
Ad-MSC iPSC day 0, diastase pretreatment (A), no diastase (B), final time point diastase pretreatment (C), no diastase (D). BM-MSC iPSC day 0, diastase pretreatment (E), no diastase (F), final time point diastase pretreatment (G), no diastase (H). CEF iPSC day 0, diastase pretreatment (I), no diastase (J), final time point diastase pretreatment (K), no diastase (L). All images x200.

7.5.10.4 Cells do not demonstrate CYP activity

Cytochrome P450 activity was low at all-time points and no significant difference was noted after phenobarbital incubation (Figure 7.20). The counts detected are likely to be background. Negative counts are due to values being below blank measurements.

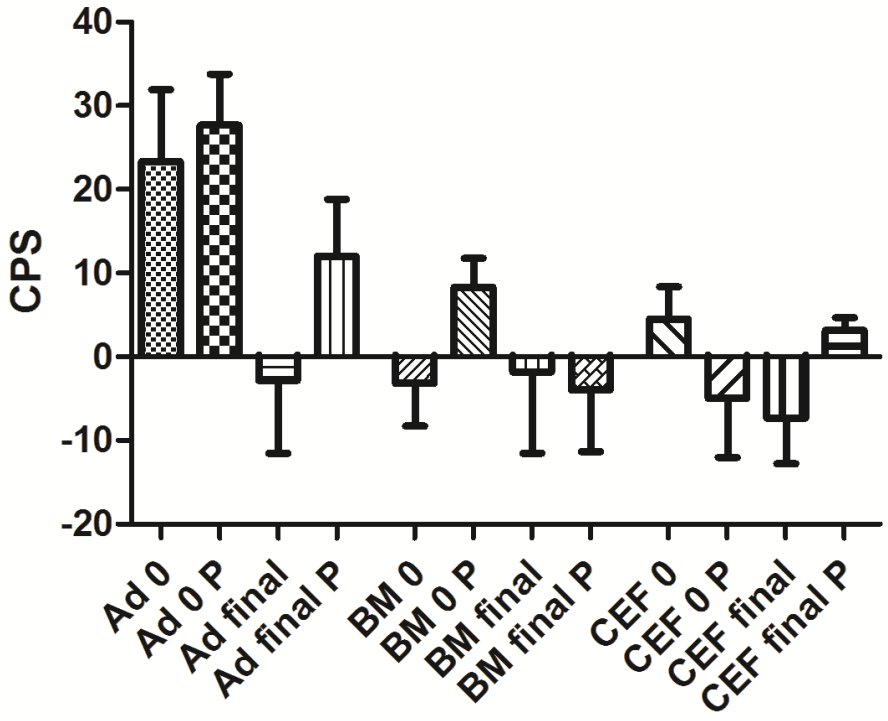

Figure 7.20 CYP activity of iPSC before and after hepatocyte differentiation. Basal activity was measured at time point 0 and day 10 (0 & final) as well as after induction with 250µM phenobarbital (P).

7.6 Discussion

7.6.1 The polycistronic vector was successfully transfected into CPEK cells

The plasmid was successfully expanded in competent *E.coli* cells, plasmid-containing cells cryopreserved, and a significant quantity was purified for subsequent use. Using the PuvI restriction endonuclease the plasmid was successfully efficiently ligated.

Using the control GFP plasmid, electroporation of the CPEK cells could be reliably performed with viable cells subsequently expressing GFP protein as demonstrated by fluorescence. The efficiency of transfection appeared lower using the 4 factor plasmid containing mOrange compared to the GFP control. In part, this may be due to the fact that plasmid quantification for transfection was based on weight rather than copy number. As the GFP control plasmid was approximately one quarter the size of the experimental plasmid (3468bp and 12939bp respectively), this would have meant that the transfection containing the experimental plasmid would contain a quarter of the amount of plasmid compared to the control. It has also been demonstrated plasmid size is inversely correlated with transfection efficiency (Yin et al., 2005). Finally, the experimental plasmid was linearised and control plasmid was not. Linearisation has been shown to reduce transfection efficiency, however it was chosen for the advantage of ensuring the integrity of the genes to be delivered (Stuchbury and Munch, 2010).

Successful plasmid transfection and protein expression is evident in the U17 cells. Fluorescent cells were present 24 hours after transfection, consistent with mOrange expression and these colonies were resistant to G418 addition. PCR analysis at day 20 confirmed the presence of plasmid DNA in the U17 cells. Considering the cells which underwent W1 transfection, an equal number were seen to be fluorescent 24 hours after transfection however this was not sustained. It is possible that cells successfully transfected using W1 were either compromised by a combination of the program and plasmid insertion, out-competed by untransfected cells or transient transfection lost at an early stage. PCR analysis at day 20 failed to detect the plasmid in remaining W1 cells.

7.6.2 The transfected cells did show signs of pluripotency

Consistent with the above findings, the morphology of colonies produced after U17 transfection is similar to that described for mouse iPSC, namely 3-dimensional domed colonies (Robinton and Daley, 2012). These colonies also demonstrated strong alkaline phosphatase staining of similar intensity to the positive control of mouse embryonic stem cells. Conversely, untransfected CPEK and remaining W1 cells showed no alkaline phosphatase staining.

After colony picking from U17 and expansion, the remaining colonies changed morphology, becoming flattened, more consistent with human iPSC (Robinton and Daley, 2012). Alkaline phosphatase staining was much weaker with the majority of cells appearing negative. End point PCR also failed to detect the presence of plasmid DNA in the expanded picked colonies. Real time PCR demonstrated no upregulation of Sox-2 gene expression, either exogenous or endogenous, compared to untransfected CPEKs, confirming the lack of expressed expression factors or conversion to a pluripotent state. Finally, no up regulation of Nanog, a key expression factor which would produce fully re-programmed cells, was detected in the remaining clones (Silva et al., 2009).

Therefore from the data, although a successful transfection was documented, the plasmid appeared to have been lost between expansion of the initial transfection and expansion of selected colonies. Transformation of cells to a pluripotent state by reprogramming is estimated to take between 10-14 days and partial reprogramming may occur (Rodolfa, 2012). It is of note that strong alkaline phosphatase staining, a marker of pluripotency, was achieved in the initial cultures (Hayat, 2012).

Possible explanations for this loss are:

- Plasmid did not integrate into genomic DNA

Rather than a stable transfection being achieved, a transient transfection was present where transcription occurred temporarily until the plasmid was lost/degraded. Although PCR of genomic DNA demonstrated the presence of the plasmid, DNA extraction would also have isolated plasmid DNA therefore this did not confirm a stable transfection. During colony picking it is possible that only transiently transfected cells were picked. Transient transfection may have been enough to initiate the process of pluripotency, as demonstrated by the change in morphology and alkaline phosphatase activity. As the plasmid was lost this may cause the cells to revert to a differentiated state as evinced by the subsequent change in morphology and loss of alkaline phosphatase staining.

- Integration was achieved then silenced/lost

It is possible that the exogenous genes were silenced by methylation or insertion into inactive heterochromatin (Adamson et al., 2011). This is less likely as a positive result would still be expected using genomic DNA PCR analysis.

- Selection pressure was insufficient to kill untransfected cells

The kill curve was performed on untransfected CPEKs grown on tissue culture plastic whilst selection was on CPEK's on SNL feeder cells which also contain the neomycin resistant gene. It is possible that this changed the susceptibility of the cells to G418, making CPEKs more resistant. An additional possibility is that the presence of the plasmid in transfected cells might have had an inhibitor effect on them compared to untransfected cells. As a result, non-transfected cells may have been picked.

7.6.3 Options for improving the outcome on subsequent experiments

- Increasing plasmid copy number at transfection
- Performing a G418 kill curve of CPEKs on SNL feeder cells
- Using G418 selection for a longer time period and/or earlier after transfection
- For monitoring, other markers of early pluripotency could be assessed such as SEA-1, could be assessed during expansion (Stadtfeld et al., 2008a).

7.6.4 Canine iPSCs can be differentiated towards hepatocyte-like cells

During differentiation, the morphology of all three cell lines changed towards a monolayer with defined cell-cell boundaries. Of the three lines, the BM-MSC iPSC exhibited the greatest transition to hepatocyte morphology with polygonal rather than rounded cells. The cytoplasm to nucleus ratio was much less than expected in mature primary hepatocytes. This change to morphology consistent with hepatocytes was mirrored in gene expression. At present no proof of function of these cells was found from glycogen storage or CYP activity. The lack of glycogen staining was difficult to assess due to cell loss during culture and subsequent staining, however no convincing evidence of glycogen storage was detected. This was despite significant upregulation of glycogen synthase gene expression after differentiation in all cell lines. Similarly, no cytochrome functional activity was detected, although a significant increase in Cyp3A12 and 3A26 (the specific enzymes required for this luciferase assay) was only noted in the Ad-MSC iPSC. Cell loss and resultant low cell density made albumin and urea measurement in the supernatant impossible.

The iPSC used were still expressing the transfected pluripotency genes *Oct4, Sox2, Klf4* and *C-Myc* and would thus be class II iPSC (Ruchi Sharma, Personal Communication 2014). As pluripotency genes were delivered by a lentivirus, the exogenous genes which integrate are less likely to be naturally silenced than by

retroviral delivery (Stadtfeld and Hochedlinger, 2010). The continued expression of these pluripotency genes may pose a block to differentiation. Despite this, convincing phenotypic change towards hepatocytes was achieved in all three cell lines.

7.6.5 Strategies for improving differentiation capacity

Although it can be stated a hepatocyte-like phenotype was achieved, a key goal was to produce functional hepatocyte-like cells, specifically with cytochrome P450 activity. Using this protocol, although *CYP* gene expression increased, no cytochrome activity was detected. This experiment was a promising start and there are many avenues that can be explored to improve phenotype and function.

7.6.5.1 Removal of transgene transcription factors

As continued expression of transgenes can reduce the differentiation capacity of the iPSC, removal of the transgenes using Cre-recombinase would likely enhance the differentiation capacity.

7.6.5.2 Alternative protocols

The protocol chosen for hepatocyte-directed differentiation is described as a "rapid protocol" and used human induced pluripotent stem cells (Chen et al., 2012b). The resultant cells were demonstrated to be functional in vitro by positive PAS staining, LDL uptake, cytochrome activity and urea secretion. There are a multitude of protocols described for generation of hepatocyte-like cells, with the majority describing a longer duration than the Chen study e.g. Roelandt et al. (2013) 25 days, Duan et al. (2010) 19-31 days, Roelandt et al. (2013) 28 days. Therefore utilizing a longer protocol may allow development of a more mature hepatic phenotype including CYP activity and glycogen storage.

7.6.5.3 Culture substrates

These include 3D culture system with collagen matrix and alginate scaffolds which significantly improved function and longevity compared to 2D culture (Gieseck Iii et al., 2014; Ramasamy et al., 2013). Also synthetic polymers have been developed which improve hepatic phenotype of differentiated pluripotent stem cells (Hay et al., 2011).

7.6.5.4 Co-culture systems

Javed et al. (2014) recently described co-culture of iPSC embroid bodies co-cultured with hepatic stellate cells whilst Nagamoto et al. (2012) utilized Swiss 3T cells (a fibroblast cell line). It is thought that these cells secrete additional growth factors which enhance hepatic maturation.

More complex 3D co-culture systems combining iPSC-derived hepatocyte-like cells, mesenchymal stem cells and endothelial cells have been successful in forming an "organ bud" , demonstrating hepatic functions, which then vascularized in immunodeficient mice (Takebe et al., 2013; Takebe et al., 2014).

At a more basic level, the iPSC lines and especially BM-MSC and CEF-derived lines were very poorly adherent in culture and as a result, many cells were lost during differentiation, limiting especially the tests of function. Methods of maintaining cell numbers such as trapping cells in a Matrigel overlay could be investigated. A high confluence has been reported to improve differentiation and therefore simply maintaining cell numbers may improve differentiation (Cai et al., 2012).

The Ad-MSC iPSC and BM-MSC iPSC were originally derived from mesenchymal stem cells which failed to transdifferentiate to hepatocyte-like cells from their mesenchymal state. This demonstrates that re-programming with *Oct4, Sox2, Klf4* and *C-Myc* increased the differentiation capacity of these cells.

7.7 Summary

- A polycistronic vector containing the 4 Yamanaka factors could be successfully transfected into CPEK.
- These cells demonstrated early markers of pluripotency namely consistent morphology and alkaline phosphatase activity.
- During single colony expansion alkaline phosphatase activity was lost.
- Three lines of canine iPSC were successfully differentiated towards a hepatocyte-like phenotype based on morphology and gene expression.
- No hepatocyte function has been demonstrated at present.
- This is the first demonstration of production of canine hepatocyte-like cells from iPSC sources.

Chapter 8: Conclusions and future perspectives

8.1 Introduction

The aim of this thesis was to produce an in vitro source of functional hepatocytes from stem cell sources. The fact that primary hepatocyte cultures do not expand in vitro and lose function rapidly, combined with poor recovery after cryopreservation, means that a constant supply of hepatic tissue from research animals is required for this resource. Differentiation of stem cells to hepatocytes would provide potentially an inexhaustible supply of functional hepatocytes. This resource would have a major impact, allowing the replacement or reduction of animals used in research, a key objective in the science community (http://www.nc3rs.org.uk/).

8.1.1 Primary canine hepatocyte cultures

To achieve this aim, what would constitute a canine hepatocyte in vitro had to be defined and a panel of tests developed. The question as to what would be adequate demonstration of hepatocyte-like cell has been discussed in the literature (Hengstler et al., 2005; Sancho-Bru et al., 2009; Zhang et al., 2013). No single test is sufficient and both gene expression and functional assays are recommended. In particular, and crucially for drug metabolism studies, demonstration of cytochrome P450 activity is important. To validate potential tests, in vitro canine primary hepatocyte cultures were produced using hepatic tissue from recently euthanased dogs. With these, a panel of primers to assess gene expression were developed along with tests of functionality; albumin secretion, glycogen storage and cytochrome P450 activity.

To further characterise the differentiation pathway of stem cells to hepatocyte-like cells, the ability to assess gene expression at the definitive endoderm stage would be useful, for example Sox17 (Sancho-Bru et al., 2009). One hurdle was the lack of canine cDNA from definitive endoderm and hepatic progenitor cells with which to validate primer efficiency and specificity. Adult hepatic tissue was used; however, only αfoetal protein and keratin 7 expression was present in sufficient quantity to allow primer validation. Material from foetal endoderm and hepatic tissue would

allow primer optimisation so that this crucial stage could be assessed during differentiation.

One test which is widely described in stem cell to hepatocyte research was found to be unreliable, at least in canine primary hepatocyte cultures. The in vitro indocyanine green (ICG) uptake and subsequent excretion test, which appears to have arisen in the field of stem cell to hepatocyte research rather than from primary hepatocyte cultures, was assessed. The majority of canine hepatocytes failed to demonstrate ICG uptake and those that did were found to be dead. These cells also subsequently appeared to lose staining intensity presumably by diffusion. Therefore this test was not thought to be specific for canine hepatocyte function and not included in the final panel of tests. It is unknown if this represents a species-specific idiosyncrasy or is a fundamental problem with this in vitro test. Previous papers which show images of ICG uptake and subsequent excretion range from convincing demonstrations with primary hepatocytes as a positive control (Takayama et al., 2012), to images which may be ICG staining of dead cells and debris (Zamule et al., 2011). The fact that ICG has been demonstrated to be cytotoxic in its own right further complicates this finding (Balaiya et al., 2011; Kawahara et al., 2007). Evaluation of ICG uptake in primary hepatocyte cultures of other species, especially human and mouse, would be useful to assess if ICG uptake is truly a valid test in other species.

Another test which is commonly employed in differentiation of stem cell to hepatocyte-like cells is low density lipoprotein uptake. As stated in chapter 3, LDL and acetylated LDL appear to be used interchangeably despite these compounds being endocytosed via different receptors. Unequivocally canine primary hepatocytes took up native LDL rather than acetylated LDL. This appeared to be a useful functional test of hepatocyte phenotype until undifferentiated adipose and bone marrow mesenchymal stem cells were also demonstrated to endocytose LDL. The

presence of the LDL receptor on primary hepatocytes as well as Ad-MSC and BM-MSC was confirmed by gene expression and also immunocytochemistry. Commercial BM-MSC from the mouse and human were purchased and also demonstrated to endocytose LDL and express the LDL receptor. Previous researchers have shown LDL receptor expression on human BM-MSC as well as a body of evidence of LDL receptor expression on fibroblasts. Therefore LDL uptake is not specific for hepatocyte function and invalid for mesenchymal to hepatocyte transdifferentiation (Drevon et al., 1981; Gross and Webb, 1986; Haniffa et al., 2009; Liesveld et al., 1989; Quaschning et al., 1997; Sasaki and Cottam, 1982).

At present only one method of cytochrome P450 activity has been validated namely the Promega Pro-Glo PFBE-Luciferase assay. This is catalysed by human and murine Cyp3A4. The isoenzymes in the dog are Cyp3A12 and 3A26. It is anticipated that the assay would measure enzymatic activity of these specific isoenzymes however this in unknown as differences between species in substrate specificity and affinity are recognised (Martinez et al., 2013). Additionally, relative gene expression of Cyp3A12 and Cyp3A24 is much lower in the canine liver than Cyp3A4 is in the human liver (Martinez et al., 2013). Therefore further tests to expand the range of Cyp activity would be useful. This could include measurement of drug metabolites by high performance liquid chromatography, or investigating other compounds which produce fluorescence after Cyp metabolism e.g. production of resorufin from ethoxy-, methoxy-, pentoxy- and benzyloxyresorufin which can then be measured using a standard plate reader (Sakai et al., 2010; Walsky and Obach, 2004).

Using the validated tests, the rapid decline in primary hepatocyte gene expression and function in vitro was noted. Culture of hepatocytes with Matrigel overlay improved total cell number viability but not gene expression or function. This rapid decline in function is well documented in other species, such that tests of hepatocyte function such as drug metabolism are recommended only in the initial 72 hours.

One area of further study would be optimising culture conditions to maintain primary hepatocyte cultures for longer. Despite primary hepatocyte cultures having been described for over 40 years, optimisation of culture systems has received little attention until recently. This is likely to be a combination of increased emphasis on reducing the number of animals used in research and also the development of bioartifical liver devices (BAL) which utilise primary hepatocytes in large numbers to provide bridging support for human patients with acute liver disease and awaiting transplant (Struecker et al., 2013). Improving the lifespan of the primary hepatocytes in this situation vastly reduces the cost of these devices (Shulman and Nahmias, 2013). It would be anticipated that optimised conditions for canine primary hepatocytes would also be likely to improve function of stem cell derived hepatocyte-like cells. Strategies to optimise primary hepatocyte culture can be broadly divided into three categories; media formulation, substrate/matric and co-cultures.

8.1.2 Media formulation

Different culture media has been demonstrated to have a significant impact on primary hepatocyte function (Nelson et al., 2013). This would be a useful initial step utilising hepatocyte cultures and tests developed during the study.

8.1.3 Substrate/matrix

8.1.3.1 Two- dimensional cultures

Although collagen type I is most commonly employed in primary hepatocyte cultures, other substrates have been recommended. Matrigel overlay only improved viability and not function in this study, however it is reported to enhance gene expression in human hepatocytes (Page et al., 2007). Equally, collagen sandwich overlay has been shown to improve function in rat hepatocytes (Dunn et al., 1992; Tuschl et al., 2009). Conversely, Nelson et al. (2013) demonstrated that matrix-free

culture of porcine hepatocytes maintained good morphology and function, therefore optimum conditions cannot necessarily be predicted between species. Therefore assessing different matrix substrates would help define optimum conditions for canine hepatocytes.

8.1.3.2 Three dimensional cultures

The above culture conditions would continue to utilise 2D culture techniques. As discussed in Chapter 3, these conditions are inherently different from in vivo hepatocyte conditions where cell to cell contacts are three dimensional and a heterogeneous cell population is in intimate contact with the hepatocytes. Hepatocytes depend on cell attachment to maintain function. Various techniques have been described based on artificial and natural biological matrixes (Godoy et al., 2013). There are three main 3D culture techniques; hydrogels, synthetic scaffolds and hepatospheres. These all have inherent advantages and disadvantages but are an improvement on 2D culture systems. Commercially available polystyrene scaffold "Alvetex ™" (Reinnervate, Co Durham) supports 3D culture of primary hepatocytes however, polymers could be screened to assess if canine hepatocytes retain function on a specific substrate (Hay et al., 2011).

8.1.3.3 Co-culture systems

As the liver comprises a heterogeneous cell network, co-culture systems have been reported which used various cell types. This could be easily investigated with expertise and ability to culture the second cell type available within the research group. Co-culture with mesenchymal stem cells has been demonstrated to improve hepatocyte function and this would utilise the cell isolated in Chapter 5 (Fitzpatrick et al., 2013; Yang et al., 2013). Endothelial cell co-culture prolongs rat hepatocyte function (Kang et al., 2013; Kim et al., 2012). Canine endothelial cells are routinely isolated from vascular endothelia, readily cryopreserved and are available for co-culture.

Co-cultures and 3D systems can be combined into more complex systems such as has been described by Takebe et al. (2013). In this study, iPSC-derived hepatocytes, endothelial cells and mesenchymal stem cells were co-cultured. This mix of cells, despite being plated in 2D, formed a 3D "liver bud" which then vascularised and became functional when implanted into NOD/SCID mice. Ultimately the aim would be to perform this using a canine stem-cell source of hepatocyte-like cells; however, optimising and demonstrating proof-of-concept using primary hepatocytes would be a useful exercise.

8.1.4 Hepatic progenitor cells

Cells morphologically consistent with hepatic stem cells and hepatoblasts were successfully isolated. Using MACS for CD133 produced colonies which expanded on initial plating. The intermittent availability of primary tissue along with difficulty in passaging cells meant that optimum conditions for expansion were not completely defined. Despite this, from the experiments, it appears that these cells require mechanical passaging, co-culture and laminin substrate. This is similar to what has been described for human HpSCs. One key hurdle is the low number of HPC in healthy tissue. Isolation of HPC in other species often starts with induction of liver injury to stimulate proliferation of HPC. This would only be possible using experimental animals. Reports that mature hepatocytes de-differentiate into hepatic progenitor cells are intriguing and could be the source of the HPC colonies detected in this case (Chen et al., 2012; Krause et al., 2013). Longer term culture of mature canine primary hepatocytes would assess if these could yield a population of HPC and therefore circumvent the problem of low density in hepatic tissue. This could potentially allow a larger quantity to optimize culture conditions.

8.1.5 Canine mesenchymal stem cells

Canine adipose-derived and bone marrow-derived mesenchymal stem cells could be repeatedly isolated and demonstration of their capacity to differentiate into mesenchymal tissues achieved. Although adult Ad-MSC and BM-MSCs from a variety of species have been successfully differentiated towards hepatocyte-like cells, this was not achieved. The one other report describing differentiation of canine MSCs to hepatocyte-like cells used both amniotic MSC and BM-MSC (Choi et al., 2013). Expression of pluripotency genes Oct4 and Sox2 was only detected in the amniotic cells and Nanog expression was much higher in the amniotic cells. Characterisation of the subsequent cells was limited and based on gene expression. Only α1-AT was expressed by the differentiated BM-MSC, which was also seen using the day 50 protocol in the current study. The amniotic MSC's expressed α1-AT, albumin and tyrosine aminotransferase. It is thought that amniotic mesenchymal stem cells have greater pluripotency which is backed up by the increased expression of pluripotency genes compared to the BM-MSC.

Methods of improving the pluripotent potential of the MSC were used, namely DNA demethylation using 5AZA and increasing histone acetylation using valproic acid. These demonstrated no advantage. The efficacy of these compounds in achieving the desired end result should be assessed. Methylation status before and after 5AZA treatment may be assessed via PCR (Hernandez et al., 2013). Similarly, the effect of valproic acid on histone deacetylase I expression could be evaluated using immunocytochemistry (Kurihara et al., 2014).

If canine amniotic mesenchymal stem cells became available, comparing these to the Ad-MSC and BM-MSCs would be useful to assess if they had increased capacity to differentiate towards hepatocytes.

8.1.6 Canine iPSC to hepatocyte-like cells

Although the iPSC used for differentiation towards hepatocyte-like cells were not fully reprogrammed i.e. the continued expression of transgenes, an increase in hepatocyte gene expression was seen in all three cell lines. Morphology of the cell lines was variable, with the BM-MSC iPSC achieving the morphology of small

hepatocytes. The large amount of cell loss due to poor adherence prevented functional testing apart from cytochrome P450 activity therefore subsequent experiments will assess methods of reducing cell loss. Alternative differentiation protocols, perhaps involving a longer time scale would also be assessed as these may result in an improved hepatocyte phenotype. When fully reprogrammed canine iPSC become available it is likely that these will have improved differentiation capacity due to silencing of the pluripotent transgenes.

Ultimately, if canine functional hepatocyte-like cells are derived from stem cells sources, assessment of the ability of these cells to produce canine albumin in NOD/SCID mice or rescue animal models of liver dysfunction would be the next step in demonstrating a hepatocyte-like phenotype.

8.2 Summary

The work in this thesis has generated a primary hepatocyte culture system and methods of assessing hepatocyte phenotype in vitro that can be used to optimise the function and lifespan of canine primary hepatocytes in vitro. In addition, the isolation and characterisation of canine mesenchymal stem cells opens up the option of co-culture systems. Results of this would be a useful basis for maintaining the hepatocyte phenotype in hepatocyte-like cells derived from stem cell sources. From the stem cell sources investigated the class I canine iPSC displayed gene expression compatible with differentiation towards hepatocytes. Additional research to improve the hepatocyte phenotype of these cells and assess functionality of the cells would be useful.

Appendix 1 Digestion/Perfusion buffers

Chelation Buffer

490ml Earle's Balanced Salt Solution without Calcium or Magnesium (Invitrogen, UK)

10ml 25mM EGTA, pH 7.4 (Sigma-Aldrich, UK)

Collagenase Buffer

100ml Earle's Balanced Salt Solution without Calcium or Magnesium (Invitrogen, UK)

200µL 1M Calcium chloride

50mg Collagenase Type II (Sigma-Aldrich)

Appendix 2: Hepatocyte isolations

Dog Id	Breed	Sex	Age (months)	Digestion Protocol/ culture substrate	Viable cells	Viability %	Culture Comments
Dog218211	SBT X	ME	48	1.1/plastic	5.2 x 10^6	45	Poor attachment
D318811	SBTX	ME	36	1.1/0.5% Gelatin	2.3 x 10^6	30	Few viable
AR25211	Dalmatian	MN	48	1.3/ Plastic	1.3 x 10^3	10	No cells
DE22711	Labrador	FN	62	1.5/	----	0	------
DJ41011	SBT	ME	36	1.6/0.05% Collagen	2.7 x 10^6	54	Few cells. No expansion and died
DL251111	Boxer X	MN	62	1.6/0.05% Collagen	0.6 x 10^6	13	No cells
DM251111	Collie X	MN	50	16/0.05% Collagen	2 x 10^4	14	Infection
D13112	SBT	ME	48	1.7/0.05% collagen	1 x 10^7	60	60-70% confluence
DR 18112	Rottweiler X	ME	36	1.8/0.05% collagen	7.5 x 10^7	83	90% confluent
DS18112	Mastiff	ME	24	1.8/0.05% collagen	2.1 x 10^7	91	90% confluent
DT8212	Lab X	ME	36	1.8/0.05% collagen	6.3 x 10^7	70	Confluent
DU23212	Cairn	ME	36	1.8/0.05%	4.3 x	65	Confluent

	Terrier			collagen	10^7		
D8812	Poodle X	ME	36	1.8/0.05% collagen	2.3 x 10^6	70	Confluent
D28812	SBTX	ME	36	1.8/0.05% collagen	1.2 x 10^6	92	Confluent
D17812	Labrador	MN	156	1.8/0.05% collagen	4.4 x 10^8	86	Confluent
D113912	SBT	FN	48	1.8/0.05% collagen	9.2 x 10^7	76	Confluent
D213912	SBT	ME	62	1.8/0.05% collagen	6.8 x 10^5	72	Confluent
D21112	SBT	Me	72	1.8/0.05% collagen	2.4 x10^8	78	Confluent
D10513	Labrador	ME	84	1.8/0.05mg/ml collagen	3 x 10^8	81	Confluent
D17513	Labrador	ME	120	1.8/0.05mg/ml collagen	3.2 x10^8	83%	Confluent
D19713	SBT	FE	72	1.8/0.05mg/ml collagen	5 x10^7	78%	Confluent
D20913	Mastiff	ME	48	1.8/0.05mg/ml collagen	3 x10^7	85%	Confluent
D41013	JRT	MN	50	1.8/0.05mg/ml collagen	5.4 x10^7	77%	Confluent

Appendix 3: Kubota's medium

500mls RPMI (Invitrogen,UK)
0.5g Bovine serum albumin (Sigma-Aldrich, UK)
270mg Niacinamide (Sigma-Aldrich, UK)
2.5mg Insulin (Gibco, UK)
5mg Transferrin (Sigma-Aldrich, UK)
L-Glutamine (Invitrogen,UK)
100 U/mL penicillin G (Invitrogen, UK)
100 µg/mL streptomycin (Invitrogen, UK)
18µg Hydrocortisone (Invitrogen,UK)
0.1mM β Mercaptoethanol (Gibco)
0.001µM Sodium selenite (Sigma-Aldrich, UK)
0.001µM Zinc Sulphate hepahydrate (Sigma-Aldrich, UK)
5mg HDL (Sigma-Aldrich, UK)

Fatty Acid Mix- 100mM of each (all Sigma-Aldrich, UK)
Palmatic acid
Palmitoleic acid
Stearic acid
Oleic acid
Linoleic acid salt
Linoleic acid (free)
Add 38µl to 500ml media

(Kubota and Reid, 2000)

Appendix 4: Hepatic progenitor cell isolations

Dog Id	Breed	Sex	Age (mths)	Protocol/ culture substrate	Viable cells %	Culture Comments
D20411	SBT X	ME	36	Percoll/ collagen	unable to count Much debris	very few adherent cells, mixed population
D22711	Labrador	FN	62	Percoll/collagen	unable to count Much debris	very few adherent cells, mixed morphology
D19811a	Rottweiler	MN	62	Percoll/collagen	unable to count Much debris	Few cells. No expansion and died
D19811b	Akita	MN	36	Percoll/collagen	unable to count Much debris	Sparse cells, less debris, no expansion
DM251111	Collie X	MN	50	Percoll/collagen	Less debris	Sparse cells, no expansion
D13112	SBT	ME	48	Percoll/collagen	Little debris	Sparse cells, small clusters, no expansion
D 18112a	Rottweiler X	ME	36	Ficoll/collagen	--	No viable cells
D18112b	Mastiff	ME	24	Ficoll/collagen	--	No viable cells
D8212	Lab X	ME	36	Ficoll/collagen	1.2 x10 ^{5}	Mixed cell population, fibroblastic and macrophage morphology

References

Abass, K., Lamsa, V., Reponen, P., Kublbeck, J., Honkakoski, P., Mattila, S., Pelkonen, O., Hakkola, J., 2012. Characterization of human cytochrome P450 induction by pesticides. Toxicology 294, 17-26.

Adamson, A.D., Jackson, D., Davis, J.R., 2011. Novel approaches to in vitro transgenesis. The Journal of endocrinology 208, 193-206.

Agarwal, S., Holton, K.L., Lanza, R., 2008. Efficient differentiation of functional hepatocytes from human embryonic stem cells. Stem cells 26, 1117-1127.

Ahboucha, S., 2011. Neurosteroids and hepatic encephalopathy: an update on possible pathophysiologic mechanisms. Curr Mol Pharmacol 4, 1-13.

Akiyama, H., Chaboissier, M.C., Martin, J.F., Schedl, A., de Crombrugghe, B., 2002. The transcription factor Sox9 has essential roles in successive steps of the chondrocyte differentiation pathway and is required for expression of Sox5 and Sox6. Genes & development 16, 2813-2828.

Al Battah, F., De Kock, J., Vanhaecke, T., Rogiers, V., 2011. Current status of human adipose-derived stem cells: differentiation into hepatocyte-like cells. TheScientificWorldJournal 11, 1568-1581.

Alliston, T., Choy, L., Ducy, P., Karsenty, G., Derynck, R., 2001. TGF-beta-induced repression of CBFA1 by Smad3 decreases cbfa1 and osteocalcin expression and inhibits osteoblast differentiation. The EMBO journal 20, 2254-2272.

Anokye-Danso, F., Trivedi, C.M., Juhr, D., Gupta, M., Cui, Z., Tian, Y., Zhang, Y., Yang, W., Gruber, P.J., Epstein, J.A., Morrisey, E.E., 2011. Highly efficient miRNA-mediated reprogramming of mouse and human somatic cells to pluripotency. Cell stem cell 8, 376-388.

Arends, B., Spee, B., Schotanus, B.A., Roskams, T., van den Ingh, T.S., Penning, L.C., Rothuizen, J., 2009a. In vitro differentiation of liver progenitor cells derived from healthy dog livers. Stem cells and development 18, 351-358.

Arends, B., Vankelecom, H., Vander Borght, S., Roskams, T., Penning, L.C., Rothuizen, J., Spee, B., 2009b. The dog liver contains a "side population" of cells with hepatic progenitor-like characteristics. Stem cells and development 18, 343-350.

Arias, I., Wolkoff, A., Boyer, J., Shafritz, D., Fausto, N., Alter, H., Cohen, D., 2011. The Liver: Biology and Pathobiology. Wiley.

Asari, S., Itakura, S., Ferreri, K., Liu, C.P., Kuroda, Y., Kandeel, F., Mullen, Y., 2009. Mesenchymal stem cells suppress B-cell terminal differentiation. Experimental hematology 37, 604-615.

Asgari, S., Moslem, M., Bagheri-Lankarani, K., Pournasr, B., Miryounesi, M., Baharvand, H., 2013. Differentiation and transplantation of human induced pluripotent stem cell-derived hepatocyte-like cells. Stem cell reviews 9, 493-504.

Aupet, S., Simone, G., Heyd, B., Bachellier, P., Vidal, I., Richert, L., Martin, H., 2013. Isolation of viable human hepatic progenitors from adult livers is possible even after 48 hours of cold ischemia. Tissue engineering. Part C, Methods 19, 497-506.

Babaev, V.R., Kosykh, V.A., Tsibulsky, V.P., Ivanov, V.O., Repin, V.S., Smirnov, V.N., 1989. Binding and uptake of native and modified low-density lipoproteins by human hepatocytes in primary culture. Hepatology 10, 56-60.

Baertschiger, R.M., Serre-Beinier, V., Morel, P., Bosco, D., Peyrou, M., Clement, S., Sgroi, A., Kaelin, A., Buhler, L.H., Gonelle-Gispert, C., 2009. Fibrogenic potential of human multipotent mesenchymal stromal cells in injured liver. PloS one 4, e6657.

Balaiya, S., Brar, V.S., Murthy, R.K., Chalam, K.V., 2011. Comparative in vitro safety analysis of dyes for chromovitrectomy: indocyanine green, brilliant blue green, bromophenol blue, and infracyanine green. Retina 31, 1128-1136.

Banas, A., Teratani, T., Yamamoto, Y., Tokuhara, M., Takeshita, F., Osaki, M., Kawamata, M., Kato, T., Okochi, H., Ochiya, T., 2008. IFATS collection: in vivo therapeutic potential of human adipose tissue mesenchymal stem cells after transplantation into mice with liver injury. Stem cells 26, 2705-2712.

Bar-Nur, O., Russ, H.A., Efrat, S., Benvenisty, N., 2011. Epigenetic memory and preferential lineage-specific differentiation in induced pluripotent stem cells derived from human pancreatic islet beta cells. Cell stem cell 9, 17-23.

Beerheide, W., von Mach, M.A., Ringel, M., Fleckenstein, C., Schumann, S., Renzing, N., Hildebrandt, A., Brenner, W., Jensen, O., Gebhard, S., Reifenberg, K., Bender, J., Oesch, F., Hengstler, J.G., 2002. Downregulation of beta2-microglobulin in human cord blood somatic stem cells after transplantation into livers of SCID-mice: an escape mechanism of stem cells? Biochemical and biophysical research communications 294, 1052-1063.

Beier, D., Hau, P., Proescholdt, M., Lohmeier, A., Wischhusen, J., Oefner, P.J., Aigner, L., Brawanski, A., Bogdahn, U., Beier, C.P., 2007. CD133(+) and CD133(-) glioblastoma-derived cancer stem cells show differential growth characteristics and molecular profiles. Cancer research 67, 4010-4015.

Beigel, J., Fella, K., Kramer, P.J., Kroeger, M., Hewitt, P., 2008. Genomics and proteomics analysis of cultured primary rat hepatocytes. Toxicology in vitro : an international journal published in association with BIBRA 22, 171-181.

Benedetti, E., Kirby, J.P., Asolati, M., Blanchard, J., Ward, M.G., Williams, R., Hewett, T.A., Fontaine, M., Pollak, R., 1997. Intrasplenic hepatocyte allotransplantation in dalmation dogs with and without cyclosporine immunosuppression. Transplantation 63, 1206-1209.

Bernardo, M.E., Zaffaroni, N., Novara, F., Cometa, A.M., Avanzini, M.A., Moretta, A., Montagna, D., Maccario, R., Villa, R., Daidone, M.G., Zuffardi, O., Locatelli, F., 2007. Human bone marrow derived mesenchymal stem cells do not undergo transformation after long-term in vitro culture and do not exhibit telomere maintenance mechanisms. Cancer research 67, 9142-9149.

Berridge, M.V., Tan, A.S., 1993. Characterization of the Cellular Reduction of 3-(4,5-dimethylthiazol-2-yl)-2,5-diphenyltetrazolium bromide (MTT): Subcellular Localization, Substrate Dependence, and Involvement of Mitochondrial Electron Transport in MTT Reduction. Archives of biochemistry and biophysics 303, 474-482.

Berry, M.N., Friend, D.S., 1969. High-yield preparation of isolated rat liver parenchymal cells: a biochemical and fine structural study. The Journal of cell biology 43, 506-520.

Bexfield, N.H., Watson, P.J., Heaney, J., Heeney, J.L., Tiley, L., 2014. Canine hepacivirus is not associated with chronic liver disease in dogs. J Viral Hepat 21, 223-228.

Bian, Z.Y., Fan, Q.M., Li, G., Xu, W.T., Tang, T.T., 2010. Human mesenchymal stem cells promote growth of osteosarcoma: involvement of interleukin-6 in the interaction between human mesenchymal stem cells and Saos-2. Cancer science 101, 2554-2560.

Bianco, P., Robey, P.G., Saggio, I., Riminucci, M., 2010. "Mesenchymal" stem cells in human bone marrow (skeletal stem cells): a critical discussion of their nature, identity, and significance in incurable skeletal disease. Human gene therapy 21, 1057-1066.

Bilzer, M., Roggel, F., Gerbes, A.L., 2006. Role of Kupffer cells in host defense and liver disease. Liver international : official journal of the International Association for the Study of the Liver 26, 1175-1186.

Black, L.L., Gaynor, J., Adams, C., Dhupa, S., Sams, A.E., Taylor, R., Harman, S., Gingerich, D.A., Harman, R., 2008. Effect of intraarticular injection of autologous adipose-derived mesenchymal stem and regenerative cells on clinical signs of chronic osteoarthritis of the elbow joint in dogs. Veterinary therapeutics : research in applied veterinary medicine 9, 192-200.

Black, L.L., Gaynor, J., Gahring, D., Adams, C., Aron, D., Harman, S., Gingerich, D.A., Harman, R., 2007. Effect of adipose-derived mesenchymal stem and regenerative cells on lameness in dogs with chronic osteoarthritis of the coxofemoral joints: a randomized, double-blinded, multicenter, controlled trial. Veterinary therapeutics : research in applied veterinary medicine 8, 272-284.

Blaisdell, J., Goldstein, J.A., Bai, S.A., 1998. Isolation of a new canine cytochrome P450 CDNA from the cytochrome P450 2C subfamily (CYP2C41) and evidence for

polymorphic differences in its expression. Drug metabolism and disposition: the biological fate of chemicals 26, 278-283.

Boomkens, S.Y., Penning, L.C., Egberink, H.F., van den Ingh, T.S., Rothuizen, J., 2004. Hepatitis with special reference to dogs. A review on the pathogenesis and infectious etiologies, including unpublished results of recent own studies. The Veterinary quarterly 26, 107-114.

Boomkens, S.Y., Slump, E., Egberink, H.F., Rothuizen, J., Penning, L.C., 2005. PCR screening for candidate etiological agents of canine hepatitis. Veterinary microbiology 108, 49-55.

Bourin, P., Bunnell, B.A., Casteilla, L., Dominici, M., Katz, A.J., March, K.L., Redl, H., Rubin, J.P., Yoshimura, K., Gimble, J.M., 2013. Stromal cells from the adipose tissue-derived stromal vascular fraction and culture expanded adipose tissue-derived stromal/stem cells: a joint statement of the International Federation for Adipose Therapeutics and Science (IFATS) and the International Society for Cellular Therapy (ISCT). Cytotherapy 15, 641-648.

Breton, A., Sharma, R., Diaz, A.C., Parham, A.G., Graham, A., Neil, C., Whitelaw, C.B., Milne, E., Donadeu, F.X., 2013. Derivation and characterization of induced pluripotent stem cells from equine fibroblasts. Stem cells and development 22, 611-621.

Bruckner, S., Tautenhahn, H.M., Winkler, S., Stock, P., Dollinger, M., Christ, B., 2013. A Fat Option for the pig: Hepatocytic Differentiated Mesenchymal Stem Cells for Translational Research. Experimental cell research.

Bucher, N.L., Oakman, N.J., 1969. Thymidine triphosphate content of regenerating rat liver. Biochimica et biophysica acta 186, 13-20.

Cai, J., DeLaForest, A., Fisher, J., Urick, A., Wagner, T., Twarosli, K., Cayo, M., HNagaoka, M., Duncan, S.A., 2012. Protocol for directed differentiation of human pluripotent stem cells toward a hepatocyte fate In: Stembook Harvard Stem Cell Institute, Cambridge, MA.

Campard, D., Lysy, P.A., Najimi, M., Sokal, E.M., 2008. Native umbilical cord matrix stem cells express hepatic markers and differentiate into hepatocyte-like cells. Gastroenterology 134, 833-848.

Cao, H., Yang, J., Yu, J., Pan, Q., Li, J., Zhou, P., Li, Y., Pan, X., Li, J., Wang, Y., Li, L., 2012. Therapeutic potential of transplanted placental mesenchymal stem cells in treating Chinese miniature pigs with acute liver failure. BMC medicine 10, 56.

Caplan, A.I., 2009. Why are MSCs therapeutic? New data: new insight. The Journal of pathology 217, 318-324.

Caplan, A.I., Bruder, S.P., 2001. Mesenchymal stem cells: building blocks for molecular medicine in the 21st century. Trends in molecular medicine 7, 259-264.

Carr, B.I., Hayashi, I., Branum, E.L., Moses, H.L., 1986. Inhibition of DNA synthesis in rat hepatocytes by platelet-derived type beta transforming growth factor. Cancer research 46, 2330-2334.

Case, J.B., Palmer, R., Valdes-Martinez, A., Egger, E.L., Haussler, K.K., 2013. Gastrocnemius tendon strain in a dog treated with autologous mesenchymal stem cells and a custom orthosis. Veterinary surgery : VS 42, 355-360.

Chan, C., Berthiaume, F., Nath, B.D., Tilles, A.W., Toner, M., Yarmush, M.L., 2004. Hepatic tissue engineering for adjunct and temporary liver support: critical technologies. Liver Transpl 10, 1331-1342.

Charles, J.A., Cullen, J.M., Van den Ingh, T.S., Van Winkle, T., Desmet, V.J., 2006. Morphological classification of neoplastic disorders of the canine and feline liver, In: WSAVA standards for clinical and histological diagnosis of canine and feline liver disease. WSAVA Saunders, Edinburgh, pp. 117-124.

Chen, Y., Pan, R.L., Zhang, X.L., Shao, J.Z., Xiang, L.X., Dong, X.J., Zhang, G.R., 2009. Induction of hepatic differentiation of mouse bone marrow stromal stem cells by the histone deacetylase inhibitor VPA. Journal of cellular and molecular medicine 13, 2582-2592.

Chen, Y., Wong, P.P., Sjeklocha, L., Steer, C.J., Sahin, M.B., 2012a. Mature hepatocytes exhibit unexpected plasticity by direct dedifferentiation into liver progenitor cells in culture. Hepatology 55, 563-574.

Chen, Y., Zhou, H., Sarver, A.L., Zeng, Y., Roy-Chowdhury, J., Steer, C.J., Sahin, M.B., 2010. Hepatic differentiation of liver-derived progenitor cells and their characterization by microRNA analysis. Liver Transpl 16, 1086-1097.

Chen, Y.F., Tseng, C.Y., Wang, H.W., Kuo, H.C., Yang, V.W., Lee, O.K., 2012b. Rapid generation of mature hepatocyte-like cells from human induced pluripotent stem cells by an efficient three-step protocol. Hepatology 55, 1193-1203.

Cheng, D., Guo, Y., Li, Z., Liu, Y., Gao, X., Gao, Y., Cheng, X., Hu, J., Wang, H., 2012. Porcine induced pluripotent stem cells require LIF and maintain their developmental potential in early stage of embryos. PloS one 7, e51778.

Cherrick, G.R., Stein, S.W., Leevy, C.M., Davidson, C.S., 1960. Indocyanine green: observations on its physical properties, plasma decay, and hepatic extraction. The Journal of clinical investigation 39, 592-600.

Choi, S.A., Choi, H.S., Kim, K.J., Lee, D.S., Lee, J.H., Park, J.Y., Kim, E.Y., Li, X., Oh, H.Y., Lee, D.S., Kim, M.K., 2013. Isolation of canine mesenchymal stem cells from amniotic fluid and differentiation into hepatocyte-like cells. In vitro cellular & developmental biology. Animal 49, 42-51.

Christman, J.K., 2002. 5-Azacytidine and 5-aza-2'-deoxycytidine as inhibitors of DNA methylation: mechanistic studies and their implications for cancer therapy. Oncogene 21, 5483-5495.

Chung, D.J., Wong, A., Hayashi, K., Yellowley, C.E., 2013. Effect of hypoxia on generation of neurospheres from adipose tissue-derived canine mesenchymal stromal cells. Vet J.

Conigliaro, A., Brenner, D.A., Kisseleva, T., 2010. Hepatic progenitors for liver disease: current position. Stem cells and cloning : advances and applications 3, 39-47.

Cook, D., Genever, P., 2013. Regulation of mesenchymal stem cell differentiation. Advances in experimental medicine and biology 786, 213-229.

Crisan, M., Corselli, M., Chen, C.W., Peault, B., 2011. Multilineage stem cells in the adult: a perivascular legacy? Organogenesis 7, 101-104.

Crisan, M., Yap, S., Casteilla, L., Chen, C.W., Corselli, M., Park, T.S., Andriolo, G., Sun, B., Zheng, B., Zhang, L., Norotte, C., Teng, P.N., Traas, J., Schugar, R., Deasy, B.M., Badylak, S., Buhring, H.J., Giacobino, J.P., Lazzari, L., Huard, J., Peault, B., 2008. A perivascular origin for mesenchymal stem cells in multiple human organs. Cell stem cell 3, 301-313.

Csaki, C., Matis, U., Mobasheri, A., Ye, H., Shakibaei, M., 2007. Chondrogenesis, osteogenesis and adipogenesis of canine mesenchymal stem cells: a biochemical, morphological and ultrastructural study. Histochemistry and cell biology 128, 507-520.

Cui, L., Shi, Y., Zhou, X., Wang, X., Wang, J., Lan, Y., Wang, M., Zheng, L., Li, H., Wu, Q., Zhang, J., Fan, D., Han, Y., 2013. A set of microRNAs mediate direct conversion of human umbilical cord lining-derived mesenchymal stem cells into hepatocytes. Cell death & disease 4, e918.

Cyranoski, D., 2013. Stem cells boom in vet clinics. Nature 496, 148-149.

Dalgetty, D.M., Medine, C.N., Iredale, J.P., Hay, D.C., 2009. Progress and future challenges in stem cell-derived liver technologies. American journal of physiology. Gastrointestinal and liver physiology 297, G241-248.

Darwiche, H., Petersen, B.E., 2010. Biology of the adult hepatic progenitor cell: "ghosts in the machine". Progress in molecular biology and translational science 97, 229-249.

Davis, C.D., Zech, L., Greger, J.L., 1993. Manganese metabolism in rats: an improved methodology for assessing gut endogenous losses. Proceedings of the Society for Experimental Biology and Medicine. Society for Experimental Biology and Medicine 202, 103-108.

De Silvestro, G., Vicarioto, M., Donadel, C., Menegazzo, M., Marson, P., Corsini, A., 2004. Mobilization of peripheral blood hematopoietic stem cells following liver resection surgery. Hepato-gastroenterology 51, 805-810.

De Ugarte, D.A., Morizono, K., Elbarbary, A., Alfonso, Z., Zuk, P.A., Zhu, M., Dragoo, J.L., Ashjian, P., Thomas, B., Benhaim, P., Chen, I., Fraser, J., Hedrick, M.H., 2003. Comparison of multi-lineage cells from human adipose tissue and bone marrow. Cells, tissues, organs 174, 101-109.

Dezawa, M., Kanno, H., Hoshino, M., Cho, H., Matsumoto, N., Itokazu, Y., Tajima, N., Yamada, H., Sawada, H., Ishikawa, H., Mimura, T., Kitada, M., Suzuki, Y., Ide, C., 2004. Specific induction of neuronal cells from bone marrow stromal cells and application for autologous transplantation. The Journal of clinical investigation 113, 1701-1710.

Dieppe, P.A., Ebrahim, S., Martin, R.M., Juni, P., 2004. Lessons from the withdrawal of rofecoxib. Bmj 329, 867-868.

Ditewig, A.C., Cugier, D.J., Liguori, M.J., Yang, Y., Blomme, E.A., 2013. Transcriptomic evaluation of canine suspension-shipped and pre-plated hepatocytes: comparison to liver. Toxicology mechanisms and methods 23, 479-490.

Dolle, L., Best, J., Mei, J., Al Battah, F., Reynaert, H., van Grunsven, L.A., Geerts, A., 2010. The quest for liver progenitor cells: a practical point of view. Journal of hepatology 52, 117-129.

Dominici, M., Le Blanc, K., Mueller, I., Slaper-Cortenbach, I., Marini, F., Krause, D., Deans, R., Keating, A., Prockop, D., Horwitz, E., 2006. Minimal criteria for defining multipotent mesenchymal stromal cells. The International Society for Cellular Therapy position statement. Cytotherapy 8, 315-317.

Donato, M.T., Jover, R., Gomez-Lechon, M.J., 2013. Hepatic Cell Lines for Drug Hepatotoxicity Testing: Limitations and Strategies to Upgrade their Metabolic Competence by Gene Engineering. Current drug metabolism 14, 946-968.

Dong, X., Pan, R., Zhang, H., Yang, C., Shao, J., Xiang, L., 2013. Modification of histone acetylation facilitates hepatic differentiation of human bone marrow mesenchymal stem cells. PloS one 8, e63405.

Drevon, C.A., Attie, A.D., Pangburn, S.H., Steinberg, D., 1981. Metabolism of homologous and heterologous lipoproteins by cultured rat and human skin fibroblasts. Journal of lipid research 22, 37-46.

Duan, Y., Ma, X., Zou, W., Wang, C., Bahbahan, I.S., Ahuja, T.P., Tolstikov, V., Zern, M.A., 2010. Differentiation and characterization of metabolically functioning hepatocytes from human embryonic stem cells. Stem cells 28, 674-686.

Dunn, J.C., Yarmush, M.L., Koebe, H.G., Tompkins, R.G., 1989. Hepatocyte function and extracellular matrix geometry: long-term culture in a sandwich

configuration. FASEB journal : official publication of the Federation of American Societies for Experimental Biology 3, 174-177.

Dunn, T.B., Kumins, N.H., Raofi, V., Holman, D.M., Mihalov, M., Blanchard, J., Law, W.R., Rastellini, C., Benedetti, E., 2000. Multiple intrasplenic hepatocyte transplantations in the dalmatian dog. Surgery 127, 193-199.

El-Ansary, M., Abdel-Aziz, I., Mogawer, S., Abdel-Hamid, S., Hammam, O., Teaema, S., Wahdan, M., 2012. Phase II trial: undifferentiated versus differentiated autologous mesenchymal stem cells transplantation in Egyptian patients with HCV induced liver cirrhosis. Stem cell reviews 8, 972-981.

Elaut, G., Henkens, T., Papeleu, P., Snykers, S., Vinken, M., Vanhaecke, T., Rogiers, V., 2006. Molecular mechanisms underlying the dedifferentiation process of isolated hepatocytes and their cultures. Current drug metabolism 7, 629-660.

Esteban, M.A., Xu, J., Yang, J., Peng, M., Qin, D., Li, W., Jiang, Z., Chen, J., Deng, K., Zhong, M., Cai, J., Lai, L., Pei, D., 2009. Generation of induced pluripotent stem cell lines from Tibetan miniature pig. The Journal of biological chemistry 284, 17634-17640.

European Medicines Agency, 2011. Reflection paper on stem cell-based medicinal products. . Committee for Advanced Therapies EMA CAT/571134/09,, pp 1-14

Evans, M.J., Kaufman, M.H., 1981. Establishment in culture of pluripotential cells from mouse embryos. Nature 292, 154-156.

Faldyna, M., Leva, L., Knotigova, P., Toman, M., 2001. Lymphocyte subsets in peripheral blood of dogs--a flow cytometric study. Veterinary immunology and immunopathology 82, 23-37.

Fanali, G., di Masi, A., Trezza, V., Marino, M., Fasano, M., Ascenzi, P., 2012. Human serum albumin: from bench to bedside. Molecular aspects of medicine 33, 209-290.

Fausto, N., Campbell, J.S., Riehle, K.J., 2006. Liver regeneration. Hepatology 43, S45-53.

Favier, R.P., Spee, B., Schotanus, B.A., van den Ingh, T.S., Fieten, H., Brinkhof, B., Viebahn, C.S., Penning, L.C., Rothuizen, J., 2012. COMMD1-deficient dogs accumulate copper in hepatocytes and provide a good model for chronic hepatitis and fibrosis. PloS one 7, e42158.

Felgner, J.H., Kumar, R., Sridhar, C.N., Wheeler, C.J., Tsai, Y.J., Border, R., Ramsey, P., Martin, M., Felgner, P.L., 1994. Enhanced gene delivery and mechanism studies with a novel series of cationic lipid formulations. The Journal of biological chemistry 269, 2550-2561.

Fiegel, H.C., Bruns, H., Hoper, C., Lioznov, M.V., Kluth, D., 2006. Cell growth and differentiation of different hepatic cells isolated from fetal rat liver in vitro. Tissue engineering 12, 123-130.

Filioli Uranio, M., Valentini, L., Lange-Consiglio, A., Caira, M., Guaricci, A.C., L'Abbate, A., Catacchio, C.R., Ventura, M., Cremonesi, F., Dell'Aquila, M.E., 2011. Isolation, proliferation, cytogenetic, and molecular characterization and in vitro differentiation potency of canine stem cells from foetal adnexa: a comparative study of amniotic fluid, amnion, and umbilical cord matrix. Molecular reproduction and development 78, 361-373.

Fleischer, S., Sharkey, M., Mealey, K., Ostrander, E.A., Martinez, M., 2008. Pharmacogenetic and metabolic differences between dog breeds: their impact on canine medicine and the use of the dog as a preclinical animal model. The AAPS journal 10, 110-119.

Forbes, S.J., 2008. Stem cell therapy for chronic liver disease--choosing the right tools for the job. Gut 57, 153-155.

Forbes, S.J., Alison, M.R., 2006. Side population (SP) cells: taking center stage in regeneration and liver cancer? Hepatology 44, 23-26.

Forbes, S.J., Russo, F.P., Rey, V., Burra, P., Rugge, M., Wright, N.A., Alison, M.R., 2004. A significant proportion of myofibroblasts are of bone marrow origin in human liver fibrosis. Gastroenterology 126, 955-963.

Forman, O.P., Boursnell, M.E., Dunmore, B.J., Stendall, N., van den Sluis, B., Fretwell, N., Jones, C., Wijmenga, C., Rothuizen, J., van Oost, B.A., Holmes, N.G., Binns, M.M., Jones, P., 2005. Characterization of the COMMD1 (MURR1) mutation causing copper toxicosis in Bedlington terriers. Animal genetics 36, 497-501.

Fraczek, J., Bolleyn, J., Vanhaecke, T., Rogiers, V., Vinken, M., 2013. Primary hepatocyte cultures for pharmaco-toxicological studies: at the busy crossroad of various anti-dedifferentiation strategies. Archives of toxicology 87, 577-610.

Frevert, U., Engelmann, S., Zougbede, S., Stange, J., Ng, B., Matuschewski, K., Liebes, L., Yee, H., 2005. Intravital observation of Plasmodium berghei sporozoite infection of the liver. PLoS biology 3, e192.

Friedenstein, A.J., Piatetzky, S., II, Petrakova, K.V., 1966. Osteogenesis in transplants of bone marrow cells. Journal of embryology and experimental morphology 16, 381-390.

Friedmann, T., Rossi, J.J., 2007. Gene transfer : delivery and expression of DNA and RNA : a laboratory manual. Cold Spring Harbor Laboratory Press, Cold Spring Harbor, N.Y.

Frith, J., Genever, P., 2008. Transcriptional control of mesenchymal stem cell differentiation. Transfusion medicine and hemotherapy : offizielles Organ der

Deutschen Gesellschaft fur Transfusionsmedizin und Immunhamatologie 35, 216-227.

Gadue, P., Huber, T.L., Paddison, P.J., Keller, G.M., 2006. Wnt and TGF-beta signaling are required for the induction of an in vitro model of primitive streak formation using embryonic stem cells. Proceedings of the National Academy of Sciences of the United States of America 103, 16806-16811.

Garcia, M.C., Ma, D., Dicioccio, A.T., Cali, J., 2008. The use of a high-throughput luminescent method to assess CYP3A enzyme induction in cultured rat hepatocytes. In vitro cellular & developmental biology. Animal 44, 129-134.

Gentile, A., Trusolino, L., Comoglio, P.M., 2008. The Met tyrosine kinase receptor in development and cancer. Cancer metastasis reviews 27, 85-94.

Gerbal-Chaloin, S., Duret, C., Raulet, E., Navarro, F., Blanc, P., Ramos, J., Maurel, P., Daujat-Chavanieu, M., 2010. Isolation and culture of adult human liver progenitor cells: in vitro differentiation to hepatocyte-like cells. Methods in molecular biology 640, 247-260.

Gerbal-Chaloin, S., Funakoshi, N., Caillaud, A., Gondeau, C., Champon, B., Si-Tayeb, K., 2014. Human induced pluripotent stem cells in hepatology: beyond the proof of concept. The American journal of pathology 184, 332-347.

Gieseck Iii, R.L., Hannan, N.R., Bort, R., Hanley, N.A., Drake, R.A., Cameron, G.W., Wynn, T.A., Vallier, L., 2014. Maturation of Induced Pluripotent Stem Cell Derived Hepatocytes by 3D-Culture. PloS one 9, e86372.

Godoy, P., Hewitt, N.J., Albrecht, U., Andersen, M.E., Ansari, N., Bhattacharya, S., Bode, J.G., Bolleyn, J., Borner, C., Bottger, J., Braeuning, A., Budinsky, R.A., Burkhardt, B., Cameron, N.R., Camussi, G., Cho, C.S., Choi, Y.J., Craig Rowlands, J., Dahmen, U., Damm, G., Dirsch, O., Donato, M.T., Dong, J., Dooley, S., Drasdo, D., Eakins, R., Ferreira, K.S., Fonsato, V., Fraczek, J., Gebhardt, R., Gibson, A., Glanemann, M., Goldring, C.E., Gomez-Lechon, M.J., Groothuis, G.M., Gustavsson, L., Guyot, C., Hallifax, D., Hammad, S., Hayward, A., Haussinger, D., Hellerbrand, C., Hewitt, P., Hoehme, S., Holzhutter, H.G., Houston, J.B., Hrach, J., Ito, K., Jaeschke, H., Keitel, V., Kelm, J.M., Kevin Park, B., Kordes, C., Kullak-Ublick, G.A., LeCluyse, E.L., Lu, P., Luebke-Wheeler, J., Lutz, A., Maltman, D.J., Matz-Soja, M., McMullen, P., Merfort, I., Messner, S., Meyer, C., Mwinyi, J., Naisbitt, D.J., Nussler, A.K., Olinga, P., Pampaloni, F., Pi, J., Pluta, L., Przyborski, S.A., Ramachandran, A., Rogiers, V., Rowe, C., Schelcher, C., Schmich, K., Schwarz, M., Singh, B., Stelzer, E.H., Stieger, B., Stober, R., Sugiyama, Y., Tetta, C., Thasler, W.E., Vanhaecke, T., Vinken, M., Weiss, T.S., Widera, A., Woods, C.G., Xu, J.J., Yarborough, K.M., Hengstler, J.G., 2013. Recent advances in 2D and 3D in vitro systems using primary hepatocytes, alternative hepatocyte sources and non-parenchymal liver cells and their use in investigating mechanisms of hepatotoxicity, cell signaling and ADME. Archives of toxicology 87, 1315-1530.

Goldstein, J.L., Brown, M.S., 1987. Regulation of low-density lipoprotein receptors: implications for pathogenesis and therapy of hypercholesterolemia and atherosclerosis. Circulation 76, 504-507.

Gomez, M.C., Serrano, M.A., Pope, C.E., Jenkins, J.A., Biancardi, M.N., Lopez, M., Dumas, C., Galiguis, J., Dresser, B.L., 2010. Derivation of cat embryonic stem-like cells from in vitro-produced blastocysts on homologous and heterologous feeder cells. Theriogenology 74, 498-515.

Gonzalez, F., Barragan Monasterio, M., Tiscornia, G., Montserrat Pulido, N., Vassena, R., Batlle Morera, L., Rodriguez Piza, I., Izpisua Belmonte, J.C., 2009. Generation of mouse-induced pluripotent stem cells by transient expression of a single nonviral polycistronic vector. Proceedings of the National Academy of Sciences of the United States of America 106, 8918-8922.

Gow, A.G., Fairbanks, L.D., Simpson, J.W., Jacinto, A.M., Ridyard, A.E., 2011. Xanthine urolithiasis in a Cavalier King Charles spaniel. The Veterinary record 169, 209.

Graham, M.J., Lake, B.G., 2008. Induction of drug metabolism: species differences and toxicological relevance. Toxicology 254, 184-191.

Graham, R.A., Downey, A., Mudra, D., Krueger, L., Carroll, K., Chengelis, C., Madan, A., Parkinson, A., 2002. In vivo and in vitro induction of cytochrome P450 enzymes in beagle dogs. Drug metabolism and disposition: the biological fate of chemicals 30, 1206-1213.

Graham, R.A., Tyler, L.O., Krol, W.L., Silver, I.S., Webster, L.O., Clark, P., Chen, L., Banks, T., LeCluyse, E.L., 2006. Temporal kinetics and concentration-response relationships for induction of CYP1A, CYP2B, and CYP3A in primary cultures of beagle dog hepatocytes. Journal of biochemical and molecular toxicology 20, 69-78.

Greenhough, S., Medine, C.N., Hay, D.C., 2010. Pluripotent stem cell derived hepatocyte like cells and their potential in toxicity screening. Toxicology 278, 250-255.

Gross-Steinmeyer, K., Stapleton, P.L., Tracy, J.H., Bammler, T.K., Lehman, T., Strom, S.C., Eaton, D.L., 2005. Influence of Matrigel-overlay on constitutive and inducible expression of nine genes encoding drug-metabolizing enzymes in primary human hepatocytes. Xenobiotica; the fate of foreign compounds in biological systems 35, 419-438.

Gross, D., Webb, W.W., 1986. Molecular counting of low-density lipoprotein particles as individuals and small clusters on cell surfaces. Biophysical journal 49, 901-911.

Guercio, A., Di Bella, S., Casella, S., Di Marco, P., Russo, C., Piccione, G., 2013. Canine mesenchymal stem cells (MSCs): characterization in relation to donor age and adipose tissue-harvesting site. Cell biology international 37, 789-798.

Guercio, A., Di Marco, P., Casella, S., Cannella, V., Russotto, L., Purpari, G., Di Bella, S., Piccione, G., 2012. Production of canine mesenchymal stem cells from adipose tissue and their application in dogs with chronic osteoarthritis of the humeroradial joints. Cell biology international 36, 189-194.

Guha, P., Morgan, J.W., Mostoslavsky, G., Rodrigues, N.P., Boyd, A.S., 2013. Lack of immune response to differentiated cells derived from syngeneic induced pluripotent stem cells. Cell stem cell 12, 407-412.

Hamilton, B.S., Paglia, D., Kwan, A.Y., Deitel, M., 1995. Increased obese mRNA expression in omental fat cells from massively obese humans. Nature medicine 1, 953-956.

Handorf, A.M., Li, W.J., 2014. Induction of mesenchymal stem cell chondrogenesis through sequential administration of growth factors within specific temporal windows. Journal of cellular physiology 229, 162-171.

Haniffa, M.A., Collin, M.P., Buckley, C.D., Dazzi, F., 2009. Mesenchymal stem cells: the fibroblasts' new clothes? Haematologica 94, 258-263.

Hannan, N.R., Rashid, S.T., Vallier, L., 2012. Applying pluripotent stem cell technology to modelling human liver disease, In: Regenerative medicine, stem cells and the liver. Science Publishers ; London : Taylor & Francis [distributor], Enfield, N.H.

Harada-Shiba, M., Takagi, A., Marutsuka, K., Moriguchi, S., Yagyu, H., Ishibashi, S., Asada, Y., Yokoyama, S., 2004. Disruption of autosomal recessive hypercholesterolemia gene shows different phenotype in vitro and in vivo. Circulation research 95, 945-952.

Hatoya, S., Torii, R., Kondo, Y., Okuno, T., Kobayashi, K., Wijewardana, V., Kawate, N., Tamada, H., Sawada, T., Kumagai, D., Sugiura, K., Inaba, T., 2006. Isolation and characterization of embryonic stem-like cells from canine blastocysts. Molecular reproduction and development 73, 298-305.

Hay, D.C., Pernagallo, S., Diaz-Mochon, J.J., Medine, C.N., Greenhough, S., Hannoun, Z., Schrader, J., Black, J.R., Fletcher, J., Dalgetty, D., Thompson, A.I., Newsome, P.N., Forbes, S.J., Ross, J.A., Bradley, M., Iredale, J.P., 2011. Unbiased screening of polymer libraries to define novel substrates for functional hepatocytes with inducible drug metabolism. Stem cell research 6, 92-102.

Hay, D.C., Zhao, D., Fletcher, J., Hewitt, Z.A., McLean, D., Urruticoechea-Uriguen, A., Black, J.R., Elcombe, C., Ross, J.A., Wolf, R., Cui, W., 2008. Efficient differentiation of hepatocytes from human embryonic stem cells exhibiting markers recapitulating liver development in vivo. Stem cells 26, 894-902.

Hay, D.C., Zhao, D., Ross, A., Mandalam, R., Lebkowski, J., Cui, W., 2007. Direct differentiation of human embryonic stem cells to hepatocyte-like cells exhibiting functional activities. Cloning and stem cells 9, 51-62.

Hayat, A., 2012. Stem Cells and Cancer Stem Cells, Volume 4: Therapeutic Applications in Disease and Injury. Springer.

Hayes, B., Fagerlie, S.R., Ramakrishnan, A., Baran, S., Harkey, M., Graf, L., Bar, M., Bendoraite, A., Tewari, M., Torok-Storb, B., 2008. Derivation, characterization, and in vitro differentiation of canine embryonic stem cells. Stem cells 26, 465-473.

He, H., Liu, X., Peng, L., Gao, Z., Ye, Y., Su, Y., Zhao, Q., Wang, K., Gong, Y., He, F., 2013. Promotion of hepatic differentiation of bone marrow mesenchymal stem cells on decellularized cell-deposited extracellular matrix. BioMed research international 2013, 406871.

Hellerbrand, C., 2013. Hepatic stellate cells--the pericytes in the liver. Pflugers Archiv : European journal of physiology 465, 775-778.

Hematti, P., 2012. Mesenchymal stromal cells and fibroblasts: a case of mistaken identity? Cytotherapy 14, 516-521.

Hengstler, J.G., Brulport, M., Schormann, W., Bauer, A., Hermes, M., Nussler, A.K., Fandrich, F., Ruhnke, M., Ungefroren, H., Griffin, L., Bockamp, E., Oesch, F., von Mach, M.A., 2005. Generation of human hepatocytes by stem cell technology: definition of the hepatocyte. Expert opinion on drug metabolism & toxicology 1, 61-74.

Hennig, T., Lorenz, H., Thiel, A., Goetzke, K., Dickhut, A., Geiger, F., Richter, W., 2007. Reduced chondrogenic potential of adipose tissue derived stromal cells correlates with an altered TGFbeta receptor and BMP profile and is overcome by BMP-6. Journal of cellular physiology 211, 682-691.

Hewitt, N.J., 2010. Optimisation of the cryopreservation of primary hepatocytes. Methods in molecular biology 640, 83-105.

Higgins, G., Anderson, R., 1931. Restoration of the liver of the white rat following partial surgical removal. Archives of Pathology and Laboratory Medicine 12, 186-202.

Ho, C.M., Dhawan, A., Hughes, R.D., Lehec, S.C., Puppi, J., Philippeos, C., Lee, P.H., Mitry, R.R., 2012. Use of indocyanine green for functional assessment of human hepatocytes for transplantation. Asian journal of surgery / Asian Surgical Association 35, 9-15.

Hodgkiss-Geere, H.M., Argyle, D.J., Corcoran, B.M., Whitelaw, B., Milne, E., Bennett, D., Argyle, S.A., 2012. Characterisation and differentiation potential of bone marrow derived canine mesenchymal stem cells. Vet J 194, 361-368.

Home Office, 2012. Statistics of scientific procedures on living animals, Great Britain 2012. https://www.gov.uk/government/publications/statistics-of-scientific-procedures-on-living-animals-great-britain-2012 (accessed 07/11/2013 2013).

Horiuchi, S., Sakamoto, Y., Sakai, M., 2003. Scavenger receptors for oxidized and glycated proteins. Amino acids 25, 283-292.

Horwitz, E.M., Le Blanc, K., Dominici, M., Mueller, I., Slaper-Cortenbach, I., Marini, F.C., Deans, R.J., Krause, D.S., Keating, A., International Society for Cellular, T., 2005. Clarification of the nomenclature for MSC: The International Society for Cellular Therapy position statement. Cytotherapy 7, 393-395.

Hou, P., Li, Y., Zhang, X., Liu, C., Guan, J., Li, H., Zhao, T., Ye, J., Yang, W., Liu, K., Ge, J., Xu, J., Zhang, Q., Zhao, Y., Deng, H., 2013. Pluripotent stem cells induced from mouse somatic cells by small-molecule compounds. Science 341, 651-654.

Hristov, M., Weber, C., 2004. Endothelial progenitor cells: characterization, pathophysiology, and possible clinical relevance. Journal of cellular and molecular medicine 8, 498-508.

http://www.nc3rs.org.uk/. http://www.nc3rs.org.uk/ (accessed 06/11/2013 2013).

Huang, P., He, Z., Ji, S., Sun, H., Xiang, D., Liu, C., Hu, Y., Wang, X., Hui, L., 2011. Induction of functional hepatocyte-like cells from mouse fibroblasts by defined factors. Nature 475, 386-389.

Hussain, S.Z., Strom, S.C., Kirby, M.R., Burns, S., Langemeijer, S., Ueda, T., Hsieh, M., Tisdale, J.F., 2005. Side population cells derived from adult human liver generate hepatocyte-like cells in vitro. Digestive diseases and sciences 50, 1755-1763.

Innes, J.F., Gordon, C., Vaughan-Thomas, A., Rhodes, N.P., Clegg, P.D., 2013. Evaluation of cartilage, synovium and adipose tissue as cellular sources for osteochondral repair. Vet J 197, 619-624.

Irollo, E., Pirozzi, G., 2013. CD133: to be or not to be, is this the real question? American journal of translational research 5, 563-581.

Izadpanah, R., Trygg, C., Patel, B., Kriedt, C., Dufour, J., Gimble, J.M., Bunnell, B.A., 2006. Biologic properties of mesenchymal stem cells derived from bone marrow and adipose tissue. Journal of cellular biochemistry 99, 1285-1297.

Jang, Y.O., Kim, Y.J., Baik, S.K., Kim, M.Y., Eom, Y.W., Cho, M.Y., Park, H.J., Park, S.Y., Kim, B.R., Kim, J.W., Soo Kim, H., Kwon, S.O., Choi, E.H., Kim, Y.M., 2013. Histological improvement following administration of autologous bone marrow-derived mesenchymal stem cells for alcoholic cirrhosis: a pilot study. Liver international : official journal of the International Association for the Study of the Liver.

Javed, M.S., Yaqoob, N., Iwamuro, M., Kobayashi, N., Fujiwara, T., 2014. Generation of Hepatocyte-like Cells from Human Induced Pluripotent Stem (iPS) Cells By Co-culturing Embryoid Body Cells with Liver Non-parenchymal Cell Line

TWNT-1. Journal of the College of Physicians and Surgeons--Pakistan : JCPSP 24, 91-96.

Jeong, S.G., Ohn, T., Kim, S.H., Cho, G.W., 2013. Valproic acid promotes neuronal differentiation by induction of neuroprogenitors in human bone-marrow mesenchymal stromal cells. Neuroscience letters 554, 22-27.

Joo, S., Ko, I.K., Atala, A., Yoo, J.J., Lee, S.J., 2012. Amniotic fluid-derived stem cells in regenerative medicine research. Archives of pharmacal research 35, 271-280.

Jung, Y., Witek, R.P., Syn, W.K., Choi, S.S., Omenetti, A., Premont, R., Guy, C.D., Diehl, A.M., 2010. Signals from dying hepatocytes trigger growth of liver progenitors. Gut 59, 655-665.

Juttermann, R., Li, E., Jaenisch, R., 1994. Toxicity of 5-aza-2'-deoxycytidine to mammalian cells is mediated primarily by covalent trapping of DNA methyltransferase rather than DNA demethylation. Proceedings of the National Academy of Sciences of the United States of America 91, 11797-11801.

Kadiyala, S., Young, R.G., Thiede, M.A., Bruder, S.P., 1997. Culture expanded canine mesenchymal stem cells possess osteochondrogenic potential in vivo and in vitro. Cell transplantation 6, 125-134.

Kaji, K., Norrby, K., Paca, A., Mileikovsky, M., Mohseni, P., Woltjen, K., 2009. Virus-free induction of pluripotency and subsequent excision of reprogramming factors. Nature 458, 771-775.

Kamimura, H., 2006. Genetic polymorphism of cytochrome P450s in beagles: possible influence of CYP1A2 deficiency on toxicological evaluations. Archives of toxicology 80, 732-738.

Kamiya, A., Kinoshita, T., Miyajima, A., 2001. Oncostatin M and hepatocyte growth factor induce hepatic maturation via distinct signaling pathways. FEBS letters 492, 90-94.

Kanawa, M., Igarashi, A., Ronald, V.S., Higashi, Y., Kurihara, H., Sugiyama, M., Saskianti, T., Pan, H., Kato, Y., 2013. Age-dependent decrease in the chondrogenic potential of human bone marrow mesenchymal stromal cells expanded with fibroblast growth factor-2. Cytotherapy 15, 1062-1072.

Kaneko, J.J., Harvey, J.W., Bruss, M.L., 2008. Clinical Biochemistry of Domestic Animals. Elsevier Science.

Kang, B.J., Ryu, H.H., Park, S.S., Koyama, Y., Kikuchi, M., Woo, H.M., Kim, W.H., Kweon, O.K., 2012. Comparing the osteogenic potential of canine mesenchymal stem cells derived from adipose tissues, bone marrow, umbilical cord blood, and Wharton's jelly for treating bone defects. Journal of veterinary science 13, 299-310.

Karnoub, A.E., Dash, A.B., Vo, A.P., Sullivan, A., Brooks, M.W., Bell, G.W., Richardson, A.L., Polyak, K., Tubo, R., Weinberg, R.A., 2007. Mesenchymal stem cells within tumour stroma promote breast cancer metastasis. Nature 449, 557-563.

Kawahara, S., Hata, Y., Miura, M., Kita, T., Sengoku, A., Nakao, S., Mochizuki, Y., Enaida, H., Ueno, A., Hafezi-Moghadam, A., Ishibashi, T., 2007. Intracellular events in retinal glial cells exposed to ICG and BBG. Investigative ophthalmology & visual science 48, 4426-4432.

Kern, S., Eichler, H., Stoeve, J., Kluter, H., Bieback, K., 2006. Comparative analysis of mesenchymal stem cells from bone marrow, umbilical cord blood, or adipose tissue. Stem cells 24, 1294-1301.

Khurana, S., Mukhopadhyay, A., 2008. In vitro transdifferentiation of adult hematopoietic stem cells: an alternative source of engraftable hepatocytes. Journal of hepatology 49, 998-1007.

Kia, R., Sison, R.L., Heslop, J., Kitteringham, N.R., Hanley, N., Mills, J.S., Park, B.K., Goldring, C.E., 2013. Stem cell-derived hepatocytes as a predictive model for drug-induced liver injury: are we there yet? British journal of clinical pharmacology 75, 885-896.

Kiani, C., Chen, L., Wu, Y.J., Yee, A.J., Yang, B.B., 2002. Structure and function of aggrecan. Cell research 12, 19-32.

Kim, J.W., Lee, J.H., Lyoo, Y.S., Jung, D.I., Park, H.M., 2013. The effects of topical mesenchymal stem cell transplantation in canine experimental cutaneous wounds. Veterinary dermatology 24, 242-e253.

Kim, K., Doi, A., Wen, B., Ng, K., Zhao, R., Cahan, P., Kim, J., Aryee, M.J., Ji, H., Ehrlich, L.I., Yabuuchi, A., Takeuchi, A., Cunniff, K.C., Hongguang, H., McKinney-Freeman, S., Naveiras, O., Yoon, T.J., Irizarry, R.A., Jung, N., Seita, J., Hanna, J., Murakami, P., Jaenisch, R., Weissleder, R., Orkin, S.H., Weissman, I.L., Feinberg, A.P., Daley, G.Q., 2010. Epigenetic memory in induced pluripotent stem cells. Nature 467, 285-290.

Kim, N., Yoo, W., Lee, J., Kim, H., Lee, H., Kim, Y.S., Kim, D.U., Oh, J., 2009. Formation of vitamin A lipid droplets in pancreatic stellate cells requires albumin. Gut 58, 1382-1390.

Kim, T.K., Eberwine, J.H., 2010. Mammalian cell transfection: the present and the future. Analytical and bioanalytical chemistry 397, 3173-3178.

Kinoshita, T., Sekiguchi, T., Xu, M.J., Ito, Y., Kamiya, A., Tsuji, K., Nakahata, T., Miyajima, A., 1999. Hepatic differentiation induced by oncostatin M attenuates fetal liver hematopoiesis. Proceedings of the National Academy of Sciences of the United States of America 96, 7265-7270.

Kisiel, A.H., McDuffee, L.A., Masaoud, E., Bailey, T.R., Esparza Gonzalez, B.P., Nino-Fong, R., 2012. Isolation, characterization, and in vitro proliferation of canine mesenchymal stem cells derived from bone marrow, adipose tissue, muscle, and periosteum. American journal of veterinary research 73, 1305-1317.

Kisseberth, W.C., Murahari, S., London, C.A., Kulp, S.K., Chen, C.S., 2008. Evaluation of the effects of histone deacetylase inhibitors on cells from canine cancer cell lines. American journal of veterinary research 69, 938-945.

Kmiec, Z., 2001. Cooperation of Liver Cells in Health and Disease: With 18 Tables. Springer Berlin Heidelberg.

Knobeloch, D., Ehnert, S., Schyschka, L., Buchler, P., Schoenberg, M., Kleeff, J., Thasler, W.E., Nussler, N.C., Godoy, P., Hengstler, J., Nussler, A.K., 2012. Human hepatocytes: isolation, culture, and quality procedures. Methods in molecular biology 806, 99-120.

Kocarek, T.A., Schuetz, E.G., Guzelian, P.S., 1993. Expression of multiple forms of cytochrome P450 mRNAs in primary cultures of rat hepatocytes maintained on matrigel. Molecular pharmacology 43, 328-334.

Koh, S., Thomas, R., Tsai, S., Bischoff, S., Lim, J.H., Breen, M., Olby, N.J., Piedrahita, J.A., 2013. Growth requirements and chromosomal instability of induced pluripotent stem cells generated from adult canine fibroblasts. Stem cells and development 22, 951-963.

Kola, I., 2008. The state of innovation in drug development. Clinical pharmacology and therapeutics 83, 227-230.

Kordes, C., Haussinger, D., 2013. Hepatic stem cell niches. The Journal of clinical investigation 123, 1874-1880.

Kordes, C., Sawitza, I., Muller-Marbach, A., Ale-Agha, N., Keitel, V., Klonowski-Stumpe, H., Haussinger, D., 2007. CD133+ hepatic stellate cells are progenitor cells. Biochemical and biophysical research communications 352, 410-417.

Krause, P., Unthan-Fechner, K., Probst, I., Koenig, S., 2013. Cultured hepatocytes adopt progenitor characteristics and display bipotent capacity to repopulate the liver. Cell transplantation. 23(7):805-17

Kubota, H., Reid, L.M., 2000. Clonogenic hepatoblasts, common precursors for hepatocytic and biliary lineages, are lacking classical major histocompatibility complex class I antigen. Proceedings of the National Academy of Sciences of the United States of America 97, 12132-12137.

Kucerova, L., Matuskova, M., Hlubinova, K., Altanerova, V., Altaner, C., 2010. Tumor cell behaviour modulation by mesenchymal stromal cells. Molecular cancer 9, 129.

Kulterer, B., Friedl, G., Jandrositz, A., Sanchez-Cabo, F., Prokesch, A., Paar, C., Scheideler, M., Windhager, R., Preisegger, K.H., Trajanoski, Z., 2007. Gene expression profiling of human mesenchymal stem cells derived from bone marrow during expansion and osteoblast differentiation. BMC genomics 8, 70.

Kuntz, E., Kuntz, H.D., 2009. Hepatology: Textbook and Atlas. Springer.

Kuo, T.K., Hung, S.P., Chuang, C.H., Chen, C.T., Shih, Y.R., Fang, S.C., Yang, V.W., Lee, O.K., 2008. Stem cell therapy for liver disease: parameters governing the success of using bone marrow mesenchymal stem cells. Gastroenterology 134, 2111-2121, 2121 e2111-2113.

Lagasse, E., Connors, H., Al-Dhalimy, M., Reitsma, M., Dohse, M., Osborne, L., Wang, X., Finegold, M., Weissman, I.L., Grompe, M., 2000. Purified hematopoietic stem cells can differentiate into hepatocytes in vivo. Nature medicine 6, 1229-1234.

Lange, C., Bassler, P., Lioznov, M.V., Bruns, H., Kluth, D., Zander, A.R., Fiegel, H.C., 2005a. Hepatocytic gene expression in cultured rat mesenchymal stem cells. Transplantation proceedings 37, 276-279.

Lange, C., Bassler, P., Lioznov, M.V., Bruns, H., Kluth, D., Zander, A.R., Fiegel, H.C., 2005b. Liver-specific gene expression in mesenchymal stem cells is induced by liver cells. World J Gastroenterol 11, 4497-4504.

Lankford, S.M., Bai, S.A., Goldstein, J.A., 2000. Cloning of canine cytochrome P450 2E1 cDNA: identification and characterization of two variant alleles. Drug metabolism and disposition: the biological fate of chemicals 28, 981-986.

Le Blanc, K., Frassoni, F., Ball, L., Locatelli, F., Roelofs, H., Lewis, I., Lanino, E., Sundberg, B., Bernardo, M.E., Remberger, M., Dini, G., Egeler, R.M., Bacigalupo, A., Fibbe, W., Ringden, O., Developmental Committee of the European Group for, B., Marrow, T., 2008. Mesenchymal stem cells for treatment of steroid-resistant, severe, acute graft-versus-host disease: a phase II study. Lancet 371, 1579-1586.

Le Blanc, K., Rasmusson, I., Sundberg, B., Gotherstrom, C., Hassan, M., Uzunel, M., Ringden, O., 2004. Treatment of severe acute graft-versus-host disease with third party haploidentical mesenchymal stem cells. Lancet 363, 1439-1441.

Leckie, P., Davenport, A., Jalan, R., 2012. Extracorporeal liver support. Blood purification 34, 158-163.

LeCluyse, E., Madan, A., Hamilton, G., Carroll, K., DeHaan, R., Parkinson, A., 2000. Expression and regulation of cytochrome P450 enzymes in primary cultures of human hepatocytes. Journal of biochemical and molecular toxicology 14, 177-188.

Lee, A.S., Xu, D., Plews, J.R., Nguyen, P.K., Nag, D., Lyons, J.K., Han, L., Hu, S., Lan, F., Liu, J., Huang, M., Narsinh, K.H., Long, C.T., de Almeida, P.E., Levi, B., Kooreman, N., Bangs, C., Pacharinsak, C., Ikeno, F., Yeung, A.C., Gambhir, S.S., Robbins, R.C., Longaker, M.T., Wu, J.C., 2011. Preclinical derivation and imaging

of autologously transplanted canine induced pluripotent stem cells. The Journal of biological chemistry 286, 32697-32704.

Lee, H.J., Jung, J., Cho, K.J., Lee, C.K., Hwang, S.G., Kim, G.J., 2012. Comparison of in vitro hepatogenic differentiation potential between various placenta-derived stem cells and other adult stem cells as an alternative source of functional hepatocytes. Differentiation; research in biological diversity 84, 223-231.

Lee, K.D., Kuo, T.K., Whang-Peng, J., Chung, Y.F., Lin, C.T., Chou, S.H., Chen, J.R., Chen, Y.P., Lee, O.K., 2004. In vitro hepatic differentiation of human mesenchymal stem cells. Hepatology 40, 1275-1284.

Lee, S., Park, J.R., Seo, M.S., Roh, K.H., Park, S.B., Hwang, J.W., Sun, B., Seo, K., Lee, Y.S., Kang, S.K., Jung, J.W., Kang, K.S., 2009. Histone deacetylase inhibitors decrease proliferation potential and multilineage differentiation capability of human mesenchymal stem cells. Cell proliferation 42, 711-720.

Li, D., Mehta, J.L., 2005. Oxidized LDL, a critical factor in atherogenesis. Cardiovascular research 68, 353-354.

Li, X., Yuan, J., Li, W., Liu, S., Hua, M., Lu, X., Zhang, H., 2013a. Direct Differentiation of Homogeneous Human Adipose Stem Cells into Functional Hepatocytes by Mimicking Liver Embryogenesis. Journal of cellular physiology.

Li, Z., Chen, J., Li, L., Ran, J.H., Liu, J., Gao, T.X., Guo, B.Y., Li, X.H., Liu, Z.H., Liu, G.J., Gao, Y.C., Zhang, X.L., 2013b. In vitro proliferation and differentiation of hepatic oval cells and their potential capacity for intrahepatic transplantation. Brazilian journal of medical and biological research = Revista brasileira de pesquisas medicas e biologicas / Sociedade Brasileira de Biofisica ... [et al.] 46, 681-688.

Liesveld, J.L., Abboud, C.N., Duerst, R.E., Ryan, D.H., Brennan, J.K., Lichtman, M.A., 1989. Characterization of human marrow stromal cells: role in progenitor cell binding and granulopoiesis. Blood 73, 1794-1800.

Lim, J.H., Byeon, Y.E., Ryu, H.H., Jeong, Y.H., Lee, Y.W., Kim, W.H., Kang, K.S., Kweon, O.K., 2007. Transplantation of canine umbilical cord blood-derived mesenchymal stem cells in experimentally induced spinal cord injured dogs. Journal of veterinary science 8, 275-282.

Liu, S.Q., Lei, P., Cui, X.H., Lv, Y., Li, J.H., Song, Y.L., Zhao, G., 2013. Sutureless anastomoses using magnetic rings in canine liver transplantation model. The Journal of surgical research.

Lubet, R.A., Mayer, R.T., Cameron, J.W., Nims, R.W., Burke, M.D., Wolff, T., Guengerich, F.P., 1985. Dealkylation of pentoxyresorufin: a rapid and sensitive assay for measuring induction of cytochrome(s) P-450 by phenobarbital and other xenobiotics in the rat. Archives of biochemistry and biophysics 238, 43-48.

Luo, J., Suhr, S.T., Chang, E.A., Wang, K., Ross, P.J., Nelson, L.L., Venta, P.J., Knott, J.G., Cibelli, J.B., 2011. Generation of Leukemia Inhibitory Factor and Basic Fibroblast Growth Factor-Dependent Induced Pluripotent Stem Cells from Canine Adult Somatic Cells. Stem cells and development.

Lyra, A.C., Soares, M.B., da Silva, L.F., Braga, E.L., Oliveira, S.A., Fortes, M.F., Silva, A.G., Brustolim, D., Genser, B., Dos Santos, R.R., Lyra, L.G., 2010. Infusion of autologous bone marrow mononuclear cells through hepatic artery results in a short-term improvement of liver function in patients with chronic liver disease: a pilot randomized controlled study. European journal of gastroenterology & hepatology 22, 33-42.

Maffei, M., Halaas, J., Ravussin, E., Pratley, R.E., Lee, G.H., Zhang, Y., Fei, H., Kim, S., Lallone, R., Ranganathan, S., et al., 1995. Leptin levels in human and rodent: measurement of plasma leptin and ob RNA in obese and weight-reduced subjects. Nature medicine 1, 1155-1161.

Makino, T., Kinoshita, J., Arakawa, S., Ito, K., Ando, Y., Yamoto, T., Teranishi, M., Sanbuissho, A., Nakayama, H., 2009. Comprehensive analysis of hepatic gene and protein expression profiles on phenobarbital- or clofibrate-induced hepatic hypertrophy in dogs. The Journal of toxicological sciences 34, 647-661.

Mallat, A., Lotersztajn, S., 2013. Cellular mechanisms of tissue fibrosis. 5. Novel insights into liver fibrosis. American journal of physiology. Cell physiology 305, C789-799.

Martignoni, M., Groothuis, G.M., de Kanter, R., 2006. Species differences between mouse, rat, dog, monkey and human CYP-mediated drug metabolism, inhibition and induction. Expert opinion on drug metabolism & toxicology 2, 875-894.

Martinez, M.N., Antonovic, L., Court, M., Dacasto, M., Fink-Gremmels, J., Kukanich, B., Locuson, C., Mealey, K., Myers, M.J., Trepanier, L., 2013. Challenges in exploring the cytochrome P450 system as a source of variation in canine drug pharmacokinetics. Drug metabolism reviews 45, 218-230.

Matsumoto, K., Nakamura, T., 1997. Hepatocyte growth factor (HGF) as a tissue organizer for organogenesis and regeneration. Biochemical and biophysical research communications 239, 639-644.

McClelland, R., Wauthier, E., Zhang, L., Melhem, A., Schmelzer, E., Barbier, C., Reid, L.M., 2008. Ex vivo conditions for self-replication of human hepatic stem cells. Tissue engineering. Part C, Methods 14, 341-351.

Meier, R.P., Muller, Y.D., Morel, P., Gonelle-Gispert, C., Buhler, L.H., 2013. Transplantation of mesenchymal stem cells for the treatment of liver diseases, is there enough evidence? Stem cell research 11, 1348-1364.

Mellersh, C., 2012. DNA testing and domestic dogs. Mammalian genome : official journal of the International Mammalian Genome Society 23, 109-123.

Meng, Z., Liu, N., Fu, X., Wang, X., Wang, Y.D., Chen, W.D., Zhang, L., Forman, B.M., Huang, W., 2011. Insufficient bile acid signaling impairs liver repair in CYP27(-/-) mice. Journal of hepatology 55, 885-895.

Mise, M., Hashizume, T., Matsumoto, S., Terauchi, Y., Fujii, T., 2004. Identification of non-functional allelic variant of CYP1A2 in dogs. Pharmacogenetics 14, 769-773.

Miura, M., Miura, Y., Padilla-Nash, H.M., Molinolo, A.A., Fu, B., Patel, V., Seo, B.M., Sonoyama, W., Zheng, J.J., Baker, C.C., Chen, W., Ried, T., Shi, S., 2006. Accumulated chromosomal instability in murine bone marrow mesenchymal stem cells leads to malignant transformation. Stem cells 24, 1095-1103.

Miyaoka, Y., Ebato, K., Kato, H., Arakawa, S., Shimizu, S., Miyajima, A., 2012. Hypertrophy and unconventional cell division of hepatocytes underlie liver regeneration. Current biology : CB 22, 1166-1175.

Miyaoka, Y., Miyajima, A., 2013. To divide or not to divide: revisiting liver regeneration. Cell division 8, 8.

Miyoshi, N., Ishii, H., Nagano, H., Haraguchi, N., Dewi, D.L., Kano, Y., Nishikawa, S., Tanemura, M., Mimori, K., Tanaka, F., Saito, T., Nishimura, J., Takemasa, I., Mizushima, T., Ikeda, M., Yamamoto, H., Sekimoto, M., Doki, Y., Mori, M., 2011. Reprogramming of mouse and human cells to pluripotency using mature microRNAs. Cell stem cell 8, 633-638.

Mizuguchi, T., Hui, T., Palm, K., Sugiyama, N., Mitaka, T., Demetriou, A.A., Rozga, J., 2001. Enhanced proliferation and differentiation of rat hepatocytes cultured with bone marrow stromal cells. Journal of cellular physiology 189, 106-119.

Mokbel, A., El-Tookhy, O., Shamaa, A.A., Sabry, D., Rashed, L., Mostafa, A., 2011. Homing and efficacy of intra-articular injection of autologous mesenchymal stem cells in experimental chondral defects in dogs. Clinical and experimental rheumatology 29, 275-284.

Mor, F., Cohen, I.R., 2013. Beta-lactam antibiotics modulate T-cell functions and gene expression via covalent binding to cellular albumin. Proceedings of the National Academy of Sciences of the United States of America 110, 2981-2986.

Moradpour, D., Blum, H.E., 2005. Pathogenesis of hepatocellular carcinoma. European journal of gastroenterology & hepatology 17, 477-483.

Moschidou, D., Mukherjee, S., Blundell, M.P., Jones, G.N., Atala, A.J., Thrasher, A.J., Fisk, N.M., De Coppi, P., Guillot, P.V., 2013. Human mid-trimester amniotic fluid stem cells cultured under embryonic stem cell conditions with valproic acid acquire pluripotent characteristics. Stem cells and development 22, 444-458.

Murakami, S., Kan, M., McKeehan, W.L., de Crombrugghe, B., 2000. Up-regulation of the chondrogenic Sox9 gene by fibroblast growth factors is mediated by the

mitogen-activated protein kinase pathway. Proceedings of the National Academy of Sciences of the United States of America 97, 1113-1118.

Naeem, N., Haneef, K., Kabir, N., Iqbal, H., Jamall, S., Salim, A., 2013. DNA methylation inhibitors, 5-azacytidine and zebularine potentiate the transdifferentiation of rat bone marrow mesenchymal stem cells into cardiomyocytes. Cardiovascular therapeutics 31, 201-209.

Nagamoto, Y., Tashiro, K., Takayama, K., Ohashi, K., Kawabata, K., Sakurai, F., Tachibana, M., Hayakawa, T., Furue, M.K., Mizuguchi, H., 2012. The promotion of hepatic maturation of human pluripotent stem cells in 3D co-culture using type I collagen and Swiss 3T3 cell sheets. Biomaterials 33, 4526-4534.

Nahmias, Y., Casali, M., Barbe, L., Berthiaume, F., Yarmush, M.L., 2006. Liver endothelial cells promote LDL-R expression and the uptake of HCV-like particles in primary rat and human hepatocytes. Hepatology 43, 257-265.

Nahon, J.L., Tratner, I., Poliard, A., Presse, F., Poiret, M., Gal, A., Sala-Trepat, J.M., Legres, L., Feldmann, G., Bernuau, D., 1988. Albumin and alpha-fetoprotein gene expression in various nonhepatic rat tissues. The Journal of biological chemistry 263, 11436-11442.

Nakamura, T., Sakai, K., Nakamura, T., Matsumoto, K., 2011. Hepatocyte growth factor twenty years on: Much more than a growth factor. Journal of gastroenterology and hepatology 26 Suppl 1, 188-202.

Need, A.C., Motulsky, A.G., Goldstein, D.B., 2005. Priorities and standards in pharmacogenetic research. Nature genetics 37, 671-681.

Nelson, D.R., 2009. The Cytochrome P450 Homepage Human Genomics 4, 59-65. http://drnelson.uthsc.edu/CytochromeP450.html (accessed 06/11/13 2013).

Nelson, L.J., Treskes, P., Howie, A.F., Walker, S.W., Hayes, P.C., Plevris, J.N., 2013. Profiling the Impact of Medium Formulation on Morphology and Functionality of Primary Hepatocytes in vitro. Scientific reports 3, 2735.

Ning, H., Lin, G., Lue, T.F., Lin, C.S., 2011. Mesenchymal stem cell marker Stro-1 is a 75 kd endothelial antigen. Biochemical and biophysical research communications 413, 353-357.

Nishimura, T., Hatoya, S., Kanegi, R., Sugiura, K., Wijewardana, V., Kuwamura, M., Tanaka, M., Yamate, J., Izawa, T., Takahashi, M., Kawate, N., Tamada, H., Imai, H., Inaba, T., 2013. Generation of functional platelets from canine induced pluripotent stem cells. Stem cells and development 22, 2026-2035.

O'Malley, J., Woltjen, K., Kaji, K., 2009. New strategies to generate induced pluripotent stem cells. Current opinion in biotechnology 20, 516-521.

Obokata, H., Sasai, Y., Niwa, H., Kadota, M., Andrabi, M., Takata, N., Tokoro, M., Terashita, Y., Yonemura, S., Vacanti, C.A., Wakayama, T., 2014a. Bidirectional developmental potential in reprogrammed cells with acquired pluripotency. Nature 505, 676-680.

Obokata, H., Wakayama, T., Sasai, Y., Kojima, K., Vacanti, M.P., Niwa, H., Yamato, M., Vacanti, C.A., 2014b. Stimulus-triggered fate conversion of somatic cells into pluripotency. Nature 505, 641-647.

Ock, S.A., Maeng, G.H., Lee, Y.M., Kim, T.H., Kumar, B.M., Lee, S.L., Rhoa, G.J., 2012. Donor Matched Functional and Molecular Characterization of Canine Mesenchymal Stem Cells Derived from Different Origins. Cell transplantation.

Oh, H.J., Park, J.E., Kim, M.J., Hong, S.G., Ra, J.C., Jo, J.Y., Kang, S.K., Jang, G., Lee, B.C., 2011. Recloned dogs derived from adipose stem cells of a transgenic cloned beagle. Theriogenology 75, 1221-1231.

Okita, K., Ichisaka, T., Yamanaka, S., 2007. Generation of germline-competent induced pluripotent stem cells. Nature 448, 313-317.

Olsavsky Goyak, K., Laurenzana, E., Omiecinski, C., 2010. Hepatocyte Differentiation, In: Hepatocytes. Humana Press, pp. 115-138.

Ornitz, D.M., Itoh, N., 2001. Fibroblast growth factors. Genome biology 2, REVIEWS3005.

Ouyang, J.F., Lou, J., Yan, C., Ren, Z.H., Qiao, H.X., Hong, D.S., 2010. In-vitro promoted differentiation of mesenchymal stem cells towards hepatocytes induced by salidroside. The Journal of pharmacy and pharmacology 62, 530-538.

Pal, R., Mamidi, M.K., Das, A.K., Bhonde, R., 2012. Diverse effects of dimethyl sulfoxide (DMSO) on the differentiation potential of human embryonic stem cells. Archives of toxicology 86, 651-661.

Palakkan, A.A., Hay, D.C., Anil Kumar, P.R., Kumary, T.V., Ross, J.A., 2013. Liver tissue engineering and cell sources: issues and challenges. Liver international : official journal of the International Association for the Study of the Liver 33, 666-676.

Pan, M.X., Cai, L., Wang, X.Y., Zhang, Q.J., Kong, F.D., Xu, S.Y., Wang, Y., Gao, Y., 2013. Establishment of a simple living donor liver transplantation dog model using a two-step nonvenous bypass hepatectomy. Transplantation proceedings 45, 2425-2432.

Panchision, D.M., Chen, H.L., Pistollato, F., Papini, D., Ni, H.T., Hawley, T.S., 2007. Optimized flow cytometric analysis of central nervous system tissue reveals novel functional relationships among cells expressing CD133, CD15, and CD24. Stem cells 25, 1560-1570.

Pareja, E., Gomez-Lechon, M.J., Cortes, M., Bonora-Centelles, A., Castell, J.V., Mir, J., 2013. Human hepatocyte transplantation in patients with hepatic failure awaiting a graft. European surgical research. Europaische chirurgische Forschung. Recherches chirurgicales europeennes 50, 273-281.

Parekkadan, B., Milwid, J.M., 2010. Mesenchymal stem cells as therapeutics. Annual review of biomedical engineering 12, 87-117.

Parekkadan, B., van Poll, D., Megeed, Z., Kobayashi, N., Tilles, A.W., Berthiaume, F., Yarmush, M.L., 2007. Immunomodulation of activated hepatic stellate cells by mesenchymal stem cells. Biochemical and biophysical research communications 363, 247-252.

Park, S.A., Reilly, C.M., Wood, J.A., Chung, D.J., Carrade, D.D., Deremer, S.L., Seraphin, R.L., Clark, K.C., Zwingenberger, A.L., Borjesson, D.L., Hayashi, K., Russell, P., Murphy, C.J., 2013. Safety and immunomodulatory effects of allogeneic canine adipose-derived mesenchymal stromal cells transplanted into the region of the lacrimal gland, the gland of the third eyelid and the knee joint. Cytotherapy 15, 1498-1510.

Park, S.S., Lee, Y.J., Lee, S.H., Lee, D., Choi, K., Kim, W.H., Kweon, O.K., Han, H.J., 2012. Functional recovery after spinal cord injury in dogs treated with a combination of Matrigel and neural-induced adipose-derived mesenchymal Stem cells. Cytotherapy 14, 584-597.

Perry, M., Nelson, D., Moore, M., Chalkley, R., 1979. Histone deacetylation in nuclei isolated from hepatoma tissue culture cells. Inhibition by sodium butyrate. Biochimica et biophysica acta 561, 517-525.

Peters, T.S., 2005. Do preclinical testing strategies help predict human hepatotoxic potentials? Toxicologic pathology 33, 146-154.

Pfaffl, M.W., 2001. A new mathematical model for relative quantification in real-time RT-PCR. Nucleic acids research 29, e45.

Phillips, J.E., Gersbach, C.A., Wojtowicz, A.M., Garcia, A.J., 2006. Glucocorticoid-induced osteogenesis is negatively regulated by Runx2/Cbfa1 serine phosphorylation. Journal of cell science 119, 581-591.

Pichard, L., Raulet, E., Fabre, G., Ferrini, J.B., Ourlin, J.C., Maurel, P., 2006. Human hepatocyte culture. Methods in molecular biology 320, 283-293.

Pittenger, M.F., Mackay, A.M., Beck, S.C., Jaiswal, R.K., Douglas, R., Mosca, J.D., Moorman, M.A., Simonetti, D.W., Craig, S., Marshak, D.R., 1999. Multilineage potential of adult human mesenchymal stem cells. Science 284, 143-147.

Pogue, B., Estrada, A.H., Sosa-Samper, I., Maisenbacher, H.W., Lamb, K.E., Mincey, B.D., Erger, K.E., Conlon, T.J., 2013. Stem-cell therapy for dilated

cardiomyopathy: a pilot study evaluating retrograde coronary venous delivery. The Journal of small animal practice 54, 361-366.

Poldervaart, J.H., Favier, R.P., Penning, L.C., van den Ingh, T.S., Rothuizen, J., 2009. Primary hepatitis in dogs: a retrospective review (2002-2006). Journal of veterinary internal medicine / American College of Veterinary Internal Medicine 23, 72-80.

Potter, H., 2001. Transfection by electroporation. Current protocols in immunology / edited by John E. Coligan ... [et al.] Chapter 10, Unit 10 15.

Pournasr, B., Mohamadnejad, M., Bagheri, M., Aghdami, N., Shahsavani, M., Malekzadeh, R., Baharvand, H., 2011. In vitro differentiation of human bone marrow mesenchymal stem cells into hepatocyte-like cells. Archives of Iranian medicine 14, 244-249.

Prasajak, P., Leeanansaksiri, W., 2013. Developing a New Two-Step Protocol to Generate Functional Hepatocytes from Wharton's Jelly-Derived Mesenchymal Stem Cells under Hypoxic Condition. Stem cells international 2013, 762196.

Promega Technical Manual P450-Glo Assays, 2013. P450-Glo Assays Technical Manual. http://www.promega.co.uk/~/media/Files/Resources/Protocols/Technical%20Bulletins/101/P450%20Glo%20Assays%20Protocol.pdf (accessed 18th November 2013).

Qihao, Z., Xigu, C., Guanghui, C., Weiwei, Z., 2007. Spheroid formation and differentiation into hepatocyte-like cells of rat mesenchymal stem cell induced by co-culture with liver cells. DNA and cell biology 26, 497-503.

Quaschning, T., Koniger, M., Kramer-Guth, A., Greiber, S., Pavenstadt, H., Nauck, M., Schollmeyer, P., Wanner, C., 1997. Receptor-mediated lipoprotein uptake by human glomerular cells: comparison with skin fibroblasts and HepG2 cells. Nephrology, dialysis, transplantation : official publication of the European Dialysis and Transplant Association - European Renal Association 12, 2528-2536.

Quintanilha, L.F., Takami, T., Hirose, Y., Fujisawa, K., Murata, Y., Yamamoto, N., Goldenberg, R.C., Terai, S., Sakaida, I., 2013. Canine mesenchymal stem cells show antioxidant properties against thioacetamide-induced liver injury in vitro and in vivo. Hepatology research : the official journal of the Japan Society of Hepatology.

Rajan, J.C., Klein, L., 1982. Periodic acid-Schiff staining of type II collagen and its cyanogen bromide peptides after polyacrylamide gel electrophoresis. Electrophoresis 3, 106-109.

Rajasingh, J., Thangavel, J., Siddiqui, M.R., Gomes, I., Gao, X.P., Kishore, R., Malik, A.B., 2011. Improvement of cardiac function in mouse myocardial infarction after transplantation of epigenetically-modified bone marrow progenitor cells. PloS one 6, e22550.

Ramasamy, T.S., Yu, J.S., Selden, C., Hodgson, H., Cui, W., 2013. Application of three-dimensional culture conditions to human embryonic stem cell-derived definitive endoderm cells enhances hepatocyte differentiation and functionality. Tissue engineering. Part A 19, 360-367.

Reich, C.M., Raabe, O., Wenisch, S., Bridger, P.S., Kramer, M., Arnhold, S., 2012. Isolation, culture and chondrogenic differentiation of canine adipose tissue- and bone marrow-derived mesenchymal stem cells--a comparative study. Veterinary research communications 36, 139-148.

Requicha, J.F., Viegas, C.A., Albuquerque, C.M., Azevedo, J.M., Reis, R.L., Gomes, M.E., 2012. Effect of anatomical origin and cell passage number on the stemness and osteogenic differentiation potential of canine adipose-derived stem cells. Stem cell reviews 8, 1211-1222.

Rimbault, M., Ostrander, E.A., 2012. So many doggone traits: mapping genetics of multiple phenotypes in the domestic dog. Human molecular genetics 21, R52-57.

Robinton, D.A., Daley, G.Q., 2012. The promise of induced pluripotent stem cells in research and therapy. Nature 481, 295-305.

Rodolfa, K.T., 2012. Inducing pluripotency, In: StemBook.

Rodriguez-Antona, C., Donato, M.T., Boobis, A., Edwards, R.J., Watts, P.S., Castell, J.V., Gomez-Lechon, M.J., 2002. Cytochrome P450 expression in human hepatocytes and hepatoma cell lines: molecular mechanisms that determine lower expression in cultured cells. Xenobiotica; the fate of foreign compounds in biological systems 32, 505-520.

Roelandt, P., Vanhove, J., Verfaillie, C., 2013. Directed differentiation of pluripotent stem cells to functional hepatocytes. Methods in molecular biology 997, 141-147.

Roskams, T., 2006. Different types of liver progenitor cells and their niches. Journal of hepatology 45, 1-4.

Rountree, C.B., Ding, W., Dang, H., Vankirk, C., Crooks, G.M., 2011. Isolation of CD133+ liver stem cells for clonal expansion. Journal of visualized experiments : JoVE.

Ryu, H.H., Kang, B.J., Park, S.S., Kim, Y., Sung, G.J., Woo, H.M., Kim, W.H., Kweon, O.K., 2012. Comparison of mesenchymal stem cells derived from fat, bone marrow, Wharton's jelly, and umbilical cord blood for treating spinal cord injuries in dogs. The Journal of veterinary medical science / the Japanese Society of Veterinary Science 74, 1617-1630.

Safra, N., Schaible, R.H., Bannasch, D.L., 2006. Linkage analysis with an interbreed backcross maps Dalmatian hyperuricosuria to CFA03. Mammalian genome : official journal of the International Mammalian Genome Society 17, 340-345.

Sakaida, I., Terai, S., Yamamoto, N., Aoyama, K., Ishikawa, T., Nishina, H., Okita, K., 2004. Transplantation of bone marrow cells reduces CCl4-induced liver fibrosis in mice. Hepatology 40, 1304-1311.

Sancho-Bru, P., Najimi, M., Caruso, M., Pauwelyn, K., Cantz, T., Forbes, S., Roskams, T., Ott, M., Gehling, U., Sokal, E., Verfaillie, C.M., Muraca, M., 2009. Stem and progenitor cells for liver repopulation: can we standardise the process from bench to bedside? Gut 58, 594-603.

Sasaki, J., Cottam, G.L., 1982. Glycosylation of LDL decreases its ability to interact with high-affinity receptors of human fibroblasts in vitro and decreases its clearance from rabbit plasma in vivo. Biochimica et biophysica acta 713, 199-207.

Sasaki, K., Kon, J., Mizuguchi, T., Chen, Q., Ooe, H., Oshima, H., Hirata, K., Mitaka, T., 2008. Proliferation of hepatocyte progenitor cells isolated from adult human livers in serum-free medium. Cell transplantation 17, 1221-1230.

Sato, K., Ozaki, K., Oh, I., Meguro, A., Hatanaka, K., Nagai, T., Muroi, K., Ozawa, K., 2007. Nitric oxide plays a critical role in suppression of T-cell proliferation by mesenchymal stem cells. Blood 109, 228-234.

Schmelz, M., Schmid, V.J., Parrish, A.R., 2001. Selective disruption of cadherin/catenin complexes by oxidative stress in precision-cut mouse liver slices. Toxicological sciences : an official journal of the Society of Toxicology 61, 389-394.

Schmelzer, E., Reid, L.M., 2008. EpCAM expression in normal, non-pathological tissues. Frontiers in bioscience : a journal and virtual library 13, 3096-3100.

Schmelzer, E., Zhang, L., Bruce, A., Wauthier, E., Ludlow, J., Yao, H.L., Moss, N., Melhem, A., McClelland, R., Turner, W., Kulik, M., Sherwood, S., Tallheden, T., Cheng, N., Furth, M.E., Reid, L.M., 2007. Human hepatic stem cells from fetal and postnatal donors. The Journal of experimental medicine 204, 1973-1987.

Schneider, M.R., Adler, H., Braun, J., Kienzle, B., Wolf, E., Kolb, H.J., 2007. Canine embryo-derived stem cells--toward clinically relevant animal models for evaluating efficacy and safety of cell therapies. Stem cells 25, 1850-1851.

Schoen, J.M., Wang, H.H., Minuk, G.Y., Lautt, W.W., 2001. Shear stress-induced nitric oxide release triggers the liver regeneration cascade. Nitric oxide : biology and chemistry / official journal of the Nitric Oxide Society 5, 453-464.

Schotanus, B.A., van den Ingh, T.S., Penning, L.C., Rothuizen, J., Roskams, T.A., Spee, B., 2009. Cross-species immunohistochemical investigation of the activation of the liver progenitor cell niche in different types of liver disease. Liver international : official journal of the International Association for the Study of the Liver 29, 1241-1252.

Schwartz, R.E., Reyes, M., Koodie, L., Jiang, Y., Blackstad, M., Lund, T., Lenvik, T., Johnson, S., Hu, W.S., Verfaillie, C.M., 2002. Multipotent adult progenitor cells

from bone marrow differentiate into functional hepatocyte-like cells. The Journal of clinical investigation 109, 1291-1302.

Seeliger, C., Culmes, M., Schyschka, L., Yan, X., Damm, G., Wang, Z., Kleeff, J., Thasler, W.E., Hengstler, J., Stockle, U., Ehnert, S., Nussler, A.K., 2013. Decrease of global methylation improves significantly hepatic differentiation of Ad-MSCs: possible future application for urea detoxification. Cell transplantation 22, 119-131.

Seglen, P.O., 1976. Preparation of isolated rat liver cells. Methods in cell biology 13, 29-83.

Sekiya, I., Tsuji, K., Koopman, P., Watanabe, H., Yamada, Y., Shinomiya, K., Nifuji, A., Noda, M., 2000. SOX9 enhances aggrecan gene promoter/enhancer activity and is up-regulated by retinoic acid in a cartilage-derived cell line, TC6. The Journal of biological chemistry 275, 10738-10744.

Sellaro, T.L., Ranade, A., Faulk, D.M., McCabe, G.P., Dorko, K., Badylak, S.F., Strom, S.C., 2010. Maintenance of human hepatocyte function in vitro by liver-derived extracellular matrix gels. Tissue engineering. Part A 16, 1075-1082.

Semba, I., Nonaka, K., Takahashi, I., Takahashi, K., Dashner, R., Shum, L., Nuckolls, G.H., Slavkin, H.C., 2000. Positionally-dependent chondrogenesis induced by BMP4 is co-regulated by Sox9 and Msx2. Developmental dynamics : an official publication of the American Association of Anatomists 217, 401-414.

Seo, M.J., Suh, S.Y., Bae, Y.C., Jung, J.S., 2005. Differentiation of human adipose stromal cells into hepatic lineage in vitro and in vivo. Biochemical and biophysical research communications 328, 258-264.

Seo, M.S., Jeong, Y.H., Park, J.R., Park, S.B., Rho, K.H., Kim, H.S., Yu, K.R., Lee, S.H., Jung, J.W., Lee, Y.S., Kang, K.S., 2009. Isolation and characterization of canine umbilical cord blood-derived mesenchymal stem cells. Journal of veterinary science 10, 181-187.

Sevior, D.K., Pelkonen, O., Ahokas, J.T., 2012. Hepatocytes: the powerhouse of biotransformation. The international journal of biochemistry & cell biology 44, 257-261.

Sgodda, M., Aurich, H., Kleist, S., Aurich, I., Konig, S., Dollinger, M.M., Fleig, W.E., Christ, B., 2007. Hepatocyte differentiation of mesenchymal stem cells from rat peritoneal adipose tissue in vitro and in vivo. Experimental cell research 313, 2875-2886.

Shamay, A., Homans, R., Fuerman, Y., Levin, I., Barash, H., Silanikove, N., Mabjeesh, S.J., 2005. Expression of albumin in nonhepatic tissues and its synthesis by the bovine mammary gland. Journal of dairy science 88, 569-576.

Sharma, N.S., Shikhanovich, R., Schloss, R., Yarmush, M.L., 2006. Sodium butyrate-treated embryonic stem cells yield hepatocyte-like cells expressing a glycolytic phenotype. Biotechnology and bioengineering 94, 1053-1063.

Shawcross, D., Jalan, R., 2005. The pathophysiologic basis of hepatic encephalopathy: central role for ammonia and inflammation. Cell Mol Life Sci 62, 2295-2304.

Shawcross, D.L., Olde Damink, S.W., Butterworth, R.F., Jalan, R., 2005. Ammonia and hepatic encephalopathy: the more things change, the more they remain the same. Metab Brain Dis 20, 169-179.

Shen, H., 2013. Stricter standards sought to curb stem-cell confusion. Nature 499, 389.

Shimada, H., Nakada, A., Hashimoto, Y., Shigeno, K., Shionoya, Y., Nakamura, T., 2010. Generation of canine induced pluripotent stem cells by retroviral transduction and chemical inhibitors. Molecular reproduction and development 77, 2.

Shimano, K., Satake, M., Okaya, A., Kitanaka, J., Kitanaka, N., Takemura, M., Sakagami, M., Terada, N., Tsujimura, T., 2003. Hepatic oval cells have the side population phenotype defined by expression of ATP-binding cassette transporter ABCG2/BCRP1. The American journal of pathology 163, 3-9.

Shiraki, N., Yamazoe, T., Qin, Z., Ohgomori, K., Mochitate, K., Kume, K., Kume, S., 2011. Efficient differentiation of embryonic stem cells into hepatic cells in vitro using a feeder-free basement membrane substratum. PloS one 6, e24228.

Shu, J., Wu, C., Wu, Y., Li, Z., Shao, S., Zhao, W., Tang, X., Yang, H., Shen, L., Zuo, X., Yang, W., Shi, Y., Chi, X., Zhang, H., Gao, G., Shu, Y., Yuan, K., He, W., Tang, C., Zhao, Y., Deng, H., 2013. Induction of pluripotency in mouse somatic cells with lineage specifiers. Cell 153, 963-975.

Shui, C., Spelsberg, T.C., Riggs, B.L., Khosla, S., 2003. Changes in Runx2/Cbfa1 expression and activity during osteoblastic differentiation of human bone marrow stromal cells. Journal of bone and mineral research : the official journal of the American Society for Bone and Mineral Research 18, 213-221.

Shupe, T.D., Piscaglia, A.C., Oh, S.H., Gasbarrini, A., Petersen, B.E., 2009. Isolation and characterization of hepatic stem cells, or "oval cells," from rat livers. Methods in molecular biology 482, 387-405.

Si-Tayeb, K., Lemaigre, F.P., Duncan, S.A., 2010. Organogenesis and development of the liver. Developmental cell 18, 175-189.

Sidhu, J.S., Farin, F.M., Omiecinski, C.J., 1993. Influence of extracellular matrix overlay on phenobarbital-mediated induction of CYP2B1, 2B2, and 3A1 genes in primary adult rat hepatocyte culture. Archives of biochemistry and biophysics 301, 103-113.

Silva, G.V., Litovsky, S., Assad, J.A., Sousa, A.L., Martin, B.J., Vela, D., Coulter, S.C., Lin, J., Ober, J., Vaughn, W.K., Branco, R.V., Oliveira, E.M., He, R., Geng, Y.J., Willerson, J.T., Perin, E.C., 2005. Mesenchymal stem cells differentiate into an endothelial phenotype, enhance vascular density, and improve heart function in a canine chronic ischemia model. Circulation 111, 150-156.

Silva, J., Nichols, J., Theunissen, T.W., Guo, G., van Oosten, A.L., Barrandon, O., Wray, J., Yamanaka, S., Chambers, I., Smith, A., 2009. Nanog is the gateway to the pluripotent ground state. Cell 138, 722-737.

Simek, J., Melka, J., Pospisil, M., Neradilkova, M., 1965. Effect of protracted glucose infusion on the development of early biochemical changes and initiation of regeneration in rat liver after partial hepatectomy. Physiologia bohemoslovenica 14, 366-370.

Sirico, M.L., Guida, B., Procino, A., Pota, A., Sodo, M., Grandaliano, G., Simone, S., Pertosa, G., Riccio, E., Memoli, B., 2012. Human mature adipocytes express albumin and this expression is not regulated by inflammation. Mediators of inflammation 2012, 236796.

Smith, A., 2014. Cell biology: Potency unchained. Nature 505, 622-623.

Snykers, S., De Kock, J., Rogiers, V., Vanhaecke, T., 2009a. In vitro differentiation of embryonic and adult stem cells into hepatocytes: state of the art. Stem cells 27, 577-605.

Snykers, S., Henkens, T., De Rop, E., Vinken, M., Fraczek, J., De Kock, J., De Prins, E., Geerts, A., Rogiers, V., Vanhaecke, T., 2009b. Role of epigenetics in liver-specific gene transcription, hepatocyte differentiation and stem cell reprogrammation. Journal of hepatology 51, 187-211.

Snykers, S., Vanhaecke, T., De Becker, A., Papeleu, P., Vinken, M., Van Riet, I., Rogiers, V., 2007. Chromatin remodeling agent trichostatin A: a key-factor in the hepatic differentiation of human mesenchymal stem cells derived of adult bone marrow. BMC developmental biology 7, 24.

Soldatow, V.Y., Lecluyse, E.L., Griffith, L.G., Rusyn, I., 2013. models for liver toxicity testing. Toxicology research 2, 23-39.

Sommer, C.A., Sommer, A.G., Longmire, T.A., Christodoulou, C., Thomas, D.D., Gostissa, M., Alt, F.W., Murphy, G.J., Kotton, D.N., Mostoslavsky, G., 2010. Excision of reprogramming transgenes improves the differentiation potential of iPS cells generated with a single excisable vector. Stem cells 28, 64-74.

Southern, P.J., Berg, P., 1982. Transformation of mammalian cells to antibiotic resistance with a bacterial gene under control of the SV40 early region promoter. Journal of molecular and applied genetics 1, 327-341.

Spaggiari, G.M., Abdelrazik, H., Becchetti, F., Moretta, L., 2009. MSCs inhibit monocyte-derived DC maturation and function by selectively interfering with the generation of immature DCs: central role of MSC-derived prostaglandin E2. Blood 113, 6576-6583.

Spaggiari, G.M., Capobianco, A., Becchetti, S., Mingari, M.C., Moretta, L., 2006. Mesenchymal stem cell-natural killer cell interactions: evidence that activated NK cells are capable of killing MSCs, whereas MSCs can inhibit IL-2-induced NK-cell proliferation. Blood 107, 1484-1490.

St Aubin, P.M., Bucher, N.L., 1952. A study of binucleate cell counts in resting and regenerating rat liver employing a mechanical method for the separation of liver cells. The Anatomical record 112, 797-809.

Stachelscheid, H., Urbaniak, T., Ring, A., Spengler, B., Gerlach, J.C., Zeilinger, K., 2009. Isolation and characterization of adult human liver progenitors from ischemic liver tissue derived from therapeutic hepatectomies. Tissue engineering. Part A 15, 1633-1643.

Stadtfeld, M., Hochedlinger, K., 2010. Induced pluripotency: history, mechanisms, and applications. Genes & development 24, 2239-2263.

Stadtfeld, M., Maherali, N., Breault, D.T., Hochedlinger, K., 2008a. Defining molecular cornerstones during fibroblast to iPS cell reprogramming in mouse. Cell stem cell 2, 230-240.

Stadtfeld, M., Nagaya, M., Utikal, J., Weir, G., Hochedlinger, K., 2008b. Induced pluripotent stem cells generated without viral integration. Science 322, 945-949.

Steinert, A.F., Rackwitz, L., Gilbert, F., Noth, U., Tuan, R.S., 2012. Concise review: the clinical application of mesenchymal stem cells for musculoskeletal regeneration: current status and perspectives. Stem cells translational medicine 1, 237-247.

Strioga, M., Viswanathan, S., Darinskas, A., Slaby, O., Michalek, J., 2012. Same or not the same? Comparison of adipose tissue-derived versus bone marrow-derived mesenchymal stem and stromal cells. Stem cells and development 21, 2724-2752.

Stuchbury, G., Munch, G., 2010. Optimizing the generation of stable neuronal cell lines via pre-transfection restriction enzyme digestion of plasmid DNA. Cytotechnology 62, 189-194.

Su, T., Waxman, D.J., 2004. Impact of dimethyl sulfoxide on expression of nuclear receptors and drug-inducible cytochromes P450 in primary rat hepatocytes. Archives of biochemistry and biophysics 424, 226-234.

Sullivan, G.J., Hay, D.C., Park, I.H., Fletcher, J., Hannoun, Z., Payne, C.M., Dalgetty, D., Black, J.R., Ross, J.A., Samuel, K., Wang, G., Daley, G.Q., Lee, J.H., Church, G.M., Forbes, S.J., Iredale, J.P., Wilmut, I., 2010. Generation of functional

human hepatic endoderm from human induced pluripotent stem cells. Hepatology 51, 329-335.

Suzuki, A., Sekiya, S., Onishi, M., Oshima, N., Kiyonari, H., Nakauchi, H., Taniguchi, H., 2008. Flow cytometric isolation and clonal identification of self-renewing bipotent hepatic progenitor cells in adult mouse liver. Hepatology 48, 1964-1978.

Szatmari, V., Rothuizen, J., 2009. Ultrasonographic identification and characterisation of congenital portosystemic shunts and portal hypertensive disorders in dogs and cats, In: Standards fro Clinical and Histological Diagnosis of Canine and Feline Liver Diseases, 2009/06/16 ed. Saunders Elsevier, Philadelphia, pp. 15-40.

Tabibian, J.H., Masyuk, A.I., Masyuk, T.V., O'Hara, S.P., LaRusso, N.F., 2013. Physiology of cholangiocytes. Comprehensive Physiology 3, 541-565.

Takahashi, K., Tanabe, K., Ohnuki, M., Narita, M., Ichisaka, T., Tomoda, K., Yamanaka, S., 2007. Induction of pluripotent stem cells from adult human fibroblasts by defined factors. Cell 131, 861-872.

Takahashi, K., Yamanaka, S., 2006. Induction of pluripotent stem cells from mouse embryonic and adult fibroblast cultures by defined factors. Cell 126, 663-676.

Takayama, K., Inamura, M., Kawabata, K., Sugawara, M., Kikuchi, K., Higuchi, M., Nagamoto, Y., Watanabe, H., Tashiro, K., Sakurai, F., Hayakawa, T., Furue, M.K., Mizuguchi, H., 2012. Generation of metabolically functioning hepatocytes from human pluripotent stem cells by FOXA2 and HNF1alpha transduction. Journal of hepatology 57, 628-636.

Takebe, T., Sekine, K., Enomura, M., Koike, H., Kimura, M., Ogaeri, T., Zhang, R.R., Ueno, Y., Zheng, Y.W., Koike, N., Aoyama, S., Adachi, Y., Taniguchi, H., 2013. Vascularized and functional human liver from an iPSC-derived organ bud transplant. Nature 499, 481-484.

Takebe, T., Zhang, R.R., Koike, H., Kimura, M., Yoshizawa, E., Enomura, M., Koike, N., Sekine, K., Taniguchi, H., 2014. Generation of a vascularized and functional human liver from an iPSC-derived organ bud transplant. Nature protocols 9, 396-409.

Takemitsu, H., Zhao, D., Yamamoto, I., Harada, Y., Michishita, M., Arai, T., 2012. Comparison of bone marrow and adipose tissue-derived canine mesenchymal stem cells. BMC veterinary research 8, 150.

Talens-Visconti, R., Bonora, A., Jover, R., Mirabet, V., Carbonell, F., Castell, J.V., Gomez-Lechon, M.J., 2007. Human mesenchymal stem cells from adipose tissue: Differentiation into hepatic lineage. Toxicology in vitro : an international journal published in association with BIBRA 21, 324-329.

Tan, J., Wu, W., Xu, X., Liao, L., Zheng, F., Messinger, S., Sun, X., Chen, J., Yang, S., Cai, J., Gao, X., Pileggi, A., Ricordi, C., 2012. Induction therapy with autologous mesenchymal stem cells in living-related kidney transplants: a randomized controlled trial. JAMA : the journal of the American Medical Association 307, 1169-1177.

Tancos, Z., Nemes, C., Polgar, Z., Gocza, E., Daniel, N., Stout, T.A., Maraghechi, P., Pirity, M.K., Osteil, P., Tapponnier, Y., Markossian, S., Godet, M., Afanassieff, M., Bosze, Z., Duranthon, V., Savatier, P., Dinnyes, A., 2012. Generation of rabbit pluripotent stem cell lines. Theriogenology 78, 1774-1786.

Tanimoto, H., Terai, S., Taro, T., Murata, Y., Fujisawa, K., Yamamoto, N., Sakaida, I., 2013. Improvement of liver fibrosis by infusion of cultured cells derived from human bone marrow. Cell and tissue research.

Terai, S., Ishikawa, T., Omori, K., Aoyama, K., Marumoto, Y., Urata, Y., Yokoyama, Y., Uchida, K., Yamasaki, T., Fujii, Y., Okita, K., Sakaida, I., 2006. Improved liver function in patients with liver cirrhosis after autologous bone marrow cell infusion therapy. Stem cells 24, 2292-2298.

Terrace, J.D., Hay, D.C., Samuel, K., Payne, C., Anderson, R.A., Currie, I.S., Parks, R.W., Forbes, S.J., Ross, J.A., 2009. Side population cells in developing human liver are primarily haematopoietic progenitor cells. Experimental cell research 315, 2141-2153.

Terry, C., Dhawan, A., Mitry, R.R., Hughes, R.D., 2006. Cryopreservation of isolated human hepatocytes for transplantation: State of the art. Cryobiology 53, 149-159.

Thomson, J.A., Itskovitz-Eldor, J., Shapiro, S.S., Waknitz, M.A., Swiergiel, J.J., Marshall, V.S., Jones, J.M., 1998. Embryonic stem cell lines derived from human blastocysts. Science 282, 1145-1147.

Tomlin, M.E., 2010. Pharmacology & Pharmacokinetics: A Basic Reader. Springer.

Tontonoz, P., Hu, E., Spiegelman, B.M., 1994. Stimulation of adipogenesis in fibroblasts by PPAR gamma 2, a lipid-activated transcription factor. Cell 79, 1147-1156.

Trepanier, L.A., 2006. Cytochrome P450 and its role in veterinary drug interactions. The Veterinary clinics of North America. Small animal practice 36, 975-985, v.

Tsuchiya, H., Matsunaga, T., Aikawa, K., Kamada, N., Nakamura, K., Ichikawa, H., Sasaki, K., Ohmori, S., 2012. Evaluation of human embryonic stem cell-derived hepatocyte-like cells for detection of CYP1A inducers. Drug metabolism and pharmacokinetics 27, 598-604.

Turner, R., Lozoya, O., Wang, Y., Cardinale, V., Gaudio, E., Alpini, G., Mendel, G., Wauthier, E., Barbier, C., Alvaro, D., Reid, L.M., 2011. Human hepatic stem cell and maturational liver lineage biology. Hepatology 53, 1035-1045.

Ubeaud, G., Schiller, C.D., Hurbin, F., Jaeck, D., Coassolo, P., 2001. Comparison of the stability of some major cytochrome P450 and conjugation reactions in rat, dog and human hepatocyte monolayers. European journal of drug metabolism and pharmacokinetics 26, 37-45.

Vaags, A.K., Rosic-Kablar, S., Gartley, C.J., Zheng, Y.Z., Chesney, A., Villagomez, D.A., Kruth, S.A., Hough, M.R., 2009. Derivation and characterization of canine embryonic stem cell lines with in vitro and in vivo differentiation potential. Stem cells 27, 329-340.

Van den Ingh, T.S.G.A.M., Van Winkle, T., Cullen, J.M., J.A., C., Desmet, V.J., 2006. Morphological classification of parenchymal disorders of the canine and feline liver., In: WSAVA Standards for Clinical and Histological Diagnosis of Canine and Feline Liver Disease, first edition ed. Elsevier Limited, Oxford, pp. 85–101.

Verma, R., Holland, M.K., Temple-Smith, P., Verma, P.J., 2012. Inducing pluripotency in somatic cells from the snow leopard (Panthera uncia), an endangered felid. Theriogenology 77, 220-228, 228 e221-222.

Vieira, N.M., Brandalise, V., Zucconi, E., Secco, M., Strauss, B.E., Zatz, M., 2010. Isolation, characterization, and differentiation potential of canine adipose-derived stem cells. Cell transplantation 19, 279-289.

Vilar, J.M., Morales, M., Santana, A., Spinella, G., Rubio, M., Cuervo, B., Cugat, R., Carrillo, J.M., 2013. Controlled, blinded force platform analysis of the effect of intraarticular injection of autologous adipose-derived mesenchymal stem cells associated to PRGF-Endoret in osteoarthritic dogs. BMC veterinary research 9, 131.

Volk, S.W., Wang, Y., Hankenson, K.D., 2012. Effects of donor characteristics and ex vivo expansion on canine mesenchymal stem cell properties: implications for MSC-based therapies. Cell transplantation 21, 2189-2200.

Vosough, M., Omidinia, E., Kadivar, M., Shokrgozar, M.A., Pournasr, B., Aghdami, N., Baharvand, H., 2013. Generation of functional hepatocyte-like cells from human pluripotent stem cells in a scalable suspension culture. Stem cells and development 22, 2693-2705.

Wagner, W., Horn, P., Castoldi, M., Diehlmann, A., Bork, S., Saffrich, R., Benes, V., Blake, J., Pfister, S., Eckstein, V., Ho, A.D., 2008. Replicative senescence of mesenchymal stem cells: a continuous and organized process. PloS one 3, e2213.

Wang, H., Gao, X., Fukumoto, S., Tademoto, S., Sato, K., Hirai, K., 1998. Post-isolation inducible nitric oxide synthase gene expression due to collagenase buffer perfusion and characterization of the gene regulation in primary cultured murine hepatocytes. Journal of biochemistry 124, 892-899.

Wang, T., Hu, H.S., Feng, Y.X., Shi, J., Li, N., Guo, W.X., Xue, J., Xie, D., Liu, S.R., Wu, M.C., Cheng, S.Q., 2010. Characterisation of a novel cell line (CSQT-2)

with high metastatic activity derived from portal vein tumour thrombus of hepatocellular carcinoma. Br J Cancer 102, 1618-1626.

Wang, T., Warren, S.T., Jin, P., 2013a. Toward pluripotency by reprogramming: mechanisms and application. Protein & cell 4, 820-832.

Wang, Y., He, J., Pei, X., Zhao, W., 2013b. Systematic review and meta-analysis of mesenchymal stem/stromal cells therapy for impaired renal function in small animal models. Nephrology 18, 201-208.

Wang, Y., Nan, X., Li, Y., Zhang, R., Yue, W., Yan, F., Pei, X., 2005. Induction of umbilical cord blood-derived beta2m-c-Met+ cells into hepatocyte-like cells by coculture with CFSC/HGF cells. Liver Transpl 11, 635-643.

Wang, Y.J., Liu, H.L., Guo, H.T., Wen, H.W., Liu, J., 2004. Primary hepatocyte culture in collagen gel mixture and collagen sandwich. World J Gastroenterol 10, 699-702.

Watanabe, M., Umenai, T., Ohori, H., Ishida, N., 1976. Evidence for the multiplication of hepatitis B virus in "oval cell" culture originated from human embryonic liver. British journal of experimental pathology 57, 211-216.

Watson, P.J., 2004. Chronic hepatitis in dogs: a review of current understanding of the aetiology, progression, and treatment. Vet J 167, 228-241.

Watson, P.J., Roulois, A.J., Scase, T.J., Irvine, R., Herrtage, M.E., 2010. Prevalence of hepatic lesions at post-mortem examination in dogs and association with pancreatitis. The Journal of small animal practice 51, 566-572.

Wauthier, E., Schmelzer, E., Turner, W., Zhang, L., LeCluyse, E., Ruiz, J., Turner, R., Furth, M.E., Kubota, H., Lozoya, O., Barbier, C., McClelland, R., Yao, H.L., Moss, N., Bruce, A., Ludlow, J., Reid, L.M., 2008. Hepatic stem cells and hepatoblasts: identification, isolation, and ex vivo maintenance. Methods in cell biology 86, 137-225.

Wei, X., Runnels, J.M., Lin, C.P., 2003. Selective uptake of indocyanine green by reticulocytes in circulation. Investigative ophthalmology & visual science 44, 4489-4496.

Wells, J.M., Melton, D.A., 1999. Vertebrate endoderm development. Annual review of cell and developmental biology 15, 393-410.

Wernig, M., Meissner, A., Cassady, J.P., Jaenisch, R., 2008. c-Myc is dispensable for direct reprogramming of mouse fibroblasts. Cell stem cell 2, 10-12.

Whitworth, D.J., Ovchinnikov, D.A., Wolvetang, E.J., 2012. Generation and characterization of LIF-dependent canine induced pluripotent stem cells from adult dermal fibroblasts. Stem cells and development 21, 2288-2297.

Willenbring, H., Bailey, A.S., Foster, M., Akkari, Y., Dorrell, C., Olson, S., Finegold, M., Fleming, W.H., Grompe, M., 2004. Myelomonocytic cells are sufficient for therapeutic cell fusion in liver. Nature medicine 10, 744-748.

Williams, A.R., Hare, J.M., 2011. Mesenchymal stem cells: biology, pathophysiology, translational findings, and therapeutic implications for cardiac disease. Circulation research 109, 923-940.

Woltjen, K., Michael, I.P., Mohseni, P., Desai, R., Mileikovsky, M., Hamalainen, R., Cowling, R., Wang, W., Liu, P., Gertsenstein, M., Kaji, K., Sung, H.K., Nagy, A., 2009. piggyBac transposition reprograms fibroblasts to induced pluripotent stem cells. Nature 458, 766-770.

Wu, X.B., Tao, R., 2012. Hepatocyte differentiation of mesenchymal stem cells. Hepatobiliary & pancreatic diseases international : HBPD INT 11, 360-371.

Xu, F., Hu, Y., Zhou, J., Wang, X., 2013. Mesenchymal stem cells in acute lung injury: are they ready for translational medicine? Journal of cellular and molecular medicine 17, 927-935.

Yamada, T., Yoshikawa, M., Kanda, S., Kato, Y., Nakajima, Y., Ishizaka, S., Tsunoda, Y., 2002. In vitro differentiation of embryonic stem cells into hepatocyte-like cells identified by cellular uptake of indocyanine green. Stem cells 20, 146-154.

Yamaguchi, M., Igarashi, A., Misawa, H., Tsurusaki, Y., 2003. Enhancement of albumin expression in bone tissues with healing rat fractures. Journal of cellular biochemistry 89, 356-363.

Yamazoe, T., Shiraki, N., Toyoda, M., Kiyokawa, N., Okita, H., Miyagawa, Y., Akutsu, H., Umezawa, A., Sasaki, Y., Kume, K., Kume, S., 2013. A synthetic nanofibrillar matrix promotes in vitro hepatic differentiation of embryonic stem cells and induced pluripotent stem cells. Journal of cell science 126, 5391-5399.

Yin, W., Xiang, P., Li, Q., 2005. Investigations of the effect of DNA size in transient transfection assay using dual luciferase system. Analytical biochemistry 346, 289-294.

Yoo, C.B., Cheng, J.C., Jones, P.A., 2004. Zebularine: a new drug for epigenetic therapy. Biochemical Society transactions 32, 910-912.

Yoo, W., Lee, J., Park, S., Kim, Y.S., Lim, C., Yoon, E., Hur, G., Oh, J., 2010. Albumin expression is required for adipocyte differentiation of 3T3-L1 cells. Biochemical and biophysical research communications 397, 170-175.

Yoshioka, K., Enaga, S., Taniguchi, K., Fukushima, U., Uechi, M., Mutoh, K., 2004. Morphological characterization of ductular reactions in canine liver disease. J Comp Pathol 130, 92-98.

Yovchev, M.I., Grozdanov, P.N., Zhou, H., Racherla, H., Guha, C., Dabeva, M.D., 2008. Identification of adult hepatic progenitor cells capable of repopulating injured rat liver. Hepatology 47, 636-647.

Yu, J., Hu, K., Smuga-Otto, K., Tian, S., Stewart, R., Slukvin, II, Thomson, J.A., 2009. Human induced pluripotent stem cells free of vector and transgene sequences. Science 324, 797-801.

Yusa, K., Rashid, S.T., Strick-Marchand, H., Varela, I., Liu, P.Q., Paschon, D.E., Miranda, E., Ordonez, A., Hannan, N.R., Rouhani, F.J., Darche, S., Alexander, G., Marciniak, S.J., Fusaki, N., Hasegawa, M., Holmes, M.C., Di Santo, J.P., Lomas, D.A., Bradley, A., Vallier, L., 2011. Targeted gene correction of alpha1-antitrypsin deficiency in induced pluripotent stem cells. Nature 478, 391-394.

Zamule, S.M., Coslo, D.M., Chen, F., Omiecinski, C.J., 2011. Differentiation of human embryonic stem cells along a hepatic lineage. Chemico-biological interactions 190, 62-72.

Zang, W.Y., de Almedia, P.E., Wu, J.C., 2012. Teratoma formation: A tool for monitoring pluripotency in stem cell research, In: StemBook.

Zaret, K.S., 2001. Hepatocyte differentiation: from the endoderm and beyond. Current opinion in genetics & development 11, 568-574.

Zemel, R., Bachmetov, L., Ad-El, D., Abraham, A., Tur-Kaspa, R., 2009. Expression of liver-specific markers in naive adipose-derived mesenchymal stem cells. Liver international : official journal of the International Association for the Study of the Liver 29, 1326-1337.

Zhang, F., Wang, C., Jing, S., Ren, T., Li, Y., Cao, Y., Lin, J., 2013a. Lectin-like oxidized LDL receptor-1 expresses in mouse bone marrow-derived mesenchymal stem cells and stimulates their proliferation. Experimental cell research 319, 1054-1059.

Zhang, F., Wang, C., Wang, H., Lu, M., Li, Y., Feng, H., Lin, J., Yuan, Z., Wang, X., 2013b. Ox-LDL promotes migration and adhesion of bone marrow-derived mesenchymal stem cells via regulation of MCP-1 expression. Mediators of inflammation 2013, 691023.

Zhang, H., Chen, Z., Bie, P., 2012. Bone marrow-derived mesenchymal stem cells as immunosuppressants in liver transplantation: a review of current data. Transfusion medicine reviews 26, 129-141.

Zhang, K., Kuroha, M., Shibata, Y., Kokue, E., Shimoda, M., 2006. Effect of oral administration of clinically relevant doses of dexamethasone on regulation of cytochrome P450 subfamilies in hepatic microsomes from dogs and rats. American journal of veterinary research 67, 329-334.

Zhang, L., Theise, N., Chua, M., Reid, L.M., 2008. The stem cell niche of human livers: symmetry between development and regeneration. Hepatology 48, 1598-1607.

Zhang, Q., Yang, Y., Zhang, J., Wang, G.Y., Liu, W., Qiu, D.B., Hei, Z.Q., Ying, Q.L., Chen, G.H., 2011. Efficient derivation of functional hepatocytes from mouse induced pluripotent stem cells by a combination of cytokines and sodium butyrate. Chinese medical journal 124, 3786-3793.

Zhang, Z., Liu, J., Liu, Y., Li, Z., Gao, W.Q., He, Z., 2013c. Generation, characterization and potential therapeutic applications of mature and functional hepatocytes from stem cells. Journal of cellular physiology 228, 298-305.

Zhao, T., Zhang, Z.N., Rong, Z., Xu, Y., 2011. Immunogenicity of induced pluripotent stem cells. Nature 474, 212-215.

Zhou, H., Wu, S., Joo, J.Y., Zhu, S., Han, D.W., Lin, T., Trauger, S., Bien, G., Yao, S., Zhu, Y., Siuzdak, G., Scholer, H.R., Duan, L., Ding, S., 2009. Generation of induced pluripotent stem cells using recombinant proteins. Cell stem cell 4, 381-384.

Zhou, Y.F., Bosch-Marce, M., Okuyama, H., Krishnamachary, B., Kimura, H., Zhang, L., Huso, D.L., Semenza, G.L., 2006. Spontaneous transformation of cultured mouse bone marrow-derived stromal cells. Cancer research 66, 10849-10854.

Zorn, A.M., 2008. Liver development, In: StemBook.

Zucconi, E., Vieira, N.M., Bueno, D.F., Secco, M., Jazedje, T., Ambrosio, C.E., Passos-Bueno, M.R., Miglino, M.A., Zatz, M., 2010. Mesenchymal stem cells derived from canine umbilical cord vein--a novel source for cell therapy studies. Stem cells and development 19, 395-402.